

Development of Signal Processing and Machine  
Learning Methods for Inertial Sensor Based Motion  
Information Systems

by

Heike Katrein Brock

A thesis submitted in partial fulfillment of the requirements for the degree of

Doctor of Philosophy

Graduate School of Media and Governance,

Keio University



November 2016

Supervisor

Yuji Ohgi, Professor

Reviewers

Jin Mitsugi

Takeshi Kawazoe

Yasuto Nakanishi



# Abstract

The provision of augmented motion information is a new research problem with increasing relevance for motor skill acquisition and performance analysis in sports. Focusing on mobility and usability, this thesis demonstrates how to obtain intelligent, computer-directed motion information for diverse recipients from the measurement data of inertial sensor devices. Methods for the implementation of respective motion information systems were developed and put into use within an original data analysis framework. This framework was based on four principal procedural stages and largely consisted of signal processing methods for the inertial sensor data and machine learning methods for the recognition of motion activity. First, numeric motion data for subsequent machine data processing was collected using inertial measurement devices. Second, the information content of the acquired motion data was augmented to provide accurate and reliable kinematic motion information. Third, the augmented data was transformed so that meaningful data representations were created. Lastly, biological or artificial motion knowledge was utilized to enable the retrieval of relevant motion properties and its subsequent provision to the user. Every computational stage required sophisticated algorithms that were illustrated with practical motion data from rehabilitation, ski jumping and every day motion actions. The latter processing steps were furthermore designed under two variant sample applications: the provision of auditive feedback by means of movement sonification and the provision of performance scores by means of motion evaluation. To date, no other work is known that would have used computational methods on actual sport motion data in a similarly universal, yet applicable way. Therefore, this work constitutes an important contribution to the future implementation of motion analysis and training software tools that support multiple aspects of a motion performance. Especially for judging-based sports, the presented intelligent style assessment could provide fundamental and unique information to increase objectivity and measurability of the final competition scores.

Key words: computational motion analysis, augmented motion feedback, body sensor networks, inertial motion capturing, motion signal processing, motion information retrieval





# Acknowledgements

I would like to express thanks to the many people, in many countries, who so generously contributed to the work presented in this thesis.

First of all, I would like to express my sincerest gratitude to my main supervisor, Professor Yuji Ohgi, whose expertise and support added considerably to my academic experience and my life in Japan. I want to thank you for encouraging my research, supporting me in the acquisition of research grants as well as the organization of experiments. Furthermore, your assistance in settling my life in Japan has been very helpful and gave me more freedom to grow as a research scientist. My gratitude also goes to all current and former members of the Ohgi lab, who supported me in the execution of experiments and presentations of my thesis work.

I would also like to thank the remaining members of my research advisory group, Professor Jin Mitsugi and Professor Takeshi Kawazoe, for serving as my research advisers despite their busy schedules. I also want to thank you for your insightful comments and encouragement, but also for the hard questions which stimulated me to widen my research and made my dissertation hearing an enjoyable moment. I would also like to thank the remaining member of my final defense committee, Professor Yasuto Nakanishi, for his time to review this thesis.

My sincere thanks also goes to Professor Alfred Effenberg and Dr. Gerd Schmitz from the Institute of Sport Science, Leibniz University Hanover. By making me a part of their movement science research team they not only gave me access to the laboratory and research facilities of their working group, but also very valuable insights into the research and working style of a sport scientist. I furthermore thank all the other colleagues I met during my time in Hanover. The group has been a source of friendships as well as good advice and collaboration. I also want to thank Professor James B. Lee, Charles-Darwin University Australia, for proof-reading my writings on the ski jump measurement system. Lastly, I want to thank all institutions that invited me for giving a lecture or workshop all over the world. By discussing my work with other scientists from related research fields, I could gather a lot of valuable feedback and impact for my current and future research activities.

I gratefully acknowledge the funding sources that made my Ph.D. work possible. I was funded by the Japanese Ministry of Education, Culture, Sports, Science and Technology (MEXT) and the German Academic Exchange Service (DAAD). The financial support enabled me to concentrate on my research and hence contributed a lot to the fruitful outcome of my work.

I must also acknowledge all athletes who supported my work by participating in my experiments. Without their numerous motion performances, no motion data for the development of my information and feedback system could have been collected. In this context, I also

## Acknowledgements

---

owe my gratitude to the ski jump judge who agreed to serve as ground truth data for the development of my jump evaluation system. Moreover, I thank the employees of the ski jump hill in Myoko Kogen, Niigata, who supported the smooth operation of the data collection.

My time in Tokyo was and is made enjoyable in large part due to the many friends and groups that became a part of my life. I am grateful for time spent away from my work desk in karaoke boxes, restaurants, public parks, beaches and mountains with a variety of friends. My time at Keio University was furthermore enriched by the Keio Women's Lacrosse Team, who made me a member of their team for 2 years despite my advanced postgraduate student age.

Last but not the least, I would like to thank my family: my parents and my sister for letting me go to such a far away place without any (spoken or obvious) objection and for supporting my life in general. It has always been a source of inspiration and happiness and made me the person I am now.

*Tokyo, July 2016*

Heike Katrein Brock



# Contents

<b>Abstract</b>	<b>i</b>
<b>Acknowledgements</b>	<b>iii</b>
<b>List of figures</b>	<b>ix</b>
<b>List of tables</b>	<b>xvii</b>
<b>I What is Inertial Sensor Based Motion Information?</b>	<b>1</b>
<b>1 Introduction</b>	<b>3</b>
1.1 Thesis Structure . . . . .	9
1.1.1 Appeal Points and Innovations . . . . .	12
<b>2 Fundamental Definitions and Terminology</b>	<b>15</b>
2.1 Motion Information from the Perspective of Sport Science . . . . .	15
2.1.1 Motion Feedback Parameters . . . . .	16
2.1.2 Motion Feedback Variables . . . . .	17
2.1.3 Augmented Motion Feedback . . . . .	18
2.2 Motion Information from the Perspective of Computer Science . . . . .	19
<b>3 Thesis Fundamentals and Related Works</b>	<b>21</b>
3.1 Ski Jumping . . . . .	21
3.1.1 Competition Rules . . . . .	22
3.1.2 Technical Specifications . . . . .	24
3.2 Representing Orientation . . . . .	27
3.2.1 Quaternion Representations . . . . .	28
3.2.2 Transformation Between Representations . . . . .	30
3.3 Related Works . . . . .	30
3.3.1 Supporting Motor Learning . . . . .	31
3.3.2 Processing Sensor Signals . . . . .	32
3.3.3 Measuring Ski Jumps . . . . .	33
3.3.4 Recognizing Motion Activities . . . . .	34
<b>II Collecting and Augmenting Numeric Motion Data</b>	<b>39</b>
<b>4 Collecting Numeric Motion Data</b>	<b>43</b>
4.1 Motion Capture Devices . . . . .	43

## Contents

---

4.2	Current Inertial Sensor Hardware . . . . .	45
4.2.1	Used Sensor Hardware . . . . .	47
4.3	Created Motion Data Bases . . . . .	48
4.3.1	Simulation and Test Data Base . . . . .	49
4.3.2	Field Motion Data Base . . . . .	50
<b>5</b>	<b>Augmentation of the Collected Motion Data</b>	<b>55</b>
5.1	Estimating Initial Posture . . . . .	55
5.2	Estimating Sensor Orientations . . . . .	57
5.2.1	Global Coordinate Frame Settings . . . . .	57
5.2.2	Angular Velocity Integration . . . . .	58
5.2.3	Fusion Filter . . . . .	59
5.2.4	Filter Designation . . . . .	68
5.3	Determining Body Segment Orientations . . . . .	70
5.4	Estimating Positions . . . . .	71
5.4.1	Orientation Based Position Estimation . . . . .	72
5.5	Processing Work Flow . . . . .	73
<b>6</b>	<b>Validation and Enhancement of the Augmented Motion Data</b>	<b>77</b>
6.1	Accuracy of the Augmented Data . . . . .	78
6.1.1	Verification of The General System Applicability . . . . .	78
6.1.2	Verification of The In-field System Applicability . . . . .	81
6.2	Enhancing Usability of the Data Augmentation Step . . . . .	85
6.2.1	Intelligent Gyroscope Drift Reduction . . . . .	85
6.2.2	Intelligent Compensation of Heading Variability . . . . .	97
6.3	Results and Discussion . . . . .	99
6.3.1	Usability Enhancement . . . . .	103
<b>III</b>	<b>Utilizing Numeric Motion Data</b>	<b>105</b>
<b>7</b>	<b>Making Sense of the Motion Data</b>	<b>109</b>
7.1	Transforming Data into Visual Features . . . . .	109
7.2	Transforming Data into Sound Features . . . . .	111
7.2.1	Data Representations for Sonification . . . . .	111
7.2.2	Sound Mapping Strategies . . . . .	113
7.3	Transforming Data into Motion Features . . . . .	115
7.3.1	Segmenting Motion Data into Parts . . . . .	116
7.3.2	Computation of Motion Features . . . . .	120
<b>8</b>	<b>Retrieving Auditory Motion Information</b>	<b>125</b>
8.1	Movement Sonification . . . . .	125
8.1.1	Sonification for Rehabilitation . . . . .	126

8.2 Discussion . . . . .	128
<b>9 Retrieving Motion Style Information</b>	<b>131</b>
9.1 Motion Feature Categories for Performance Assessment . . . . .	132
9.1.1 Technical Motion Features . . . . .	132
9.1.2 Aesthetic Motion Features . . . . .	135
9.2 Fundamental Information Retrieval Methods . . . . .	137
9.2.1 General Data Base Separation . . . . .	137
9.2.2 Classification Methods for Error Recognition . . . . .	138
9.3 Ski Jump Style Assessment . . . . .	142
9.3.1 Style Error Recognition . . . . .	145
9.3.2 Full Performance Quality Assessments . . . . .	158
9.3.3 Feature Type Evaluation . . . . .	163
9.3.4 Numeric Style Error Assessment . . . . .	165
9.4 Discussion . . . . .	170
9.4.1 Outlook: Rating Further Sports . . . . .	172
 <b>IV The Future of Training and Competitions</b>	 <b>175</b>
<b>10 Information Provision</b>	<b>177</b>
10.1 Athlete Feedback . . . . .	177
10.1.1 Outlook: Auditory Feedback in Sports . . . . .	178
10.1.2 Motion and Style Feedback in Ski Jumping . . . . .	180
10.2 Judging Knowledge . . . . .	184
10.3 Discussion . . . . .	186
<b>11 Final Words</b>	<b>187</b>
11.1 Summary and Conclusion . . . . .	187
11.2 Outlook and Future Work . . . . .	194
 <b>V Appendix</b>	 <b>197</b>
<b>A Author Publications</b>	<b>199</b>
<b>B System Promotion</b>	<b>205</b>
<b>C Overview Ski Jump Data Base</b>	<b>213</b>
<b>D Judge Score Sheets</b>	<b>219</b>
 <b>VI Bibliography</b>	 <b>225</b>







# List of Figures

1.1	General design of the computer-based motion information system developed in this thesis. The structure builds a framework for the evolution of the whole thesis. . . . .	4
1.2	Motion information types selected as sample applications for this thesis and their interrelation to signal processing and machine learning methods. . . . .	6
1.3	Four main internal processing stages ((1) – (4), red) have to be passed through before motion information can be obtained from wearable motion sensors. . .	8
1.4	Overview of the main innovations presented in this thesis. The combination of methods from computer science and sport science is unique and has not been found to be presented in a similar form anywhere else. . . . .	14
2.1	Closed-loop model of motor learning processes developed by Schmidt in 1975.	16
2.2	Confirmed (solid) and hypothesized (dashed) effectiveness of a feedback strategy for the enhancement of motor learning in dependence on functional task complexity after Sigrist. . . . .	18
2.3	Differences in the definition of motion information respectively feedback from a sport scientific (left) and computer scientific (right) perspective. . . . .	19
3.1	Illustration of the current scoring system in ski jumping. By adding style points, wind and in-run length scores, the final ranking does not necessarily conform with the jump length. . . . .	23
3.2	Take-off and landing divide a ski jump into the three main motion phases in-run, flight and outrun. Motion characteristics further separate in-run and flight into the four sub-phases take-off initiation, transition to stable flight, stable flight and landing initiation. . . . .	24
3.3	The most characteristic flight elements of contemporary ski jumping are the V-style flight position (left) and the Telemark landing (right). . . . .	25
3.4	Definition of orientation for the description of human posture following naming conventions from navigation. Roll $\phi$ depicts the rotation around the sagittal axis, pitch $\theta$ the elevation around the transversal axis and yaw $\psi$ the rotation around the vertical axis. . . . .	28
3.5	The orientation of frame $B$ (purple, with the axes $X_B$ , $Y_B$ and $Z_B$ ) in relation to frame $A$ (blue, with the axes $X_A$ , $Y_A$ and $Z_A$ ) is represented by a rotation around axis $\hat{n}$ . . . . .	29
4.1	Output of the three currently most common motion capture systems. Left: optical marker-based devices, middle: optical marker-less devices, right: wearable sensor-based devices. . . . .	44

## List of Figures

---

4.2	Capture volumes as they can be covered by optical marker-based and marker-less systems are easily exceeded in many sports. Therefore, it is sensible to choose wearable (inertial) sensors as motion capture device. . . . .	45
4.3	General hardware specifications of inertial measurement units (MARG sensors) and the special demands of sports that require independent sensor technology.	46
4.4	Waterproof sensor from Logical Product used in this thesis and its local sensor coordinate system (orange). . . . .	48
4.5	Sensor placement for the collection of the simulation data base and the four corresponding optical markers attached to every sensor for the acquisition of ground truth reference data. . . . .	50
4.6	Sensor placement for the collection of the field ski jumping motion data base. The sensors are directly attached to the body with adhesive and kinesiology tape.	51
4.7	Impressions of the data acquisition of summer ski jumping. Pictures of the measurement equipment used and the sensor attachment can be found on the following pages. . . . .	52
5.1	Working principle of the vector-based orientation estimator $VB$ to estimate the initial posture in static position at the beginning of every data capture. . . . .	56
5.2	Inertial capturing in the defined global coordinate system under the laboratory setting ( $\mathcal{D}_S$ , left) and at the ski jump hill ( $\mathcal{D}_R$ , right). . . . .	57
5.3	Working principle of the angular velocity integration estimator $GI$ . . . . .	58
5.4	Simplified working principle of the gradient descent optimization based complementary fusion filter $CF1$ . . . . .	60
5.5	Detailed description of the working principle of $CF1$ illustrating all computation steps. . . . .	62
5.6	Simplified working principle of the rotation matrix based complementary fusion filter $CF2$ . . . . .	63
5.7	Detailed description of the working principle of $CF2$ with all computation steps.	64
5.8	Simplified working principle of the optimization based pseudo-linear Kalman fusion filter $KF$ . . . . .	65
5.9	Detailed description of the working principle of $KF$ with all computation steps.	66
5.10	Working principle of the external orientation estimation and convergence step used by $KF$ . . . . .	67
5.11	Working principle of a sensor-bone alignment. Calibration movements have to be executed before the main data processing to determine the displacement of every sensor placement. . . . .	71
5.12	Forward kinematics under the defined global coordinate system for the estimation of relative joint positions at the left arm. . . . .	72
5.13	Working principle of the relative pose estimation under the FK principle. . . . .	73
5.14	Overview on all data augmentation methods and their natural flow within the motion information system. . . . .	75

6.1	Orientation estimates obtained with <i>CF1</i> (purple), <i>CF2</i> (green) and <i>KF</i> (light blue) and the ground truth orientation determined from optical camera data (black). Upper row: estimates for pitch $\theta$ in throwing and kicking at P. Bottom row: estimates for pitch $\theta$ in jumping (rope skipping) and jumping jacks at P. . . . .	80
6.2	$E_{RMS}$ averaged over all motions in $\mathcal{D}_S$ at (a) P and (b) an extremity (right shank or arm) and their standard deviation with the chosen filter values. Possible error values range between 0 and 1. . . . .	82
6.3	Sample plot of a throwing motion with the ground truth data and the respective estimate from the three filter models along x, y and z. . . . .	83
6.4	Magnetic disturbances between different takes on the start gate at the top of the ski jump hill led to differences in heading $\phi$ of estimated segment orientations, as well as differences in joint positions estimated from the posture data. . . . .	84
6.5	Changes in the accuracy values $E_{RMS}$ of all filter models with a fixed noise value in relation to the $E_{RMS}$ values of <i>GI</i> (here depicted as base value 0) per motion pattern and their mean relative change values RC. . . . .	86
6.6	Changes in the accuracy values $E_{RMS}$ of <i>CF1</i> in relation to the $E_{RMS}$ values of <i>GI</i> (here depicted as base value 0) per sensor location and their mean relative change values RC. . . . .	87
6.7	Visualization of the three main principal components for (left column) the Vicon ground truth data and (right column) <i>GI</i> for highly accurate data captures (kicking, top) and less accurate data captures (jumping jacks, bottom) at P and IS. . . . .	89
6.8	Power-Frequency plots of the DFT of the angular velocity data at IS for (a-c) kicking and (d-f) jumping jacks as well as for (g-i) throwing at P along x (red), y (green) and z (blue). . . . .	91
6.9	a) Global ground truth pitch $\theta$ (blue, solid), roll $\phi$ (red, dotted) and yaw $\psi$ (yellow, line) in degree for a continuous sequence of jumping jacks at P. b) Angles estimated from the sensor data with <i>GI</i> for the same motion with drift. c) Same estimated angles with <i>GI</i> and drift compensation. . . . .	92
6.10	Angular velocities at x (blue, dotted), y (green, solid) and z (red, line) for three sample motion types jogging (a), jumping jacks (b) and throwing (c) at rA in relation to the thresholds $th_{lm}$ at $\pm 400$ dps and $th_{mh}$ at $\pm 800$ dps. . . . .	93
6.11	Graph visualization of the relative change in $E_{RMS}$ for the drift compensated <i>GI</i> estimates under a logarithmic scale. Every motion type is represented by a unique color, whereas color saturation represents the different bias rate values (from little saturation for $b_{l1}$ to high saturation for $b_{h2}$ ). . . . .	94
6.12	Matrix visualization of the relative change in $E_{RMS}$ for the drift compensated <i>GI</i> estimates under a logarithmic scale. . . . .	95
6.13	$E_{RMS}$ error values averaged over all motion takes and sensor locations for <i>GI</i> , <i>CF1</i> , <i>CF2</i> and <i>KF</i> without drift compensation (purple), with drift compensation of a simple fixed value (orange) and with the proposed flexible drift compensation (yellow). . . . .	96

## List of Figures

---

6.14	Working principle for the additional magnetic bias compensation method equalizing disturbances in the magnetic field measurements. . . . .	98
6.15	Visualization of the three main principal components for the Vicon ground truth data and the $CF2$ estimates with the former less jumping jack data capture at IS. The flexible value (c) brings the coefficient distribution closer to the ground truth distribution. . . . .	101
6.16	Visualization of the differences in heading $\psi$ before (top) and $\psi_C$ after (bottom) compensation. Heading angles are of positive values 0 to $\pi$ on the right side of the circle and of negative values 0 to $\pi$ on the left side of the circle, whereas 0 is at the bottom and $\pm \pi$ at the top of the circle plot. Red pies represent the angular areas in which initial heading angles occur. . . . .	102
6.17	Working principle of the complete processing system with the developed additional methods that enhance or maintain high accuracy of the derived body kinematics independently of the sporting venues and the captured motion data.	103
6.18	Sample user interface for man-machine communication to define the elementary a-priori motion knowledge for drift reduction. Simple motion descriptions are specified by the user and then internally translated to the use of a predefined filter value. . . . .	104
7.1	Data plot of the relative position of the lower back computed from of two sample data captures and their respective phase annotations for the beginning of the in-run phase, the take-off and the landing (vertical black lines). . . . .	110
7.2	Screen shots of an animated figure visualization during in-run, flight and initiation of the landing of a ski jump computed from estimated joint positions along the kinematic chains of spine, arms and legs. . . . .	110
7.3	Defined coordinate systems for (a) Cartesian, (b) spherical coordinates and (c) angular representations. Changes in the position of a joint are differently displayed within each coordinate system. The definition for the coordinate systems is corresponding to the sensorimotor reference frames in humans. . .	112
7.4	Sample PD patch to control sound by incoming motion data. . . . .	114
7.5	Raw acceleration data from the ski sensors was used to obtain a first coarse estimate on the start and end timing of the flight phase: noise superimposing the sensor signals during ground contact of the ski clearly separates in-run and landing from the flight phase. . . . .	117
7.6	Characteristics of the different jump phases made it possible to segment the jump into different phases under a fine annotation level. . . . .	117
7.7	Determination of the start and end timing of the stable flight phase using the angular velocities at the z-axis of lF and rF. The selected phases depict the end, respectively the dissolution of the v-angle opening. . . . .	118

7.8	Aligning the segmentation functions $f_{TOI}$ , $f_{TO}$ and $f_{LD}$ of all jumps to a reference peak (red line) showed that the chosen strategies for phase segmentation (maximal peaks) were consistent among athletes and capture sessions. The mean over all curves (black) as well as the minimal peak (green) and maximal peak (blue) curves are shown. All other curves lie in between the extreme curves. 119	119
7.9	Visualization of a feature matrix and a sample feature ski opening (v-angle). Every row contains another motion feature with the temporal evolution sample-wise displayed in the columns. . . . . 123	123
8.1	Schematic overview of the proposed sonification framework consisting of motion capturing procedures, motion data processing procedures and the final auditory display. . . . . 126	126
8.2	Identification rates of the sonification patterns with different dimensionalities over the course of empirical testing. . . . . 127	127
9.1	Flow of a general wearable motion rating and performance assessment system. 132	132
9.2	Visualization of technical motion features (purple) for the assessment of ski jump style. . . . . 133	133
9.3	Illustration of a possible use for the technical motion features (a) $F_{T1}$ , (b) $F_{T2}$ and (c) $F_{T3}$ with the proposed sample implementation in figure skating. . . . . 134	134
9.4	Schematic explanation of the data base preparation step separating the collected data captures into a training and a test data subset for the machine learning steps. Here, an equal split for 2-fold validation purposes is illustrated. The splitting process can be modified to any other desired multi-fold validation. 138	138
9.5	Flow of the evaluation system in ski jumping. Motions can be compared either among different athletes, giving a score and ranking for judging, or within one athlete to monitor different training sessions and the evolution of skills and jumping technology over time. . . . . 142	142
9.6	Correlation between length and flight style in the experimental data collected for this thesis. (a): style points with landing deductions, (b): style points for in-flight deductions only. . . . . 144	144
9.7	Precision and recall values and $F_1$ -measure for the DTW error classification per style criteria. The red line represents the probability border of 50%. . . . . 146	146
9.8	Precision and recall values and $F_1$ -measure for the SVM error classification per style criteria and the probability border of 50% (red line). . . . . 147	147
9.9	Scheme of the k-fold double-nested cross-validation used for error recognition along the different style criteria. . . . . 148	148
9.10	Accuracy measures for the error classification per style criteria using the DTW classifier ((a)-(d)) and the SVM classifier ((e)-(h)) for both $\mathcal{F}_D$ and $\mathcal{F}_C$ . Upper row each: $P$ , $R$ and $F_1$ values, lower row each: $CA$ and $ER$ values. . . . . 150	150

## List of Figures

---

9.11	Sample normalized confusion matrices for the full feature classification with $\mathcal{F}_D$ and DTW classification. From (a)-(d): confusion matrix for an accurate classification with $A1$ , confusion matrix for an average classification with $A2$ , confusion matrix for a poor classification with $L3$ and confusion matrix for $L5$ .	151
9.12	Visualization of the selected features for the reduced feature sets $FSS1$ (green), $FSS2$ (blue) and $FSS3$ (magenta) over all sensor locations and style criteria in absolute occurrence. Left: discrete features $\mathcal{F}_D$ . Right: continuous features $\mathcal{F}_C$ .	153
9.13	$P$ , $R$ and $F_1$ measure for k-fold CV of all sets of feature selections with the DTW classifier averaged over the jump phase for (a) and (b) $\mathcal{F}_D$ and (c) and (d) $\mathcal{F}_C$ .	154
9.14	Confusion matrices for landing error recognition with DTW classification. From (a)-(d): confusion matrices for $L1$ , $L3$ , $L4$ and the combination of $L1$ and $L3$ with $\mathcal{F}_D$ . From (e)-(h): confusion matrices for $L1$ , $L3$ and $L4$ and the combination of $L1$ and $L3$ with $\mathcal{F}_C$ .	155
9.15	Accuracy measures for the LOO error classification per style criteria and the probability border of 50% (red line) using the DTW classifier ((a)-(d)) and the SVM classifier ((e)-(h)) for both $\mathcal{F}_D$ and $\mathcal{F}_C$ . Upper row each: $P$ , $R$ and $F_1$ values, lower row each: $CA$ and $ER$ values.	157
9.16	$CA$ and $ER$ for the LOO error classification per style criteria and CV cycle using the SVM classifier and $\mathcal{F}_D$ .	158
9.17	Accuracy measures for the classification of performance quality determined by overall flight scores using the DTW classifier ((a)-(d)) and the SVM classifier ((e)-(h)) for both $\mathcal{F}_D$ and $\mathcal{F}_C$ . Upper row each: $P$ , $R$ and $F_1$ values, lower row each: $CA$ and $ER$ values.	161
9.18	Confusion matrices for the classification of performance quality determined by overall flight scores with $\mathcal{F}_C$ for M and G jumps with both DTW and SVM classification.	162
9.19	Accuracy metrics for the classification of performance quality determined by flight length with $\mathcal{F}_D$ .	163
9.20	Comparison of the averaged accuracy values for the $\mathcal{F}_D$ and $\mathcal{F}_C$ feature sets with both classifiers. Top row: accuracy metrics for the basic, criteria wise error recognition. Bottom row: accuracy metrics for the overall flight quality assessment.	164
9.21	Sorted distance measures in ascending order with their correlating ground truth point deduction for sample style criteria under $\mathcal{F}_D$ . The black line separates misclassifications and correct error recognitions.	167
9.22	Estimated error values obtained from regression analysis in relation to the awarded ground truth data with $\mathcal{F}_D$ for $A1$ , $A2$ , $L1$ and $L3$ .	169
10.1	Probable sonification scenarios for the support of motor skill and motor performance in sports.	179

10.2 Visual feedback plot providing positional motion information, as for example on the relative end position of the spine during a ski jump. Additional video figure visualization enhances motion understanding. . . . . 181

10.3 Example of a graphical user interface for the provision of directed motion feedback for ski jumping athletes. . . . . 182

10.4 Principal front and back end processes establishing a dialog between athlete and motion style training application. . . . . 183

10.5 Technical implementation of a future online judging system at the ski jump hill. 184

10.6 Illustration of a program interface and its possible functions for judging in ski jumping. . . . . 185

10.7 Illustration of a sample information output given by the judging program interface. . . . . 185

11.1 Recapitulation of the general design of the computer-based motion information system introduced in this thesis with the most important developments for system input and output highlighted in pink. . . . . 188

11.2 Recapitulation of the main innovations presented in this thesis. . . . . 191

11.3 Flowchart of the complete, developed motion information system with processing methods and its final feedback output possibilities. . . . . 193

B.1 Presentation of the real-time sonification system at the 'Ideen Expo' science fair.205

B.2 Screen shot of the homepage developed for the movement sciences group at the Leibniz University Hanover for promotion of auditory feedback system research.206

B.3 Screen shots of the homepage developed for the promotion of my PhD work and the spread of knowledge on motion sensor data processing. . . . . 212







# List of Tables

3.1	Guidelines for the judging of ski jumping style including points deduction rules for errors. The guidelines were translated from an official jump evaluation training sheet for judges from the Japanese Ski Association. . . . .	26
4.1	Comparison of the two main fundamental data sets $\mathcal{D}_S$ and $\mathcal{D}_R$ that determined their subsequent use in the computational methods of this thesis. . . . .	49
5.1	Number of process model state values $x$ and observation measurement values $z$ used by the chosen Kalman filter. . . . .	67
5.2	Overview of the implemented orientation estimation methods including the abbreviations used in the following investigations as well as references to the works describing their original concept design. . . . .	69
6.1	Mean error values of $CF1$ , $CF2$ and $KF$ for the orientation estimates of all sensor placements with filter values adapted to specific drift prevalent in every sensor placement and motion type. . . . .	81
6.2	Rounded mean maximal angular velocities ( $AV$ ) along $x,y$ and $z$ in dps at the pelvis and at an extremity $E$ (right shank or arm) with kicking, jumping and right-handed throwing and their resulting classification to a speed label. . . . .	93
6.3	$E_{RMS}$ error values over all orientation estimates for $GI$ under the presented rate bias values and the relative change values $RC$ to the uncompensated $GI$ estimates. . . . .	95
6.4	Absolute maximal variances in the heading angle $\psi$ occurring over the complete data set $\mathcal{D}_R$ . After compensation, the absolute maximal heading deviations $\psi_C$ were significantly reduced. Both heading angles are depicted in radians. . . . .	102
7.1	Description of the MIDI sound mappings chosen for experimental investigations on the effect of auditory feedback for motor learning in rehabilitation. . . . .	115
7.2	Description of the discrete (descriptive statistics) features $\mathcal{F}_D$ with their feature ID for all sensor axes. . . . .	121
7.3	Description of the continuous (time-series) features $\mathcal{F}_C$ with their feature ID for all sensor axes. . . . .	122
7.4	Description of the simple kinesiology-induced features $\mathcal{F}_K$ with their feature ID and the represented style error. . . . .	124
9.1	Overlook on all feature sets and feature selection strategies ordered by their occurrence in this thesis. . . . .	143
9.2	$P$ , $R$ and $F_1$ measures for classification of performance quality labeled under full flight scores with P, M, G and P and G only. . . . .	160

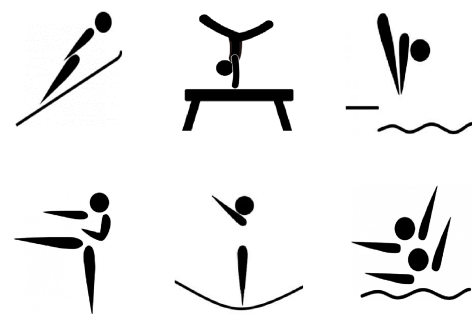
## List of Tables

---

9.3	<i>CA</i> values of the error recognition averaged over all error categories under the eight <i>CV</i> cycles. <i>ER</i> values can be determined as the difference between <i>CA</i> and 1.0. . . . .	164
B.1	Summary of all lectures and talks given during the PhD. . . . .	207

# What is Inertial Sensor Based Motion Information?

## Part I





# 1 Introduction

Improvement of the own performance and possibilities is an important motivation for most sportsmen and can also be economically important to professional athletes. Consequently, much effort is made to create an ideal training environment. One important component of motor performance optimization is the process of learning how to execute a motor task in the best and most efficient way, referred to as motor learning and motor skill acquisition. Especially for complicated motor tasks, motor learning is a very essential neural process for the acquisition of correct and flawless motor skills. Practicing sport motions under the newest findings and principles of motor training is one part of this learning process, as is the use of hard- and software for motion analysis. By combining both aspects to one training structure in a meaningful way, one can expect to achieve a more ubiquitous and professional training environment in future. Especially biological processes like the preparation, anticipation, and guidance of movement could get considerably enhanced by a suitable provision of relevant motion information. The development of augmented motion feedback systems that detect and deliver such information is therefore gaining more and more interest among both movement scientists and sport engineers. Numeric motion information obtained from motion measurement and analysis systems could however not only be utilized by the performer (respectively athlete) itself, but also by any other person actively or passively involved in a motion performance: here, the principal purpose would be to enhance the general understanding of a respective motion performance. Application examples are coaching, judging, sport broadcasting and spectator involvement. The demand for comprehensive technology that provides motion performance information under various level of detail can consequently be expected to increase within the next decade.

The implementation of such motion information system is linked to various research problems, ranging from technological aspects of data acquisition to psychological and biological aspects of information reception and perception. In this thesis, I approach the topic from the technical side. The focus is set on the development of original processing and computation strategies for numeric motion data obtained from wearable motion sensing systems. By investigating probable applications for real-world sport performances under different kind of motion information, the following questions shall be answered: how can one employ the most recent sensor technology for sensing a sports performance? How can one transform captured motion data into more meaningful numerical representations? How can one retrieve and identify relevant information from these data representations that could not be discovered otherwise? And how can such information be displayed?

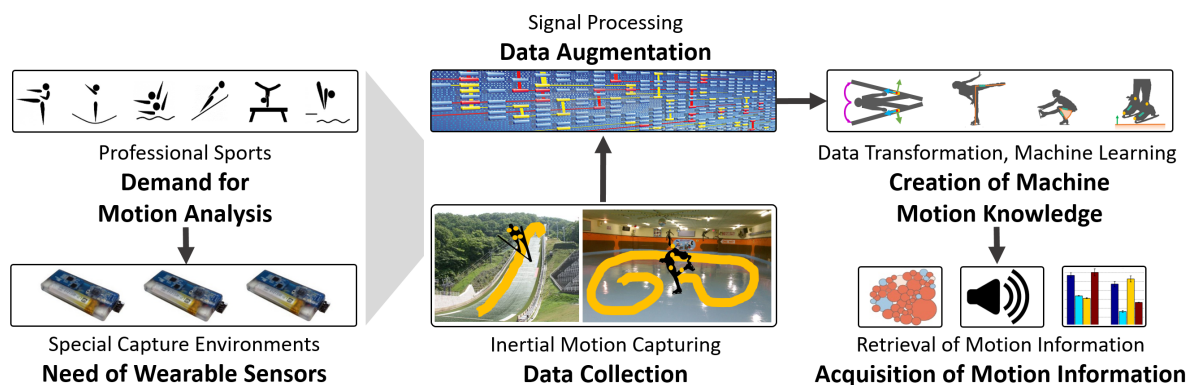


Figure 1.1: General design of the computer-based motion information system developed in this thesis. The structure builds a framework for the evolution of the whole thesis.

Under the aspect of sport informatics, the resulting motion information system shall also be denominated as computer-assisted training (CAT) tool. This term comprises the use of various hardware and software solutions for the retrieval of knowledge on motion performances and its provision to various recipients of differing interests. Universally designed, a general CAT system (Figure 1.1) should then for example provide information about motion technique, errors during motion performance and suggestions for improvements to athletes, coaches, judges, officials or spectators.

### The Rise of Mobile Motion Capture Systems

Electronic devices as video cameras and computers are common standard technologies in modern computer-assisted training, but can generally either not provide immediate motion information or numerical (and hence comparable) data. Positions can be acquired very accurately and immediately by an optical motion capture system. However, optical motion capturing cannot be applied to all kinds of sport motions. Especially movements that require daylight conditions like outdoor sports or sports that have a large motion volume can hardly be captured with an optical motion capture system. Then, it is feasible to find a different and more suitable type of motion sensing device.

In recent years, much emphasis was put on the development and use of devices that capture and transfer human motion data in an easier and more direct way. Some popular examples of such kind of motion capture device are depth-cameras, 3-D cameras and wearable devices. For this thesis, wearable sensors were chosen: with the progress of sensor technology, respective sensor units became smaller, lighter and more accurate, hence augmenting their usability for recreation and sports. In concrete, I employed multidimensional *inertial measurement units* (IMUs) in all subsequent fundamental data acquisition tasks. These devices consist of accelerometers, gyroscopes and magnetometers. This means that they yield measurement

---

data of gravity and acceleration, the earth magnetic field and angular velocities, but do not contain or represent global or local translation and position data. Therefore, their data output is sparse, abstract and less intuitive than the data output of other measurement devices. For example, they do not directly provide motion information necessary for conventional motion analysis: it is not possible to track the athlete or to directly determine motion properties such as the position of body parts from the inertial sensor data. Here, sophisticated data processing techniques are required to compute and determine meaningful motion features that can then provide athletes and coaches with valuable information on the performed motion.

In the same way as sensor hardware technology improved and mobile measurement devices became common, the demand for new methods to process and make sense of the incurring data rose, as well. Several different methods for the derivation of meaningful kinematic motion data have been developed in the last two decades. Nevertheless, none of them led to a standardized procedure so far, leaving the use and implementation of processing methods to the user. Generally, sensors can be applied well to systems with medical and rehabilitation purposes as for example gait analysis. However, those standard processing methods developed for static situations or slow-motion measurements might be less suited for use in sports where high-speed motions with large accelerations, angular velocities and high-impact phases occur. A similar concern holds for commercial inertial capture systems, which offer good accuracy, but are often restricted to their internal implemented methods that have been developed under general assumptions. It is therefore first necessary to investigate and establish accurate methods for data processing that are reasonable to use with high-dynamic sports motions. Ideally, those methods are not only accurate, but also simple to use for any system user to ensure a high level of usability of the future processing system.

After the establishment of reliable and accurate processing methods, the next question is how to transform the obtained complex kinematic information into a suitable description of the performed motion. Only then, the provision of a meaningful and (most importantly) intuitive, understandable motion information can be ensured. Humans acquired the skill to perceive, understand and evaluate sensory information on motor processes during years of practice and experience. Similar to the complex biological processes of the human brain, it is in many application scenarios reasonable to utilize machine learning algorithms. Computer science developed various strategies to build artificial neural networks that resemble the human brain. However, research generally focuses on different aspects of the human brain, such as language processing or image processing. The simulation of biological motor perception and understanding is a unique and new research problem that is – thanks to the availability of cheap and ubiquitous mobile motion capture systems – likely to become a matter of growing interest within the next years.



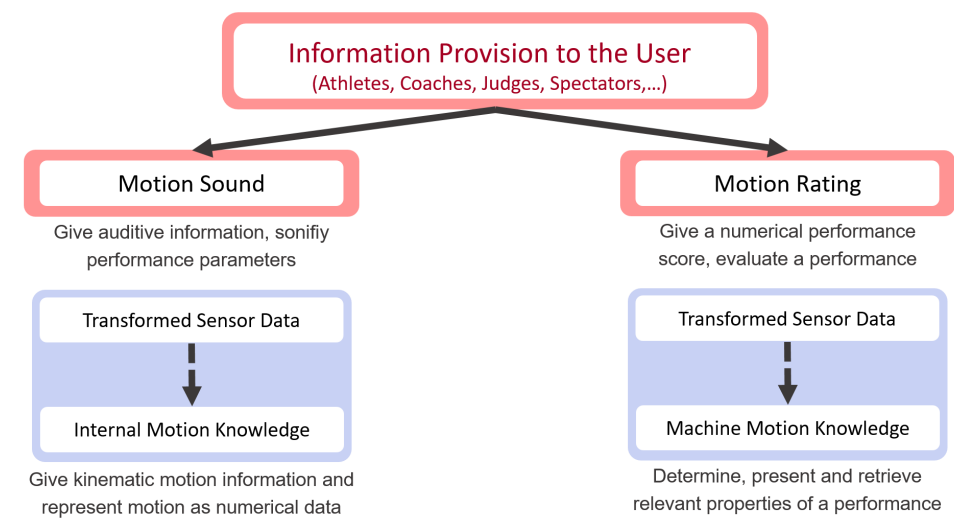


Figure 1.2: Motion information types selected as sample applications for this thesis and their interrelation to signal processing and machine learning methods.

### Computer-Assisted Training and Motion Information Systems

Two concrete sample applications for motion information systems are given in this thesis. They address different information recipients, and herewith illustrate the fundamental diverse applicability of computer algorithms for CAT systems. One type is auditory feedback information for athletes, providing either concrete or abstract auditive motion hints during movement execution. The other one is style and motion error information, providing point scores and support for judges in subjective judged-sports as well as performance quality information for athletes or coaches (Figure 1.2).

The first application illustrates a particular method of auditory information display referred to as movement sonification. Sonification expands movement acoustics to silent phases of actions which are usually not evoking sounds (e.g. actions or gestures of the limbs). It furthermore offers a wide variety of technical implementations. In general, sonification strategies depend on the underlying input motion data, the sonification purpose and the intended sound mapping. Using MIDI or combinations of oscillating sine waves, sound can be created and easily influenced with a computer program in real-time. The main question that has to be answered here is how auditory feedback should be designed to convey motion information with largest possible effect on the motor learning task. When set into meaningful correlation to motion action events, a movement sonification can then be employed as source of motion feedback information.

With the second sample application, I demonstrate the possibilities of automatic performance quality assessment on the base of a motion's common style and error conventions. By introducing a system for the measurement and automatic rating of performance quality, I

---

particularly address once certain negative aspect of sports: manipulation of competition results by fraud and unfair means. Coinciding with the commercialization of sports and the rising pressure of achievement on every individual athlete, manipulation is one of the main issues in competitive sports. In pure result-oriented sports such as track and field, swimming or cycling, the outcome of a competition can be measured objectively: the person who arrives first, throws or jumps furthest is the winner. Judges are only necessary to survey the compliance with common competition rules like for example keeping one's own designated track or starting from the official starting point. Similar conditions hold for goal-oriented sports such as soccer, handball or basketball, where the team with the higher point score wins. Here, judges (respectively referees) supervise the compliance with rules and are eligible to fine unfair behavior like fouls. The results in many individual sports, however, cannot just be put into scales and measures: their outcome is determined by several factors and elements that need to be rated in a qualitative way. Those ratings are based on the subjective perception and evaluation of referees or judges, and despite judges being trained for it, evaluations can be biased and influence the final outcome of a competition (both willingly or unwillingly). Assuring an adequate level of objectivity is therefore a major concern for most modern judged-sports like gymnastics, figure ice skating and snowboarding. This led to changes in the competition and grading rules (e.g. in figure skating), as well as to the introduction of additional, more objective measures (e.g. the time of flight in trampolining). However, for many affected sports, objectivity cannot be ensured completely, so that distrust is still remaining. The idea was therefore to develop new evaluation measures that are immediately related to the performed motion using current wireless motion sensor technologies. With this additional performance assessment, it is then moreover possible to provide augmented motion information for training of fundamental motor patterns and motion style.

As for the two presented sample applications, various different reasons exist that justify the introduction of computer-assisted training technologies in sports. Examples are personal performance improvement, performance surveillance, support to coaches and judges or additional information for spectators. The resulting system output data used to convey the desired motion information are as diverse as the intended application. Moreover, the necessary computation methodologies and algorithms that need be applied to obtain the specific information differs as well. Whereas for some applications, sufficient information can for instance be retrieved from the transformed numeric motion data gained in signal processing methods, it is necessary to additionally apply machine learning methods to the transformed data for other applications. However, the fundamental stages and principles for the provision of such augmented feedback systems are always similar and comply with the basic questions that led to the development of CAT systems in this thesis. In concrete, they comprise the following aspects: creation and collection of numeric data that can be processed by the computer respectively (mobile) training device, augmentation of the acquired numeric data into meaningful motion information, sense-making (or transformation) of the augmented data so that intelligent machine knowledge or data representations can be created, and retrieval of motion information by utilizing some sort of motion knowledge

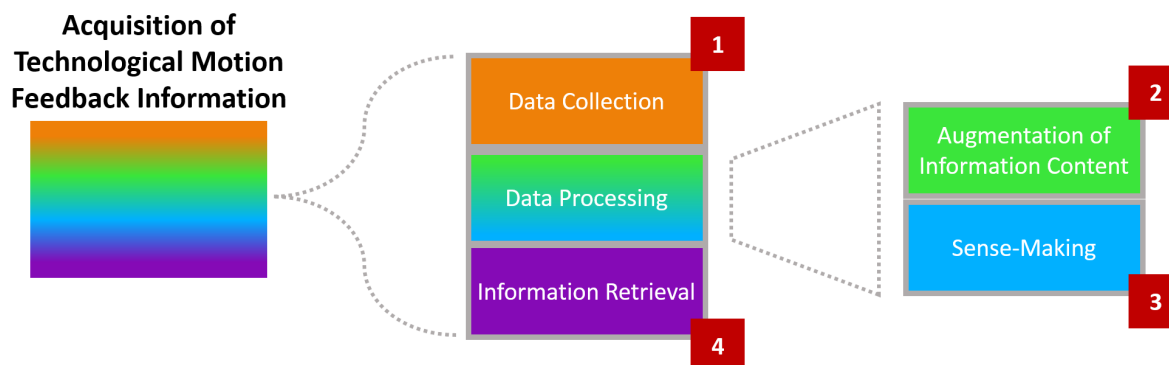


Figure 1.3: Four main internal processing stages ((1) – (4), red) have to be passed through before motion information can be obtained from wearable motion sensors.

to provide the desired motion information (Figure 1.3). All of those stages are discussed in detail in the course of this thesis. For the concrete two sample applications, especially the third and fourth step vary (Figure 1.2). For the provision of auditory feedback, the augmented motion data is transformed into acoustic sound representations. They are then displayed and can be directly retrieved by the recipient using internal biological motion knowledge. For the rating of motion, it is first necessary to train a powerful machine motion knowledge from the augmented motion data that is then used to retrieve relevant information displayed or presented to the user as external information.

Every step in the development of the presented CAT system is supported by a concrete set of inertial motion capture data takes – either by simulation motion data from a laboratory setting or by sport motions executed in their real environments. Concrete application samples for movement sonification are given in the context of rehabilitation and motor relearning. Furthermore, possibilities for sonification and auditory display in sports are discussed. Methods for style assessment were designed in such a way that they could be used in various subjective sports. Of particularly interest here were sports for which inertial sensors currently are the only way to discover new and relevant motion information. Those could be sports that are either multi-directional (so that two-dimensional analysis does not suffice), or that have a very wide motion range and are executed under difficult capture environments (so that the technical specifications of conventional motion capture systems cannot be used). Therefore, the use of inertial sensors might support advanced judging as well as further performance improvements, as for example in diving, snowboarding or ice skating. The fundamental and important computations in this thesis were based on a sample set of ski jumping data. Ski jumping is a judged-sport, despite its clear focus on length as main indicator of performance quality. It is furthermore a technically demanding and complex sport which requires very fine motor skills to adapt to even the smallest changes in aerial conditions during flight. Erroneous motion execution and use of aerodynamic forces immediately influence the performance and can furthermore increase the risk of fall and injury. Despite the complex motor

task, motion analysis is currently largely depending on visual feedback, with the quality of the general training and competitive structures bound to economical and logistical constraints. In junior and intermediate level ski jumping it is for example common that many jumps are executed within a very short span of time. Responsible coaches often observe jumps from one perspective only (generally the coaches' stand), while the assessment of every single jump performance has to be instantaneous. Similar constraints hold for the formation of a final score ranking in competitions. Ski jumping is subject to style points awarded by five judges that indicate performance quality additionally to the jump length. This style assessment has to be immediate: since the overall impression of a flight depends on several local parameters such as the flight curve and the distance to the slope, it is necessary to observe a jump within its natural environment on the ski jump hill for performance evaluation. Supporting video data cannot display all necessary environmental information. Therefore, a mobile CAT platform for performance assessment and judging can be a very valuable tool in future, which might not only improve measurability in grading but also enhance the general fundamental training environment.

## 1.1 Thesis Structure

The thesis consists of four main parts separated into multiple coherent chapters, whereas Part II and Part III constitute the two main parts. They describe the innovative and original work of this thesis and roughly follow the general application design given in Figure 1.1.

The first part of this thesis (Part I) is designed to illustrate and give elementary background knowledge necessary to understand the idea and concepts presented within this thesis:

- The current Chapter 1 gives an introduction on the fundamental topic as well as on the structure and main innovations of this thesis.
- Chapter 2 discusses the general scientific concept of motion feedback as form of motion information under a sport scientific approach and shows the differences to a motion information concept generated under a computer scientific perspective. It is explained what kind of feedback types are commonly used in sports training, and how they refer to motor learning. Furthermore, connections to the intended sample applications are drawn and the respective motion information types set into context to motor learning.
- Chapter 3 provides background information that is necessary for the understanding and lecture of this thesis. The sport of ski jumping, which was used for the main experiments, is explained in detail, including background information on the general properties of ski jumping within the family of Olympic winter sports, technical motion specifications as well as the grading and scoring guidelines. The chapter furthermore gives a general introduction into the mathematical concepts of orientation representations that underlie the main processing of the raw inertial sensor data. Lastly, I show

## Chapter 1. Introduction

---

how important works from proximate research fields (sport science, computer science and engineering) influenced this thesis and how they are related to the present work.

The first main part of this thesis (Part II) is dedicated to provide a detailed description of the process of collecting numeric motion data and its subsequent enhancement. In particular, common **signal processing methods** for inertial sensor data are introduced, discussed and set into context to the use within motion capturing of sports. Influences on the data accuracy are presented and strategies proposed that counterbalance those influences and improve the quality of the final processed data outcome. For this, innovative methods to handle possible sources of error are proposed.

- In Chapter 4, a short summary on the existing motion capture technologies is given. Furthermore, the principle of inertial sensors is illustrated. The specifications of the sensors used for the acquisition of motion data in this thesis are listed, and relations to current sensor technologies as well as problems in data processing shown. Furthermore, this chapter illustrates all performed data acquisition sessions and the resulting data bases which served as main experimental data sets for the following investigations.
- Chapter 5 then describes how the inertial capture data can be augmented so that meaningful kinematic motion data is obtained. Current orientation estimation filter methods that are widely used within many different applications are introduced. Besides, further essential data processing methods such as the estimation of initial posture and joint positions are discussed.
- Implementations of the previous processing methods are analyzed and verified in Chapter 6. Accuracies as well as influences on the data accuracy are presented. Furthermore, methodologies that can compensate those influences and eventual errors in an automatic way are developed and included in the proposed processing framework to increase accuracy and usability of the methods within motion analysis and training systems.

Whereas Chapter 5 is primarily recapitulating important technologies from literature and utilizes them as the base for the motion information system development, the results in Chapter 6 are unique and constitute an innovative output of this work. They also led to two journal publications written as lead and main author.

The second main part of this thesis (Part III) is designated to demonstrate how the data can be transformed for the provision of motion information. Important research problems that have to be solved for this task are how the derived kinematic motion data can be decomposed into meaningful information and how this transformation process can be orchestrated to conform with different levels of information content and performance and competition rules. To create artificial motion knowledge, furthermore **machine learning methods** are introduced and applied.

- In Chapter 7, I present strategies to make sense of the previously derived body kinematics and discuss three different possibilities for the transformation of the processed sensor data into motion descriptors. First, I show how body kinematics can be visualized. Second, I explain features that display motion information by sound for movement sonification. Third, I discuss the formation of motion features for use in subsequent machine learning methods. In this context, I present an algorithm to segment ski jumps into their main motion phases and extract different kind of motion features (discrete signal based, body-model based and expert-knowledge based) on the time segmented data.
- Chapter 8 then demonstrates the concept of movement sonification for rehabilitation. I illustrate how auditive motion hints can be given during performance from the previously build auditory features and discuss the efficiency of selected features for motor learning.
- Lastly, Chapter 9 demonstrates how machine learning can be used to provide motion information for style and error assessment. First, a unique concept of motion features is developed that confirms with the technical and aesthetic aspects of a motion. Next, fundamental technologies necessary for the retrieval of useful motion information from the transformed and sense-made motion information are introduced. Lastly, these are utilized to evaluate the quality of the ski jumping field data under multiple classification and style rating aspects.

Most of the methods presented in the third part have been developed exclusively for this thesis and the problem of style and performance assessment. Furthermore, it is not known that a similar work has ever been made public anywhere else before. I am therefore convinced that the presented approach to the topic of augmented motion information offers a unique composition of mathematical, algorithmic and procedural sub-parts that cannot be found anywhere else so far. The contents of this part were summarized in a journal paper as lead author as well as at three international conferences. Results of experimental studies using the movement sonification system were furthermore conducted and published by the member of the motor learning group at the Institute of Sport Science, Hanover University.

Part IV finally illustrates the chosen sample information types with a description of possible application scenarios in Chapter 10. Results have been submitted for publication at a conference and will be submitted to another journal paper as lead author soon. With the last Chapter 11, Part IV then finally completes the thesis with a summary and conclusion and an outlook on future work.

### 1.1.1 Appeal Points and Innovations

With the presented methods and technologies for data processing, this work is intended to serve as handbook containing basic, elementary information as well as guidelines for the creation of computer-based motion information systems in the sports environment. Contributing to unique ways of motion analysis by the acquisition and processing of wearable motion information, I hope this thesis to lead the way towards new applications that support training, performance improvement and talent recruiting in the future. The problem that arises in this thesis is very interdisciplinary and multi-layered. It relates to the field of engineering (sensor technology), mathematics (data processing, attitude representation and algorithm development), computer science (programming, human-computer interaction: application design and information visualization), sport sciences (principles of biomechanics and motor learning) and psychology (information visualization). Therefore, it is also a very unique research topic that is not known to have been addressed in a similar way before.

The first innovation of this thesis I want to emphasize is the development of a full-body motion capture system for ski jumping. Inertial ski jump data is a very rare numeric motion information, which has not been acquired more than three to four times before. Because I chose ski jumping as sport for my main experiments, I have collected body information from a large number of jumps that was sufficient to display all relevant parameters of a flight with the presented and developed processing methods. In fact, I believe to have built the most extensive data base of inertial ski jump data that is existing so far.

Knowing the orientation and position of body segments and joints is essential for a meaningful and detailed analysis of human motion. A big part of this work has therefore been dedicated to the acquisition of correct inertial sensor data and its processing into accurate attitude and relative position of body segments. The main methods for data processing have already been introduced several years ago and are actively used in various applications. Unique for this work is that in dependence with the characteristics of the performed motion, it is possible to choose between three different orientation estimation methods for the computation of body kinematics that can then give more detailed motion information and create higher motion information content for the end-user – athletes and coaches here. Moreover, I evaluated the accuracy of main orientation estimators with several experimental data sets. These contain data from four field experiments at ski jumping venues and data from several smaller on-campus experiments in combination with optical motion capture cameras serving as ground truth data. Based on those accuracies, I identified several data specialties that influence the accuracy of the processed data and examined methods to deal with those variations. This led to the development of two additional error compensation strategies - an intelligent drift reduction strategy and an automatic magnetic bias compensation to reduce the influence of varying magnetic field in sport venues. They contribute to the enhancement of data accuracy and reliability without additional expert input given by the user and hence considerable increase usability of future motion analysis system.

Based on the results of the proposed intelligent drift compensation, every underlying filter method might be universally applicable for any type of motion data in the future without the need to change the fundamental system settings: dependent on the characteristics of a motion, like the amount of maximal angular velocities or the number of motion dimensions, fundamental system parameters can now be chosen automatically to ensure a high accuracy of the estimated body kinematics irrespective of the motion pattern. The required information on those motion characteristics can be estimated by any future user without the need of technical background knowledge, which is an important step to enhance the usability of a future application system. Including the proposed magnetic bias compensation in the system, it furthermore becomes possible to use the sensors under any kind of magnetic field condition. In other words, the system can be yield stable and reliable estimates from data acquired at any type of sporting venue without additional complicated and time-consuming magnetic calibration measurements.

In the second part of this work, I explain how to make sense of the numeric motion data. As a first example, I introduce the concept of movement sonification, and illustrate a design made for support in motor learning and motor skill acquisition. Second, I demonstrate the application of machine learning methods for motion information retrieval and in particular motion information systems. Some problems that are currently discussed in research, personal and even public life inspired the design and development of the sample application of motion evaluation. Since all sources of inspiration are a unique and innovative application, no existing technologies could be used as references and the framework has been developed independently without any further supporting system design input. Several approaches for activity recognition from wearable sensor data have been discussed in literature, but they are mainly restricted on every day activities. Furthermore, they usually do not contain information on the quality of an action, or alternatively do not evaluate the motion from an overall, full-body kinematic perspective. The idea of rating a motion performance therefore seems to be a new unique approach to the problem of machine learning in motion activity. I believe that the innovative character of the machine learning pipeline for motion evaluation is so fundamental that its further development can and will be of great interest for many years to come in machine learning and sport engineering fields.

To summarize, the following innovations were made with the progress of this thesis (Figure 1.4<sup>1</sup>):

- Full-body motion capturing of ski jumping motions and determination of the relevant body kinematics
  - Collection of the currently most extensive inertial ski jump data base worldwide
- Development of methods to enhance the usability of body kinematic estimators for the

---

<sup>1</sup>Image courtesy movement sonification: movement sciences group, Leibniz University Hanover  
Image courtesy judging image: <http://www.langsleysports.com/>



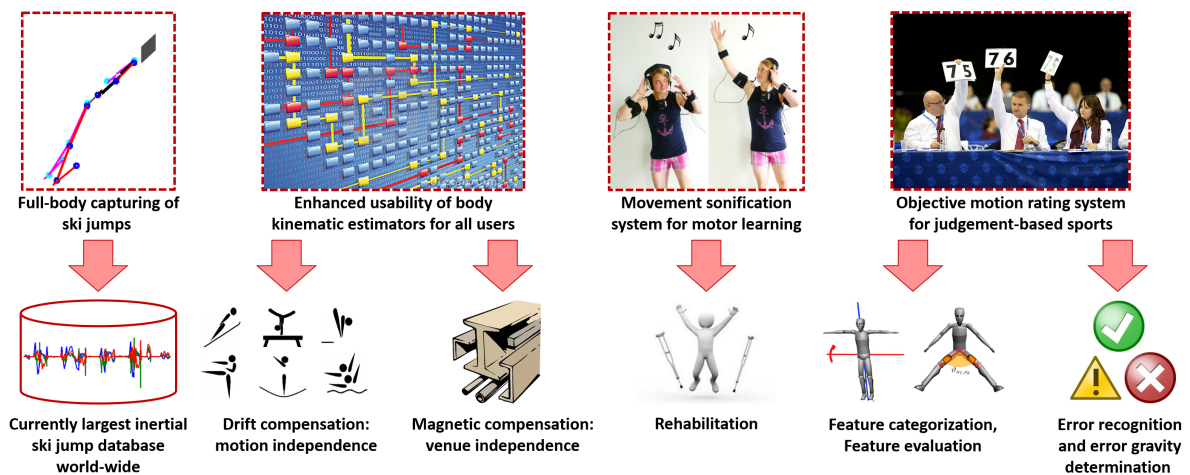


Figure 1.4: Overview of the main innovations presented in this thesis. The combination of methods from computer science and sport science is unique and has not been found to be presented in a similar form anywhere else.

diverse group of future system users

- Intelligent drift compensation using elementary a-priori motion annotations for flexible use of orientation estimation filter with sport motions
- Magnetic compensation step for determination of body kinematics from data captured at variate sporting venues
- Development and testing of a real-time movement sonification system for motor learning in rehabilitation
- Development of the system environment and methods for a kinematic data based motion rating system in subjective judging-based sports
  - Introduction of a motion feature categorization for full-body motion rating scenarios
  - Testing of feature representations for motion rating scenario by feature selection strategies
  - Implementation of algorithms for error recognition and error assessment: activity recognition in real sport motions with error gravity determination

More detailed information on the background of all concepts, as well as the related works that had an impact on the system development and that emphasize the uniqueness of the presented work, is given in Section 3.3.

## 2

# Fundamental Definitions and Terminology

Any meaningful motion analysis relies on the availability of relevant motion information. The general definition of such motion information however varies with the scientific point of view: in sport sciences, the provision of motion information is part of the problem of movement sciences and primarily supports motor learning and skill acquisition of an athlete. Research in sport informatics on the other hand addresses motion information under a more technically-focused intention that alters the fundamental sport scientific definition. As a result, the information content also varies in dependence on the analysis purpose and the target information recipient. In this chapter, basic terms are therefore explained from both the perspective of sport and computer science. Furthermore, a concrete definition is given for the implementation of all subsequent technologies and algorithms.

## 2.1 Motion Information from the Perspective of Sport Science

Sport sciences commonly refer to motion information as motion feedback. Generally speaking, this is defined as any kind of sensory information given to an athlete before, during or after performance with the goal of performance improvement. Motion feedback is perceived by the human sense organs and then derived from the descending motor command in internal efferent neural processes to master and adapt sensorimotor transformations. As a result of practice or novel experience, neural adaptation occurs that is finally retained over a longer period of time. Such neural adaptation usually comprises all types of change in motor behavior – meaning it involves not only the learning of new movement patterns, but also the improvement of smoothness and accuracy in existing movement patterns – and is referred to as **motor learning**.

One of the main research questions in motor learning is how and by which neural processes changes in motor behavior are evoked, and how they are related to the knowledge obtained from the various existing feedback parameters. From the middle of the last century, research has been subject to constant additions and changes caused by new insights won over the progress of time. To date, most studies that explore the mechanisms of motion feedback consider motor learning from a cognitive psychological approach. This means that the human brain is compared with a computer of limited capacities for the processing of information [SW76]. Associating biological and neural processes as closed control loops [Wie49], motor learning is then understood as a cause of internal error recognition (Figure 2.1 [Sch75])

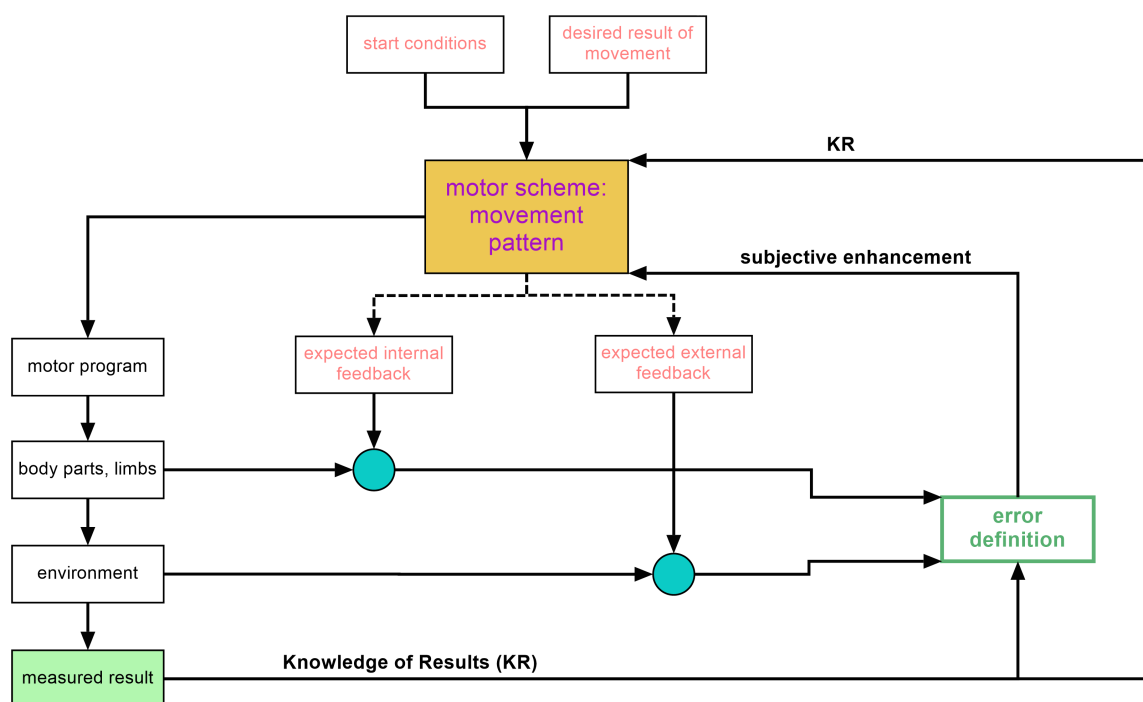


Figure 2.1: Closed-loop model of motor learning processes developed by Schmidt in 1975.

triggered by two different types of feedback parameters – intrinsic and extrinsic ones.

### 2.1.1 Motion Feedback Parameters

Intrinsic feedback is given by internal sensorimotor feedback sources like vision, proprioception and audition. It is kinaesthetic, meaning that it is received simultaneously with the execution of a movement, and always present during motor learning. Extrinsic feedback is augmented information that can only be provided by an external source. Probable sources vary within the scope of a motor task and a certain training environment. In everyday settings, the most common sources are oral recommendations and instructions by coaches. However, they can also be visual target-related (as for example when scoring or not scoring points after a basketball throw) or supplied by any kind of electronic device respectively display. With the goal of developing new machine-generated sources of motion information, I focused on applications for the provision of extrinsic motion feedback in this work. Therefore, the term motion feedback shall refer to extrinsic feedback in the following if not explicitly indicated as intrinsic feedback.

Feedback relates the learner's individual performance to either a desired performance, or to an instruction that emphasizes and reminds of certain aspects of the movement or induces a certain focus [SW08]. Such information can generally be assigned to one of the two categories

## 2.1. Motion Information from the Perspective of Sport Science

---

*knowledge of performance* (KP) and *knowledge of results* (KR).

The information that is provided by **KP** is closely related to the proprioception of a movement and motion process. It indicates the quality or pattern of a performer's movement and also includes kinematic information such as displacement, velocity or joint motion which can generally not be perceived by intrinsic feedback. KP is often employed by coaches or rehabilitation practitioners [MA07, WH79].

The information that is provided by **KR** is related to the result of a performance and indicates the success of a performer's actions with regard to an environmental goal. It can be redundant with intrinsic feedback in real-world scenarios, but also exceed the information that is received by internal processes. Visual target information for example is clearly result-related and can be perceived intrinsically (one can see the immediate result of its own throw by hitting or missing the target instead of one's own execution of motion). However, other forms of feedback can be either related to the course of a motion execution, the result of a motion or both (e.g. too high, too fast) and not be perceived intrinsically. Especially KR is considered to be a critical variable in the acquisition of motor skill [SSW84]. Its quality is dependent on several variables that significantly influence the speed and process of motor learning.

### 2.1.2 Motion Feedback Variables

Motor learning is assumed to occur in multiple stages that depend on the current skill level of a performer. With every stage, the activity and success of the learner varies. In the same way, instructions given to a learner should differ along all of the stages. General properties of a good feedback that are valid for all stages are: a timely manner of feedback provision (brief period between performance and feedback), accuracy of the information, an appropriate level of detail correlating to the individual skills of the recipient (meaning the learner's stage) and an appropriate amount of information.

Four principal variables have been identified which are known to influence the process of motor learning. They contribute largely to the success of motor training and should also be kept in mind for the implementation of any future mobile information system:

**Information type:** Motion information conveyed by a feedback strategy can either relate the execution of a motion to a target value (e.g. too high, too fast) or describe the current-state of the motion execution (e.g. 40cm, 20seconds).

**Information content:** Feedback can be negative and positive (e.g. 'wrong' and 'correct') and general and specific (e.g. 'too fast' or 'too high' in contrast with '10% too fast' or '5cm too high').

**Distribution and frequency:** Over a certain bandwidth, feedback can be continuous, intermittent, faded or controlled (e.g. after every performance, in blocks after a certain

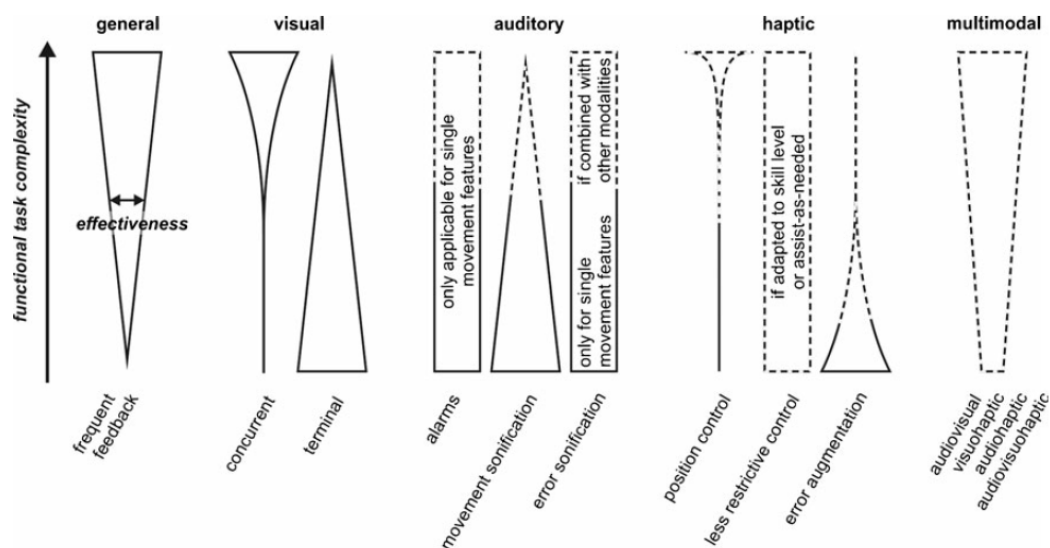


Figure 2.2: Confirmed (solid) and hypothesized (dashed) effectiveness of a feedback strategy for the enhancement of motor learning in dependence on functional task complexity after Sigrist.

number of performances or on request of the learner).

**Timing:** The placement and timing of feedback can be varied with respect to the main motion execution (e.g. before, during or after a performance).

Several aspects influence the acquisition of motor skill like the variation of practice conditions and practice stimuli or motion feedback. Amongst all of them, feedback is considered as the most prominent and influential one. With conventional and simple consumer electronics still being the main source of extrinsic feedback, the development of innovative augmented feedback systems therefore appears very promising for the future.

### 2.1.3 Augmented Motion Feedback

During the last century, augmented motion feedback was based on external motion information given by a human expert that eventually got enhanced by visual feedback from video displays. Over the last decade, additional strategies such as auditory, haptic, or multimodal augmented feedback display were gradually introduced. Technical advances made it possible to also investigate complex, realistic motor tasks with those training devices. However to date, the most effective way of augmented feedback provision is still discussed controversially among sport scientists. The potential and the limitations of concurrent unimodal and multimodal feedback strategies for motor learning has been summarized in a review by Sigrist [SRRW12]. This review can be seen as a guideline for the development of augmented

## 2.2. Motion Information from the Perspective of Computer Science

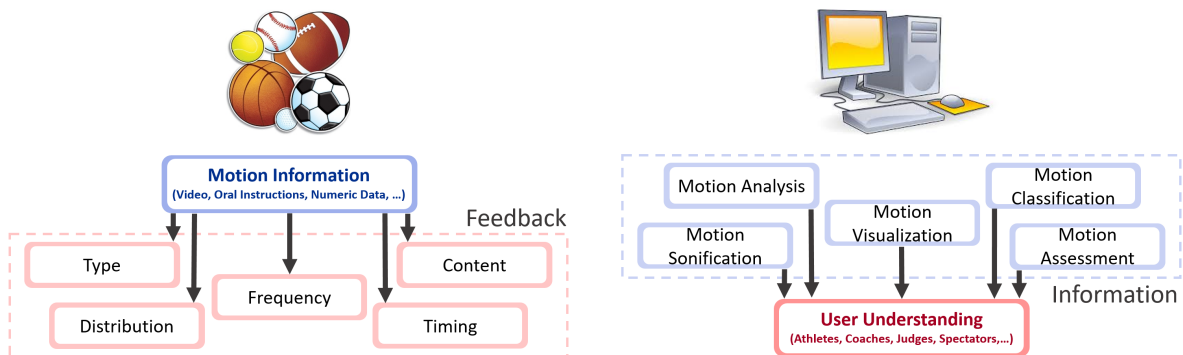


Figure 2.3: Differences in the definition of motion information respectively feedback from a sport scientific (left) and computer scientific (right) perspective.

feedback systems for the enhancement of motor learning. In particular Sigrist's definition of the relation between motor task complexity and applied feedback modality (Figure 2.2) is important information for the development of real feedback applications.

## 2.2 Motion Information from the Perspective of Computer Science

For the following work, motion information should be defined from a more technical perspective as any kind of method or action by which knowledge on the performance of an athlete is provided to a user with the goal of performance analysis. Here, the main difference to the previous definition of motion feedback is the modification of the problem's target information recipients: a possible user can either be the performer (respectively athlete) itself, or any other person involved in a motion performance like coaches, judges, officials and even spectators. This modified definition tremendously enlarges the group of possible CAT system users as well as the number of possible application scenarios. For this reason, it also correlates more closely to the general idea of human-computer systems: instead of focusing on the different parameters and variables for optimization of the feedback provision process, strategies for the enhancement and enrichment of human motor tasks are put into focus. This means that the main interest is now set on the end users and the possibilities that could be achieved with the provision of motion information (Figure 2.3). As under the sport scientific approach, the intention of a motion information system can of course still be the acquisition and improvement of motor skill then. However, intentions could additionally involve support in performance surveillance, improvement of general competition conditions or even entertainment.

Video and photographic data are currently the most common electronic source of motion information. With the evolution of time, the wide range of probable applications and informa-

## **Chapter 2. Fundamental Definitions and Terminology**

---

tion systems is however likely to attract new technologies and devices that can be employed for the acquisition of motion knowledge. Here, it is especially important to develop CAT systems that comply to the most recent knowledge on motor learning processes: although motor learning is investigated since decades, its underlying neural processes are still not decoded and understood completely. Once considering the constant change in research, possibilities for training and competition are then numerous and only bound by the state-of art in motion sensing technologies. Consequently, I believe that a successful combination of both research perspectives will notably accelerate and improve learning processes in humans of various art and kind that are not only related to sport performances or recreation.

## **3 Thesis Fundamentals and Related Works**

The development of CAT systems is a multidisciplinary and multi-layered problem that requires knowledge of different fields and studies – sports science, computer science, engineering and mathematics. Specific terms and backgrounds that cannot be expected to be known to all readers shall therefore be explained in this chapter.

For the development of a motion style assessment system, ski jumping has been chosen as main sports. Although ski jumping is one of the most popular Olympic winter sports, it is a relatively rare sport from a global perspective. It is mostly enjoyed by winter sport affine nations like Austria, Germany, Switzerland, Finland, Norway, Slovenia and Japan, and actively practiced by even a smaller group of athletes and sportsmen. If never having seen a ski jumping hill and a training or competition ski jump, it can be difficult to understand the sport's concept, as well as to assess the training and coaching circumstances that impose the use of further data insight and training machinery. Basic information on ski jumping is therefore summarized in an own section to ensure the understanding of the following sample applications under the specific motion task.

Handling human motion data, it is particularly important to know about the orientation of body parts, since these kinematics have a huge impact on the progression, form and outcome of a motion. Therefore, representation of orientation – respectively attitude and angular information – is the most essential and fundamental mathematical concept of this thesis. Strategies for the representation of orientation vary with the application purpose, and differ between pure mathematical and computational usage. The most common strategies for processing and computation are therefore explained in the second part of this chapter.

Lastly, the work made for this thesis is put into relation to important and influential research from the various contributing sub-fields at the end of this chapter.

### **3.1 Ski Jumping**

Ski Jumping originated in the 18th century in the Norwegian province of Telemark, when farmers used small hills on alpine slopes for short jumps. With time, the interest and the enthusiasm for this new discipline rose and ski jumping became a sport of its own that was added to the Olympic winter schedule in 1924. In Japan, it was first performed in 1929, when



Norwegian instructors arrived in Sapporo to train the Japanese in ski jumping. Since its origins, ski jumping has developed into a highly specialized sport. Broadly speaking, it can be described as follows: athletes sequentially descend a specially constructed take-off ramp (known as the in-run slope) and jump from its end (known as the take-off table) as precisely as possible and with as much power as they can generate to 'fly' as far as possible down a steeply sloped hill before landing and skiing safely through an outrun zone. Woman's ski jumping started during the end of the last century and finally got included in the Olympic Winter Games in Sotchi 2014. Further disciplines that have been added to the Olympic Game schedule over time are the team and mixed team competitions.

According to the Federation of International Skiing (FIS), ski jumping is currently one of the most popular disciplines in winter sports. In particular, it is enthusiastically enjoyed in Germany and Austria, with the four hills tournament constituting the climax of euphoria. The tournament is extensively broadcasted in public television and visited by several thousands of fans every winter. At the moment, the sport is practiced in about 20 countries on a World-Cup level throughout the year. The classical scenario is winter ski jumping, where the athletes jump on a surface made from ice and snow and during which all important competitions take place. However, it is also practiced in summer season for training and preparation competitions on watered artificial, grass-like surfaces made from plastic. Together with cross-country and Nordic combined skiing (which is a mix of ski jumping and cross-country skiing), ski jumping forms the Nordic skiing disciplines. As opposed to Alpine skiing, the Nordic skiing disciplines are characterized by the fact that the heel of the ski boot cannot be fixed to the ski. To enable the athletes to effectively glide long distances and for a safe landing, jumping skis are furthermore considerably wider and longer than their cross-country and Alpine skiing counterparts.

### 3.1.1 Competition Rules

After long and tedious competitions under the influence of changing wind conditions in the 90s and 2000s, the winner of a competition is nowadays determined in a more robust scoring system which combines flight distance, style points awarded by five judges as well as wind conditions and in-run length to one final output score (Figure 3.1). This mixed system compensates for the influence of variable outdoor conditions and makes the competition more compact and attractive to the spectator at the same time. In concrete, it works as described in the following.

**Distance points:** Each hill has a target landing point called the calculation point (K-point) in the middle of the landing area. The K-point is set at the landing slope's steepest point and defines the place where the majority of jumpers is expected to land. In a competition, landing on the K-point is rewarded with a certain fixed number of points. Jumpers earn extra points for flying beyond the K-point, and lose points for every meter they land before the K-point. Regular FIS World-Cup events take place on hills of three different sizes: the normal hill with

### 3.1. Ski Jumping

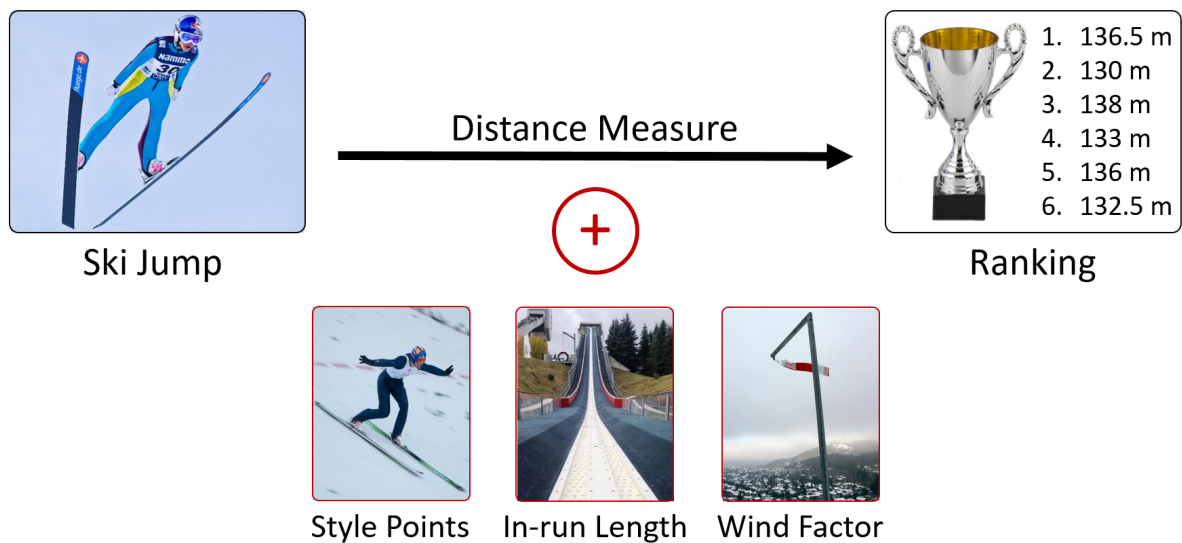


Figure 3.1: Illustration of the current scoring system in ski jumping. By adding style points, wind and in-run length scores, the final ranking does not necessarily conform with the jump length.

a K-point of approximately 90 meters, the large hill with a K-point of approximately 120-130 meters and ski flying hills that allow jump of over 200 meters. The current World Record for the longest jump without fall is 251.5 meters. It was set in February 2015 by Anders Fannemel from Norway.

**Style points:** Jump style is rated by five judges simultaneously from a judging tower at the side of the slope. Good style can be awarded with a style measure of up to 20 points per judge. Indicators for a good motion execution are steady skis during flight, balance, aerodynamic body position and a correct and safe landing.

So far until summer 2016, only 7 jumpers in the history of ski jumping are recorded to have achieved a 'perfect jump' with all five judges attributing the maximum style score: Anton Innauer and Wolfgang Loitzl from Austria, Kazuyoshi Funaki and Hideharu Miyahira from Japan, Sven Hannawald from Germany and Peter Prevc and Jurij Tepec from Slovenia.

**Wind points:** Changing wind conditions significantly influence the maximal length a jumper can achieve under an optimal technical motion execution. The more wind blows up the hill, the more a jumper-ski flying system is exposed to lift forces. This results in longer jump lengths. Tail wind on the other hand exposes an athlete to drag forces that will reduce the resulting jump length. Setting the wind condition at the start of a competition as base value, plus and minus points are given for actual wind conditions at every jump and then added or withdrawn from the original scores.

**In-run length points:** With changing wind conditions, also the optimal take-off speed to reach the K-point differs. In case the in-run length (meaning the gate from which the athlete starts the jump) has to be adjusted during a competition to adhere to changing wind conditions, additional plus or minus points are determined that are added to the final score.

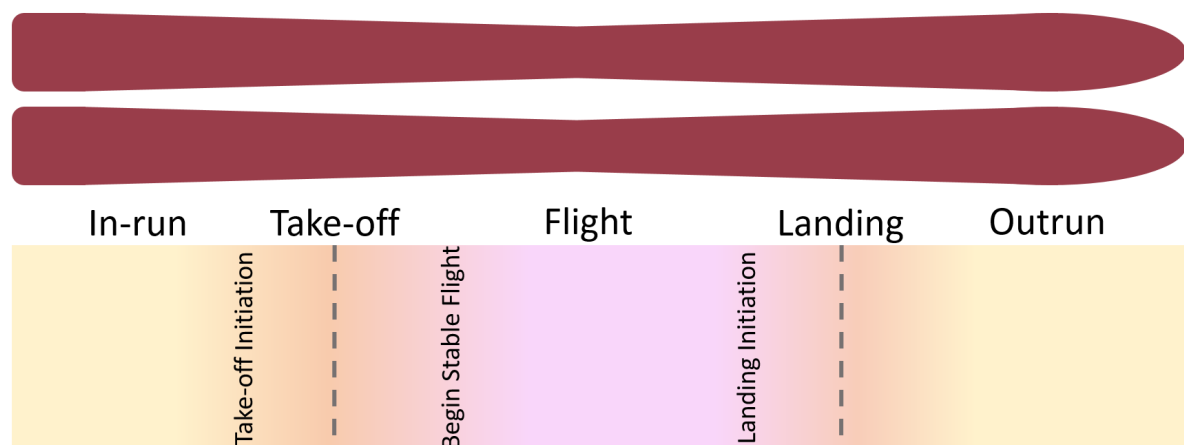


Figure 3.2: Take-off and landing divide a ski jump into the three main motion phases in-run, flight and outrun. Motion characteristics further separate in-run and flight into the four sub-phases take-off initiation, transition to stable flight, stable flight and landing initiation.

In the past years, several changes in rules and material specifications have furthermore been put into effort to regulate the use of aerodynamic effects, and to stop the trend of underweight athletes [SM02, Mül09] for a reduction of drag forces: ski jumpers below the minimum safe body mass index are penalized with a shorter maximum ski length, reducing the aerodynamic lift they can achieve.

### 3.1.2 Technical Specifications

Ski jumping is a very technical sport. This means that the main motion parameters like body posture, take-off timing and flight height are defined by biomechanical and physical laws (e.g. aerodynamic forces such as drag and lift). In general, good motion technique correlates to a higher flight curve and a longer jump length. Erroneous motion execution and use of the aerodynamic forces like wrong body pose or too high rotational impulse can furthermore increase risks of fall and injury. All these motion characteristics yield multiple indicators to identify the quality of a jump, which on the other side leave many possibilities for new application systems – as stated before, the provision of motion information and feedback is often carried out in a very traditional way by observation from coaches and video data analysis so far.

A ski jump is divided into five main parts: in-run, take-off (the actual biomechanical process of jumping), flight, landing and outrun. In-run, flight and outrun comprise more than 90% of the whole jump and are separated from each other by the take-off (separating in-run from the flight phase) and landing (separating the flight phase from the outrun). Furthermore, every ski jump consists of four sub-phases within the in-run and flight phase: the end of the in-run is marked by the take-off initiation, and the flight phase is divided into the three

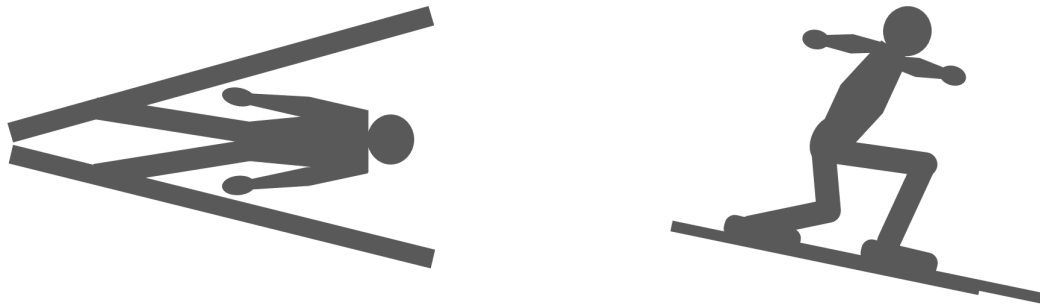


Figure 3.3: The most characteristic flight elements of contemporary ski jumping are the V-style flight position (left) and the Telemark landing (right).

parts transition into a stable flight after the takeoff, stable flight (where ideally no motion at all is supposed to happen) and initiation of the landing [CFC<sup>+</sup>13, BKTG10, OHMS08] (Figure 3.2). The creation and conservation of beneficial aerodynamic conditions during those phases largely influences the length of the jump. Two examples are an ideal take-off timing and an optimal transition of velocities and angular momentum generated during take-off into flight. They ensure the athlete to reach a stable flight position immediately after take-off, as well as to counterbalance pitching moments during the flight that might arise by wind flow. However, it is important to note that no general and universally valid ideal flight style exists, so that style recommendations cannot be quantified. How to reach and maintain advantageous body poses and angles consequently always has to be put into context with every athlete's individual physical properties and motor skills [Mül09]. From biomechanical and aerodynamic studies [MBG09a, MBG09b, SM05, VIK<sup>+</sup>05, ABVK95, SMY04, SWM04, VKK01], it is on the other hand possible to generate guidelines for the execution of a complete ski jump. They are used to learn and practice this sport and contributed to increased safety and jump length over time. Since the late 80s, it is for example common to open both skis to a V-shape during flight (Figure 3.3). This V-position enables the athlete to create an ideal balance between lift and drag forces that result in a longer flight.

#### Indicators for Flight Quality - Style

The first guidelines on how to score a ski jump date back to the beginning of the 20th century (see [Kei33] for an description of judging in the 1930s), and although flight style, material and equipment have changed drastically since then, the main core of the scoring system still remains the same: marks are not given for good style, but deducted for faults. A perfect jump is awarded with a maximal style measure of 20 points per judge, and errors and deviations from the desired motion style in every motion phase are fined by distracting points from the maximum score. The jump phases that are part of the judging evaluation are flight, landing and outrun. Faulty behavior during the flight phase and the landing can be punished with a maximum point deduction of 5 marks each and during the outrun with a maximum point

### Chapter 3. Thesis Fundamentals and Related Works

deduction of 7 marks under the current point deduction specifications set by the International Ski Federation FIS [FIS13]. The exact definition for errors and their point deductions in jump style can be found in Table 3.1, which was derived from a jump evaluation training sheet for judges from the Japanese Ski Association.

Table 3.1: Guidelines for the judging of ski jumping style including points deduction rules for errors. The guidelines were translated from an official jump evaluation training sheet for judges from the Japanese Ski Association.

<b>A</b>	<b>Aerial phase errors</b>	<b>max. 5.0</b>
1	Insufficient control over body or skis during the formation of the stable and dynamic flight posture	0.5-2.0
2	Instability (unnecessary motion of the arms, uncontrolled body position, bent knees, not completely stretched legs)	0.5-1.0
3	Unsymmetrical positioning of the arms	0.5-1.0
4	Unsymmetrical positioning of the legs	0.5-1.0
5	Unsymmetrical positioning or unevenness of the skis	0.5-1.0
<b>L</b>	<b>Landing phase errors</b>	<b>max. 5.0</b>
1	No Telemark landing at all (feet parallel, single fault)	min.2.0
2	No smooth movement/transition from the flight pose to the landing	0.5-1.0
3	Slight Telemark landing, with little bending of the knees only	0.5-1.5
4	Insufficient absorption of the landing impact by the Telemark, or Telemark position is not maintained until the end of the landing process (instability, too stiff or not fully executed Telemark position)	0.5-1.5
5	Unstable or unbalanced movement of the arms to keep the balance of the jumper-ski system	0.5-1.0
6	Insufficient ski control (skis are not parallel or more than 2 ski widths apart), or skis are not equally in contact with the gliding surface (ski upright on edge)	0.5-1.0
<b>O</b>	<b>Outrun phase errors</b>	<b>max. 7.0</b>
1	Small errors (momentary instability, skis are not equally in contact with the gliding surface or not parallel, body is not in upright position before the start of deceleration)	0.5-1.5
2	Errors (insecurity, missing impression of balance, skis are not equally in contact with the gliding surface or not parallel, body is not in upright position when reaching the fall line)	2.0-2.5
3	Large errors (instability, impression of risk of falling before or on the fall line, touching the ground or ski with one hand)	3.0
4	Loss of control or balance (touching the ground or ski with both hands, the back or lower back)	4.0-5.0
5	Fall before or on the fall line	7.0

A particularly important specification for the flight phase is the active use of air pressure

and aerodynamic conditions. This is characterized by a bold and aggressive forward leaning movement at the take-off and results in a rapid and smooth transition to the optimal flight position. During stable flight, it is important to keep a steady and symmetric ski and body positioning and good body balance. To achieve maximum landing points (meaning no point deduction for the landing execution), the athlete is expected to hit the slope in a standardized posture, the so-called Telemark position. The Telemark is a standardized, squat-like position with one leg slightly shifted in front of the other and no other body parts touching the ground (Figure 3.3). Remaining in the stable Telemark position for approximately 10 to 15 meters are the main indicators for little or no point deduction in the outrun. Faults and deviations from the defined style form are punished in dependence on their severity and time of occurrence during flight. A fall after or during landing for example is weighted much more (up to 7 points) than an asymmetrical arm position during flight (0.5-1 points).

## 3.2 Representing Orientation

Changes in position and angle of body segments and joints describe human motion. For motion analysis, it is essential to understand the fundamental concepts that define and represent those changes, especially since representations of orientation and their naming conventions differ between research fields and applications. In computer science and engineering, it is for example common to refer to spatial rotations as attitude, whereas they are generally referred to as posture in motion sciences and humanities.

Attitude representation – or orientation – of an object gives information on how an object is rotated within the three-dimensional space. In other words, the attitude of an object defines the direction in space an object is facing to. When measuring the orientation of human body parts by sensors mounted on a subject's body, orientation estimation will consequently provide an estimate of the rotation between the local coordinate frame of the sensor and a global fixed world frame.

Orientation can be expressed in different ways. Common representations are Euler angles, rotation vectors, rotation matrices or quaternion representations [Die06]. Euler angles are the most obvious and intuitive orientation representation since they are based on trigonometric functions. They are defined by three variables that represent the rotational motion (angles) around the three principal axes. Following their general definitions and naming conventions, those are **roll**  $\phi$  for rotation around the sagittal axis, **pitch**  $\theta$  for rotation around the transversal axis and **yaw** (or **azimuth**)  $\psi$  for rotation around the vertical axis (Figure 3.4). Because of their intuitive representation, Euler angles are widely used in real-life, human sciences and civil engineering as for example in navigation. However, the use of Euler angles to describe orientation can result in a loss of one dimension of freedom in situations where one of the rotation angles is equal or very close to  $90^\circ$ . This makes two rotation axes coincide, so that the orientation can then not be described uniquely anymore. One strategy to get rid of this

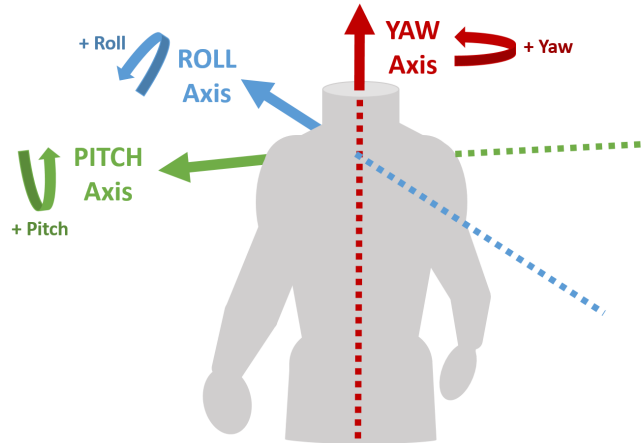


Figure 3.4: Definition of orientation for the description of human posture following naming conventions from navigation. Roll  $\phi$  depicts the rotation around the sagittal axis, pitch  $\theta$  the elevation around the transversal axis and yaw  $\psi$  the rotation around the vertical axis.

singularity problem is to use a different attitude representation that does not suffer from such an ambiguity (also called gimbal lock).

The most common alternative to Euler angles are quaternion representations. They offer three main advantages that favor their use in complex attitude computations of technical applications like computer graphics, computer vision and robotics. Those are the invariance to the previously mentioned gimbal lock, the possibility to apply fundamental arithmetic operations (whose general conventions hold for quaternions) on the orientation data, and low computational costs. For those reasons, the majority of all computations on orientation and angular change in this work is based on quaternion representations.

### 3.2.1 Quaternion Representations

Simply spoken, quaternions extend complex numbers to four dimensions and can be used to represent the orientation of a rigid body or coordinate frame in three-dimensional space. For this, the orientation of a body at a special time frame  $B$  shall be related to the orientation of the body at another (previous) time frame  $A$ . Furthermore,  ${}^A\hat{r}$  is defined as a unit vector in  $A$  constituting the rotation axis for a specific rotation. This rotation can then be seen as the rotation around an axis  ${}^A\hat{r}$  which shifts frame  $A$  to frame  $B$  (Figure 3.5).

In the following, the quaternion at frame  $B$  relative to frame  $A$  will be noted as  ${}^A_B\hat{q}$ , with the leading sub-script denoting the frame that is described and the leading super-script denoting the reference frame. The four-dimensional vector space is then for example written as

$${}^A_B\hat{q} = [q_0 \quad q_1 \quad q_2 \quad q_3] = a + bi + cj + dk,$$

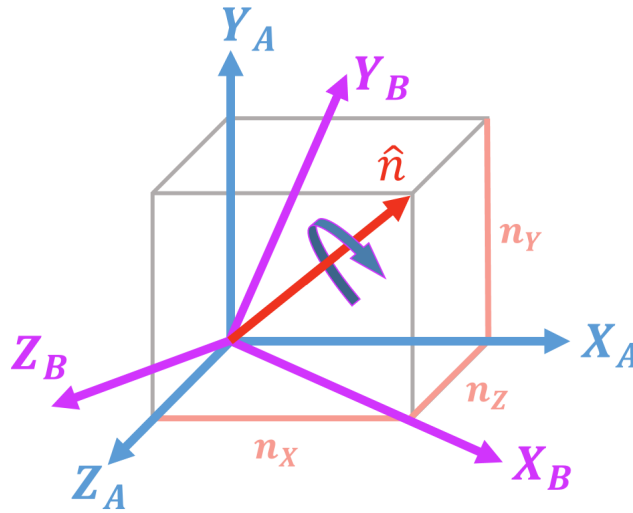


Figure 3.5: The orientation of frame  $B$  (purple, with the axes  $X_B$ ,  $Y_B$  and  $Z_B$ ) in relation to frame  $A$  (blue, with the axes  $X_A$ ,  $Y_A$  and  $Z_A$ ) is represented by a rotation around axis  $\hat{n}$ .

whereas  $q_0$  depicts the real and  $q_1$ ,  $q_2$  and  $q_3$  the complex (or vector) part.

Quaternion representations allow for arithmetic standard operations, which makes it simple to add, separate or divide spatial rotations. In particular conjugation, multiplication, and vector rotation are often used in attitude computations. For all operations, it is conventional to work with unit quaternions, meaning the parameters of the quaternion  ${}^A\hat{q}$  are normalized so that they describe an orientation of unit length as  $q_0^2 + q_1^2 + q_2^2 + q_3^2 = 1$ .

### Useful Arithmetic Conventions

*Quaternion conjugate:* The quaternion conjugate swaps the relative frames described by an orientation. For example,  ${}^A\hat{q}^*$  describes the orientation of frame  $A$  relative to frame  $B$  and is defined as  ${}^A\hat{q}^* = {}^B\hat{q} = [q_0 \quad -q_1 \quad -q_2 \quad -q_3]$ .

*Quaternion product:* The quaternion product of two quaternions  $a = {}^A\hat{q}$  and  $b = {}^B\hat{q}$  creates a compound orientation  ${}^A\hat{q} = {}^B\hat{q} \otimes {}^A\hat{q}$ . Mutually, a quaternion is decomposed into separate consecutive rotations by division with the quaternion conjugate as  ${}^B\hat{q} = {}^A\hat{q} \otimes {}^A\hat{q}^*$ . This bi-directionality makes quaternion multiplication one of the most useful operations in attitude computation. In concrete, it is defined by the Hamilton rule as

$$a \otimes b = [a_0 \quad a_1 \quad a_2 \quad a_3] \otimes [b_0 \quad b_1 \quad b_2 \quad b_3] = \begin{bmatrix} a_0 b_0 - a_1 b_1 - a_2 b_2 - a_3 b_3 \\ a_0 b_1 + a_1 b_0 + a_2 b_3 - a_3 b_2 \\ a_0 b_2 - a_1 b_3 + a_2 b_0 - a_3 b_1 \\ a_0 b_3 + a_1 b_2 - a_2 b_1 + a_3 b_0 \end{bmatrix}^T$$



It is important to note that unlike the multiplication of complex numbers, quaternion multiplication is non commutative. This means that  $a \otimes b \neq b \otimes a$ . Consequently, it is essential to check the order of multiplication when using quaternion products: for example,  $ij = k$ , whereas  $ji = -k$ .

*Vector rotation:* An arbitrary, three-dimensional vector in frame  $A$  can be rotated to frame  $B$  by a simple quaternion-vector rotation. For this, the vector is first converted into a quaternion by extending it to a four dimensional vector  ${}^A v$ : a fourth vector element is added which depicts the real part of the quaternion and is set to 0. A double multiplication  ${}^A \hat{q} \otimes {}^A v \otimes {}^A \hat{q}^*$  with the spatial rotation  ${}^A \hat{q}$  then results into the extended vector representation  ${}^B v$  in the new frame. The previous equation holds when  ${}^A v$  and  ${}^B v$  are the same vector described in the respective frames  $A$  and  $B$ .

### 3.2.2 Transformation Between Representations

Although quaternion representations are very useful, fast, accurate and simple to use, it can sometimes be necessary to transform them into other attitude representations. This is because their convenience in computation comes with a trade-off in explicitness. Both rotation matrices and Euler angles are more intuitive to understand, so that the following transformations are helpful for the examination of the computed output spatial rotations.

The orientation defined by the quaternion  ${}^A \hat{q}$  can be transformed into a rotation matrix  ${}^A R_B$  by

$${}^A R_B = \begin{bmatrix} 2q_0^2 - 1 + 2q_1^2 & 2(q_1 q_2 + q_0 q_3) & 2(q_1 q_3 - q_0 q_2) \\ 2(q_1 q_2 - q_0 q_3) & 2q_0^2 - 1 + 2q_2^2 & 2(q_2 q_3 + q_0 q_1) \\ 2(q_1 q_3 + q_0 q_2) & 2(q_2 q_3 - q_0 q_1) & 2q_0^2 - 1 + 2q_3^2 \end{bmatrix}.$$

For  $\psi$  representing rotating around  $\hat{z}_B$ , *pitch*  $\theta$  representing rotating around  $\hat{y}_B$  and *roll* representing  $\phi$  rotating around  $\hat{x}_B$ , it can furthermore be transformed into Euler angles by

$$\begin{aligned} \psi &= \text{Atan2}(2q_1 q_2 - 2q_0 q_3, 2q_0^2 + 2q_1^2 - 1) \\ \theta &= -\sin^{-1}(2q_1 q_3 + 2q_0 q_2) \\ \phi &= \text{Atan2}(2q_2 q_3 - 2q_0 q_1, 2q_0^2 + 2q_3^2 - 1). \end{aligned}$$

## 3.3 Related Works

Works and research questions related to the development of this thesis are as variate as the different layers of the actual research problem. Research from computer science, electrical and mechanical engineering, sport sciences as well as sports engineering and biomechanics

all address different parts and aspects of the present problem. All of those differing parts have to be taken into account to present a work that complies with the most current state of the art possible. Consequently, works that are usually not inter-related have been merged into one huge, combined pool of background information that influenced the development of this thesis. In the following, the multivariate parts that are essentially contributing to the work in its current form are discussed under the most relevant aspects.

#### 3.3.1 Supporting Motor Learning

Motor learning is subject to extensive research since decades. Important examples that had a big impact on the subsequent sport scientific research are the previously mentioned studies that describe motor learning processes from an information scientific perspective [SW76, Wie49]. However, research is also subject to permanent changes, and various investigations and new insights have been continuously discussed in public over the last decades [SL88, GTM02, MA07]. Basic aspects of the problem, such as the distribution of feedback information, the style of feedback distribution or the neural process behind skill acquisition are under scientific investigation until current time [SKM12, SBKF<sup>+</sup>13, Ste14]. Newer interests focus on the neural processes of adaptation, motor re-learning or multimodal feedback stimuli [SM93, SBD<sup>+</sup>09]. Only since the mid 2000s, movement sciences started to move further towards the area of augmented feedback in its various forms, from visualization to sonification and haptic systems [SRRW12]. Information on their impact on motion feedback with respect to the motor task complexity can be found in Section 2.1.3.

#### Auditive Support

Research showed that the stimulation of additional sensory systems during training can enhance motor control and motor learning within both sports and medical applications. Especially auditory feedback in form of movement sonification is considered to be effective for motor control and motor learning [Eff05, EFW11]. Sonification has been introduced for various application areas and has been used in various fields of science and life over the last two decades [DB11]. To sonify human movements, kinematic and dynamic data representations have been derived from several types of measurement and motion capture devices. Those data representations were for example signals from a force measurement plate [Eff05], motions of a German wheel from a simple magnetometer [HHFS10] or properties of a hammer during throw [ARGB04]. However, it still remains unclear how to provide and process the captured data to display sound in an effective and accurate way. Finding an efficient movement sonification strategy can hence offer various new possibilities for training applications, such as mobile devices being worn directly attached to the actor's body.

### Computer Support

In both sports engineering and computer science, the awareness of the importance of CAT and augmented motion information systems has risen. This led to a higher interest and effort for technological implementation. Studies have already brought first proof of the positive effects of augmented feedback [PFBH13, MSD<sup>+</sup>13] [AS10, KMH<sup>+</sup>13] and are likely to be subject to further investigations in future by not only movement scientists, but also natural scientists.

In general, current investigations from computer sciences are algorithmically advanced and target mainly on the implementation and application of activity recognition systems and robot control. Often, machine learning methods are applied to recognize and evaluate few constrained defined motion patterns from daily life situations [PvSMW15, XL15, CCG<sup>+</sup>15, BDP<sup>+</sup>12]. Sports engineering on the other hand approaches the subject from the other side, putting the actual movement and acquisition of motor skill or performance improvement into focus. As a result, they are generally less advanced and often focus on certain selected body parts, low level features or pure analysis tasks only [MGSR<sup>+</sup>15] [WS13, KCGC12, SNSK16, RPF15]. In this thesis, (some of) the more advanced strategies from computer science are now combined with the expert approach of a sports engineer, which is a unique approach to the topic of motion information provision under the current state of art.

### 3.3.2 Processing Sensor Signals

With the increasing popularity of inertial sensors as motion capture tools, many methods have been introduced that estimate meaningful motion information like segment orientations or body angles from the inertial sensor input data. The most famous methods are based on sensor data fusion of gyro rate integration and observation measurements from accelerometer and magnetometer like variations of the Complementary Filter and the Kalman Filter. All those methods originally got developed for non-dynamic situations like inertial navigation, and later got optimized for a use in human motion capturing. They can enable fundamental kinematic analysis in medical applications and rehabilitation where only motions of low acceleration phases occur, and are especially common in gait analysis or stroke rehabilitation [TTM13, GFF<sup>+</sup>14, BKB14, BLC<sup>+</sup>15, BBCL15]. With the absence of quick motions, it is easy to estimate the orientations from the sensors' accelerations and angular velocities. Natural constraints of the restricted motion environment like ground contact phases can furthermore help to reduce drift and increase accuracy [YBMC07]. Inertial sensors were therefore successfully employed under simulations of real motion data in laboratory settings or in low speed motion scenarios [SGIA<sup>+</sup>15, GLJ16, JSN<sup>+</sup>15, FGM<sup>+</sup>16]. They were furthermore employed to monitor activity and fatigue in slow, non-sport motor performances as rifle holding in war-fighters [DCM<sup>+</sup>16]. Most sports, however, consist of more complex motions with high accelerations and angular velocities, so that filter properties developed in the rehabilitation context might not be applicable to sports in the same way [LPR12, FSK<sup>+</sup>15, BWP08a]. One

explanation for this is that rapid motion parts within a performance induce high accelerations. They on the other hand significantly superimpose the linear accelerations originated by gravity and bias the observation measurement vectors used for the estimation correction. As a result, common methods can be insufficient here, and it might be beneficial to process the multidimensional sensor data in a different way. A popular signal processing method for inertial high speed measurements of alpine skiing for example introduces an independent fusion algorithm [BWP08b] to handle the specific characteristics of the input data. Furthermore, it could be useful to consider the specific characteristics of a motion along the various motion dimensions. Although the number of published research was steadily increasing over the last years [VDSBB<sup>+</sup>15, FFC<sup>+</sup>15, MCG<sup>+</sup>15, SNSK16, ADM<sup>+</sup>14, GTNJ13], inertial sensors are still less frequently applied for analysis of real sport motions than for medical purposes. Exactly such eventual deficiencies in accuracy as well as the difficulty to adapt the filter to the current sport situation might be the reason for this disparity. Therefore, it is essential to gain deeper insights into the processes that influence the accuracy of orientation estimation algorithms. In this regards, it is necessary to investigate common and available sensor processing methods independently under the special requirements of sports so that the strengths and weaknesses of different methods can be identified and eventual constraints and conditions that arise in the context of insufficient sensor calibration and dynamic motion be discovered to enable an appropriate use in varying sport disciplines.

#### 3.3.3 Measuring Ski Jumps

During the last century, researchers from Austria, Germany, Finland and Japan started to extensively analyze the ski jumping motion under biomechanical criteria. Findings from those studies have led to a constant increase in the maximal jump and flight distance, as well as to the adaptations and changes of competition rules to make the sports fairer and safer for the athletes. However, as exact kinematic and dynamic properties of an athlete are quite difficult to measure quantitatively during training and competition, registered research activities were usually based on simulation calculations, wind tunnel measurements, observation and video analysis [MBG09a, MBG09b, SM05, Mü109, SMY04, SWM04, ABVK95]. To set new standards for motion analysis during training and competition, it is now necessary to make detailed and accurate motion information available to coaches and athletes by means of a mobile platform.

As previously mentioned, ski jumping offers several aspects that favor an inertial motion capturing and data processing, with the main aspects being the large motion volume and the restricted number of possible conventional motion analysis methods. Especially in junior ski jumping and local training and competitions (where many jumps are performed within a short time frame), visual information often is the only source of motion information, whereas all jumps are observed from the same position at the coaches' stand. In this respect, the creation of a new training technology that provides accurate, additional and more detailed

motion information to athletes and coaches is very reasonable. Nevertheless, research efforts on the ubiquitous capturing of ski jumping motions remain very unique - only a very small number of research groups worldwide used wearable sensors for the capturing of ski jumping so far. The first reported investigation using inertial sensors was completed in 2008 at Keio University [OHMS08] and mainly focused on the extraction of direct information from the inertial raw data. Further studies concentrated on the use of single sensors for the extraction on motion characteristics and jump detections [LZL<sup>+</sup>15]. The first data capture of a ski jump with a commercial system has been performed just recently and is currently promoted as 'first ever full body 3D motion capture of an entire ski jump'<sup>1</sup>. Knowing that the present research has determined full body ski jumping data before the publishing of the respective video material, this marketing slogan cannot be considered correct in its current form. However, it clearly shows the uniqueness of the topic. Apart from my own research, multiple sensor devices have furthermore been used by two research groups in Europe. First in a study to measure the flight of an Olympic champion in 2010 [BKTG10], and second in a series of more detailed studies on the estimation of kinematic parameters during flight in 2012 and 2013 [CFLC<sup>+</sup>12, CFC<sup>+</sup>13]. Here, the different flight phases of a ski jump could be annotated based on the raw inertial sensor data. Additionally, body segments could be estimated using typical constraints found in ski jumping motion.

In contrast, the kinematic jump parameters should be computed on a more general and generic basis without the help of sport-specific natural constraints in this thesis. Given the mix of little to no acceleration and angular changes during in-run and flight, and shorter periods of high acceleration and quick angular changes during take-off and landing, ski jumping is likely to pose unique demands on the data processing. Furthermore, magnetic disturbances caused by ferromagnetic material (e.g. steel structures) of the ski jump hill may influence the accuracy of kinematic estimates obtained with conventional methods: research has shown that variations in the magnetic field have a significant impact on the orientation estimates from inertial sensor data [dVVBvdH09], and that the differences between a sensor orientation estimate to an optical ground truth are larger when the sensors are in close proximity to ferromagnetic materials such as force platforms [MGSR<sup>+</sup>15]. With no existing guidelines available to adhere to, the system's accuracy and functionality therefore needed to be thoroughly validated with respect to the intended application. This ensured then that the developed mobile system could be assumed as generic and applicable for the automatic assessment of motion performances and the supply of real-time motion information.

### 3.3.4 Recognizing Motion Activities

The main question of this work is to find specific motion knowledge from the sensor data, so that useful information can be extracted and provided to users like coaches and athletes. In an automated, technology-supported training environment this means to create mean-

---

<sup>1</sup>A video on the ski jump capturing can be found here: <https://www.youtube.com/watch?v=3Zt1q3qrriE>

ingful machine knowledge on the base of relevant motion information for classification and evaluation tasks. Features that represent the semantic content of a motion performance should be chosen in such a way that characteristics can be discovered, classified and rated for support of the user. This intended application is a new task that requires specific and extensive domain knowledge, and common machine learning algorithms need to get adapted to satisfy the present task-dependent requirements.

A wide variety of possible features exists to transform motion kinematics from wearable sensor data into meaningful information such as statistical raw-signal based features, event-based features, multilevel features derived from clustered statistical occurrences and kinematic body motion information [BBS14] [AB10]. In general, learning systems are very sensitive to the feature quality. This means that low-quality features that have no relevance for the learning task can have a negative impact on the performance when included in a feature set. Many processing methods used in the context of sports focus on low-level signal-based features and extract information directly from the raw sensor data [MF15, DMA14, GJ11a] for computational simplicity. With a sensor data processing framework that estimates angles of body segments and joint positions, additionally higher-level motion information like positional and temporal evolution of joints or relational information between body parts can be provided [HBMS11]. Such additional semantic motion information correlates to a movement's biomechanical specification and can be assumed to give more detailed motion information under the aspect of time.

Concepts and strategies for recognition of motion activity have been introduced in former research from both video and depth camera data as well as wearable motion sensors [CGG<sup>+</sup>09, ZBMM06, PDLM15, HSSL13]. However, they mostly focus on every day motions with the target of robot action handling and do not evaluate sport performances in their specific motion context [JKBH15, SWDS15, ZB15]. Consequently, they either simulate a set of data for input in the training and testing of the machine learning systems or concentrate on clearly distinguishable motion patterns [CCG<sup>+</sup>15, XL15, PvSMW15]. However, working with such simulated or manually created experimental data, learning methods can generally easier be adapted and trained to their intended application since the system environment is constrained and every activity can be simply described in a unique way. For the present work and the technical evaluation of a motion performance quality on the other hand, even small changes in body pose or the technical motion performance can significantly influence the outcome of the performance. Body posture during the flight of a ski jump for example immediately influences aerodynamic forces as drag and lift and hence the length of flight and final performance. Because of this direct relation and the absence of large angular changes like full body rotations, the general scale for changes during motion position is small. As a result, differences between jumps occur on a fine scale, requiring additional accuracy and discriminative power of eventual processing and machine learning system to retrieve relevant fine-scaled differences among the different relevant motion activities. Only few studies have tackled the problem of sport performance activity recognition so far, and usually

## Chapter 3. Thesis Fundamentals and Related Works

---

concentrated on the measurement and retrieval of few key aspects of a motion, or very simple raw sensor data features [HDK13, Sup10, HMMHJ08, HJ10, Stu12]. Most of them furthermore did not apply specific machine learning strategies as used in this work. Consequently, I believe that this work has a very innovative and unique approach that could considerably impact following works in the same field.

### Evaluating the Beauty of Performances

The more subjective decisions a sport includes, the more it usually becomes unreliable and prone to errors. While target sports as soccer and handball are mostly objective since the referee only decides on minor and major rule violations, performance-oriented sports that contain an aesthetic component such as gymnastics, diving, synchronized swimming or ski jumping are subjective and hence prone to wrong evaluation or manipulation. As a result at least every second year with the focus of the Olympic Games, discussions on fraud, manipulation and bribery come up in judged-sports [PH06]. For the Sochi 2014 Games, rumors on unfair means have been particularly strong for figure ice skating – which is exposed to rumors about fraud in many big, important competitions – and half pipe snowboarding. For the Rio 2016 Games, boxing was in the focus of judging controversies. In both cases, multiple non-scientific articles and blog entries have been published that discuss the fairness of the events, or dubious scoring and ranking processes.

Research has shown that nationalism biases competition results [Zit06] and that reformations in the competition rules initially made to increase transparency might favor corruption [Zit14] even without the existence of explicit fraud. The respective study argues that this is because a judge's individual perception is typically biased, either unconsciously or on purpose, so that it is difficult to maintain objectivity when subjective human decision making serves as the base of the ranking.

To account for this problem and to enhance transparency, the International Olympic Committee (IOC) started to impose changes in competition rules for all Olympic judged-sports at the beginning of the 21st century. Revised scoring and judging systems of respective sports nowadays aim to assure a higher level of objectivity by reducing the influence of individual judging decisions on the final results. In this process, it became a requirement for every performance-oriented sport to include at least one objective measure in the evaluation results. In trampolining for example, the time-of-flight (TOF) measurement, which designates the overall length of a trampoline routine, was added to the catalog of evaluation criteria. However, such measures quantify just a very small and often minor part of the motion and cannot record the complete performance. Inertial sensors can offer innovative motion assessment possibilities here, and contribute to new credibility, but also understandability, for both athletes and spectators. I am therefore convinced that the future of affected sports lies within the implementation and creation of independent technical judging devices.

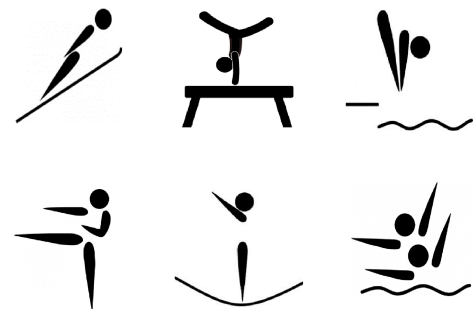
To date, the problem of skill scoring has been explored vaguely by few research groups only. One of the first works to address this issue was a study for the development of automatic scoring system of horizontal bar artistic gymnastics from video data [SO08]. A scoring support model for ballet based on ground truth data of judges was described in 2013 [YA13] with the help of an optical motion capture system. However, in this work it was not made clear how the chosen kinematic scoring features were concretely built from the identified feature descriptors from the optical motion capture data. To rate a motion on the base of wearable sensor data, subjective winter sports were the prime target so far. For snowboarding tricks, a classification and evaluation system has been presented in literature several years ago, but never got extended further to be used in general scenarios or on a worldwide scale [HMHJ08]. A related sensing solution for skill evaluation in downhill snowboarding, which focuses on one single aspect of the motion (weight balance) determined from sensor devices attached to the snowboard, was presented recently [MFTW16]. A more advanced system for skill scoring in skiing and snowboarding based on one inertial sensor attached to the athlete's trunk was implemented in 2014 [YOS14]. This study was followed by a more detailed investigation on the retrieval of retrieval skill from large body movement data bases [YKT<sup>+</sup>15].

For my evaluation algorithm, I primarily intended to find differences and similarities among ski jumps to create a ranking order as result. This can be achieved using data mining methods for activity recognition mentioned before. To date however, much more research effort has been made for the development of various music information retrieval algorithms than for motion data retrieval. Here, it is amongst others possible to recognize similar motions of different speed, pitch and beat, or to find special parts of a partition in a musical piece [FZP03, YLSC08, MRM<sup>+</sup>05, YLC09]. Most of the methods developed for music data processing have never been used for other data types, however it appears to be very promising and reasonable to also apply them to motion data evaluation, especially when evaluating beauty aspects of a motion: one of the biggest questions is how subjective, aesthetic impression of a motion as perceived by judges could be represented in a motion assessment and rating system. The problem here is that they play an important role in the computation of the final score, but can usually not be quantified and vary with every person. An idea is to consider influences on a user's aesthetic perception as a combination of certain dominant semantic data relations that can be numerically determined over time. Similar problems exist for the parametrization of aesthetic perception in music and video data and are known under the term computational media aesthetics [NDV01, Ada03]. For those non-motion multimedia data, research already generated feature description strategies as for example dynamics, flow, density, clarity and neighboring relations [ZZZ15, YLSC08, YYC11, FZP03, WDFJ13]. They can be a good starting point for the development of similar feature descriptors in future motion judging applications.





# Collecting and Augmenting Numeric Motion Data





---

As it was explained in Chapter 1 (Figure 1.3), any computer-based motion analysis system consists of a certain number of internal processing stages that have to be run through before meaningful motion information is obtained. Generalizing those internal processes, a minimum of four main steps stand out for every system – data creation, data augmentation, sense-making and retrieval of relevant information. In this part, I discuss the first two main stages, data creation and data augmentation. They are essential for any potential system as they ensure the supply with the fundamental and meaningful numeric motion data. Therefore, they also comprise many components and algorithms from signal processing.

For a meaningful and detailed analysis of human motion that satisfies all aspects of kinesiology, it is essential to know the orientation and position of body segments and joints. The first activities to capture motion with technological devices have already been performed more than hundred years ago with the aim to better understand the processes and key points of human and animal locomotion. Since this time, more and more devices to capture human motion were made available to the public audience, leading to systems of increasing accuracy and usability. To choose suitable technology for a subsequent application, it is important to know the advantages and disadvantages of commonly used motion capture devices. Local and technical specifications of sports generally demand mobility and flexibility and condition the use of wearable motion capture systems like inertial sensors. The first chapter of this part therefore introduces current inertial motion capture devices, the hardware used for the creation of the motion data bases and their strengths and weaknesses. Furthermore, I describe the main data bases that resulted from the first main processing stage and that are used in the following three processing stages.

The biggest challenge arising with the utilization of inertial sensors is that their data output has to be postprocessed to make the best use of it. Ideally, the sensor data is processed in such a way that motions can be qualitatively analyzed and evaluated under the same accuracy as optical motion capture data. Because of their sparse data output, the most extensive and important step for the acquisition of kinematic motion data therefore is to estimate the orientations of the used sensors and the body segments the sensors are attached to. Apart from this task, several other processing steps have to be made to obtain universally applicable sensor data, like estimating the initial posture or sensor-bone displacement and positional data of body joints. All methods are accumulated and described in one chapter as the base and fundamental technology for any subsequent application.

To ensure that the estimated kinematic data is reliable enough for the remaining two processing stages and any subsequent application, it is necessary to know about the accuracy of the estimated orientations and positions. Accuracy measures are discussed in the last chapter of this part. Investigating the performance of the implemented processing methods, it cannot only be possible to verify their error and deviation from the ground truth, but also to discover peculiarities in the data and the used sensors. During the course of this thesis, it was for example possible to identify several variables that influence the sensor performance. As a

---

result of this analysis, counter-measures were introduced that improved the data accuracy and made the estimated motion kinematics more robust to errors. Those findings – that have also been presented in two journal publications – enhanced the usability of the system, so that a simpler and more intuitive interface could be provided to the diverse group of target users in future. They are discussed at the end of this part.

## 4 Collecting Numeric Motion Data

A photo series about a galloping horse by Eadweard Muybridge in 1878, and two following publications about animal locomotion and human motion in 1887 and 1901 initiated the idea of motion capturing at the end of the 19th century. Since the beginning of motion analysis, motion capturing became a professional industrial branch and various kinds of technologies for different application purposes were introduced. Nowadays, the main purpose is to deliver three dimensional position information of selected points at a rigid object or body. The most common systems are: optical marker-based systems, optical marker-less systems, mechanical systems, magnetic systems and wearable capture devices as inertial sensors used in this thesis. Every contemporary motion capture system has different properties and requirements concerning the recording environment, the size of the capture volume and the expressiveness of the provided data. Consequently, every system is characterized by special setup and capture requirements, and the information content of the obtained motion capture data varies with each system specification. These special properties have to be taken into account to select the best method for every application.

### 4.1 Motion Capture Devices

**Optical motion capture systems** (as they are for example widely used in movie and game productions) base on the tracking of marker positions from multiple camera views. Consequently, they provide very rich data that is easy to interpret. On the other hand, they are very expensive and restricted to indoor capture conditions (daylight interferes with the tracking of the marker) and with respect to the size of the capture volume. They furthermore come with a relatively big overhead for the system set-up and calibration, so that they do not recommend themselves for a use in mobile consumer applications and most sport applications.

**Marker-less systems** use computer vision algorithms and methods to track motion of objects and humans with either monocular camera views or multi-perspective camera views. Since few years, it is also possible to obtain depth information from marker-less motion capture systems, such as from the Microsoft Kinect camera sensors. The main contribution of marker-less motion capture systems is that the motion can be captured in a natural capture environment. This means that subjects are not required to wear special equipment or marker for tracking. The main problem of marker-less systems is that tracking requires close proximity with the object to be tracked to maintain a sufficient level of accuracy and information content. In

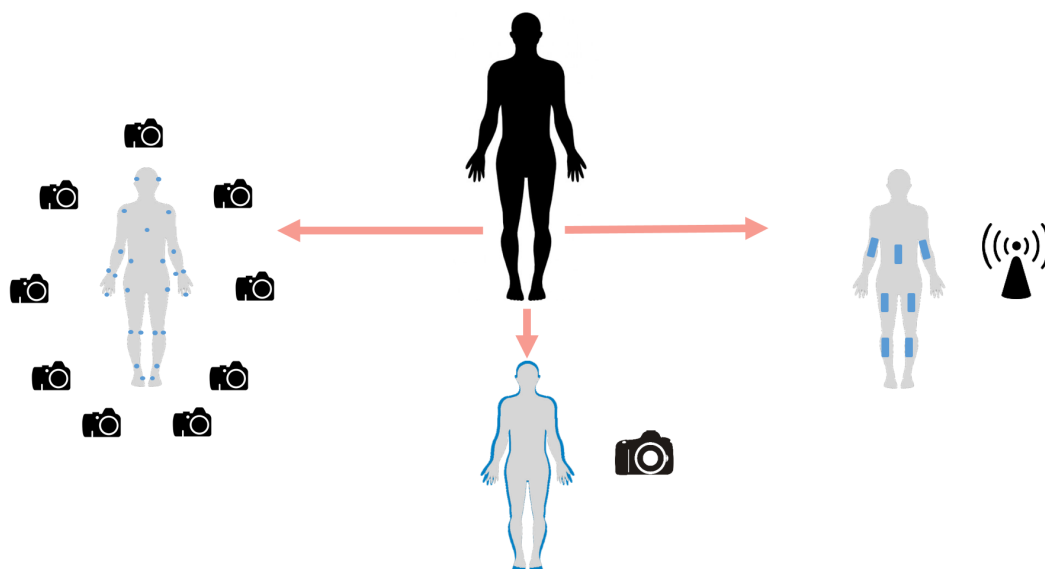


Figure 4.1: Output of the three currently most common motion capture systems. Left: optical marker-based devices, middle: optical marker-less devices, right: wearable sensor-based devices.

other words, objects in large distance to the camera cannot be captured in detail or under high resolution with respect to single specific aspects of a motion performance.

Sensors of **mechanical motion capture systems** are generally attached to the human body with a skeletal-like structure and the performer's relative motion is measured over the articulated mechanical parts that move in the same way as the actor. Because the system has an skeletal-like structure, this system considerably interferes with the actor's performance and is not used in a common way.

**Magnetic systems** utilize sensors that measure the low-frequency magnetic field generated by a transmitter source. Sensors and source are cabled to an electronic control unit that determines reported locations within the field and measures and tracks the range of motion by the relative intensity of the voltage. Markers are not occluded by nonmetallic objects but are very susceptible to magnetic and electrical interferences from ferromagnetic objects and electrical sources in the environment. Those disturbances affect the magnetic field strongly. The system is furthermore cabled to the electronic control unit and the actor's mobility restricted, making it less favorable for sports environments.

**Wearable sensors** on the other hand, do not impose any restrictions on the motion with respect to lighting conditions and mobility. The sensors (most commonly inertial sensors) are small and of low weight, and do not need any external cameras, emitters or markers. Communication with such an inertial measurement unit (IMU) is wirelessly established via Bluetooth. From a computer and software program, sensor commands can then be sent



Figure 4.2: Capture volumes as they can be covered by optical marker-based and marker-less systems are easily exceeded in many sports. Therefore, it is sensible to choose wearable (inertial) sensors as motion capture device.

out and motions be recorded, saved and viewed. Restrictions on the size of the capture volume only exist with respect to the maximal distance between sender and receiver of the capture and program commands and can nowadays also be minimized by additional data communication bridges and networks. However, ubiquity in the data acquisition comes with a drawback in data quality - positional or angular data cannot be directly obtained from the sensors, but has to be estimated from the raw sensor output that is very sparse. Besides, inertial systems that use additional magnetometers can be sensitive to magnetic and electrical interferences in the environment.

Most capture systems need to be immediately excluded as prospective data input systems once the requirements of sports are considered. Although sports generally takes place in locally restricted environments, their field of activity easily exceeds common capture volumes as they can be covered by camera systems (Figure 4.2). Consequently, optical marker-based and marker-less systems are not suited under the intended application. With additional requirements of high mobility, minimal size and weight (to not disturb the athlete), magnetic and mechanical systems also disqualify for any further use. This leaves wearable sensors, and in particular the combination of multiple sensing modules within inertial sensors, as only reasonable choice.

## 4.2 Current Inertial Sensor Hardware

IMUs offer many features that are ideal for mobile motion capture and tracking applications: they are cheap, light and capture human motion in an easy, flexible and direct way. In general, they consist of a combination of miniature three-axial accelerometers, gyro rate and magnetic field sensors. Those sensors supply the user with information about acceleration, angular velocity and the magnetic field and can then be processed in a next step to provide more intuitive and meaningful motion data.



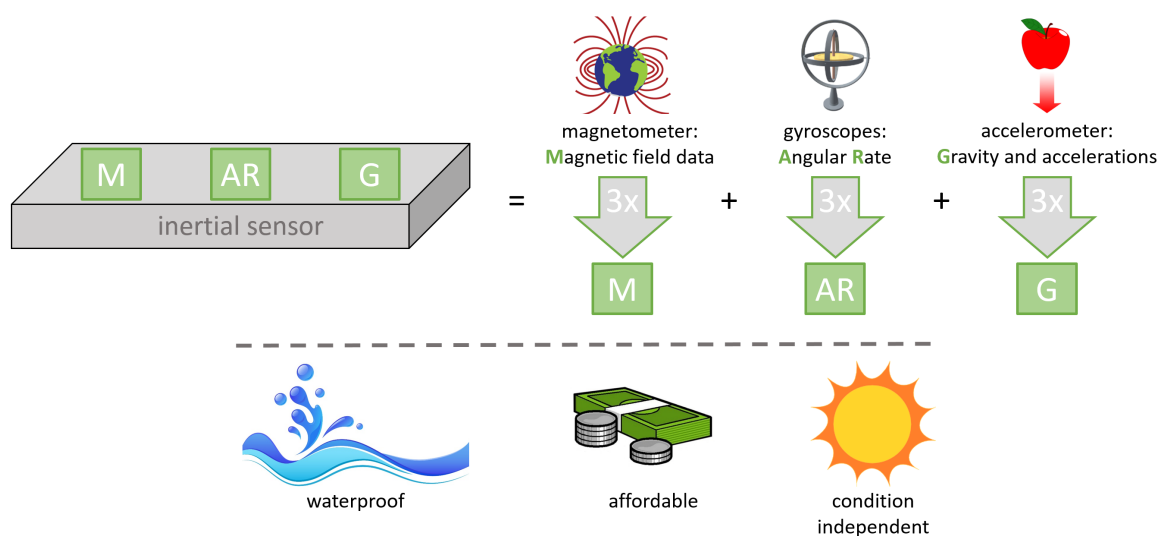


Figure 4.3: General hardware specifications of inertial measurement units (MARG sensors) and the special demands of sports that require independent sensor technology.

Technology for full body motion capturing of sport performances has been introduced commercially at the beginning of the new century using a general Kalman filter and biomechanical constraints as the rotational degree of freedom of body joints [RLS09]. Many research facilities all over the world use the commercial X-Sens system (XSens Technologies B.V. MVN/MTw, Enschede, Netherlands) for their research, and it serves as a quasi-standard since it offers high accuracy and usability [XSe]. With the included data processing and the graphical user interface software, it is especially popular in research areas with less electrical and technical know-how [EMW14]. However, the relatively high initial cost, as well as disturbing sensor sizes or vulnerability to water can detain sport research and training facilities from the acquisition of this commercial system. In those cases, alternative hardware solutions that offer a smaller and waterproof combination of inertial sensor modules are developed and employed instead. Unlike commercial systems, independent sensor systems are not bound to certain determined data processing methods and can consequently be used in a more flexible way in future mobile applications. On the other hand, they usually do not evaluate full body kinematics, but either retrieve direct knowledge from the measured accelerations and angular velocities [MF15, DMA14], or from special aspects of a motion and specific body parts that play an important role for the performance [GJ11a, TGAT11]. To enable a meaningful biomechanical full-body performance analysis, it is then additionally necessary to derive kinematic data that should be of high accuracy. This constitutes a challenge in the development and use of independent fusion filters, which is one of the reasons why many movement scientists rely on the commercial system. For similar reasons, the sample sonification system demonstrated in this thesis has also been implemented using X-Sens sensors, whereas the remaining parts have been implemented with a different, less commercialized system.

In recent years, several independent sensor modules for human motion capturing and the estimation of body segment orientations have been introduced in literature [BKB14, HAW<sup>+</sup>10, BM14, BAB<sup>+</sup>11]. One interesting example is the wireless micro IMU introduced in [HMZ<sup>+</sup>13], that is of particularly small size, high sampling rate and fast performance thanks to efficient sender to base communication and the outsourcing of data processing methods to basic hardware components. With extensive sensor calibration, it can furthermore achieve a high accuracy suitable for motion tracking that is similar to the accuracy of a commercial system. In combination with a water-proof casing, such independent and considerably cheaper sensor devices can become more useful and popular in the near future.

### 4.2.1 Used Sensor Hardware

For the majority of the subsequent applications, I used waterproof 9-axial measurement units from Logical Product (Logical Product. SS-WS1215/SS-WS1216, Fukuoka, Japan) [Log] containing triads of gyroscopes, accelerometer and magnetometer of 16 bit quantization rate for the respective x,y and z axes. Depending on the captured sport and the body segment a sensor got attached to, accelerometers with either a minimum full-scale range of  $\pm 5$  G (usually body placement) or  $\pm 16$  G (ski placement and highly accelerated body parts) have been used. Other specifications, as well as the specifications of the magnetometer and gyroscope have not been changed in any other way. The full sensor specification then is as followed:

- Gyroscope: full-scale range of  $\pm 1500$  dps with 0.67 mV/dps sensitivity
- Accelerometer: minimum full-scale range of  $\pm 16$  G with 62.7 mV/g sensitivity OR minimum full-scale range of  $\pm 5$  G with 191.7 mV/g sensitivity
- Magnetometer: full-scale range of  $\pm 1.2$  Ga

Conforming to biomechanical definitions, the sensor was placed on the human body in such a way that the y-axis was aligned to the bone of the corresponding segment (Figure 4.4). In the same way, the sensor axis measuring data on the longitudinal axis was also defined as y-axis, the axis aligned with the sensor's short side as x-axis and the normal vector to the plane spanned by the x- and y-axis as z-axis. This contradicts general naming conventions from inertial navigation and tracking, where the longitudinal axis is defined as x-axis. Consequently, this naming convention had to be considered when examining the data in subsequent analysis steps: the x-y-z-axial representation was defined by *pitch  $\theta$ -roll  $\phi$ -yaw  $\psi$*  instead of *roll  $\phi$ -pitch  $\theta$ -yaw  $\psi$* . This meant that elevating a body segment was then for example measured as a rotation around the sensor's x-axis.

Possible sampling rates per sensor module ranged from 10 to 1000 Hz. The sensors were started by a start command trigger sent from a sensor control program via Bluetooth, whereas

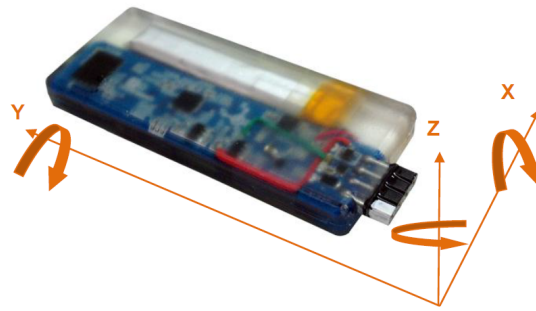


Figure 4.4: Waterproof sensor from Logical Product used in this thesis and its local sensor coordinate system (orange).

multiple sensor modules could be used simultaneously. The inertial measurement data was captured and saved within a memory hardware of the sensor until a stop command was received. Such stop command could be either sent manually from the sensor program or be internally executed after a certain predefined sampling time in seconds. The raw accelerations, angular velocities and magnetic field measures could then be read out for subsequent use.

To draw a valid conclusion on the quality of each orientation estimator, it is essential to know more about the sensor specifications in terms of drift, bias and noise. To adjust to the measurement inaccuracies of every single sensor, a simple, fundamental calibration was performed within the data acquisition processes of all following test data bases. For the accelerometers and gyroscopes, the sensor offset was determined in rest along all sensor axes under working temperature (meaning with the sensor running for a certain time in the capture environment) to avoid temperature drift. This could also mean cold temperatures below 0°C in case of winter ski jumping. For the magnetometers, I determined the local scale and offset factors by rotating the sensors around the main motion axes before or after the main data capturing.

### 4.3 Created Motion Data Bases

Two different kinds of inertial motion capture data sets have been created for this thesis (Table 4.1). A simulated motion data base ( $\mathcal{D}_S$ ) acquired in a laboratory was used to investigate and adjust the general system's accuracy for the set up of the subsequent system. For this, both inertial sensor data and optical motion capture data – serving as accuracy ground truth – were collected. Furthermore, motion data was captured in real application respectively sporting environments from the X-Sens and Logical Product sensing devices. In particular a real jump data base ( $\mathcal{D}_R$ ) of actual ski jumping data was important here since it served as input data for the motion evaluation and rating application.

### 4.3. Created Motion Data Bases

Table 4.1: Comparison of the two main fundamental data sets  $\mathcal{D}_S$  and  $\mathcal{D}_R$  that determined their subsequent use in the computational methods of this thesis.

Name	Description	Purpose	Specifications
$\mathcal{D}_S$	Simulated motions in laboratory setting: 20 sample motion patterns with varying motion dynamics were performed by two different participants. Type: Optical motion capture (Vicon) and inertial motion capture (Logical Product)	Test the accuracy and performance of implemented orientation and position estimation methods.	30 second capture intervals of permanent motion execution. Markers around every sensors captured at 500 Hz with a 11 camera optical motion capture system (calibration accuracy higher than 0.8mm). Body segment motions captured at 500 Hz by 9 inertial measurement units.
$\mathcal{D}_R$	Actual motions in real-world environments and sport locations: ski jumps (119 jumps in main data base), everyday motion, freestyle body movements. Type: Inertial motion capture (Logical Product, XSens)	Test the accuracy of the system in actual application environments. Develop and adapt machine learning methods for retrieval of relevant motion information. Demonstrate sample application of motion rating.	Capture intervals of variant length depending on application purpose (40 second capture intervals for ski jumping). Body segment motions captured at 500 Hz by 9 inertial measurement units.

#### 4.3.1 Simulation and Test Data Base

The simulation and testing motion data base  $\mathcal{D}_S$  was captured using a sensor arrangement of nine Logical Product sensors attached to pelvis (P), and both left and right thigh (rT, lT), shank (rS, lS), foot (rF, lF) and arm (rA, lA) of the athlete. The sensors were positioned to measure motion of all limbs and segments relevant for the execution of the intended target motions. 20 sample motion patterns with varying motion dynamics were performed by two different participants in a common capture studio. Simultaneous and Bluetooth synchronized data was captured by inertial sensor and optical motion capture systems for 30 second intervals. Each inertial sensor was surrounded by 4 optical markers positioned in a rectangular shape (Figure 4.5). These marker's positional changes were captured at 500 Hz with a 11 camera Vicon optical motion capture system (VICON Nexus version 1.7.1. Vicon Motion Systems Ltd, Oxford UK) [Vic] to validate inertial sensor orientation data. The performed motions were chosen in such a way that they could simulate varying motion dynamics and impact forces as they occur in sports (and ski jumping). In concrete, they included walking, jogging, jumping,

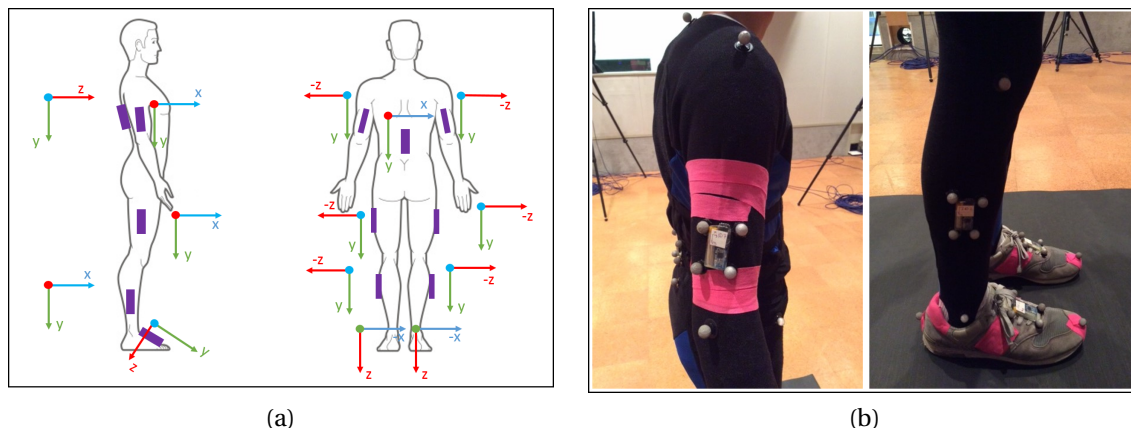


Figure 4.5: Sensor placement for the collection of the simulation data base and the four corresponding optical markers attached to every sensor for the acquisition of ground truth reference data.

turns around the longitudinal axis, jumping jacks, kicking and throwing, leading to a total of  $N = 28$  data captures.

### 4.3.2 Field Motion Data Base

The data set  $\mathcal{D}_R$  comprised multiple independent data bases with data captures of actual sport motions or movements as they occur in real life situations and training environments. In general, they were subject to two different capture devices, the sensors from Logical Product used for the development of all signal processing and machine learning methods, and the XSens sensors used for the sonification of movement. Since the final movement sonification functions in real-time without any fundamental underlying data base, only the data acquired with the Logical Product sensors shall be described here. In this respect, it is particularly important to discuss the main ski jump data captures and their acquisition processes at a ski jumping hill.

#### Ski Jumping Data Base

To obtain a good collection of ski jump data, the following particularities that result from the specifications and natural and environmental characteristics of ski jumping had to be especially taken into account:

**High impact:** High impact is registered during take-off, and particularly during landing, which can lead to perturbations in the sensor data, particularly the gyro rate measurements of the sensors attached to the skis.

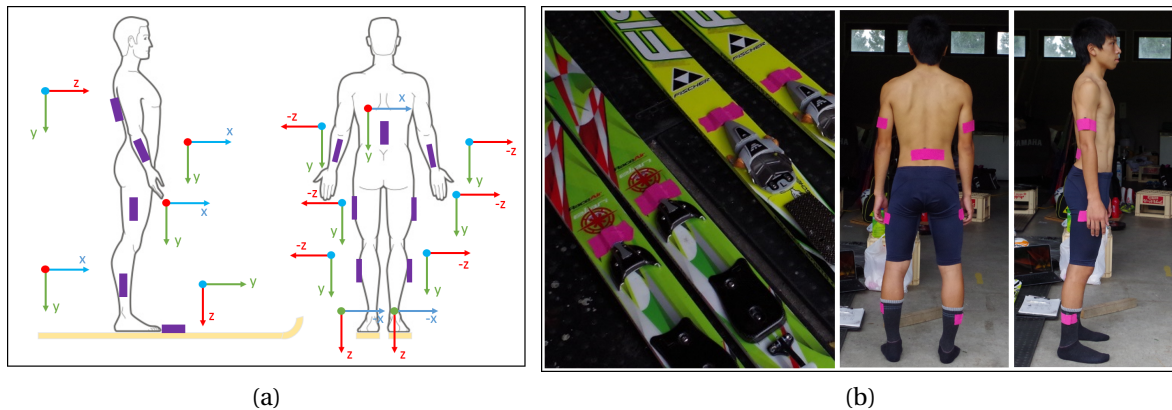


Figure 4.6: Sensor placement for the collection of the field ski jumping motion data base. The sensors are directly attached to the body with adhesive and kinesiology tape.

**Ski oscillations:** During ground contact phases, the ski surface is subject to small oscillations that lead to high noise in the acceleration measurement of the ski sensors and should be suppressed as much as possible.

**Run time:** Under suddenly changing wind conditions, an athlete can prolong the time before in-run start until the wind conditions improve. In training sessions, this phase can last longer than 30 seconds, which requires a sufficient preset run time.

**Sensor interference:** Since the risk of fall and injury is prevalent in every ski jump, the sensors should interfere as least as possible with the freedom of movement of the athlete. Ideally, they should not be perceived at all when attached to the body.

Following the previous constraints and the biomechanical description of the motion, sensor positions chosen for the subsequent jump assessment were: pelvis (P), and both left and right thigh (rT, lT), shank (rS, lS), ski directly at the beginning of the ski boot (rF, lF) and upper arm (rA, lA) of the athletes (Figure 4.6). This means that the sensor arrangement was almost identical to the one used in the simulation and testing data base, where only the sensors rF and lF have been placed differently on the top of the shoe. The sensors were securely placed directly on the athlete's body and ski using adhesive and kinesiology tape before the beginning of every training session. Particular care was taken to ensure similar positions throughout all training sessions.

Over the last two years, I performed several experiments with multiple capture sessions in both summer and winter season to optimize the capture processes and ensure high data quality. The main ski jump data base within  $\mathcal{D}_R$  was then finally created during summer ski jump season in 2015. During two experimental sessions, training jumps of four junior athletes (three ski jumpers and one Nordic combined athlete) were captured at a normal hill with a K-point of 90 meters (Figure 4.7). Every experimental session included multiple

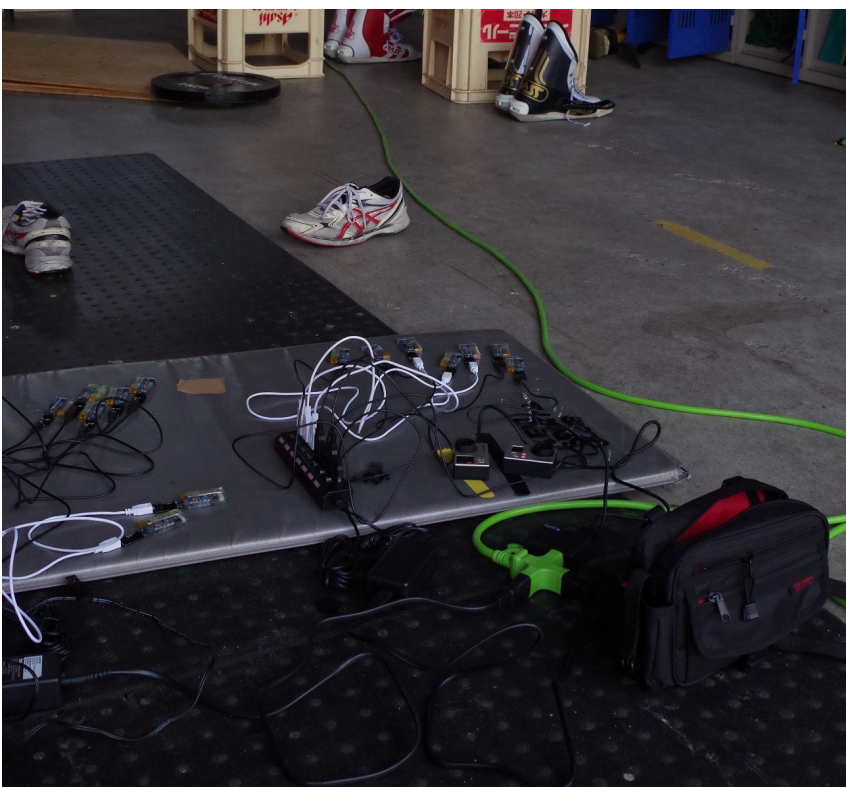
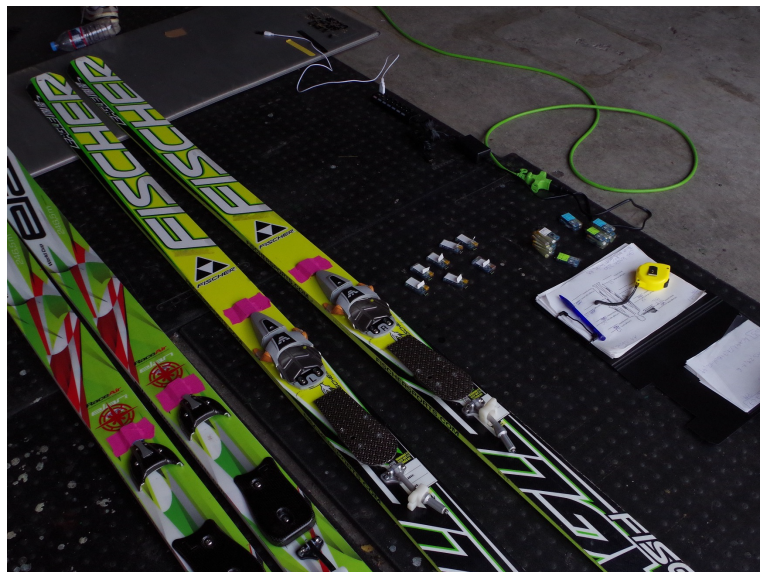


Figure 4.7: Impressions of the data acquisition of summer ski jumping. Pictures of the measurement equipment used and the sensor attachment can be found on the following pages.

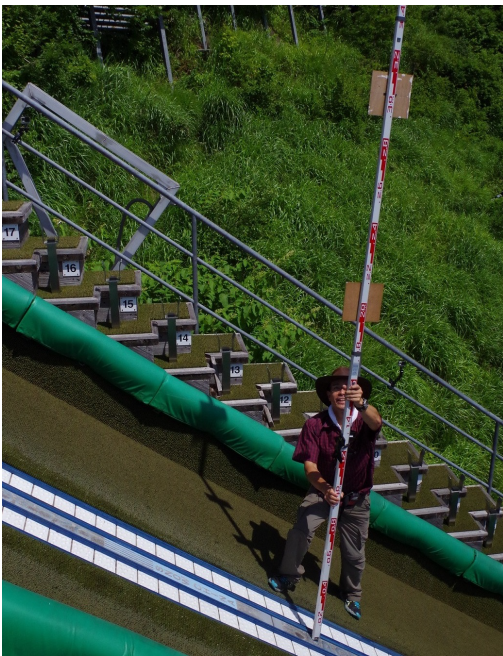
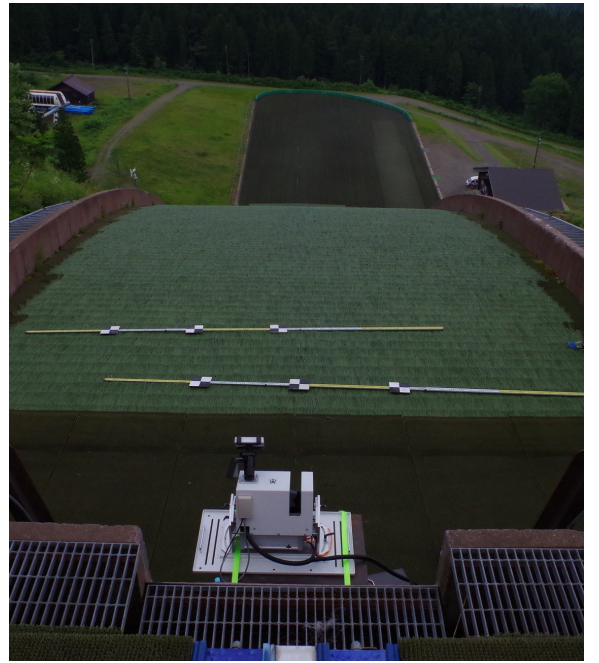
training sessions on several days with five to eight training jumps each. As a result, a total of 180 ski jumps could be captured. Impressions on the field experiments can be found on the following picture pages, which show the measurement technology, sensor device attachment and camera calibration.

In addition to the inertial sensor data, I took note of the length of every jump and its style point scores awarded by a human experienced ski jumping judge. The judge scores were collected on paper in real-time during the data capture sessions and under real judging circumstances from the judge's tower. They therefore conform with score results as they are obtained in real competitions. Collected point deductions were marked under the scoring criteria listed in Table 3.1. After data acquisition, all score sheets were digitized to be used as ground truth in the machine learning and testing step.

Out of the more than 180 jumps captured, 110 consisted of a complete data set with all sensor data files (Appendix C). They were selected as input for  $\mathcal{D}_R$ . For 85 of those data captures, furthermore jump length and judge score annotation were available, so that those captures were additionally marked for a subsequent use in the sense-making and retrieval steps.







## 5 Augmentation of the Collected Motion Data

Having created numeric motion data (bases), it is now necessary to process the data so that useful information can be retrieved in the next step. For the present motion data, this means to determine kinematic properties (namely segment orientation and joint position) of the moving body that define the motion under biomechanical and physical aspects. Therefore, I next want to explain the fundamental computation methods and algorithms chosen for use in the subsequent retrieval steps with  $\mathcal{D}_S$  and  $\mathcal{D}_R$ . They are introduced in sequential order as they occur in the complete processing pipeline.

### 5.1 Estimating Initial Posture

To compare data and their kinematic parameters within different trials, it is necessary to know the initial orientation of each sensor. Especially if trials from different venues and hence differing starting positions are compared to each other, the main performance characteristics should be independent of the starting environment and invariant to spatial variations. Furthermore, a system that provides motion information in real-time at the start of every jump is required to analyze motions during competition and training sessions. Consequently, I added a method to the processing pipeline that can determine the initial orientation of the sensors attached to the athlete's body. From the initial posture, one can then compute the spatial variations out of the data sets and hence get a uniquely valuable estimation result. Using the initial orientation guess, it furthermore becomes possible to start the subsequent data processing steps in any position, so that distraction of the athlete can be avoided.

I chose to determine the initial orientation of all sensors with a non-fusion vector-based orientation estimator method *VB*, a variation of the QUaternion ESTimator (QUEST) algorithm [YBM08]. *VB* originally got developed in the context of spacecraft attitude determination to solve the problem of determining attitude from magnetometer and accelerometer measurements only. In the algorithm, attitude is represented as a combination of the rotational displacements around the three principal axes in the global frame: a rigid body can be placed in an arbitrary orientation by consecutive rotations around the three axes. In static environments under no external acceleration, those rotations are described by trigonometric correlations from the raw sensor (field) vectors. Therefore, the algorithm is very quick and well suited to estimate the orientation of a static or slow-moving rigid body with no or little external acceleration, as it is for example the case for the ski jump start where the athlete is

## Chapter 5. Augmentation of the Collected Motion Data

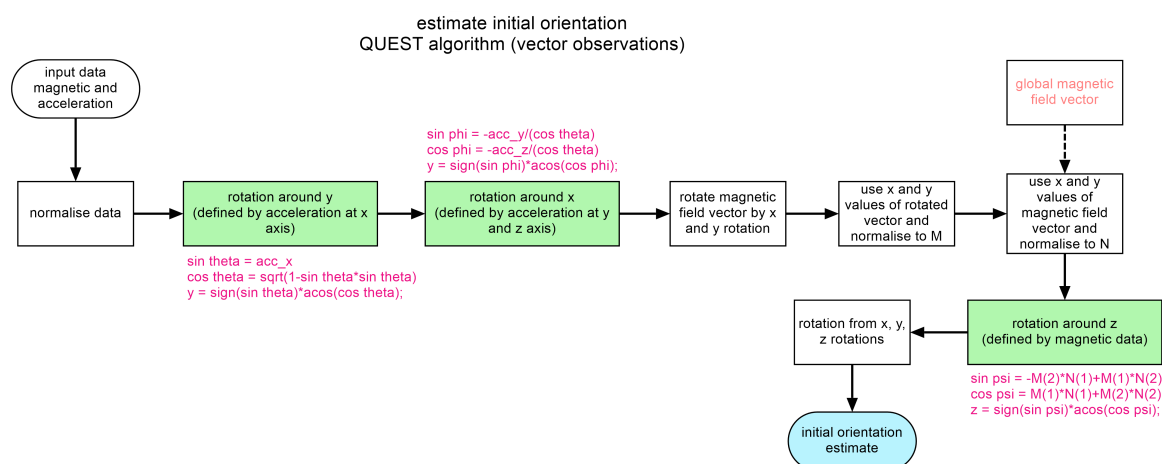


Figure 5.1: Working principle of the vector-based orientation estimator  $VB$  to estimate the initial posture in static position at the beginning of every data capture.

sitting on the start gate prior to any movement. For the creation of all other data captures, participants were instructed to stay in a motionless position for approximately two seconds before starting the performance of the requested motion task. This ensured the initial posture estimate to yield stable and reliable results. In general, one observation vector from a static time step is already sufficient to estimate the orientation at the designated frame. However, I recommend to average the orientation estimate over several frames to get a result that is more indifferent against temporary deviations and noise in the sensor data.

A principal sequence for the determination of any angular displacement in Euler angles would be to first rotate the examined rigid object (meaning the sensor) about its z-axis by the yaw angle  $\psi$ , then about its y-axis by the pitch angle  $\theta$  and finally about its x-axis by the roll angle  $\phi$ . The local accelerometer and magnetometer readings will change in accordance to the rotations and trigonometric correlations of  $\phi$  and  $\theta$ . The magnetic field measurements are computed in reference to a ground magnetic field vector, which generally constitutes the magnetic field vector of the local position on earth and are only used to determine the estimate of  $\psi$ . Consequently, magnetic distortions do not affect the estimates of roll and pitch. In this way, three quaternions for the rotations around the main axes in the sensor-earth coordinate frame are computed -  $q_p$  for pitch,  $q_r$  for roll and  $q_h$  for the heading - that are then multiplied in the order  $q_h \times q_p \times q_r$  to build the final normalized initial output quaternion  ${}^S q_{j1}$  for body segment  $j$  (Figure 5.1).

During the implementation of the initial posture estimator, two points should be kept in mind since they enable adaptations to the certain circumstances. First,  $VB$  can only yield a complete orientation estimate if both magnetometer and accelerometer data are available. Using only accelerations, it is possible to determine the initial estimates for pitch and roll angles, but not for the heading. In such a case, the heading estimate either has to be guessed,

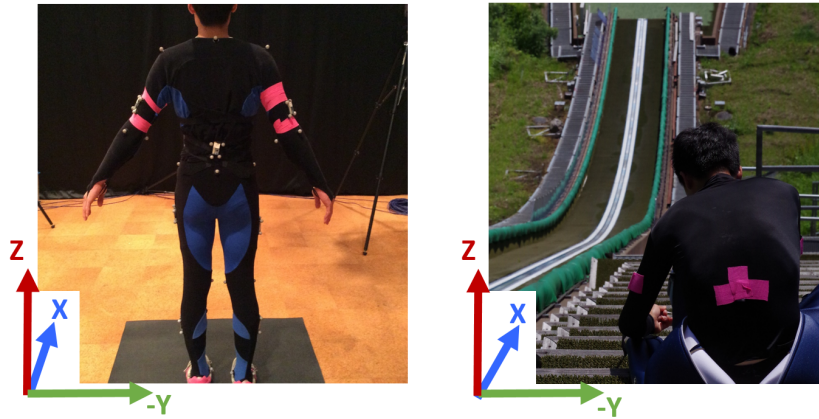


Figure 5.2: Inertial capturing in the defined global coordinate system under the laboratory setting ( $\mathcal{D}_S$ , left) and at the ski jump hill ( $\mathcal{D}_R$ , right).

set to zero or be computed by an additional preestimate. Second, the magnetic field reference vector that determines the heading from the magnetic field data input in  $VB$  can be any possible field vector appropriate for the intended application. This means, the field vector can be adapted and that the heading can be defined with the semantic content of a motion independently of general local environments and their magnetic heading. For example, the direction parallel to the direction of view or the main direction of motion can serve as zero yaw angle. Such reference vector has to be measured before the commencement of the main data acquisition to serve as data input in the computation.

## 5.2 Estimating Sensor Orientations

Apart from the  $VB$  method, I implemented different attitude determination methods. They are popular algorithms for the processing of inertial sensor data and have been widely used over the last years. Especially when capturing jumping scenarios, one can assume that free fall and aerodynamic conditions impose special requirements on the orientation estimation algorithms, or that high-impact phases influence the accuracy of estimates during the affected time periods. With several processing methods available, chances are higher to identify and choose the best processing method for a specific motion task, so that all implemented estimators shall be discussed in the following.

### 5.2.1 Global Coordinate Frame Settings

At every sample  $t$ , an orientation estimation filter returns an output orientation  ${}^S_E q_{est,t}$  in the sensor to global earth frame  ${}^S_E$ . To make further use of the estimated orientations, it is helpful to know the definition and directions of the global earth frame. Then, it becomes easier

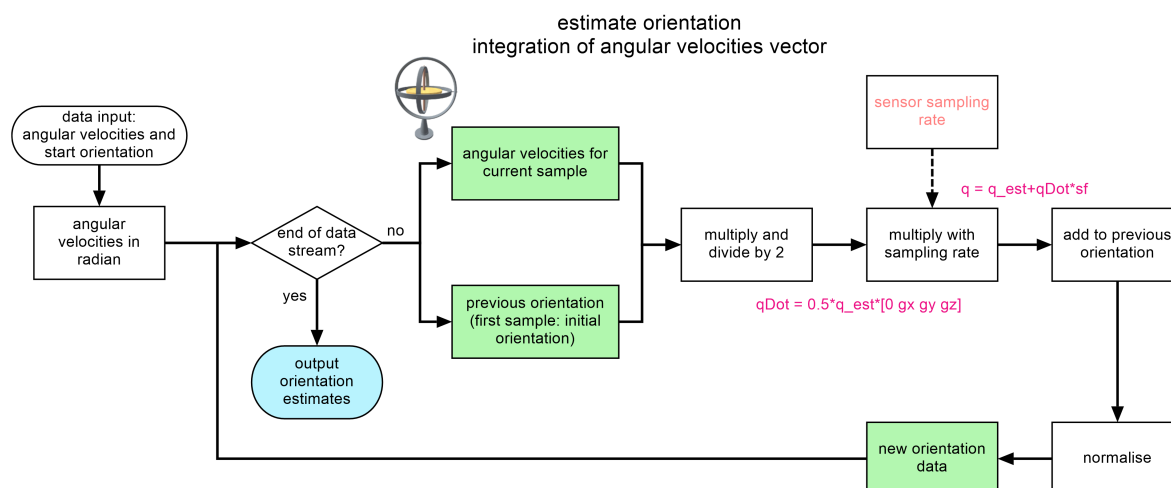


Figure 5.3: Working principle of the angular velocity integration estimator *GI*.

to reenact the computed postures and angular changes under semantic and sport-specific aspects. For the following computations, the global earth frame was defined by Z functioning as the vertical, Y as the transverse and X as the sagittal axis (Figure 5.2). For  $\mathcal{D}_S$ , X was aligned with the x-axis of the optical motion capture system, for  $\mathcal{D}_R$  X was aligned with the landing and outrun phase of the ski jump hill.

### 5.2.2 Angular Velocity Integration

Angular velocity can be derived from angular displacement in the same way as velocity and acceleration can be derived from positional displacement. In theory then also the opposite way must be true, so that orientation can be obtained by integrating angular velocity. However, integration is never absolutely exact and always contains an unknown error that sums up over time. Depending on the quality of the used gyroscopes, sensor bias might further distort the estimate. As a result, the accuracy of the integrated data estimates will deteriorate over time and the orientation estimate veer away from the actual orientation. This error is broadly known and referred to as drift. Without any further constraints that regulate the drift problem, a simple integration estimator is therefore not suitable for long term orientation determination. In this work, gyroscope integration has been implemented to test the effects of long term drift and to compare its results to other, more sophisticated methods.

There are several ways to integrate angular rates computationally. The easiest would be to work with Euler representations and numerically compute the integrated angular rate values for every time step and all three rotation axes. However, as mentioned before, all estimators in this application are intended to be free of any singularities induced by the use of Euler angles. Therefore, I estimated the orientation with a simple quaternion data integration process *GI*

on the base of quaternion multiplication (Figure 5.3). First, I expanded the three-dimensional vector  ${}^s\omega$  containing the angular rates  $\omega_x$ ,  $\omega_y$  and  $\omega_z$  of the  $x$ ,  $y$  and  $z$  axes in the sensor frame to four dimensions. A quaternion derivative  ${}^S_E\dot{q}$  that described the angular change in the earth frame  $E$  relative to the sensor frame  $S$  was then defined as  ${}^S_E\dot{q} = \frac{1}{2}{}^S\hat{q} \otimes {}^s\omega$ . Finally, the numeric integration of the earth frame relative to the sensor frame  ${}^S_Eq_{\omega,t}$  at time step  $t$  was determined by the following equations

$${}^S_E\dot{q}_{\omega,t} = \frac{1}{2}{}^S\hat{q}_{est,t-1} \otimes {}^s\omega_t \quad \text{and} \quad (5.1)$$

$${}^S_Eq_{\omega,t} = {}^S_E\hat{q}_{est,t-1} + {}^S_E\dot{q}_{\omega,t} \Delta t, . \quad (5.2)$$

Here,  $\Delta t$  is the sampling frequency, and the sub-script  $t$  indicates that the estimate is valid for time step  $t$ .

### 5.2.3 Fusion Filter

A Fusion Filter is an orientation estimator that combines the integration estimate from a gyroscope with the estimate from vector observations. The quaternion  $q_{\omega}$  obtained from integration of the angular velocities serves as fundamental orientation estimate, which is then refined by adding information from the observation vectors to the final output estimate  $q_{est,t}$  in every time step  $t$ . The idea is that this sensor combination creates a faster, more efficient and nearly drift free output quaternion. Over short periods of time and for highly-dynamic periods with much external acceleration, the integrated data from the gyroscope is used to give an orientation estimate. This is because the short term gyroscope integration is very precise and not susceptible to external forces. During phases of low external acceleration on the other hand, the estimate obtained from the vector-observations is more precise as it is drift-free and can be used to enhance the estimate. The positive effect of fusion filters on the resulting sensor estimates are well known and shown in various works [BLS<sup>+</sup>14, RLMLP16, LDJ<sup>+</sup>16].

#### Optimization Based Fusion Filter

The first implemented fusion filter *CF1* was introduced in 2010 and combines the gyro rate estimate  ${}^S_Eq_{\omega,t}$  with an estimate  ${}^S_Eq_{\Delta,t}$  obtained from the gravity and magnetic field vectors. In the simplest form, the final orientation estimate  ${}^S_Eq_{est,t}$  for every time step  $t$  is built as

$${}^S\hat{q}_{est,t} = \gamma_t {}^S_Eq_{\Delta,t} + (1 - \gamma_t) {}^S_Eq_{\omega,t}, \quad (5.3)$$

with  $\gamma$  being a filter value that represents the gyroscope measurement error that is removed in the direction of the error estimated with  ${}^S_Eq_{\Delta,t}$ . While  ${}^S_Eq_{\omega,t}$  is computed in the same way as described in Section 5.2.2, the values for  ${}^S_Eq_{\Delta,t}$  are obtained using a gradient descent opti-

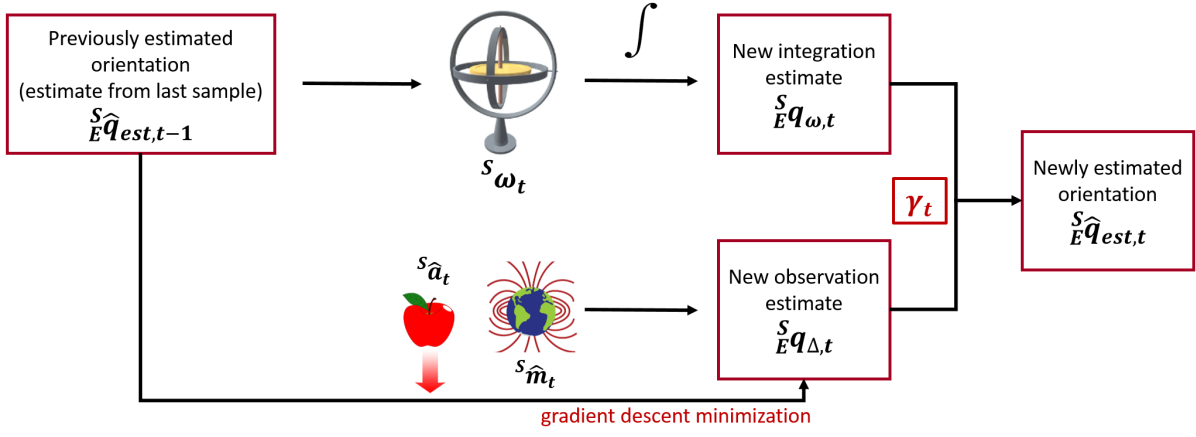


Figure 5.4: Simplified working principle of the gradient descent optimization based complementary fusion filter *CF1*.

mization approach [MHV11] motivated by the difference between the actual orientation and the orientation estimated by the data from accelerometers and magnetometers (Figure 5.4). In concrete, a unique orientation representing the spatial rotation  ${}^S_E \hat{q}$  aligning a predefined reference direction of the field  ${}^E \hat{d}$  in the earth frame with the measured direction of the field  ${}^S \hat{s}$  in the sensor frame should be found. This optimization problem can be described by an objective function  $f({}^S_E \hat{q}, {}^E \hat{d}, {}^S \hat{s})$  that can then be minimized in the optimization step.

Several computational steps are taken to determine  ${}^S_E q_{\Delta, t}$  under the formulated optimization problem. First, the reference and measured direction vectors used in the objective function are defined with respect to the observation measurements. For the accelerometer,  ${}^E \hat{d}$  can be defined in a simple way under the assumption that the vertical z-axis is parallel to the direction of gravity, so that  ${}^E \hat{g} = [0 \ 0 \ 0 \ -1]$ . Furthermore, the normalized accelerometer measurement builds  ${}^S \hat{s}$  as  ${}^S \hat{a} = [0 \ a_x \ a_y \ a_z]$ . Similar assumptions can be drawn for the magnetometer measurements: the earth's magnetic field  ${}^E \hat{b} = [0 \ b_x \ 0 \ b_z]$  has components in one horizontal axis and a vertical axis and can substitute  ${}^E \hat{d}$ . For  ${}^S \hat{s}$ , the normalized magnetometer measurement  ${}^S \hat{m} = [0 \ m_x \ m_y \ m_z]$  is used. As a result, two simplified objective functions  $f_g({}^S_E \hat{q}, {}^S \hat{a})$  and  $f_b({}^S_E \hat{q}, {}^E \hat{b}, {}^S \hat{m})$ , and two simplified Jacobian matrices  $J_g({}^S_E \hat{q})$  and  $J_b({}^S_E \hat{q}, {}^E \hat{b})$  are obtained.

Next, the two objective functions and two Jacobians are combined to generate a unique solution for the minimization problem. Based on the previous orientation estimate  ${}^S_E \hat{q}_{est, t-1}$  and the objective function gradient  $\nabla f$  built from the objective function and Jacobian for accelerometer and magnetometer, the estimated orientation  ${}^S_E \hat{q}_{\Delta, t}$  at time step  $t$  is

$${}^S_E \hat{q}_{\Delta, t} = {}^S_E \hat{q}_{est, t-1} - \mu_t \frac{\nabla f}{\|\nabla f\|}. \quad (5.4)$$

$\mu_t$  depicts the step size of the gradient decent estimation step. With  $\Delta t$  being the sampling period and  ${}^S_E \dot{q}_{\omega,t}$  being the physical orientation rate measured by the gyroscopes, it can be calculated as  $\mu_t = \alpha \|{}^S_E \dot{q}_{\omega,t}\| \Delta t$ ,  $\alpha > 1$ . The variable  $\alpha$  is an augmentation of  $\mu$  to account for noise in the accelerometer and magnetometer. Assuming that the convergence rate of  ${}^S_E q_{\Delta}$  is equal or greater than the physical rate of change of orientation, the previous equations ensures an optimal fusion between  ${}^S_E q_{\Delta,t}$  and  ${}^S_E q_{\omega,t}$ . Therefore,  $\alpha$  has no upper bound and can be assumed to be very large, which implies that  $\mu_t$  also becomes very large. A large  $\mu_t$  however means that  ${}^S_E q_{est,t-1}$  in the gradient decent estimator function becomes negligible and hence the orientation filter equation 5.4 for the vector observation simplifies to

$${}^S_E q_{\Delta,t} \approx -\mu_t \frac{\nabla f}{\|\nabla f\|}. \quad (5.5)$$

Having determined the optimization based orientation estimate, it has to be fused with the integration estimate to a final estimate in the next step. First, the optimal  $\gamma_t$  value is defined as that value which ensures that the weighted divergence of the primary input  ${}^S_E q_{\omega,t}$  is equal to the weighted convergence of the correcting input  ${}^S_E q_{\Delta,t}$ . This definition leads to

$$\gamma_t = \frac{\beta}{\frac{\mu_t}{\Delta t} + \beta} \quad \text{and} \quad (5.6)$$

$$\gamma_t \approx \frac{\beta \Delta t}{\mu_t} \quad \text{under} \quad \gamma_t \approx 0 \quad (5.7)$$

with  $\beta$  functioning as a filter gain corresponding to the gyroscope measurement error including sensor noise, signal aliasing, quantization errors, calibration errors or sensor misalignment. Finally, all elements of the simple filter definition (Equation 5.3) are replaced with one of the former variable definitions. The equation is then transformed a last time to obtain a concrete estimation from the estimated rate of change of orientation  ${}^S_E \dot{q}_{est,t}$  and the direction of the error  ${}^S_E \hat{q}_{\epsilon,t}$  of  ${}^S_E \dot{q}_{est,t}$ :

$${}^S_E \dot{q}_{est,t} = {}^S_E \dot{q}_{\omega,t} - \beta {}^S_E \hat{q}_{\epsilon,t} \quad \text{with} \quad {}^S_E \hat{q}_{\epsilon,t} = \frac{\nabla f}{\|\nabla f\|}. \quad (5.8)$$

How to implement all of the previous computation steps is shown in Figure 5.5. Furthermore, the filter can be made more robust against sensor measurement errors by adding magnetic distortion and gyroscope bias drift compensation. For further information see the official description from Magdwick [MHV11]).



## Chapter 5. Augmentation of the Collected Motion Data

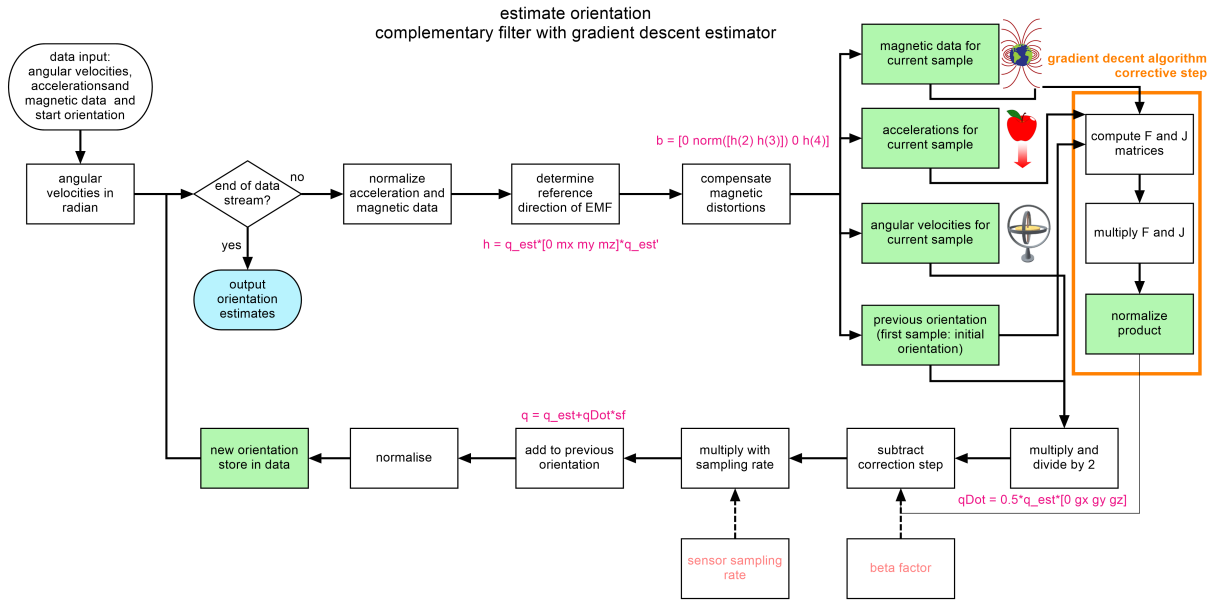


Figure 5.5: Detailed description of the working principle of CF1 illustrating all computation steps.

### Rotation Matrix Based Fusion Filter

The next filter CF2 was a modification of the simple filter fusion scheme and was introduced in 2008 by Mahony [MHP08]. Similar as for the previous fusion filter, the final orientation estimate  ${}^S_E q_{est,t}$  for every time step  $t$  is built by correcting the gyro rate estimate  ${}^S_E q_{\omega,t}$  with a vector observation estimate, whereas it is not necessary to determine the concrete values for  ${}^S_E q_{\Delta,t}$  in the present filter. The computation is based on the idea that the angular changes determined with the vector observations can be represented in a rotation matrix, the Direction Cosine Matrix (DCM) [ECM+08] (Figure 5.6). In the original DCM filter algorithm, magnetic measurements are not included as vector observations. In this work, a filter version is used that detects pitch and roll deviations from the accelerometer data and deviations in yaw from the magnetometer, similar as in the VB method for estimation of the initial posture (Section 5.1).

The divergence of integration and sensor measurement is weighted by means of two error measures for the error induced by drift and sensor bias and the numerical integration error. To determine the two error measures, one first computes the direction of gravity  $\hat{v}$  and magnetic field  $\hat{w}$  with the previous estimated quaternion  $q_{\omega}$  and the earth's magnetic field  ${}^E \hat{b}$ . Proportional (sensor induced) error feedback  $e$  is obtained by the cross product between the estimated direction vectors from  $q_{\omega}$  and the field measurements from the accelerometer  $\hat{a} = [a_x \ a_y \ a_z]$  and magnetometer  $\hat{m} = [m_x \ m_y \ m_z]$ :

$$e = \hat{a} \times \hat{v} + \hat{m} \times \hat{w}. \quad (5.9)$$

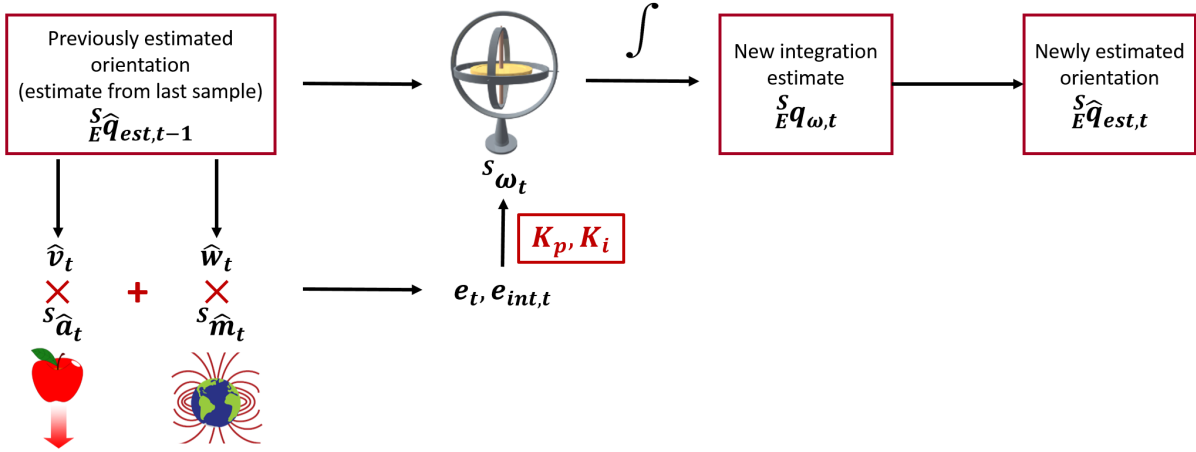


Figure 5.6: Simplified working principle of the rotation matrix based complementary fusion filter *CF2*.

The error accumulating with integration over all previous time steps per time step  $\Delta t$  constitutes the integration error correction term  $e_{int}$ :

$$e_{int,t} = e_{int,t-1} + e * \Delta t. \quad (5.10)$$

Having determined the fundamental definitions for the estimation of the error measures, the general fusion filter equation (Equation 5.3) is adapted next. Under the present problem definition, no  $\gamma_t$  value that controls the convergence between primary input  $^S_E q_{\omega,t}$  and correcting input  $^S_E q_{\Delta,t}$  is necessary. Instead,  $e$  and  $e_{int}$  are weighted and added to the angular velocities using the two filter gains  $K_p$  and  $K_i$ . They control the influence of the correction terms  $e$  and  $e_{int}$  on the output estimate by

$$^S \omega_t = ^S \omega_t + K_p * e + K_i * e_{int}. \quad (5.11)$$

Finally, the angular velocity data  $^S \omega_t$  in quaternion form is integrated (Section 5.2.2) to yield the output estimate  $^S_E q_{\omega,t}$ .

Although the algorithm's general work flow (Figure 5.7) looks very similar than the one for *CF1*, Equation 5.9 reveals that the algorithmic component of the filter is much simpler, which keeps the implementation of the algorithm east and quick. Consequently, the computational complexity of the filter is also smaller, making it very fast and convenient to use. In the same way as for *CF1*, the filter can furthermore be made more robust against variations in the magnetic measurements by adding magnetic distortion compensation in the implementation.

## Chapter 5. Augmentation of the Collected Motion Data

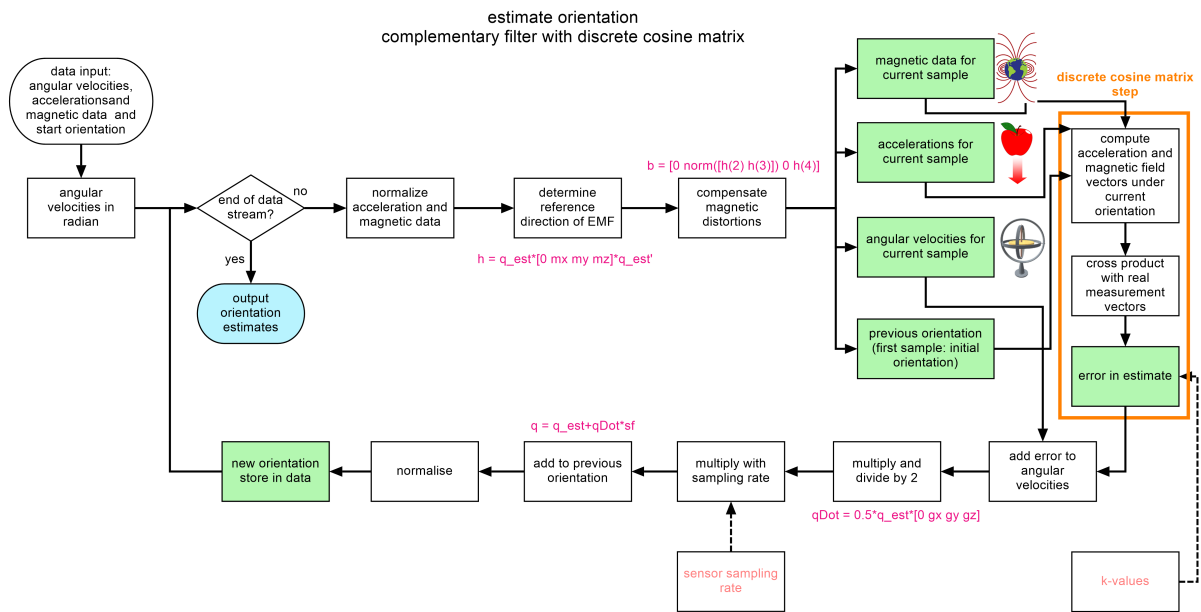


Figure 5.7: Detailed description of the working principle of *CF2* with all computation steps.

### Optimization Based Pseudo-linear Kalman Filter

The last fusion filter *KF* was a variation of the Kalman Filter, a general algorithm to estimate unknown variables from multiple time series data of (one or higher dimensional) noisy, randomly variable and inaccurate measurements. The basic idea behind the *KF* is that by combining several measurements, a more precise output estimate is computed than by using a single measurement. Consequently, it can be adapted well to the different data obtained with an IMU. Many different variations and adaptations of the *KF* for fusion of the angular velocity, accelerometer and magnetometer data have been proposed in literature, making it the most common filter type for orientation estimation with IMU sensors.

The general working principle of a *KF* for orientation estimation is as follows: from a previous or initial guess (the prior knowledge of state), a new value is predicted on the base of the angular velocities of the next time step. This prediction is then compared to the observations of the correcting sensor measurement data and the credibility of the prediction and observations dynamically rated using information about measurement noise and inaccuracies. This means that the influence of every guess on the next estimate is dynamically adapted to the certain conditions of that specific time step. As a result, an output estimate is determined that is then again used as previous guess for the next time step. For the computation of the estimates it is needed to specify the following variables at the beginning of the filter computation:

- A description of the signal value  $x_t$
- A measurement value  $z_t$

## 5.2. Estimating Sensor Orientations

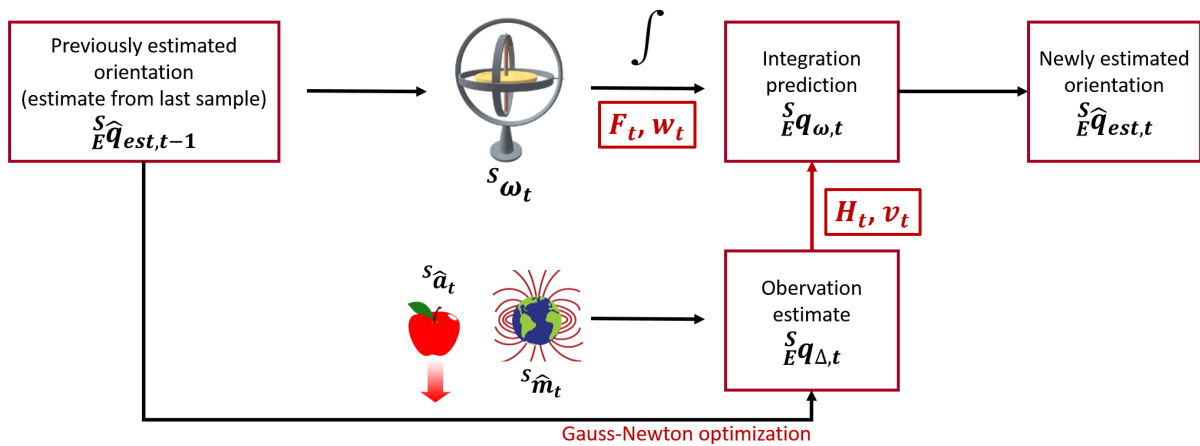


Figure 5.8: Simplified working principle of the optimization based pseudo-linear Kalman fusion filter  $KF$ .

- A value for the control signal  $u_t$
- A value for the process noise  $w_t$  representing the noise that arises by making a first orientation estimate
- A value for the measurement noise  $v_t$
- $F_t$ , which is called the state-transition model and which gets applied to the previous state  $x_{t-1}$  to compute a first guess for the new time step
- $B_t$ , which is called the control-input model and which gets applied to the control vector  $u_t$ ,
- $H_t$ , which is called the observation model and which maps the true state space into the observed space
- $Q_t$ , the covariance of the process noise
- $R_t$ , the covariance of the observation noise

The KF was first introduced for linear systems, but can be extended to nonlinear systems of complex input data. Such extended Kalman filter is the standard for the use of inertial sensor data with its different input vectors (orientation from the previous time step, accelerometer, gyroscopic and magnetometer measurements). However, its complexity and computation time is higher than in linear filters. I therefore chose to use a KF that refines the primary estimate  $^S_{\hat{E}}q_{\omega,t}$  from the integration estimate with a precomputed vector-based orientation quaternion  $^S_{\hat{E}}q_{\Delta,t}$  functioning as observation input in the Kalman Filter's update step [MYB<sup>+</sup>01, YB06] (Figure 5.8). In this way, the same number and types of input and output values are used, so that the filter is of linear complexity and faster than a conventional extended KF.

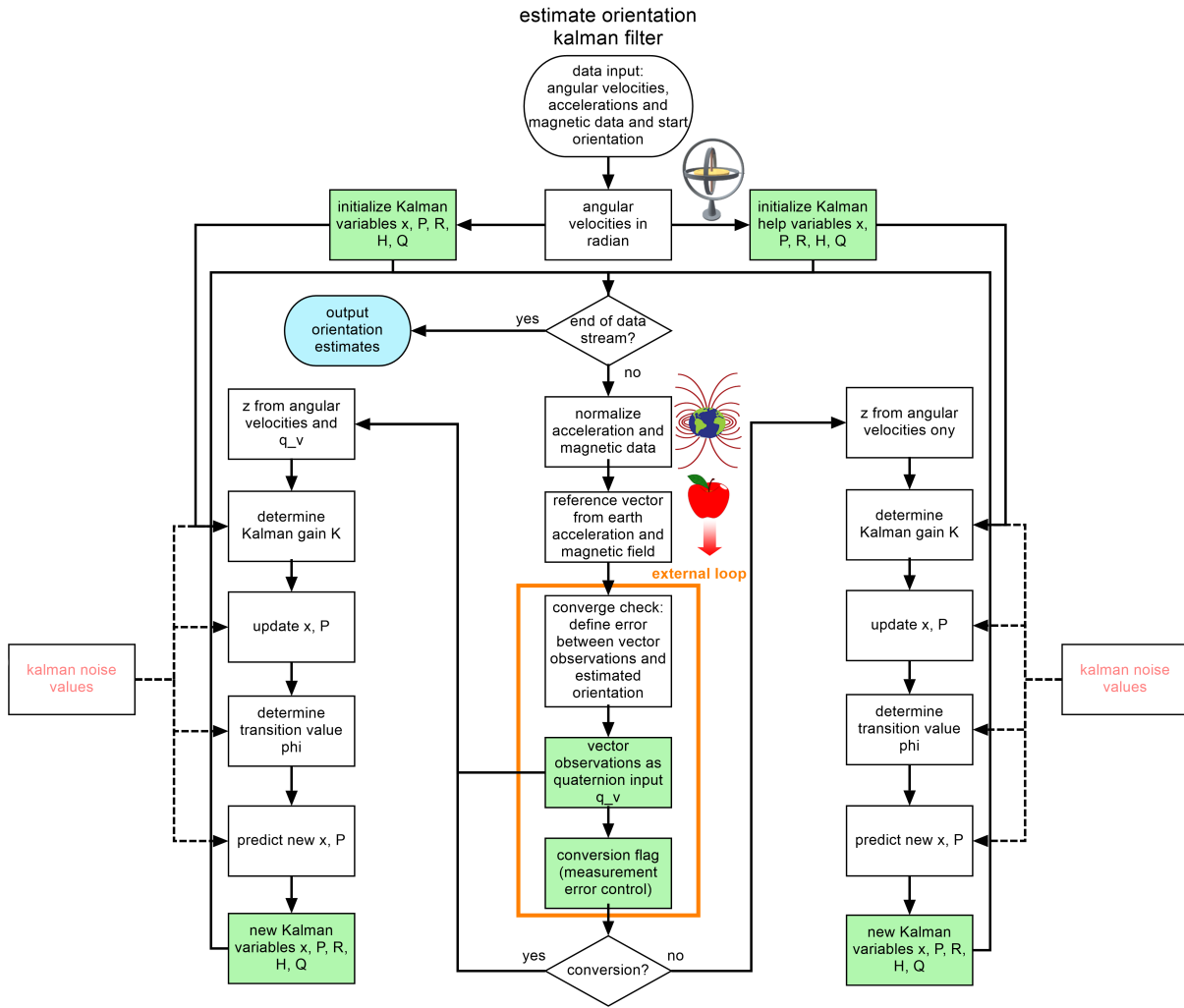


Figure 5.9: Detailed description of the working principle of  $KF$  with all computation steps.

The process model is described by the quaternion integration process as

$$x_t = F_t x_{t-1} + B_t u_{t-1} + w_t \quad (5.12)$$

$$z_t = H_t x_t + v_t. \quad (5.13)$$

In accordance to the process model, the signal value containing the states of  $x$  is a 7-dimensional vector containing the angular rates among all three dimensions and the four components of  ${}^S_E q_{\omega,t}$ .

The common approach of an extended  $KF$  would now be to use a 9-dimensional vector containing the measurements for angular rate, accelerometer and magnetometer in all three axes as measurement value vector  $z$ . To obtain the same number of input and output values for the  $KF$  (and hence keep the  $KF$  less expensive), the orientation estimation from the vector

## 5.2. Estimating Sensor Orientations

Table 5.1: Number of process model state values  $x$  and observation measurement values  $z$  used by the chosen Kalman filter.

Val #	State $x$	Observation $z$
1	angular rate of x-axis	angular rate of x-axis
2	angular rate of y-axis	angular rate of y-axis
3	angular rate of z-axis	angular rate of z-axis
4	quaternion component $q_0$ (scalar component)	quaternion component $q_0$ (scalar component)
5	quaternion component $q_1$	quaternion component $q_1$
6	quaternion component $q_2$	quaternion component $q_2$
7	quaternion component $q_3$	quaternion component $q_3$

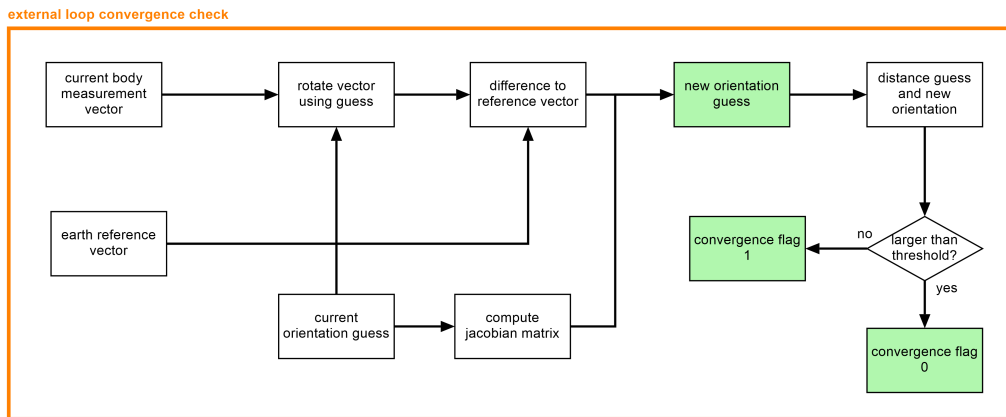


Figure 5.10: Working principle of the external orientation estimation and convergence step used by  $KF$ .

observations is moved to an independent computation step as an outside loop of the KF. This estimate is then used as observation measurement vector. Consequently, the elements are exactly the same as the states listed in Table 5.1. The values for  $R$ ,  $H$ ,  $Q$  and the noise vectors needed in the update step of the Kalman filter are determined experimentally for the individual inertial sensor used. For this thesis, their values have been determined in a long term observation of the sensors in rest. A more detailed, but also complex, possibility would be to determine the noise values by the Allan Variance [ESHN08, Hou05].

Although the output equations are linear, it is still necessary to use an extended KF because a part of the state equation is nonlinear. Therefore, the filter design is called pseudo-linear KF in this work. The success of such Kalman filter design is strongly dependent on the pre-estimation method. To find the quaternion that best relates the measured accelerations and earth magnetic field measurements to the reference directions in the earth coordinate frame, any orientation estimation strategy can be used. Here, a Gauss-Newton optimization method has been selected to be integrated in the overall filter process (Figure 5.10). This method

## Chapter 5. Augmentation of the Collected Motion Data

---

resembles the gradient descent optimization, but was shown to be faster than the gradient descent method since it requires less iterations for getting to a stable result. Furthermore, it is invariant against 'zigzag' effects, a moving around the minimal values in both left and right direction. The conversion of the measurement data that will then be minimized in the optimization step is described by an error function  $Q$  as

$${}^E Q = \varepsilon^T \varepsilon = ({}^E y_e - M^B y_b)^T ({}^E y_e - M^B y_b), \quad (5.14)$$

where  ${}^E y_e$  is a six-dimensional vector containing the measurements of accelerometer and magnetometer in the earth frame and  ${}^B y_b$  is the vector in the body frame. Furthermore,  $M = \begin{pmatrix} R & 0 \\ 0 & R \end{pmatrix}$  with  $R$  being the common general 3x3 rotation matrix. From the quaternion  $n_k$  for the current time step  $k$  one can then iteratively compute the quaternion for the following time step  $k+1$  via the Jacobian  $J$  as

$$\hat{n}_{k+1} = \hat{n}_k - [J^T(\hat{n}_k) \quad J(\hat{n}_k)]^{-1} J^T(\hat{n}_k) {}^E \varepsilon(\hat{n}_k). \quad (5.15)$$

Since there is not a quaternion that exactly converts what is measured - meaning the sensor data in body frame - into the known values - meaning the sensor data in earth frame - it is necessary to check the convergence of the preestimated observation quaternion. To make sure that the error  $Q$  for converting the measurements to the earth frame is minimized, the main goal of the algorithm is to find good initial values for the quaternion  $n$ . Besides, only few calculations are necessary for the computation of the next quaternion estimate under such good initial guess, which keeps the algorithm of low complexity.

### 5.2.4 Filter Designation

In the following chapter, I describe how the presented filters were tested for accuracy and evaluated for their use in sports. Besides, all derived body kinematics should be utilized within the sense-making step of the data processing pipeline, so that the filters herewith serve as input for a motion information system. Therefore, Table 5.2 summarizes the type, abbreviations (ID) and characteristics of all filters for reference in the subsequent chapters of this thesis.

## 5.2. Estimating Sensor Orientations

Table 5.2: Overview of the implemented orientation estimation methods including the abbreviations used in the following investigations as well as references to the works describing their original concept design.

Name	Type	ID	Description	Reference
Integration filter	non-fusion	GI	Integrates the angular velocity data by quaternion integration to a quaternion output estimate.	
FQA-QUEST filter	non-fusion	VB	Determines a quaternion output estimate by the measurement from accelerometer and magnetometer only. The computation is based on simple trigonometric relations and half-angle computations.	[YBM08]
Gradient Descent based Complementary Filter	fusion	CF1	The integration estimate is refined by accelerometer and magnetometer data with a Gradient Descent Optimization algorithm to a quaternion output estimate. The influence of the correction from the vector estimate is determined by the variable $\beta$ .	[MHV11]
Rotation Matrix based Complementary Filter	fusion	CF2	The angular velocity data used for the integration estimate to build a quaternion output estimate is corrected on the base of two error measures $K_p$ and $K_i$ determined via the rotation matrix and the accelerometer and magnetometer data.	[ECM <sup>+</sup> 08]
Pseudo-linear Kalman Filter	fusion	KF	Enhances the integration estimate with an orientation estimate precomputed by the observation data of accelerometer and magnetometer to a quaternion output estimate. The noise values $w_k$ and $v_k$ are essential parameters of the filter settings.	[YB06]



### 5.3 Determining Body Segment Orientations

Ideally but not practical, the sensor could be directly placed on the bones of an athlete and the sensor data be expected to represent the mounted body segment without any further processing. However in the real world, varying anthropometrics of participants and the manual sensor placement process create a displacement between the sensor placement and the real bone structure which has to be considered for subsequent data analysis. For this, I performed a sensor-bone calibration similar to a method previously described [LVB05] at the commencement of every capture session. From this calibration data, the difference between sensor frames to the global coordinate frame could then be determined. Since the sensor placement did not change within one session, the displacement remained the same for all captures of one training set.

Two calibration measurements are necessary. Firstly a static measurement to determine the displacement to the direction of gravity. Secondly a rotational movement around one predefined axis to determine the displacement to the respective rotational axis.

In the first step, the athletes are asked to stand still in the anatomical position with the affected body segments perpendicular to the ground surface so that the longitudinal axes of the bones are parallel to the direction of gravity and the z-axis direction of the defined global coordinate system. The displacement of the sensor placement at segment  $j$  along the global z-axis  ${}^S z_j^-$  is then given by the differences in the normalized acceleration vector to the unit vector along z. Here, the  $-$  in the notation depicts that the direction vector will be refined in a later step to keep the axes of the sensor frame perpendicular. In the second step, the participants are asked to move all sensor mounted body segments around one of the remaining two axes of the sensor frame, for example to swing the legs or to bend the torso around the transverse axis. Ideally, the deviation  ${}^S a_j$  from the respective rotation axis can then be determined from the direction of the point of maximal angular velocity at the rotation turning point.

From the two deviations one can then determine the axial displacements of the sensor to the global coordinate system. The sensor frame is completed by two cross product computations that determine the missing axis and the refined z axis  ${}^S z_j$ . The axes then build a rotation matrix  ${}^S rM$  that depicts the sensor displacement. For a rotational calibration movement around the y-axis, this is for example defined by

$${}^S rM = [{}^S y_j \times {}^S z_j^- \quad {}^S y_j \quad ({}^S y_j \times {}^S z_j^-) \times {}^S y_j]. \quad (5.16)$$

Adding the sensor displacements  ${}^S rM_{bs}$  to the respective sensor estimates  ${}^S q_{est,bs}$  then led to the final body segment orientations  ${}^S q_{bs}$ . For all jump files within  $\mathcal{D}_R$ , the computed displacements ranged between 0.7 to 13 degree. Large displacements mainly occurred as heading deviations of sensors attached to the arm, where was difficult to align the sensor

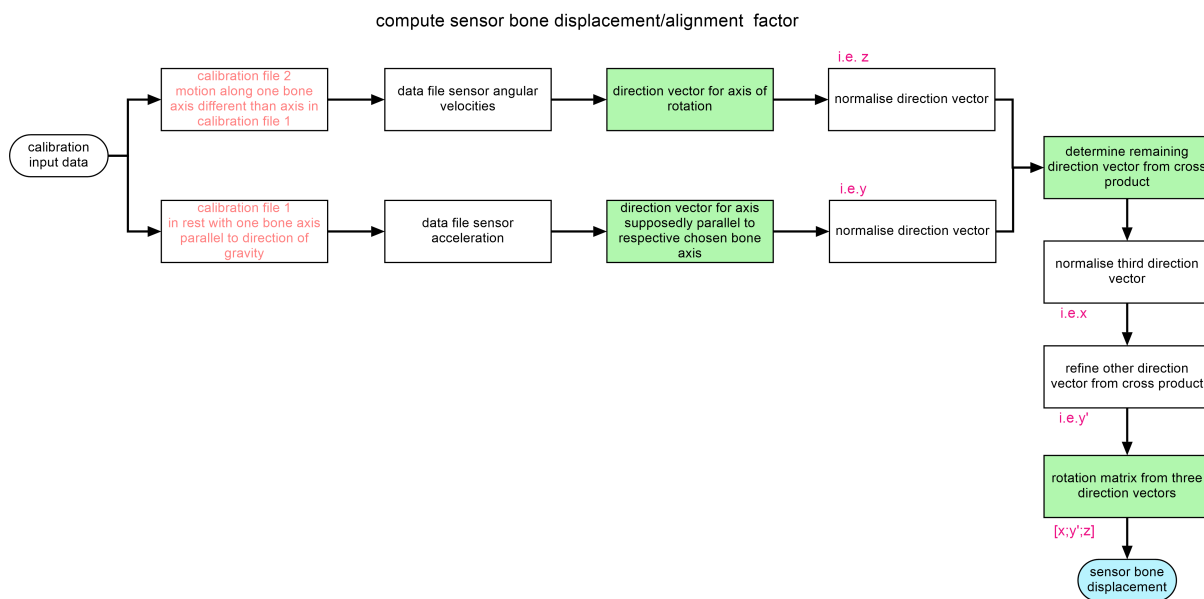


Figure 5.11: Working principle of a sensor-bone alignment. Calibration movements have to be executed before the main data processing to determine the displacement of every sensor placement.

perfectly to the bone's dorsal axis. Consequently, the alignment process can be very useful and increase the data reliability significantly in cases of large sensor bone displacements. However, it should be emphasized that the accuracy of the sensor alignment was strongly influenced by the execution of the sensor calibration movement. Since the method relies on the general axial definition of the global coordinate system, the calibration poses and movements should also be executed as closely as possible to the intended axial directions.

## 5.4 Estimating Positions

Kinematic data usually does not only comprise angular information on body segments, but also positional information on body joints. In general, there are two different strategies for the determination of positions or an athlete's posture from inertial sensor data. One is to work directly with the raw data, the other one is to use angular information to determine position as a sequence of sub-positions within a kinematic chain.

Positional displacement is computed as the velocity of a moving object over time, and velocity in turn by acceleration over time. Inverting this relation, a double integration of raw acceleration sensor data then yields information on positional changes of the position and location the sensor is mounted to. Although this double-integration is simple and theoretically correct, it is generally not practicable and cannot be used in the processing pipeline of applications without any further data correction. As for the integration of angular

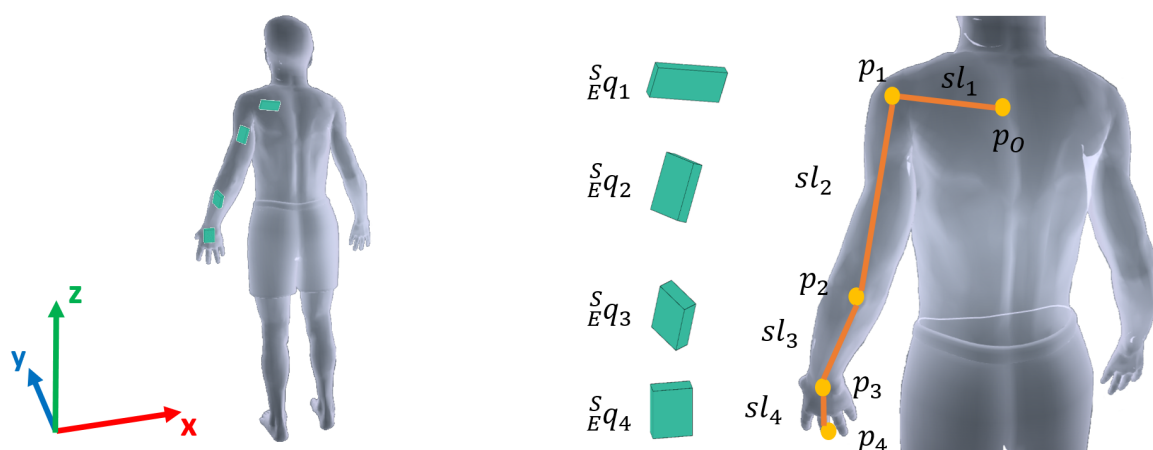


Figure 5.12: Forward kinematics under the defined global coordinate system for the estimation of relative joint positions at the left arm.

velocities, inaccuracies and noise in the sensor data accumulates quickly (errors sum up even more in the course of a double-integration), and the resulting posture can drastically differ from the real posture. One strategy to account for errors and inaccuracies that occur during the integration process is to add a control value input. In gait analysis, such a control value can for example be taken at every instance of touching the ground [YBMC07]. However, in case such motion events do not occur regularly or comprise a main part of the performance (as in many sports), the implementation and addition of such control events is much more difficult. Therefore, it shall not be discussed in more detail here. Instead, the previously estimated orientation of body segments (respectively the orientation of the sensors mounted to the body segments) were used.

### 5.4.1 Orientation Based Position Estimation

Consecutive body segments build a flexible kinematic chain by connecting segment start and end positions through joints of various degrees of freedom. An arm for example usually consists of shoulder, elbow, wrist and knuckle joints. In robotics, it is common to estimate the parameters of connecting body segments from known or desired positions of the joints and end-effectors towards the center of mass. This problem is called inverse kinematics (IK). Starting at a root position, joint positions are vice-versa determined from specified known segment parameters by forward kinematics (FK) (Figure 5.12 and Figure 5.13).

Under the condition that the sensors are aligned with the sensor bones during their attachment, FK is simple and can be used well in the processing pipeline. In this case, the sensor orientation  ${}^S_E \hat{q}$  is the same as the orientation of the affected segment. With  ${}^S_E \hat{q}$  already determined in a previous step, the only additional segment parameter necessary for the computation then is the length  $sl_j$  of the segments, which can be easily measured before data acquisition.

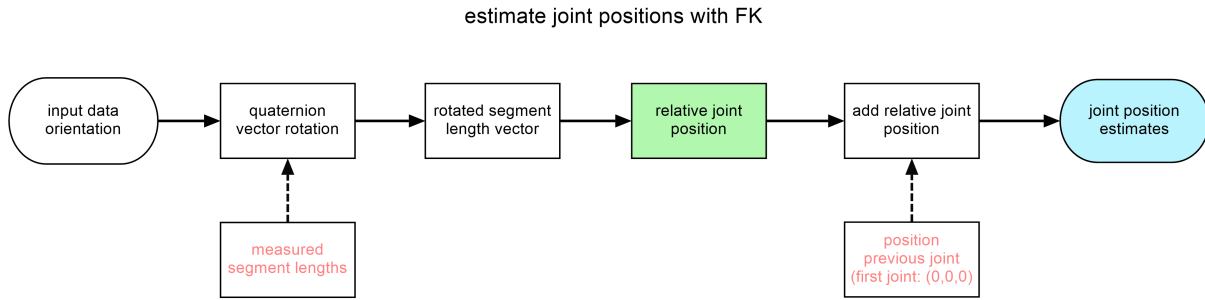


Figure 5.13: Working principle of the relative pose estimation under the FK principle.

Knowing both segment orientation and length, the segment's end position can be determined in two easy calculations. First, the relative end position of every joint  $j$  in relation to the segment's origin is determined using a vector-quaternion rotation with the measured segment length to be the rotated vector. Since it is assumed that the sensor orientations represent the real orientation of the body segments, they are known to follow a straight line in the case of no angular displacement. Then, the rotation vector can be build as a three-dimensional vector  $\vec{\vartheta} = [sl_j \ 0 \ 0]$  with the previously measured segment length  $sl_j$  of the respective  $j$ -th segment along the x-axis. Second, the absolute position  $p_j$  of every joint in the kinematic chain is computed. Starting at the origin  $p_0$  of a kinematic chain, all joint end positions  $p$  are then computed as a combination of the relative end position and the position of the previous joint as

$$p_j = p_{j-1} + {}^S_E q_j \otimes \vec{\vartheta} \otimes {}^S_E q_j^*. \quad (5.17)$$

One of the main restrictions for the FK pose estimation is that the position can only be expressed in relation to a root joint, generally the center of body. This means that translational motions of the whole athlete-sensor system cannot be determined. Since inertial sensors are mainly intended to be used in sports with a large motion volume (that hence also contain much translational motion), certain relevant motion parts will not be available from the sensors. If such information should be desired, it can be possible to determine further parameters by additional mobile devices like GPS or laser tracking systems. In this thesis, I will only use positional data within the sensor-athlete system, so that a collection of global positional data is not explicitly necessary.

## 5.5 Processing Work Flow

With the implementation of all previous sensor signal processing methods, I obtained a full framework for the estimation of body kinematics. Starting with a raw data input, it concretely consisted of the following sequence of computation steps: (1) raw data processing

## Chapter 5. Augmentation of the Collected Motion Data

---

(filter, offset noise removal), (2) sensor-bone alignment to adhere for variations in the sensor placement, (3) determination of initial sensor orientations with an algorithm based on trigonometric relations in the field measurement vectors, (4) estimation of sensor orientation estimation by a Complementary Filter, (5) combination of sensor orientation and sensor displacement for determination of segment orientations, and (6) computation of relative joint positions with a forward kinematics approach using manually measured segment lengths (Figure 5.14). A stored or incoming live inertial sensor data stream passed through all methods then results in the system's output data in form of kinematic motion information. Next, I tested whether this estimate is accurate and reliable to be used for the subsequent sense-making step. The results are discussed in the following chapter.

## 5.5. Processing Work Flow

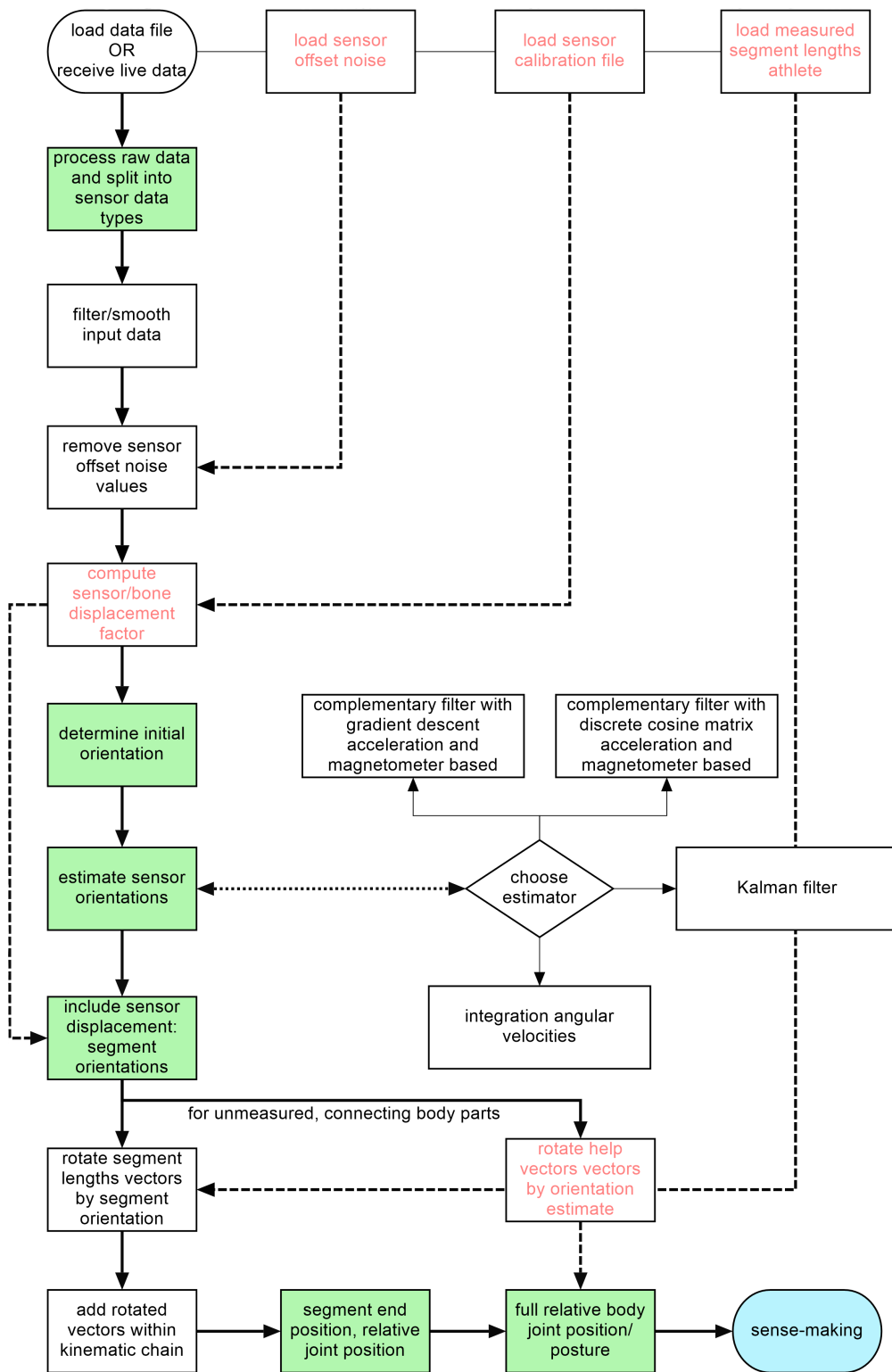


Figure 5.14: Overview on all data augmentation methods and their natural flow within the motion information system.



## 6 Validation and Enhancement of the Augmented Motion Data

Being able to determine accurate and reliable sensor orientation estimates as well as derived body kinematics is important for the usability of any inertial sensor measurement system. In order to obtain the most accurate data, it is recommended to perform initial calibrations on all sensor types before starting the data capturing and processing [HMZ<sup>+</sup>13, FSK<sup>+</sup>15]. This is because sensor data is imposed by inaccuracies – based on temperature-induced noise variations, angle misalignment and magnetic field bias – that result in errors and drift when estimating angular and positional displacements from the sensor data. Knowledge on the system noise can consequently help to reduce resulting error as much as possible. This is especially important for the present target applications using sport motion data as primary input: to represent and analyze all motion information correctly, a high level of data accuracy is necessary.

After implementation of all necessary processing methods for the derivation of body kinematics, the accuracy of the augmented data was therefore conscientiously verified. Furthermore important was to find alternative methods that enhance accuracy, in case that a correct and reliable hardware calibration cannot be performed. To determine eventual constraints and conditions that arise in the context of insufficient sensor calibration and dynamic motion, the strengths and weaknesses of the different implemented estimation filters and all those factors that have an influence on the data processing were examined.

Research was made to introduce applicable methods for system calibration and drift compensation [YB16, KS16, OBT16, MBSS16, BSDD14]. The methodologies are usually based on advanced mathematical algorithms. Considering the diverse group of future system users (Section 2.2), simple methods that can be automatized and universally applied should be better suited: then, an intuitive and universal application that does not require any technical knowledge for the system set up can be developed. However, filter settings, environmental parameters and motion characteristics might change in dependence on the motion pattern. As mentioned before, conventional orientation estimation methods could for example be insufficient when used with dynamic motion data, so that the underlying filter technologies would require adaptations and changes. As a consequence, a good understanding of the background filter methods and processes that influence the accuracy of the used filter algorithms would then be fundamental to ensure data quality. Since this cannot be presumed as valid with everybody, I introduced two simple algorithms for error reduction that can be added to the overall processing pipeline.



## 6.1 Accuracy of the Augmented Data

I verified the accuracy and functionality of the previous implementations and their resulting computations with both the data from  $\mathcal{D}_S$  and  $\mathcal{D}_R$  (Section 4.3). First, the accuracies of the orientation estimates from the three fusion filter  $CF1$ ,  $CF2$  and  $KF$  as well as their dependent joint positions were determined using the data captures from the simulation data base. Next, the filters were examined with respect to their use under the field motion data base and the system functionality validated for the intended ski jumping application. Lastly, a main system evaluation was performed with the actual ski jumping data.

### 6.1.1 Verification of The General System Applicability

To obtain information on the general system applicability, I computed sensor orientations, displacements and initial orientations of all data captures within  $\mathcal{D}_S$ . Next, I compared the resulting motion information to the optical ground truth data. With a calibration accuracy of 0.8mm or less, the orientations obtained from the Vicon system were highly accurate. The accuracy of an estimated orientation  ${}^S_E q_{est,t}$  in the global earth frame  $E$  at every time frame  $t$  could then reliably be determined as numerical deviation to the camera system orientation  ${}^C_E q_{gt,t}$ .  ${}^C_E q_{gt,t}$  was computed from two positional vectors  $\vec{p}_1$  and  $\vec{p}_2$  defined by three of the four captured marker positions around each sensor (Figure 4.5) and a third orthogonal vector  $\vec{p}_3$  built from the cross product of  $\vec{p}_1$  and  $\vec{p}_2$ . They were combined in a rotation matrix and in the last step transformed into quaternion representation to form  ${}^C_E q_{gt,t}$ .

To evaluate changes on the overall accuracy values per filter strategy, accuracies were compared in relation with each other. Using the same initial orientation values for every filter, differences between estimate and ground truth remained the same in all computations, so that just the drift and accumulating errors over time could be evaluated. The quaternion representation of both orientations furthermore made the resulting estimates comparable.

#### Accuracy Measures

The difference between  ${}^S_E q_{est,t}$  and  ${}^C_E q_{gt,t}$  could be easily quantified via the distance  $E_{IP}$  defined by the inner product  $\langle {}^S_E q_{est,i}, {}^C_E q_{gt,i} \rangle$ .  $E_{IP}$  is 0 when the quaternions represent the same orientation and 1 when the difference between the two orientations is  $180^\circ$ . The overall accuracy per take was then determined as the root mean square error  $E_{RMS}$  (RMSE) over  $E_{IP}$  as

$$E_{IP} = 1 - \langle {}^S_E q_{est,i}, {}^C_E q_{gt,i} \rangle^2 \quad \text{and} \quad (6.1)$$

$$E_{RMS} = \sqrt{\frac{1}{n} \sum_{i=1}^n (E_{IP,i})^2}, \quad (6.2)$$

whereas  $i$  stood for the current examined sample within the data capture of length  $n$ . Using the quaternion representation as a combination of the three Euler components pitch, roll, and heading, this error measure was not prone to errors caused by singularities in the Euler angles and the gimbal lock. However, it also did not give a concrete information about angular deviations per sensor rotation axis. I therefore defined an additional RMSE measure  $E_{RMS\angle}$  with  $\angle$  representing the decoupled Euler values  $\phi$ ,  $\theta$  and  $\psi$  in radians computed from the quaternion representations as

$$E_{RMS\angle} = \sqrt{\frac{1}{n} \sum_{i=1}^n (\angle_{gt,i} - \angle_{est,i})^2}. \quad (6.3)$$

For a meaningful comparison between  ${}^S_E q_{est,i}$  and  ${}^C_E q_{gt,i}$ , it was necessary to bring both into the same reference frame. Since the origin of the optical motion capture system was set parallel to the ground surface, the  $z$  axes of both coordinate frames were expected to be parallel (Section 5.2.1). Consequently, it was only necessary to compensate for the heading difference  $\psi'$  between the  $x$ -axes of the global and camera system. Such alignment was simple, while knowing the sensor heading  $\psi_S$  from the initial posture estimation step and the initial heading of the camera system  $\psi_C$ : in that case, the quaternion product  ${}^S_E q_{est,i} \otimes q_{\psi_S}^*$  with  $q_{\psi_S}$  built from  $\psi_S$  should be equal to the quaternion product  ${}^C_E q_{gt,i} \otimes q_{\psi_C}^*$  with  $q_{\psi_C}$  built from  $\psi_C$ .

### Accuracies

As principal investigation, I determined the general accuracy of the three fusion filters from Section 5.2. Their mathematical description clearly shows that the accuracy of every filter model is dependent on the filter values chosen: in general, the accuracies of the fusion filters depend on how much influence on the overall estimate is internally granted to every sensor data type (respectively the correcting sensor observation data from accelerometer and magnetometer). To obtain good orientation estimates, it was therefore essential to choose appropriate settings for the noise values  $\beta$  in  $CF1$ ,  $K_p$  and  $K_i$  in  $CF2$  and  $w_k$  in  $KF$ .

To find reasonable filter settings, I first estimated the orientations of randomly selected data captures with arbitrary filter values. From visualizations of the orientation data, I then identified a range of possible filter values for every filter method and built a sequence of linearly increasing filter values from those intervals. Estimating the orientations of all data captures with the collection of selected filter values, I finally chose the best estimates per filter, sensor location and motion pattern from the data for evaluation of the maximal accuracy. As concrete filter values, I used

$$0.01 \leq \beta \leq 0.5, 0.05 \leq K_p \leq 1.25, \quad \text{and } 0.01 \leq w_k \leq 0.2,$$

## Chapter 6. Validation and Enhancement of the Augmented Motion Data

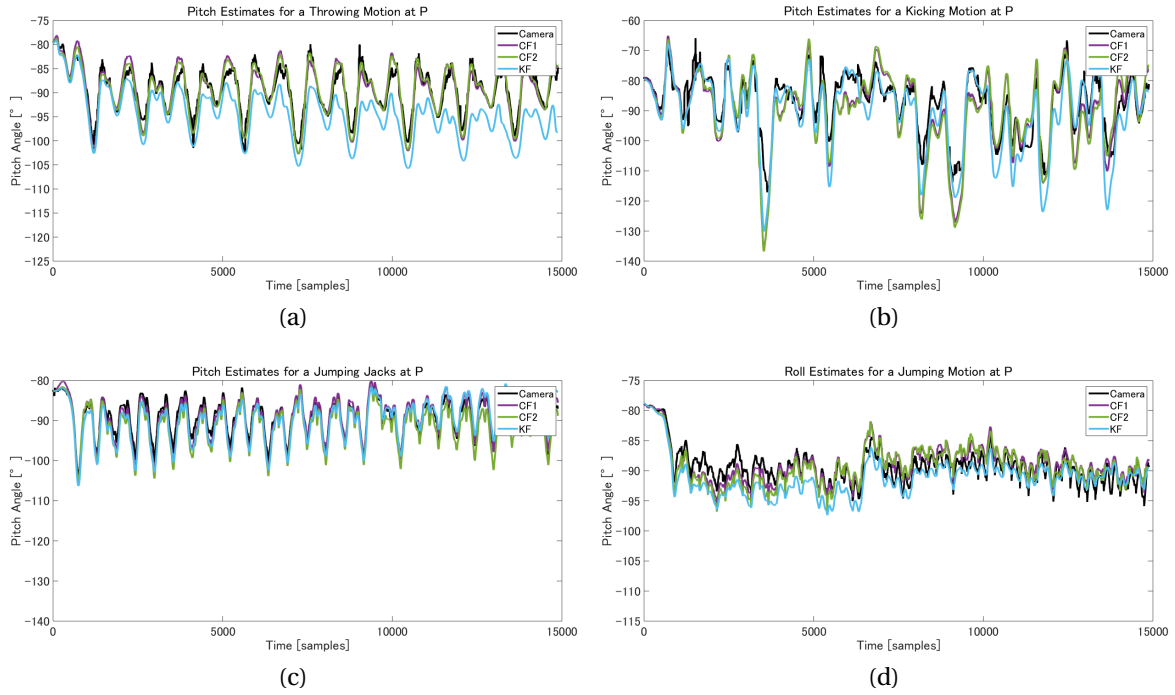


Figure 6.1: Orientation estimates obtained with *CF1* (purple), *CF2* (green) and *KF* (light blue) and the ground truth orientation determined from optical camera data (black). Upper row: estimates for pitch  $\theta$  in throwing and kicking at P. Bottom row: estimates for pitch  $\theta$  in jumping (rope skipping) and jumping jacks at P.

whereas the values for  $\beta$  were increasing by steps of 0.02, the values for  $K_p$  by steps of 0.05 and the values for  $w_k$  by steps of 0.01.  $K_i$  was set to a constant value of  $-0.45$  to reduce the number of variables.

As a result, I could obtain accurate orientation estimates for all three filter models. For all sensor placements and motion types,  $E_{RMS}$  values could be constantly brought under 0.03 for *CF1* and *CF2* and under 0.1 for *KF*. The values of  $E_{RMS\angle}$  remained within 0.2 rad (meaning  $\approx 10^\circ$  or less) along all axes of *CF1* and *CF2* and 0.4 rad for *KF* (Figure 6.1, Table 6.1). Here, it should be emphasized that *KF* might have also produced more accurate estimates under different observation noise values, which were used to build the covariance matrix  $R$  (Section 5.2.3). They were estimated from data bias measured with the sensors in rest and have not been modified in this investigation. Consequently, more accurate and specific noise measures by for example the Allan Variance could have increased results [ESHN08, Hou05]. Leaving out deviations already existing between the initial postures  ${}^S_E q_{est,1}$  and  ${}^C_E q_{gt,1}$ , the quality of the filter models could be considered as sufficiently high and accurate. These good accuracy measures brought me to the conclusion that all implemented filters could generally be well applicable for a subsequent motion analysis.

Besides the sensor orientation estimates, I furthermore determined the accuracy of the initial

## 6.1. Accuracy of the Augmented Data

Table 6.1: Mean error values of  $CF1$ ,  $CF2$  and  $KF$  for the orientation estimates of all sensor placements with filter values adapted to specific drift prevalent in every sensor placement and motion type.

Motion	$E_{RMS}$	$E_{RMS\angle}$
<i>CF1</i>		
Kicking	0.0121	[0.1412, 0.0730, 0.1334]
Jumping	0.0098	[0.1199, 0.0720, 0.0808]
Jump-Turn	0.0142	[0.1332, 0.0783, 0.1479]
Jump.Jacks	0.0204	[0.1900, 0.1260, 0.1427]
Throwing	0.0103	[0.1470, 0.0716, 0.1026]
<i>CF2</i>		
Kicking	0.0128	[0.1434, 0.0740, 0.1405]
Jumping	0.0238	[0.1655, 0.1245, 0.1122]
Jump-Turn	0.0190	[0.1649, 0.0952, 0.1681]
Jump.Jacks	0.0338	[0.2157, 0.1561, 0.1730]
Throwing	0.0091	[0.1374, 0.0679, 0.0965]
<i>KF</i>		
Kicking	0.0642	[0.2740, 0.1758, 0.3101]
Jumping	0.0516	[0.2439, 0.1601, 0.2014]
Jump-Turn	0.0913	[0.3078, 0.1912, 0.3921]
JumpJacks	0.0575	[0.2566, 0.1586, 0.2524]
Throwing	0.0419	[0.2483, 0.1499, 0.2479]

posture estimates obtained with  $VB$  as well as the positional accuracy with deviations in mm. Comparing the accuracy of pitch  $\theta$  and roll  $\phi$  from  $E_{RMS\angle}$  with the initial orientation obtained with the Vicon system, accuracies were within  $\approx 2.5^\circ$  for  $\theta$  and  $\approx 5^\circ$  for  $\phi$ . Since the roll depended on the preceding pitch estimate, the error accumulated in the roll estimate. However, accuracy should be considered as accurate enough - especially given the fact that the orientation obtained from the optical marker points could also not be considered as absolutely identical to the sensor casing and proportions. Lastly, the deviations between estimated joint positions and ground truth marker positions from the optical motion capture system were considered. Under the previous highly accurate sensor (and hence segment) orientations, positional differences could be kept within 25 mm for all orientation estimates, sensor locations and samples. For the best estimates, deviation was less than 10 mm distance, which I considered a highly satisfying value given the intended follow-up application as well as reference values from literature [Sab06, LVB05].

### 6.1.2 Verification of The In-field System Applicability

With the confirmed general system accuracy, the functionality of all fusion filters should subsequently be tested with the data captures  $\mathcal{D}_R$  acquired at actual sporting venues. In those

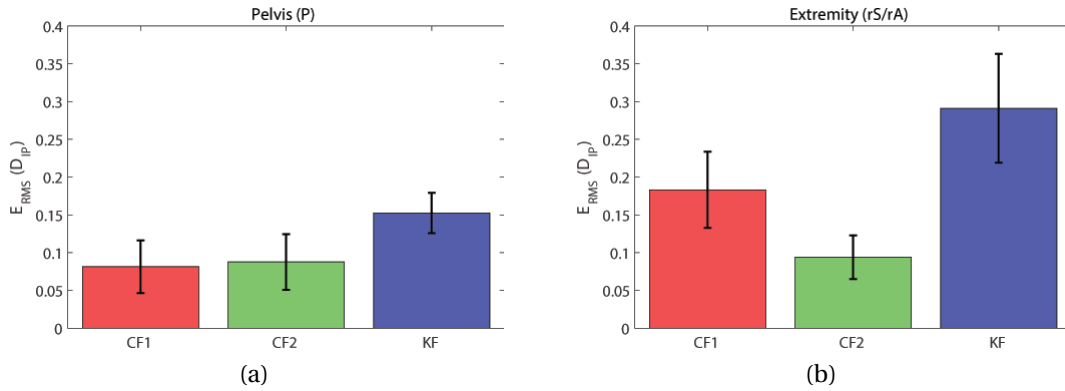


Figure 6.2:  $E_{RMS}$  averaged over all motions in  $\mathcal{D}_S$  at (a) P and (b) an extremity (right shank or arm) and their standard deviation with the chosen filter values. Possible error values range between 0 and 1.

locations, generally no ground truth data is available that could provide information on the system's error and accuracy. Therefore, it is difficult to modify the filter values in a variable way for every individual data stream and with changing conditions or sensor placement. In contrast to the previous accuracy validation, it is hence economical to employ a fixed filter value. However, such fixed filter setting cannot guarantee for permanently accurate estimates. To find the best method under the present prerequisites, I therefore first examined the sensor estimates of the simulation data in more detail, before I then progressed my evaluation with the ski jump data from  $\mathcal{D}_R$ .

### Conclusions from Simulation Data Base

To evaluate accuracies of the implemented methods with one filter value, I determined the best filter value on average for every filter model. For this, I weighted all selected best filter values with their accuracy and averaged them to  $\mathcal{V}_I$  constituting of the rounded  $\beta = 0.19$ ,  $K_p = 0.56$  and  $w_k = 0.02$ . The accuracies of all data files with  $\mathcal{V}_I$  were then computed and then compared to the Vicon ground truth data. Taking effects of inconstant sensor background noise out of account, results indicated that the performance and applicability of every filter model varied with the motion pattern. Those differences were likely to be induced by each filter's algorithm. To identify suitable motions of every fusion algorithm, I averaged the  $\mathcal{V}_I$   $E_{RMS}$  values for two sensor locations of differentiating motion characteristics (Figure 6.2). While the averaged  $E_{RMS}$  values of the *KF* estimates showed the largest deviations to the ground truth in both cases, *CF1* had slightly better averaged accuracies for the static sensor data than *CF2*, but also a higher standard deviation. Furthermore, *CF2* suffered from less drift at the higher accelerated sensor data.

General observations were slightly different when looking at the changes in accuracy every filter achieved in relation to the *GI* estimates: the difference between the accuracy of *GI* and

## 6.1. Accuracy of the Augmented Data

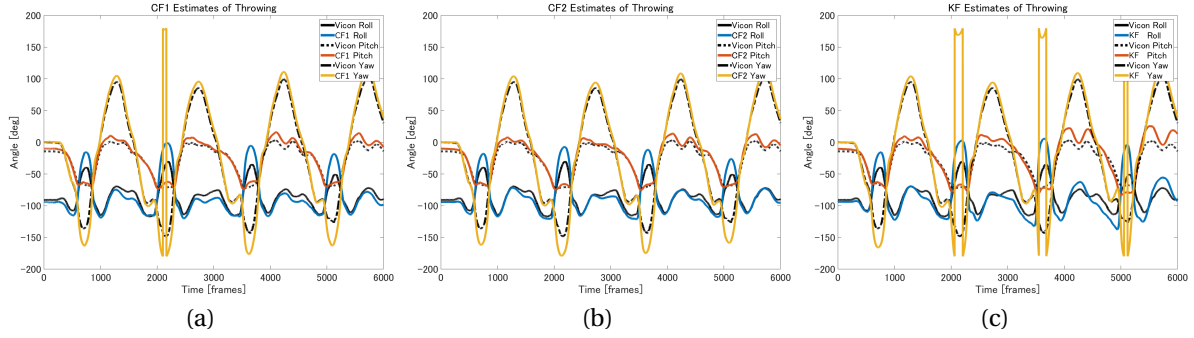


Figure 6.3: Sample plot of a throwing motion with the ground truth data and the respective estimate from the three filter models along x, y and z.

a more sophisticated fusion filter gave an idea about the effect and impact of the fusion filter with the chosen filter settings. Mathematically, I described this difference as relative change RC between the error values  $E_{RMS,TV}$  of the fusion filter estimates to the error value  $E_{RMS,BV}$  of the base error values from the  $GI$ :

$$RC_{TV} = \frac{(E_{RMS,TV} - E_{RMS,BV})}{E_{RMS,BV}}. \quad (6.4)$$

The RC for  $KF$  for example was defined as  $RC_{KF} = \frac{(E_{RMS,KF,i} - E_{RMS,GI,i})}{E_{RMS,GI,i}}$  at every frame  $i$  in a motion take. The average relative change  $RC_{KF} = -0.7843$  gave the impression that  $KF$  was especially useful for primary low speed motions. With an average relative change of  $RC_{CF2} = -0.7725$ ,  $CF2$  in contrast offered particularly high accuracy for motions and body segments that constantly reached high angular velocities.  $CF1$  improved the estimator performance in all cases, but was of lower accuracy or higher standard deviation than  $CF2$ .

To draw a conclusion about the main  $\mathcal{D}_R$  field data, I examined only motions of similar characteristics as ski jumping in the next step. Motions were considered a similar motion pattern when they contained both static and high-impact motion phases as for example a sequence of throwing motions of the throwing arm. Angular changes during quick and high-impact phases could not be represented to a full extent by any of the estimation methods (Figure 6.3). However, less accurate estimates during dynamic motion phases were stabilized well during the more accurate data in the static motion phases. In those phases, data was stabilized best by  $CF2$  that was of constantly accurate values and seemed to be less prone to drift than the other two estimators. As a result, I chose  $CF2$  as principal orientation estimator for the actual ski jump data captures.

### In-field Accuracy

The ski jump data captures were verified from two high-speed video cameras facing towards the take-off table and the middle of the flight path and one consumer camera facing towards

## Chapter 6. Validation and Enhancement of the Augmented Motion Data

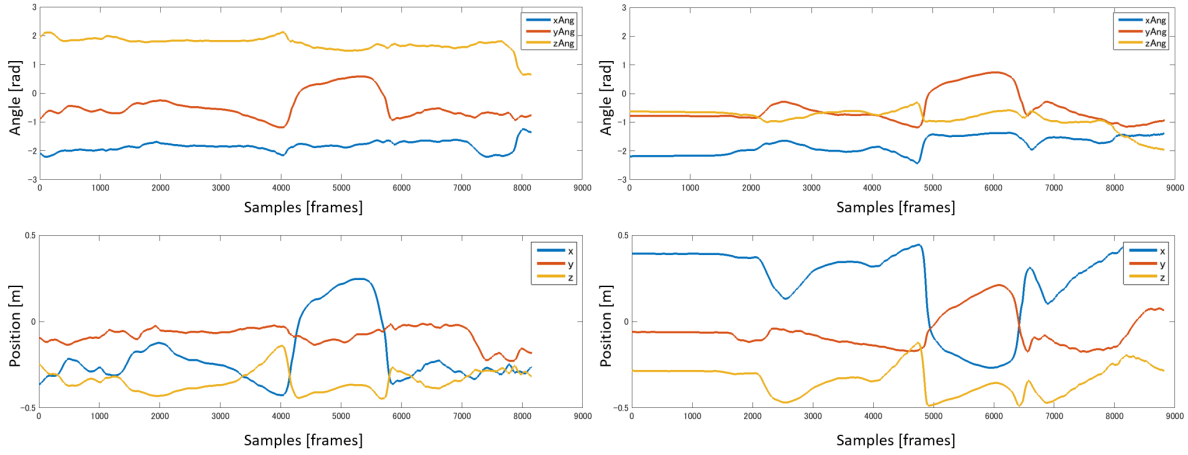


Figure 6.4: Magnetic disturbances between different takes on the start gate at the top of the ski jump hill led to differences in heading  $\phi$  of estimated segment orientations, as well as differences in joint positions estimated from the posture data.

the start gate. Pitch values of body segments were manually annotated from the camera data and correlated to pitch values  $\theta$  of the estimated orientations within a  $5^\circ$  accuracy range. Furthermore, pitch values from the orientation estimates at the ski were compared to the hill construction properties of the in-run slope with an elevation angle  $\theta_{IR} = 35^\circ$ , the take-off table with an elevation angle  $\theta_{TO} = 10^\circ$  and the landing slope with an elevation angle  $\theta_{KP} = 34.7^\circ$  at the K-point. Their difference was in a range of less than  $3 - 5^\circ$  during all annotated motion phases. To examine the progression of error caused by drift, I additionally computed the average changes in ski elevation and heading during in-run. Given the natural constraints of the slope, variations along both X and Y axis should be minimal during those approximately 10 seconds. Within all jumps, pitch angles varied by maximally  $0.5 - 5^\circ$  with an average change of orientation of  $1.15^\circ$  per data capture, and heading angles by  $1.4 - 3^\circ$  with an average change of orientation of  $1.56^\circ$  per take. Consequently, drift could be assumed to be sufficiently small in the chosen setting.

However, large variations could be found in the sensors' heading values  $\psi$  among all jumps. In particular, initial heading differences were present throughout the complete data set  $\mathcal{D}_R$  in dependence on the sensors used during every capture session, the mounted body segment and the date of the data acquisition. Since the angular changes  ${}^S_E q_{bs}$  were used to determine body joint positions, large variations were observed in the positional data as well. Visualizing the estimated data as data plots or stick figure animations, it was not possible to reliably display the full body kinematics. Figure 6.4 shows animation visualizations of sample jumps during the in-run and their corresponding time-series plot for the segment orientation  ${}^S_E q_{rT}$  and knee position  $p_{rT}$  obtained from the sensor attached to rT. Differences  $> \pi$  in  $\psi$  (visible in the top row of the figure as the yellow curve for the angular changes in z) led to sign errors in the relative positional data (visible in the middle row of the figure as the blue curve for the positional changes in x-direction and red curve for the positional changes

---

## 6.2. Enhancing Usability of the Data Augmentation Step

in y-direction) and unnatural and impossible body poses. Similar differences and errors appeared randomly within other jumps of  $\mathcal{D}_{\mathcal{R}}$  and different capture sessions. They were also numerically represented within the full data set as heading variations with an unnaturally large range of occurring  $\psi$  values (Table 6.4, Figure 6.16). In the top row of the pie chart (Figure 6.16) for example, the heading values of rF varied within the complete range of 0 to  $-\pi$  as well as around +0.6 to +1 rad – a heading range that is not possible to fulfill naturally given the fact that all jumps have been captured on the same jump hill, with the athlete sitting at the start gate.

As a conclusion, body kinematics were unreliable with respect to their initial heading states that appeared to be influenced by the following properties: varying sensitivities in the sensor's magnetometers (every sensor measured a slightly different magnetic field at the same position of the ski jump hill), proximity to the in-run slope and jump hill (with evidence: sensors attached to the arms were less variant than those attached to the thigh, or near the magnetic start gate), as well as differences in the magnetic field with changing weather conditions. To enable a generic system it was consequently necessary to find the reason of those heading variations, in order for the variations to be held to a minimum.

## 6.2 Enhancing Usability of the Data Augmentation Step

I have seen that the system accuracy can be high when the filter values and noise simulations were adapted well to the requirements of a certain motion task. However, this adaptation can be very complicated, time-consuming and tedious. Especially for users that are not familiar with the underlying mathematical concepts, the adaptation of the sensor noise can be a very difficult task. In other words, a future analysis system would either be little user-friendly (in case that filter settings get fine-tuned) or inaccurate (in case that filter settings would not get fine-tuned) when the previous processing framework is employed. A similar trade-off persists when compensating the variation in heading angle discovered in the real field motion data: using additional settings and filter values might be successful for reduction of distortions, but would on the other hand complicate the system use. Therefore, I aimed to develop additional intelligent strategies for data enhancement that would contribute to both higher data quality and system usability.

### 6.2.1 Intelligent Gyroscope Drift Reduction

Indexing all filter values that achieved best accuracy values in the previous accuracy evaluation (Section 6.1.1), I could observe large differences for every specific sensor placement and motion pattern. Best filter values were variate and could differ considerably between the data captures and under various properties of the motion data stream. One reason for this variation was that huge differences among sensors and rotation axes were already present in



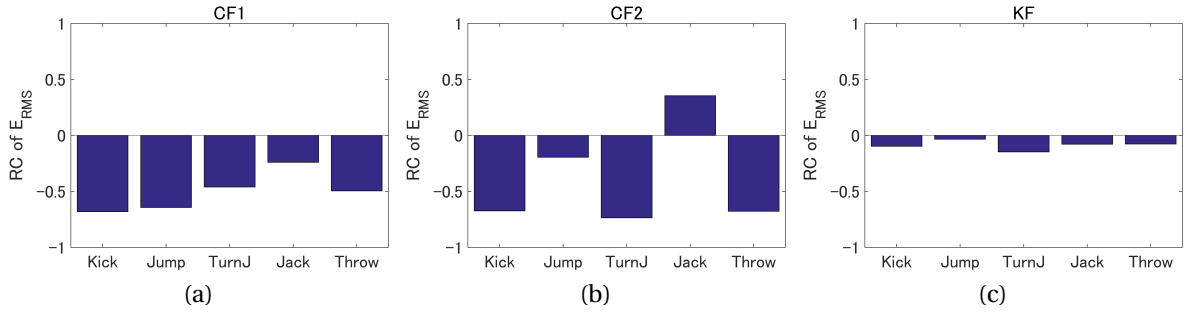


Figure 6.5: Changes in the accuracy values  $E_{RMS}$  of all filter models with a fixed noise value in relation to the  $E_{RMS}$  values of  $GI$  (here depicted as base value 0) per motion pattern and their mean relative change values  $RC$ .

the accuracies of the pure  $GI$  estimates: specific sensors for example continuously generated estimates of higher accuracy than other sensors independent of their mounted position. Therefore, a fusion filter of one fixed noise value was not equally suitable for all sensor estimates. A  $KF$  noise value of  $w_k = 0.07$  for example could produce better estimates than  $w_k = 0.01$  for certain sensors, but on the other hand significantly deteriorate the estimates of other sensor data. Those differences were likely to stem from technological hardware differences between sensors or insufficient calibration of specific sensors. The other main reason for this variation was drift. Evolving from white noise in the gyro rate sensor readings, it cannot be controlled as a constant offset – even tiny deviations from the underlying raw sensor data like very small oscillations around a sensor’s reading in rest are significantly enhanced in the integration process. To determine fluctuations in drift over different motion patterns, I examined the  $RC$  values averaged over all data captures in  $\mathcal{D}_S$  with the  $\mathcal{V}_I$  filter values (Figure 6.5). With their relation to the  $GI$  estimates, they comprise accuracy differences per sensor: the better the sensors, the more accurate already integration estimates from  $GI$ .

The different distributions of accuracy per filter model can be easily distinguished from the data plot: while the chosen  $w_k$  for  $KF$  generates the least improvement,  $CF1$  yields stable and large improvements for all motion pattern.  $CF2$  on the other hand can both considerably improve and degrade accuracies in dependance on the motion pattern. For jumping motions and jumping jacks for example, the filter models could be considered as less effective as for kicking, throwing or jumps with turn. From Equation 5.11 and Equation 5.12, one can see that  $CF2$  and  $KF$  already include an error measure for the sensor noise induced drift and require additional noise input values. The resulting accuracy values showed that this internal drift compensation was not sufficient to equally remove the drift from the sensor signal of all data captures, respectively of all motion types. Positive  $RC$  values furthermore denoted that the chosen noise values could even influence the final output estimate in a negative way for certain motion patterns.

To get more detailed information on the accuracy distributions, the  $RC_{CF1}$  values of different

## 6.2. Enhancing Usability of the Data Augmentation Step

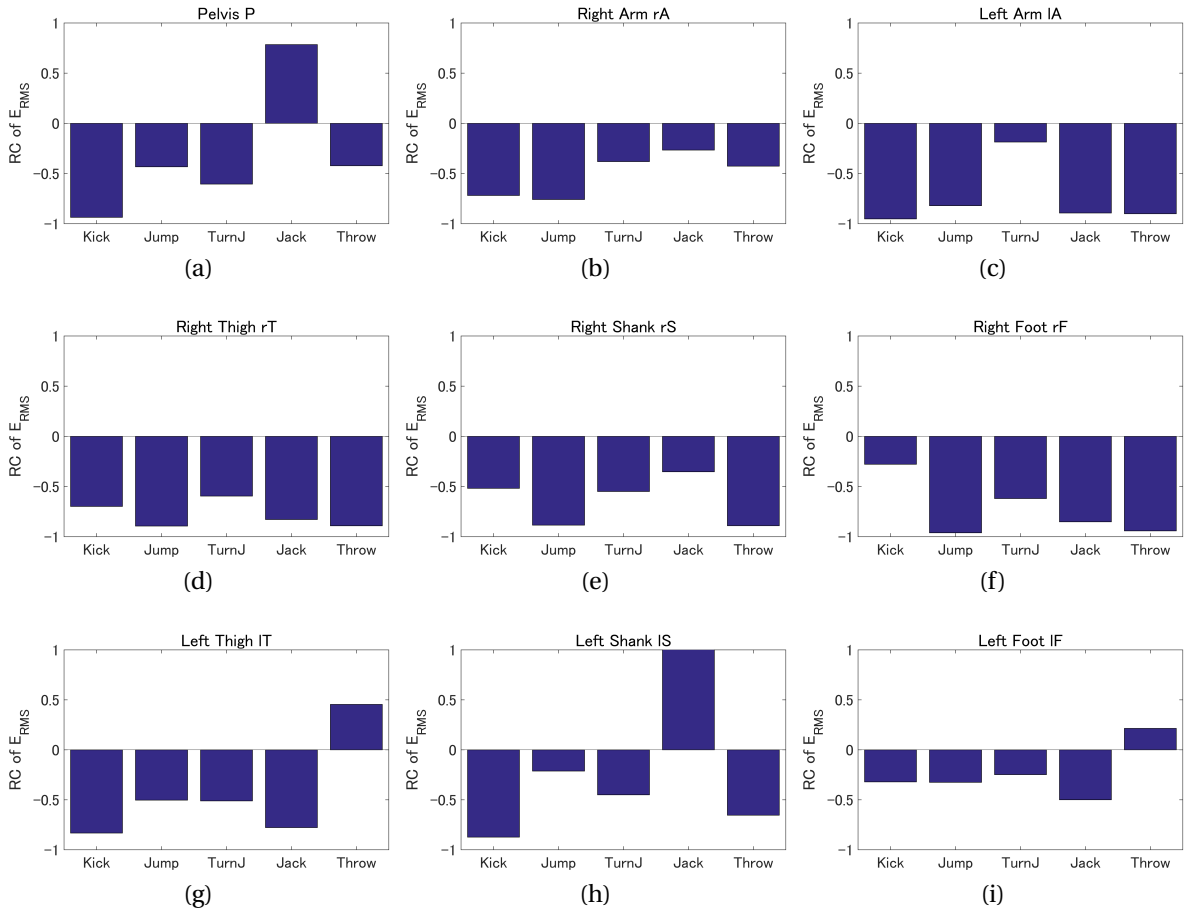


Figure 6.6: Changes in the accuracy values  $E_{RMS}$  of  $CF1$  in relation to the  $E_{RMS}$  values of  $GI$  (here depicted as base value 0) per sensor location and their mean relative change values RC.

sensor placements should be examined next, since  $CF1$  is the only filter model whose accuracy only depended on one variable ( $\beta$ ). It became clear that different sensor locations were not equally accurate, but varied along the different motion categories (Figure 6.6). Jumping jacks for example could not be estimated well with the measurements of P and lS, but with rF. Kicking in reverse could be handled well by P and lS, but not with rF. In throwing, the chosen filter values contributed to higher data accuracy of the right leg (middle row) than of the left leg (bottom row), whereas the relation was inverse for the arms. Considering the execution of the present right-handed throwing motion, the left leg was used as swing leg and exposed to high impact during ground contact and release of the thrown object, whereas the grounded right leg and the left arm were more static.

It is logical to assume that specialties within the underlying measurement affected the data accuracy of the fixed value estimates. To be able to automatically react to such variances and inconstancy, my idea was to introduce a flexible drift compensation that could be added to the processing framework if necessary (meaning in cases where the chosen filter setting

could not yield accurate results). For the implementation of such method, I first verified the variation in accuracy, examined influences responsible for it and then developed a strategy for their compensation.

### Verification Using Principal Component Analysis

To verify the previous assumptions, I determined the principal components of all data captures with *GI* and the Vicon ground truth data and visualized their coefficients in the space of the first three principal components. Using *GI* estimates, results were not influenced by any filter specific properties, but only represented the variance obtained with the simple and fundamental data processing.

As a result, I could observe that the coefficients of data captures that were estimated well with the simple integration estimate were of similar distribution than the coefficients of the ground truth data. For data captured with the same sensor, component coefficients on the other hand had a distribution very variate to the ground truth distribution when orientation estimates were less accurate. Estimates for P and IS for example were similarly scattered with a kicking motion, but seemed unrelated during jumping jacks (Figure 6.7). Although differences in distributions are obvious, the circular motion shape is clearly visible for both Vicon and estimated orientation in kicking. Coefficients of the estimated orientation appear more noisy and variant, especially as the outer extremity, which constituted the higher accelerated motion parts. Distributions of the coefficients of jumping jacks on the other hand did not suggest any visual similarities. Here, the ground truth coefficients were scattered in a point cloud (for P) and U-shaped form (for IS), the estimate coefficients were distributed along a line. For IS, even a repetitive sequential pattern was visible, which could be associated to the sequential motion form of jumping jacks. Reconfirming the data plot of Figure 6.6, the same interrelation was also represented in the  $RC_{CF1}$  values.

The component visualization and analysis brought me to the conclusion that indeed certain data captures must be more prone to drift than others, which is independent and unrelated to hardware specifications and sensor background noise. Consequently, the task was to create a processing system able to handle those motion data streams differently in consideration of their internal drift potential. For this, rules describing the occurrence of drift had to be found in the first step.

## 6.2. Enhancing Usability of the Data Augmentation Step

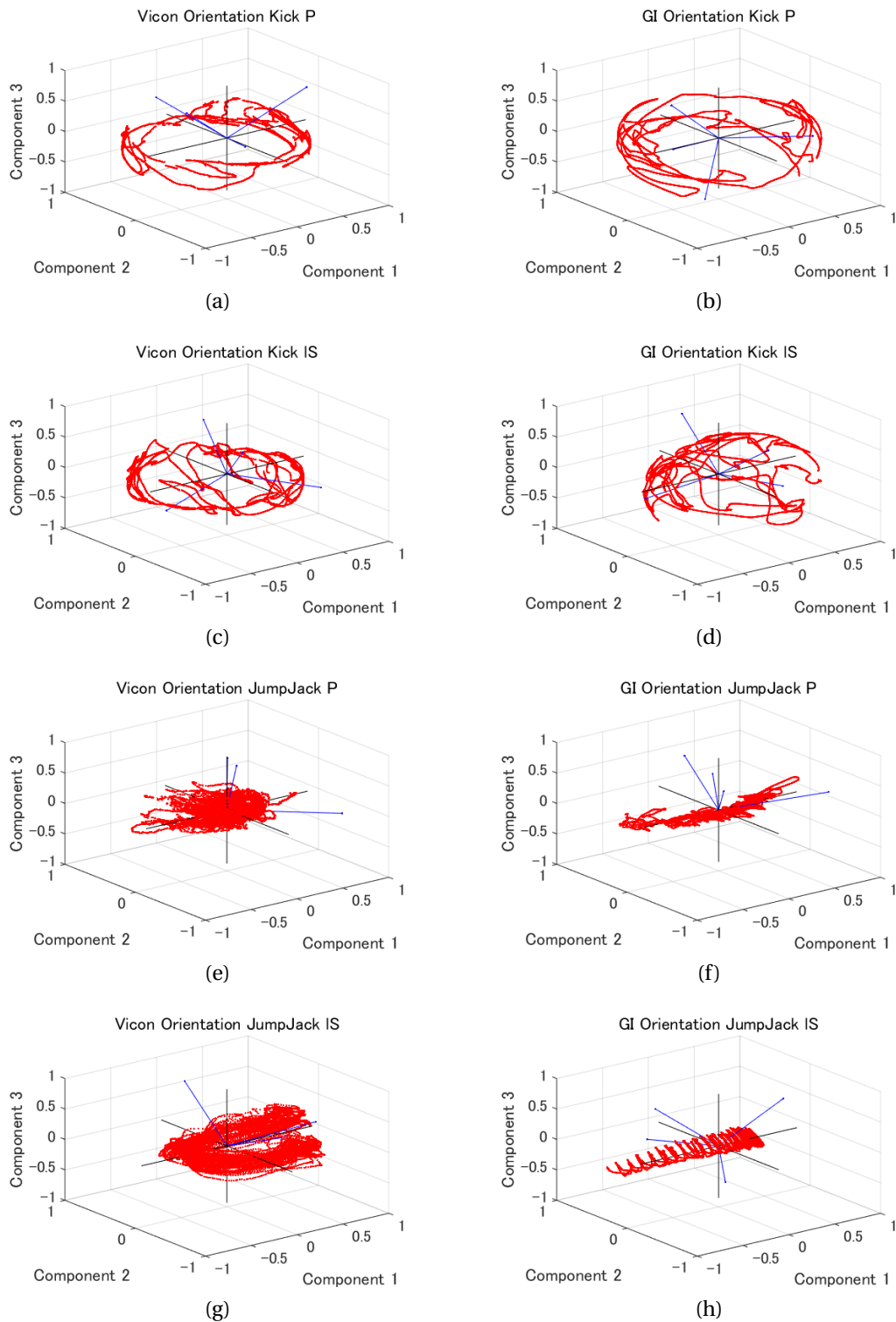


Figure 6.7: Visualization of the three main principal components for (left column) the Vicon ground truth data and (right column) *GI* for highly accurate data captures (kicking, top) and less accurate data captures (jumping jacks, bottom) at P and IS.

### Identifying Influences on the Accuracy

Motions that were suffering from higher drift could be identified by either high indexed ideal filter values (as estimates of strong data fusion) or by reaching smaller or positive *RC* values. Considering the differences and commonalities within the variate motion types for different sensors and sensor placements, I came to the conclusion that the maximal amount of angular velocity within a motion could impact the estimation accuracy. For every motion pattern, different body segments underwent different angular velocities (Table 6.2). Angular velocities during a kicking motion for example were much higher at the outer lower extremities than around the body center. In the same way, high rotational movement occurred at the right arm in a right-handed throwing motion, whereas less rotational movement occurred at the left arm and the relatively static legs. It was therefore logical to conclude that varying angular velocities between different motions influenced the filter performance, especially when considering the conventional target use of orientation estimation filters: generally, they are designed for slow motions like walking and gait analysis where all sensors are only exposed to low angular velocities.

The second parameter that appeared to influence the data accuracy was the dimensionality of a motion pattern: the principal motion axis, the amount of changes along a motion axis and the number of motion planes involved in a motion also differed between the captured motion patterns. Generally, data takes containing motions in primarily one motion plane (e.g. jumping motions) seemed to suffer more from drift than data takes containing motions with rotations around more than one motion axis (e.g. throwing or kicking). Besides, the accuracy of an estimate increased with larger angular changes along a motion axis. One explanation for this behavior could be that white sensor noise remaining after an imperfect sensor calibration and leading to drift during the integration was automatically reduced with changing and varying motion directions.

Finding rules for the prevalence of drift in an orientation estimate, it should also be possible to introduce a compensation that could react to the drift (and change the filter values accordingly). Since the integration of the gyro rate measurements is the base for all orientation estimators, reducing the integration drift should also help to improve the overall accuracy of an orientation estimator. A similar approach to drift reduction was introduced before [LBCP08] and should function as inspiration in the following: noisy frequencies prevalent in the measurement data have been analyzed and could then be prefiltered to reduce the drift of the final estimate.

### Frequency Band Analysis

To verify the influences of speed and motion dimension, I investigated the frequency band of the angular velocity data of different motion patterns. The angular velocities of all motions had their frequencies within the interval [0,20] Hz, whereas variances in the spectrum of gyro

## 6.2. Enhancing Usability of the Data Augmentation Step

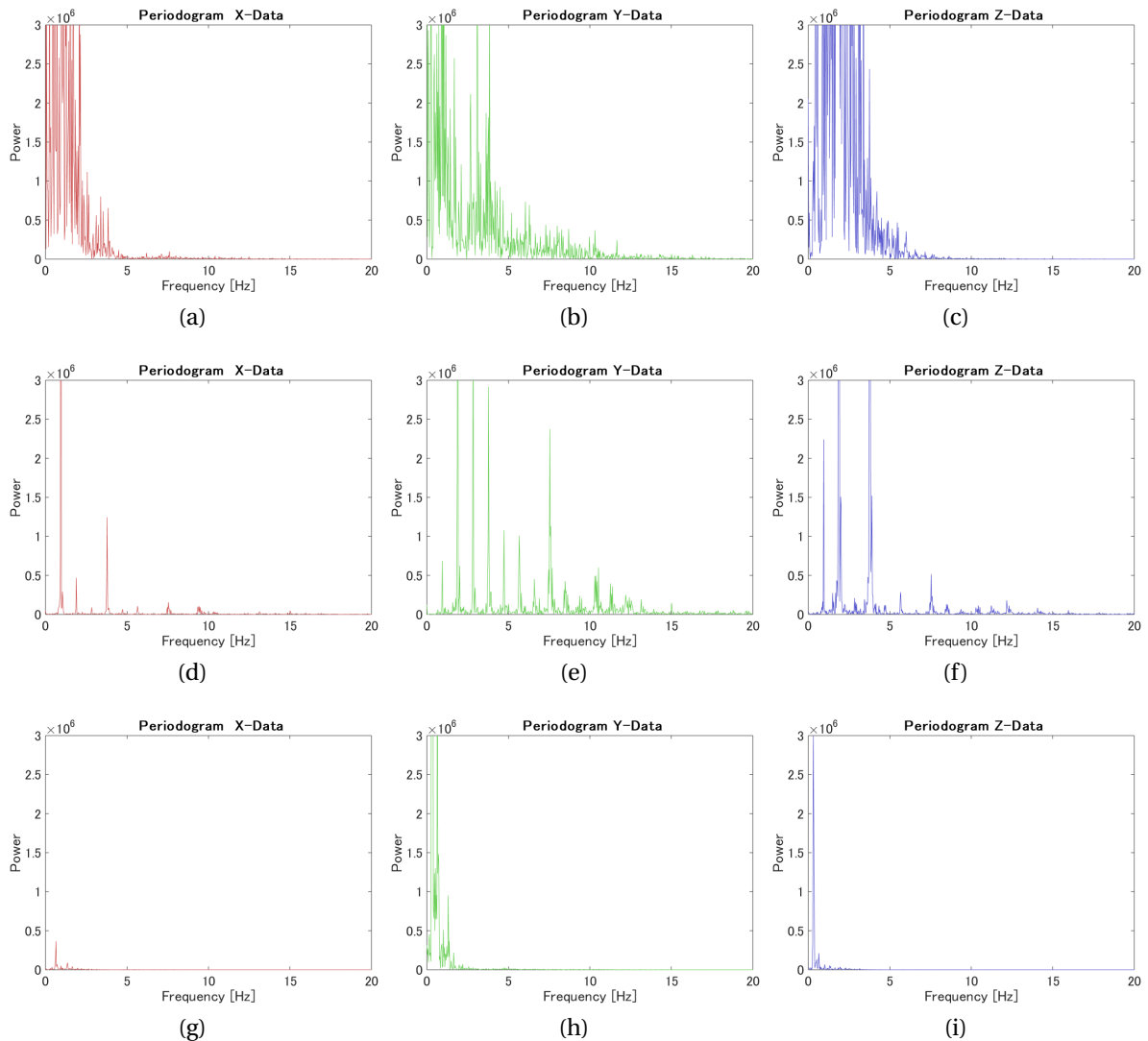


Figure 6.8: Power-Frequency plots of the DFT of the angular velocity data at IS for (a-c) kicking and (d-f) jumping jacks as well as for (g-i) throwing at P along x (red), y (green) and z (blue).

rate data streams were visible per motion pattern and sensor placement. Visualizing the data plots (Figure 6.8), I discovered that gyro rate data of high motion dimensionality (e.g. IS in kicking) had a unspecific range of frequencies contributing to the measured signal. Gyro rate data of higher drift potential (e.g. IS at jumping jacks) on the other hand had multiple frequencies contributing to the measured signal. Lastly, gyro rate data of little drift potential and small angular velocities (e.g. P in throwing) had mostly one main frequency contributing to the measured signal. In other words, the frequency band of the angular velocity data of different motion pattern conformed with the factors previously identified as influences on the estimation drift. Consequently, I could progress with the development of an intelligent drift reduction on the base of the assumptions in the next step.

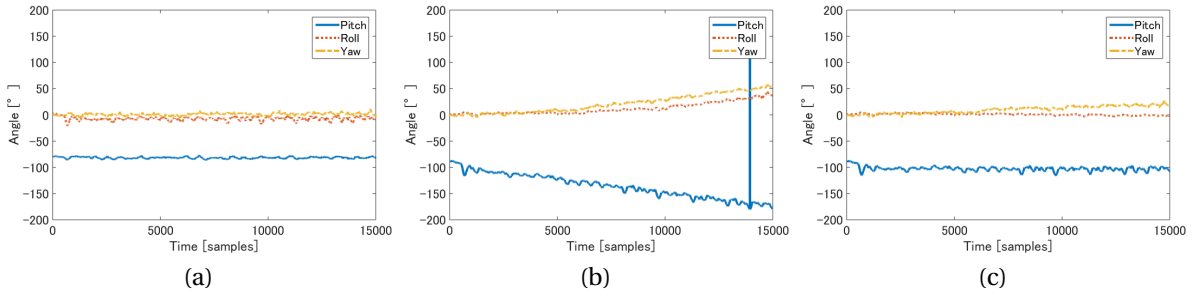


Figure 6.9: a) Global ground truth pitch  $\theta$  (blue, solid), roll  $\phi$  (red, dotted) and yaw  $\psi$  (yellow, line) in degree for a continuous sequence of jumping jacks at P. b) Angles estimated from the sensor data with *GI* for the same motion with drift. c) Same estimated angles with *GI* and drift compensation.

### Simulating Intelligent Drift Reduction

To develop an intelligent drift reduction strategy, I simulated the effects of flexible filter values with a simple drift compensation first. Various drift compensation approaches exist, and I chose to use a very simple one here: assuming the sensor offset value to be varying around the zero value, I responded to the resulting drift by subtracting an additional, small offset from the gyro rate sensor reading in the angular velocity integration step. First, I computed the drift  $d_i$  per frame  $i$  as multiplication between its angular velocities  $\omega_i$  and a defined gyro rate bias (e.g.  $b = 0.05$ ) with the respective sampling rate  $f_s$ , whereas the gyro bias rate was a constant that included all possible sources of error like sensor noise, signal aliasing, quantization errors or variations caused by temperature differences. I then added the current drift  $d_i$  to the previous drift  $d_{i-1}$ . In the subsequent computation step, the new summed drift was subtracted from the next angular velocities, and the influence of the sensor noise reduced. In this way, an accumulated drift compensation value was created over time, functioning as low pass and hence accounting to the temporal progression of drift. As for the noise values of the filter models, this simple drift compensation could have positive or negative effects on the data streams: for highly drifting estimates  $b$  reduced the linear accumulating drift errors visibly (Figure 6.9), for estimates with low drift rates  $b$  could reverse the positive effect and lead to negative compensation. In such cases, a better adaptation to the present motion data could be obtained with a different, smaller  $b$  value (e.g.  $b = 0.02$ ). Therefore, the compensation could be utilized well to develop and examine the effects of a flexible filter.

To categorize drift types, I built three semantic groups  $L$  low speed,  $M$  medium speed and  $H$  high speed rotational movement. Under consideration of the general sensor specifications, the threshold ranges  $th_{lm} = \pm 400$  and  $th_{mh} = \pm 800$  [dps] were chosen. Based on the rounded measured maximal angular velocity averaged over all three motion axes, every sensor data was then assigned to one of the respective groups. Body parts that were exposed to a rotational movement of equal or less than  $\pm 400$ [dps] in average over all three motion axes were classified as low speed, body parts exposed to rotational movement between  $\pm 400$ [dps] and  $\pm 800$ [dps]

## 6.2. Enhancing Usability of the Data Augmentation Step

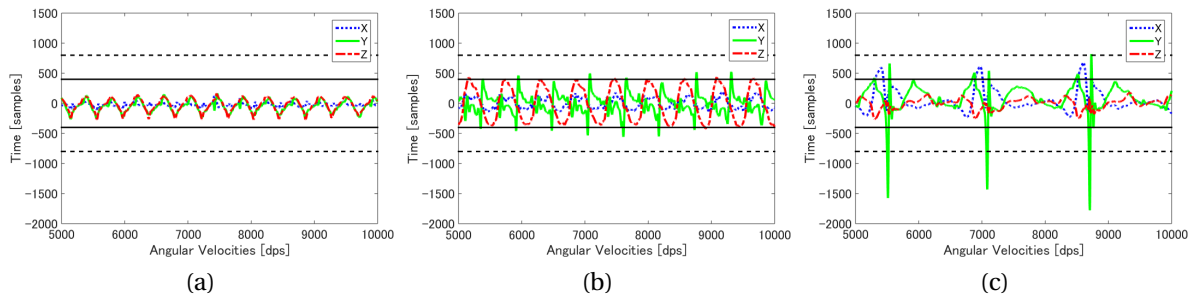


Figure 6.10: Angular velocities at x (blue, dotted), y (green, solid) and z (red, line) for three sample motion types jogging (a), jumping jacks (b) and throwing (c) at rA in relation to the thresholds  $th_{lm}$  at  $\pm 400$ dps and  $th_{mh}$  at  $\pm 800$  dps.

in average as medium speed and any other as high speed motion. According to the definitions of  $th_{lm}$  and  $th_{mh}$ , the sensor attached to rA was for example classified as low speed motion for jogging with angular velocities lower than  $th_{lm}$ , as medium speed motion for jumping jacks with angular velocities lower than  $th_{mh}$  and as high speed motion for throwing (Figure 6.10). Other body parts were not necessarily classified under the same motion speed. During throwing for example, P with a maximal angular velocity of  $\omega_{max} = 295$  dps was annotated as low speed, while the legs with rS, lS and rT and lT underwent medium angular velocities (Table 6.2).

Table 6.2: Rounded mean maximal angular velocities (AV) along x,y and z in dps at the pelvis and at an extremity E (right shank or arm) with kicking, jumping and right-handed throwing and their resulting classification to a speed label.

Motion	AV P max/mean	Classif.	AV E max/mean	Classif.
Kicking	[209, 367, 212]/263	low	[338, 716, 501]/518	medium
Jumping	[250, 565, 133]/316	low	[529, 925, 480]/645	medium
Jump-Turn	[519, 803, 326]/549	medium	[1011, 1750, 1101]/1287	high
Jump.Jacks	[179, 290, 110]/193	low	[458, 762, 494]/571	medium
Throwing	[423, 265, 68]/252	low	[935, 1487, 413]/945	high

As second categorization criteria, I defined two further groups that referred to the discussed variations in the number of rotation axes involved within a motion. Sensor data from motions that were of generally less drift did not require a high compensation value, even if only small angular velocities were measured by the gyro rate sensors. In other words, the effect of drift compensation values did not only depend on the angular velocities, but also on the general drift potential of every motion pattern. Therefore, motions around one principal rotation axes should be classified as Type 1 (designating high drift potential) and motions around more than one rotation axis as Type 2 (designating low drift potential).

The previous categorizations finally led to the six different bias compensation categories  $L1$ ,  $M1$  and  $H1$  and  $L2$ ,  $M2$  and  $H2$ , whose values have been determined experimentally



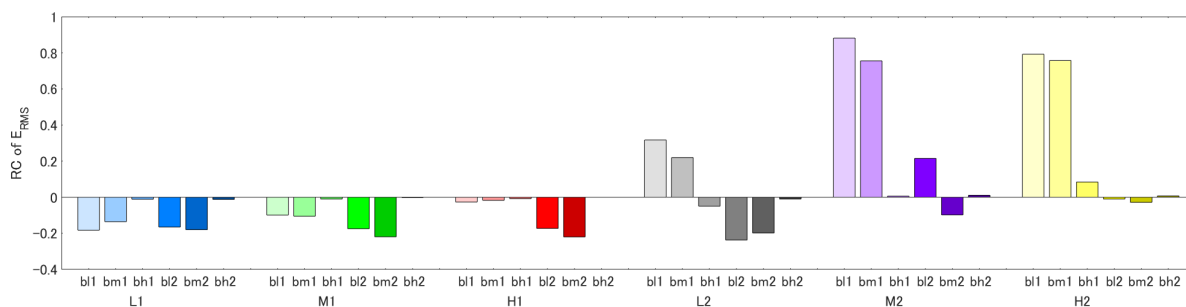


Figure 6.11: Graph visualization of the relative change in  $E_{RMS}$  for the drift compensated  $GI$  estimates under a logarithmic scale. Every motion type is represented by a unique color, whereas color saturation represents the different bias rate values (from little saturation for  $b_{l1}$  to high saturation for  $b_{h2}$ ).

for the subsequent comparison. First, the sensor data of all data captures was annotated and assigned to one of the six respective categories. Every category was then tested under several probable bias rate values of linearly increasing distance, and the value of best average accuracy over all estimation filters per sensor category chosen. This brought me to the error values  $b_{l1} = 0.05$ ,  $b_{m1} = 0.026$  and  $b_{h1} = 0.002$  as well as  $b_{l2} = 0.003$ ,  $b_{m2} = 0.001$  and  $b_{h2} = -0.001$ .

### Evaluating Enhanced Accuracies

For verification of the previously defined flexible compensation values, I first estimated the angular changes of all data captures with  $GI$  and the respective variant  $b$  values. Next, I compared the resulting  $E_{RMS}$  values to the  $E_{RMS}$  values of pure  $GI$  estimates without drift compensation. To emphasize changes on the overall accuracy values, I compared accuracies in relation with each other, whereas in all computations, the initial difference between estimate and ground truth remained the same. By this data consistency, just the drift and accumulating errors over time were evaluated.

Visualizing the relative accuracy changes, it became clear that the drift compensation worked well when appropriately put into context to the motion type and bias rate values (Figure 6.11, Figure 6.12). Accuracy could especially be increased for Type 1 motions that were suffering from larger drift (meaning the motions categorized as  $L1$  and  $M1$ ). For those motions - as for example P in jumping or the thighs in throwing - the average relative changes  $RC_{l1}$  and  $RC_{m1}$  under  $b_{l1}$  and  $b_{m1}$  were very good. In those cases, drift was dominant along certain motion axes, but could be efficiently reduced to a large extent with the compensation. For Type 2 motions of high angular velocities (meaning the motions categorized as  $M2$  and  $H2$ ) on the other hand, additional drift compensation was not recommendable under the generalized gyro bias rate values. I concluded that the drift arising as a result of missing variation in the rotational axes had a much bigger effect on the estimates as the motion speed. The amount of angular velocities mainly had an influencing effect on Type 2 motions, where drift was gen-

## 6.2. Enhancing Usability of the Data Augmentation Step

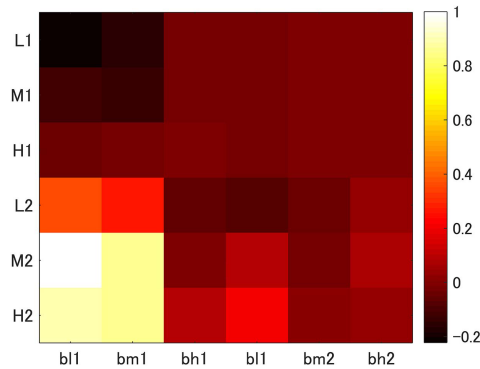


Figure 6.12: Matrix visualization of the relative change in  $E_{RMS}$  for the drift compensated  $GI$  estimates under a logarithmic scale.

erally smaller. It furthermore became obvious that accuracy values did not notably improve with drift compensation for high speed motions and even deteriorated for most motions of Type 2 when the chosen bias compensation value was not ideal. Consequently, finding useful bias rate values was more difficult in those cases due to the higher compensation effect on the overall estimates: already small changes in the  $b$  value could turn an appropriate drift compensation into an overcompensating value or vice-versa. In accordance with the previous results and assumptions, it was especially difficult to compensate  $H2$  motions.

From the relative changes of all drift compensated accuracy values I could see that accuracy improvements were primarily achieved when drift was heavily prevalent in the data (Table 6.3). However, error values were relatively high since only the  $GI$  method was used for analysis. Therefore, accuracies should be improved by applying data fusion filtering in the next step. For simulation, I added a drift compensation to the implementation of all fusion filter models that was performed before the integration of the gyro rate data.

Table 6.3:  $E_{RMS}$  error values over all orientation estimates for  $GI$  under the presented rate bias values and the relative change values  $RC$  to the uncompensated  $GI$  estimates.

Motion Type	$b_{l1}$	$b_{m1}$	$b_{h1}$	$b_{l2}$	$b_{m2}$	$b_{h2}$
Type L1	0.0907	0.1314	0.2295	0.2246	0.2343	0.2440
Rel. Changes	-0.5950	-0.4640	-0.0435	-0.0655	-0.0213	0.0239
Type M1	0.1446	0.1777	0.2825	0.2772	0.2878	0.2986
Rel. Changes	-0.3564	-0.3769	-0.0497	-0.0689	-0.0302	0.0098
Type H1	0.1834	0.2009	0.2219	0.2189	0.2251	0.2325
Rel. Changes	-0.1065	-0.0707	-0.0354	-0.0481	-0.0211	0.0124
Type L2	0.5036	0.3608	0.1802	0.1736	0.1909	0.2222
Rel. Changes	1.8595	1.1396	-0.1867	-0.2339	-0.1079	0.1310
Type M2	0.5749	0.5047	0.1720	0.1856	0.1649	0.1672
Rel. Changes	11.4479	8.1154	0.0212	0.3035	-0.0676	0.2314
Type H2	0.6089	0.5542	0.1563	0.1748	0.1468	0.1574
Rel. Changes	8.9963	8.1570	0.3694	0.8323	0.0820	0.1197

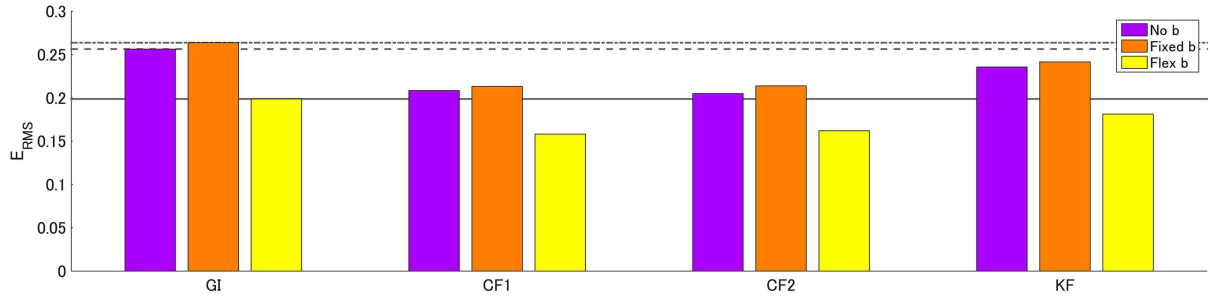


Figure 6.13:  $E_{RMS}$  error values averaged over all motion takes and sensor locations for  $GI$ ,  $CF1$ ,  $CF2$  and  $KF$  without drift compensation (purple), with drift compensation of a simple fixed value (orange) and with the proposed flexible drift compensation (yellow).

As for the  $GI$  estimates only, an additional drift compensation step could enhance the orientation estimates, whereas the effect was again especially obvious in motions prevalent to high drift. With no additional drift compensation, the filter models improved the accuracy measures of  $GI$  by  $RC_{CF1} = -0.6508$  for  $CF1$ ,  $RC_{CF2} = -0.5981$  for  $CF2$  and  $RC_{KF} = -0.0326$  for  $KF$  on average. Using the additional two step drift compensation improved the relative changes to  $RC_{CF1} = -0.6687$ ,  $RC_{CF2} = -0.6975$  and  $RC_{KF} = -0.6358$ . Especially for the  $KF$  estimates, a much higher accuracy could be achieved. Here, the chosen  $w_k$  noise values might have not been ideal for all motions beforehand. Under  $H2$  motion types, where it was difficult to predict and compensate drift, I abstained from additional drift-compensation and used only the fundamental fusion filter algorithm, which enhanced the estimates by an average relative change of  $RC_{CF1} = -0.4668$ ,  $RC_{CF2} = -0.4933$  and  $RC_{KF} = -0.1473$ .

Furthermore, I investigated the effects achieved with the flexible filter in comparison to an identical drift compensation using a simple, fixed bias rate value (Figure 6.13). This fixed value was chosen as the mean value between the six values of the flexible strategy and hence set to  $b = 0.0135$ . Results showed that the compensation with flexible filter values could address and reduce drift effects much better than the compensation with the fixed bias rate value. The former increased accuracy and performance of every investigated filter strategy in comparison to the averaged  $E_{RMS}$  error values without drift compensation. The latter did not perform better than the conventional filter design without additional drift compensation, since no ideal  $b$  value that respected all different motion types was set. As a result, I concluded that it is reasonable to extend the filter design by the proposed drift compensator when the flexible strategy that respects a motion's innate drift potential is employed. Then, the general applicability of orientation estimation methods can be improved, independently of the chosen fusion filter algorithm. Moreover, it was again obvious that a flexible use of the orientation estimation method is highly necessary when the underlying system should be employed for inertial data captures of different motion characteristics.

### 6.2.2 Intelligent Compensation of Heading Variability

To enable a generic measurement system it was not only necessary to employ a structure for accurate and target-specific orientation estimation, but also to hold any other variation in the data to a minimum. For the jumping data  $\mathcal{D}_R$ , this meant to identify the reasons for the discovered variations in the sensor headings.

In common simple sensor applications, the heading  $\psi$  of a sensor is determined with the measurement vector from the three magnetic field sensors. This was also the case for the proposed processing framework, where  $\psi_S$  of every sensor  $S$  was computed during the initial orientation estimation. Research has shown the negative influence of ferromagnetic materials on the accuracy of orientation estimates [dVVBvdH09, MGSR<sup>+</sup>15]. Further work suggested that even in free field measurements, where only the earth's magnetic field should be prevalent, sensors are subject to magnetic measurement errors that should be removed in a calibration step [HMZ<sup>+</sup>13]. Considering that differences already occur in less electric and magnetic environments, magnetic bias is likely to be even larger in man-made environments that include jumping ramps, slopes and technical equipment. The magnetic measurements should consequently not be blindly accepted. Indeed, magnetic bias in form of randomly varying sensor measurement offset could be observed in the raw magnetic field measurement data that may be responsible for the registered heading variations. Before deriving body kinematics from the sensor measurements, the processing system should therefore be made invariant to variances in the magnetic field first [RLBV05]. Magnetic bias in form of variation within the magnetic field measurement was included in the used orientation estimator *CF2*. However, constant differences present over a complete data capture as observed with  $\mathcal{D}_R$  were not addressed. As a consequence, an additional compensation method for variant initial field measurements was introduced and added to the full measurement system.

#### Compensating Magnetic Disturbances

To compensate for magnetic disturbances, I made use of the fact that the sensors' heading angle was defined in reference to the direction of the location's magnetic field. In a first step, a premeasure was added to the processing system to compensate for constant larger variations in  $\psi$ . For this, an independent set  $S_{fV}$  was created containing reference magnetic field vectors for the individual sensors at the jump start location. As explained before, the x-axis of the global coordinate system was set to be aligned in the direction of motion (Section 5.2.1). Consequently, the reference field vectors were built from the magnetic sensor readings of the x-axis alignment without roll and pitch rotation considered. For every sensor  $n$ , its initial heading angle was then determined with the respective field vector  $f\vec{V}_n$  in  $S_{fV}$ .

The second step addressed inconstant differences in the field measurements by integrating an additional field compensation method to the framework after the initial orientation estimate (Figure 6.14). The general idea here was to compare  $f\vec{V}_n$  with the current real magnetic

## Chapter 6. Validation and Enhancement of the Augmented Motion Data

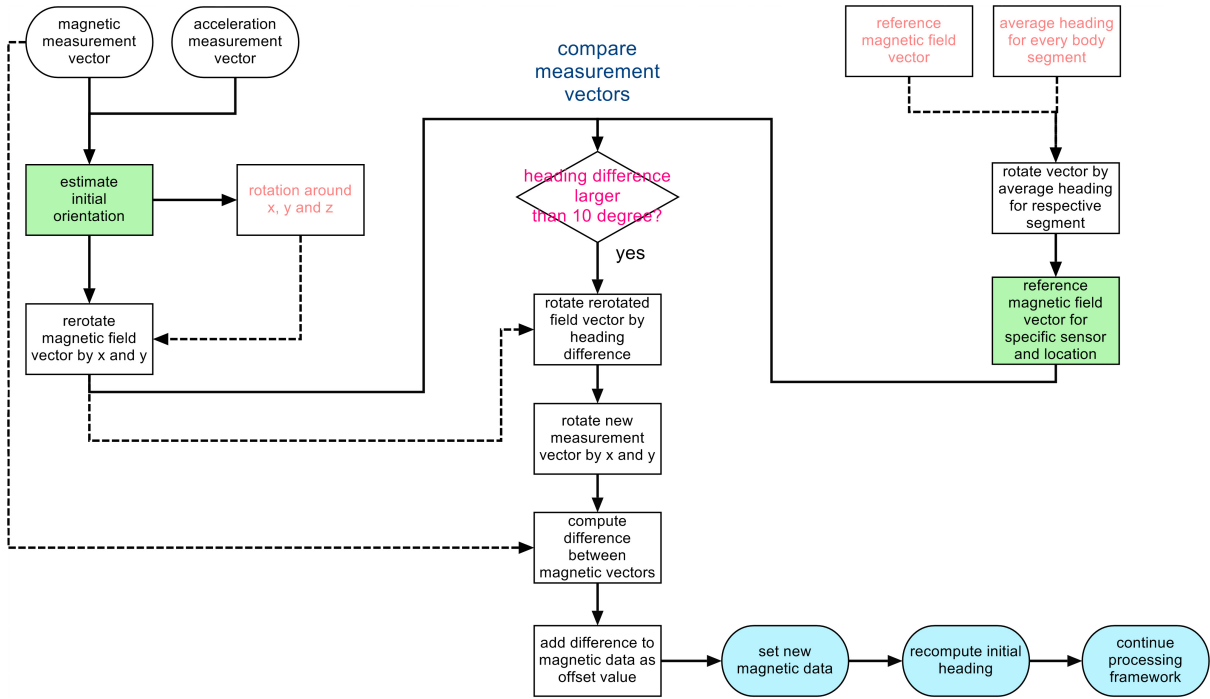


Figure 6.14: Working principle for the additional magnetic bias compensation method equalizing disturbances in the magnetic field measurements.

data  $m\vec{V}_n$ . The difference is then added to the magnetic measurements as offset values to stabilize and equalize the distorted magnetic field measurements over all data takes. For this,  $m\vec{V}_n$  was rotated by the estimated initial pitch and roll values  $\theta_i$  and  $\phi_i$  to get a vector  $r\vec{V}_n$  that was only influenced by the heading component. Furthermore,  $f\vec{V}_n$  was rotated by an average heading  $\psi_{aj}$  for the respective sensor location at segment  $j$ : the longitudinal axes for the sensors attached to rF, lF and P in the start position were for example bound to the in-run slope and start gate (ignoring changes that occur from pitch). They were therefore aligned forward, approximately parallel to the coordinate system's x-axis, so that  $\psi_a$  was close to  $0^\circ$ . The hip joint is generally lightly spread in a natural relaxed sitting position - stable magnetic conditions should consequently lead to an average  $\psi_a$  of approximately  $30^\circ$  for rT and lT. Finally, the rotation of  $f\vec{V}_n$  yielded a reference vector  $h\vec{V}_n$  that represented the field measure for the general start position per placement and sensor. This allowed to determine the heading difference  $\psi'$  from  $r\vec{V}_n$  and  $h\vec{V}_n$  by the simple trigonometric relation in the x-y plane

$$\begin{bmatrix} H_{nx} \\ H_{ny} \end{bmatrix} = \begin{bmatrix} \cos \psi' & -\sin \psi' \\ \sin \psi' & \cos \psi' \end{bmatrix} \begin{bmatrix} R_{nx} \\ R_{ny} \end{bmatrix},$$

where  $R_n$  and  $H_n$  are the two-dimensional normalized vectors built from  $r\vec{V}_n$  and  $h\vec{V}_n$ . To account for style differences from the average sitting start position, existing deviations in the magnetic data were only compensated if  $\psi'$  was larger than a certain threshold  $t_c$  set to  $10^\circ$ .

In the main compensation cycle, the difference  $\vec{d}_n$  to the current magnetic field vector  $m\vec{V}_n$  was then determined with a new vector  $c\vec{V}_n$  built from  $r\vec{V}_n$ , a quaternion  $q_\psi$  representing the heading difference  $\psi$  and a quaternion  $q_{er}$  representing the previously determined initial pitch and roll values as

$$\begin{aligned} r\vec{V}_n &= q_\psi \otimes r\vec{V}_n \otimes q_\psi^* \\ c\vec{V}_n &= q_{er} \otimes r\vec{V}_n \otimes q_{er}^* \\ \vec{d}_n &= m\vec{V}_n - c\vec{V}_n. \end{aligned}$$

In a last step,  $\vec{d}_n$  was added as offset value to the magnetic field data of the full jump and the initial orientation estimated a second time with the new magnetic data. Finally, the general processing and determination of body kinematics could be resumed with the new initial states to estimate the necessary orientations and joint positions.

Since only the initial heading state was changed by this bias compensation, the proposed magnetic compensator did not have any influence on the general estimation of the angular changes with *CF2*. Instead, the magnetic field measurements were corrected in form of a general offset only. Therefore, the resulting orientation estimates within the captured jumps were invariant and only changed with respect to their initial start values.

## 6.3 Results and Discussion

The presented data augmentation and processing methods could be considered a robust tool for the determination of kinematic motion data. Final accuracies deviated less than  $3^\circ$  from the Vicon ground truth data, and less than  $10^\circ$  from environmental and biomechanical constraints. As a conclusion, the methods could be considered as well suited for use in augmented motion information systems. However, I have shown that the accuracy of orientation estimates varied with the characteristics of a performed motion and environmental conditions. Of particular influence were the amount of angular velocity and the number of rotation axes occurring in a motion, as well as disturbances in the magnetic field. By manually adapting the processing settings to those influences, a system can be made invariant to errors in the data, but cannot be considered user-friendly anymore. To ensure a generic framework, I introduced additional methods for intelligent enhancement of the basic numeric motion data. For the purpose of system re-implementation, the most important findings shall be summarized in the following.

### Simulation Data

Common strategies for the estimation of orientation estimates address measurement and system process errors (drift) by combining the data of multiple measurement sources. In

## Chapter 6. Validation and Enhancement of the Augmented Motion Data

---

general, the performance and accuracy of such a filter model is determined by a predefined fixed value. However under diverse applications of the motion measurement devices, it might not be sufficient to rely on one fixed filter value – under specific motion performances, the set filter values might not be able to remove drift that occurred as a result of accumulated variate sensor noise.

Differences in the individual sensor specifications led to variations in the amount of drift per sensor: to handle those fundamental differences, I recommend to investigate each sensor's behavior in a prestudy, so that hardware specific differences could be taken into account in the experimental setup.

Moreover, data analysis showed that the accuracy of attitude estimators varied in dependence on the performed motions, their occurring angular velocities, the number of rotation axes involved and the amount of external acceleration acting on the measurement sensors. Motions that underwent high angular velocities over several dimensions for example suffered from significantly less drift than monotonous motion patterns of low angular velocities. Using an extra computation step, I simulated an intelligent drift computation that could flexibly adapt to the characteristics of specific motion patterns. Results suggested that under motion data of varying dynamics, it is recommendable to employ an automated motion classification system that annotates the drift potential of a motion: taking into account simple elementary motion knowledge like the amount of angular velocities and motion dimensionality, the chosen drift compensation could be adapted well to the expected amount of drift per motion, and the accuracy be improved considerably. Those accuracy improvements were independent of the chosen filter design, and can hence be expected to apply to any orientation estimation filter.

Including the proposed intelligent drift compensation as flexible filter strategy to the orientation estimates, variations within the data could be significantly reduced. Repeating the previous principal component analysis, distribution of the first three components was clearly modified, so that it is resembling the distribution of the ground truth data (Figure 6.15). For example for the sensor data at IS illustrated beforehand, one can see that the flexible filter values resulted in a u-shaped distribution of the principal components' coefficients similar to the ones of the ground truth data. A fixed value on the other hand resulted in a variant distribution pattern.

As a conclusion, a flexible system that adapts to the specifications and characteristics of a captured motion does not impose the need of changing the fundamental system parameters while providing better, more accurate and significant kinematic motion data. Analyzed motion types should be annotated with respect to the amount of rotational axes involved and the expected maximal angular velocities, ideally before the main motion analysis task: both factors considerably influence and change the general accuracy values, whereas the amount of rotational axes involved had a bigger impact on the simulation data. Biomechanical knowledge of the performed motion and its principal axes is useful to further advance and automatize the data processing from inertial measurement units, whereas it is also possible

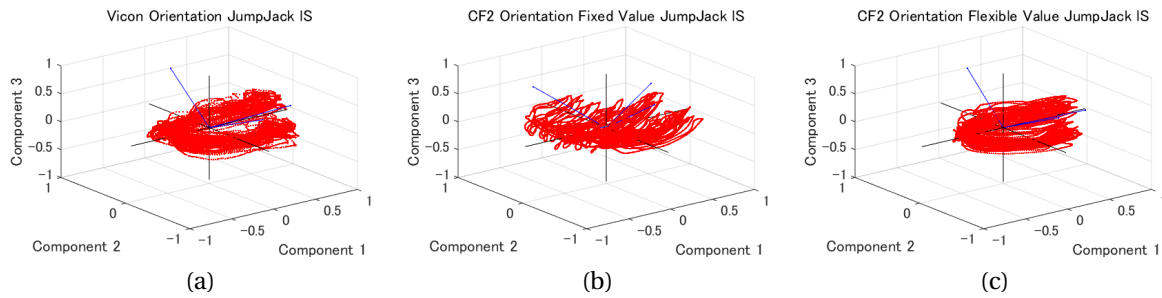


Figure 6.15: Visualization of the three main principal components for the Vicon ground truth data and the *CF2* estimates with the former less jumping jack data capture at IS. The flexible value (c) brings the coefficient distribution closer to the ground truth distribution.

to retrieve the fundamental information from the user by a user interface or text input.

### Field Data

Investigations on the field data showed that magnetic sensor data from a standardized or conventional inertial capture framework cannot be expected to be reliable within the ski jumping environment. Rather, it should be considered that standard processing methods are not appropriate under magnetic disturbances of the ski jump hill. This observation is likely to hold for other motions being executed at sporting venues of high ferromagnetic construction material as well.

While accuracies could be determined to be within  $3 - 5^\circ$  accuracy in pitch and roll with an appropriate noise value of the utilized filter model, body segments' heading estimates were influenced by magnetic bias. This heading variation did not allow for automatic processing of the computed data and required additional compensation of the magnetic bias during the data processing framework.

Orientations and heading values after error compensation allow for the conclusion that the newly developed magnetic bias compensation algorithm made the measurement system robust against magnetic variations under different capture situations: results were considerably improved for both data visualizations and the range of computed initial heading angles. Before compensation, many different  $\psi$  values for all sensor placements of all data base captures could be observed that appeared randomized and uncontrollable. After compensation, the largest variances in the sensors' heading angle could be eliminated or at least be reduced to a very small range of heading difference (Table 6.4). The remaining differences can be considered natural variations created by differences in the initial start position per athlete and jump. It was clearly visible (Figure 6.16 bottom row) that the proposed compensation method drastically reduced the variation in initial alignment, as the motion ranges within the initial heading values  $\psi$  were reduced significantly. With the additional compensator, the



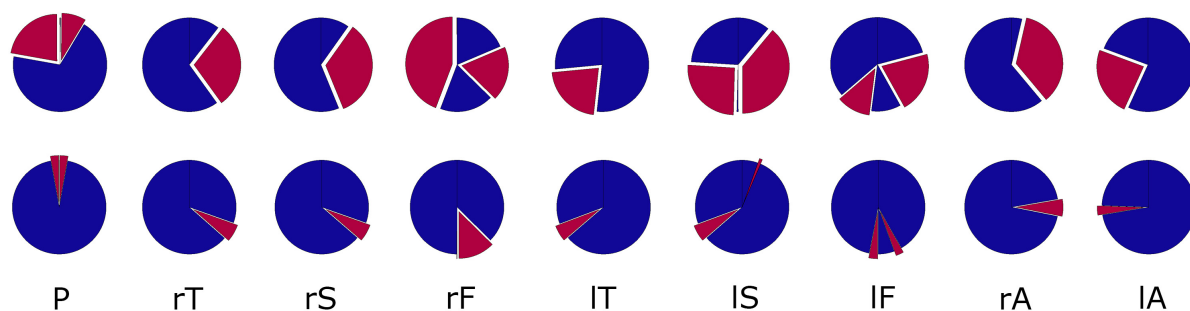


Figure 6.16: Visualization of the differences in heading  $\psi$  before (top) and  $\psi_C$  after (bottom) compensation. Heading angles are of positive values  $0$  to  $\pi$  on the right side of the circle and of negative values  $0$  to  $\pi$  on the left side of the circle, whereas  $0$  is at the bottom and  $\pm\pi$  at the top of the circle plot. Red pies represent the angular areas in which initial heading angles occur.

Table 6.4: Absolute maximal variances in the heading angle  $\psi$  occurring over the complete data set  $\mathcal{D}_R$ . After compensation, the absolute maximal heading deviations  $\psi_C$  were significantly reduced. Both heading angles are depicted in radians.

Sensor	max Variance $\psi$	max Variance $\psi_C$
P	1.39	0.18
rT	1.85	0.38
rS	2.13	0.37
rF	2.77	0.79
rA	1.37	0.35
IT	2.44	0.36
IS	1.32	0.20
IF	2.22	0.37
IA	1.50	0.20

framework is therefore likely to produce meaningful results that allow for further data use under real-time conditions in various sporting events.

The additional compensation method requires initial sensor orientation estimates, which does not only help to detect variations in magnetic heading, but also yields stable results in the orientation estimate directly from the beginning of data capture. It is furthermore relative to the local properties of the capture and sporting venue and can therefore be used in various locations and environments. This is not only useful for ski jumping, but also any other inertial capture application in both sports and rehabilitation. Since both the magnetic heading compensation and the initial orientation estimate are based on very simple trigonometric relations and quaternion calculations, they hardly influence the overall computation time and are eligible for a possible future use under real-time conditions.

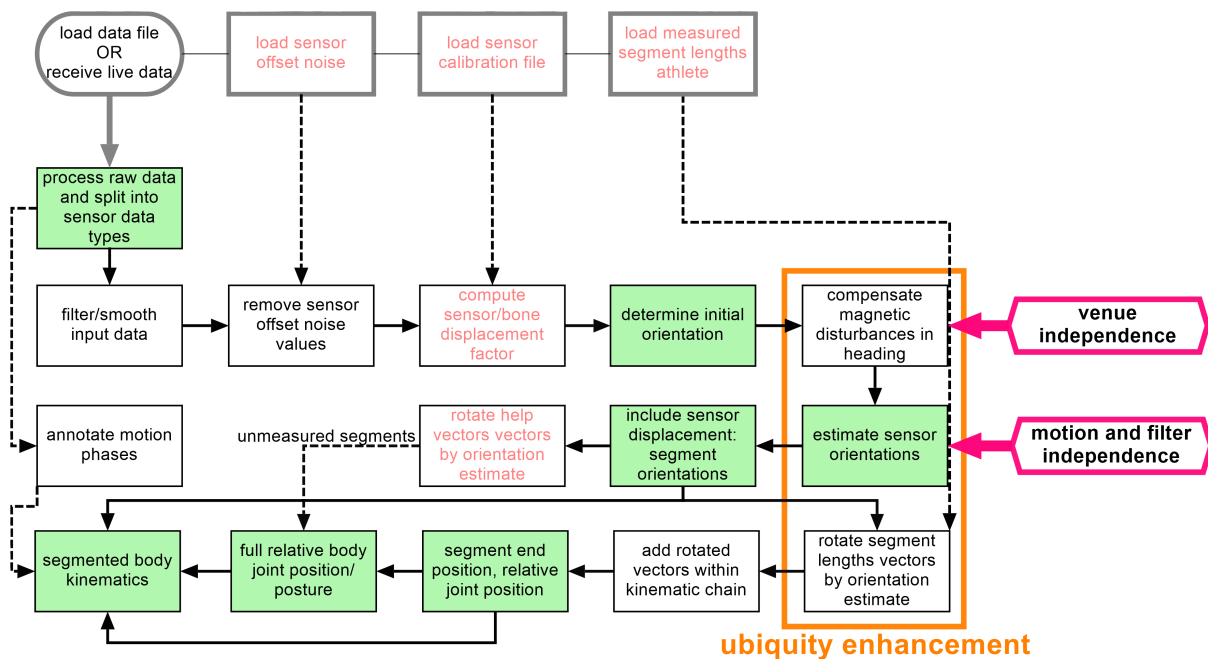


Figure 6.17: Working principle of the complete processing system with the developed additional methods that enhance or maintain high accuracy of the derived body kinematics independently of the sporting venues and the captured motion data.

### 6.3.1 Usability Enhancement

I believe that the utilization of the previous two strategies will notably enhance the usability of an overall motion data processing pipeline (Figure 6.17). This is because they ensure the derivation of accurate and reliable data without any user interventions. Herewith, they allow for a subsequent use of generic and automated information retrieval methods in the overall feedback pipeline which would not be possible otherwise: accuracy values suggested that to obtain accurate orientation estimates in the conventional way, the filter values have to be manually adapted. Moreover, random magnetic bias at sporting venues can lead to unreliable body joint positions and kinematic motion information from the sensor data.

Whereas the flexible drift compensation is subject to system user input data, the magnetic bias compensation is a self-contained, autonomous method. For this reason, I will first dwell on the usability factor of the latter strategy. Being included in the processing pipeline, the presented magnetic compensation does not require any additional interaction with the system. The only parameter necessary for the execution of the compensation function within the processing framework are reference direction vectors of every sensor's magnetic field in the capture environment. Those reference vectors can be easily obtained as measurement data from the static sensors placed close to the start of motor action and aligned in forward direction. By adding one additional measurement to the data collection procedures, the system is consequently made robust to variances in the magnetic field, and the simplicity of

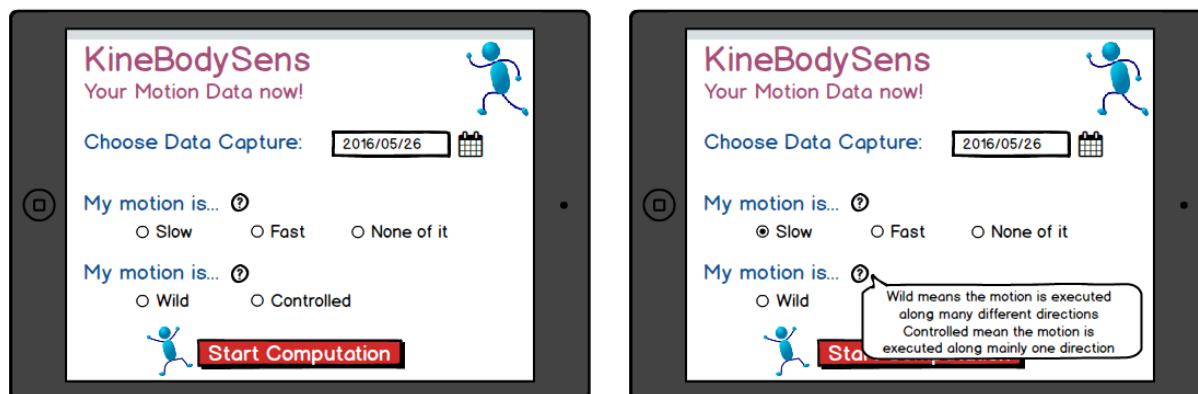


Figure 6.18: Sample user interface for man-machine communication to define the elementary a-priori motion knowledge for drift reduction. Simple motion descriptions are specified by the user and then internally translated to the use of a predefined filter value.

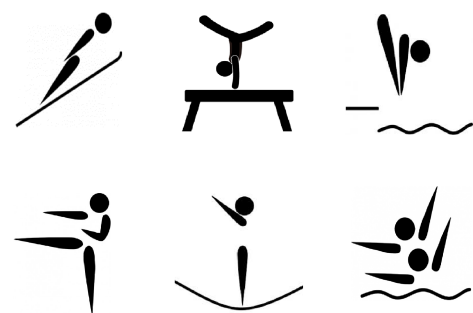
use for inexperienced or technically less versed users maintained.

Implementing the intelligent drift compensation, accuracy values of orientation estimates should ideally be improved on an individual basis for every specific motion performance. A certain number of possible filter values could for example be saved beforehand for every used (or the chosen) fundamental estimation filter. Filter values of the processing system could then change dynamically with the current motion characteristics. Such strategy could be implemented in a very simple set up: the target motion is annotated with respect to its angular velocities and motion dimensions in a basic way before the motion performance. This annotation can for example be provided by a simple, elementary user interface (Figure 6.18). The program's filter values and drift compensation could then be automatically modified according to the annotations and predefined internal motion specifications, and the estimation filter be universally used for all motion patterns. In a more ubiquitous scenario, the filter values could furthermore change dynamically under the currently measured angular velocities, taking into account also sudden phases of high impact or angular changes of body parts. As a result, the accuracy values of orientation estimates are improved on an individual basis for every specific sport motion performance, while it is not required to individually change the fundamental setting.

The successful implementation of a generic and universally applicable estimation filter is a key factor for the future use of inertial sensors in motion performance scenarios. Providing a simple use for any kind of system users, the proposed drift and magnetic bias compensation consequently constitute valuable data enhancement strategies: by refining the estimates while maintaining simplicity and universality of the processing framework at the same time, it should be possible to ensure more sophisticated data analysis applications and software tools in future.

# Utilizing Numeric Motion Data

## Part III





---

In the next part, the remaining two processing stages of a motion information system (sense-making and retrieval of relevant information) are examined. They can take up various forms, and their algorithms mainly depend on how the final stage of information retrieval is designed to occur within any specific system. This means that information retrieval can be induced by both internal perception of a user, or by external enforced impulses. However, both scenarios target on the existence of information understanding and retrieval intelligence, either from an existing biological motion knowledge or from an artificially created one. Much information given in this part therefore comprises components and algorithms from machine learning.

In the first chapter, I discuss three different strategies for the sense-making of the derived body kinematics that prepare the implementation of the final application samples. One is the transformation of motion data into visual information, one is the transformation of motion data into sound feature representations that can then be used to sonify a motion, and the last one is the transformation of motion data into motion feature representations that can be used to learn machine knowledge for a certain information retrieval. Whereas the first one is a very universal transformation, the idea of the latter two is to extract highly discriminative and representative features from a motion performance that can give information on specific points of interests during the motion exertion. An additional part of the numeric feature transformation is furthermore the semantically significant segmentation of the input data. With respect to the sport scenario, this means for example to use either raw inertial or processed motion data to determine different motion phases and to segment and temporally annotate motion performances. This can help to investigate only specific parts of a motion instead of a complete motion take, making the computation faster, quicker and also more specialized towards specific analysis targets like the exertion and motion behavior in key motion phases.

Lastly, the two final applications – movement sonification and motion rating – are discussed in more detail in the remaining two chapters of this part. Since motion sonification is subject to internal feedback reception, I mainly focus on the evaluation and rating of performance qualities (a new, innovative scenario which was initially born out of personal interest and affliction). To automatically retrieve motion information necessary for the provision of specific style and error assessment, it is reasonable to include intelligent learning methods in the processing pipeline. They can create permanent, latent machine knowledge that is then retrieved and used to provide deeper data insights at all times. For example, they are very likely to be useful for performance surveillance, monitoring of aerodynamic conditions, motion evaluation and further motion analysis tasks. Common methods are introduced and explained with respect to the present problem. This comprises the implementation and training of learning methods for classification and error recognition of a motion action, as well as the identification and selection of meaningful motion features by means of automatic, unsupervised motion feature selection.

As a result, a categorization system is introduced that labels the transformed motion features

---

as either technical or aesthetic rating features with respect to various style criteria. Moreover, a design for a full ski jump evaluation system is presented. Here, the focus of the demonstrated and implemented methods was put on the creation of methods to rate technical aspects of a motion, since it is much easier to numerically define a motion quality with respect to technical descriptors (e.g. body angles or conduct in landing) than with regard to aesthetic impressions of a performance.

## 7 Making Sense of the Motion Data

The main task for every augmented motion information system is to process the collected sensor data in such a way that useful information is extracted and provided to users like coaches and athletes. More and more training and activity surveillance devices appeared in leisure, health and recreation over the last years, providing data insights or recommendations on future activities. However, similar technologies did not become standard in competitive and professional sports so far. With more complex motion data and the demand for higher information content, more accurate information retrieval and computation algorithms are necessary in those application fields.

To enhance the information content of available numeric motion data, it is very useful to define meaningful features that represent the structure and characteristic of the underlying data. Common strategies to build such features used in many motion action recognition learning scenarios are segmentation and motion feature transformations. Either raw inertial or processed motion data can for example be used to determine and temporally annotate a motion performance into semantically significant motion parts. Instead of a complete motion take, only specific parts of a motion need to be investigated then, making the computation faster, quicker and also more specialized towards phase-related analysis targets. Besides, the present numeric motion data can be used to extract highly representative features from a motion performance that give information on specific points of interests during the motion exertion. Apart from the previous two strategies, also other approaches and possibilities can be applicable for a transformation into usable features such as auditive or visual representations.

Knowledge about the specific characteristics of a certain motion is beneficial for the success of any kind of feature transformation. In the following, I discuss how to use knowledge on motion techniques for the creation of meaningful feature representations under the two sample applications movement sonification and motion rating.

### 7.1 Transforming Data into Visual Features

The simplest way of transforming the augmented kinematic motion information into more intuitive and comprehensible data is visualization. Body segment orientations, joint positions and joint angles can be easily presented to the user (may it be athletes, coaches or



## Chapter 7. Making Sense of the Motion Data

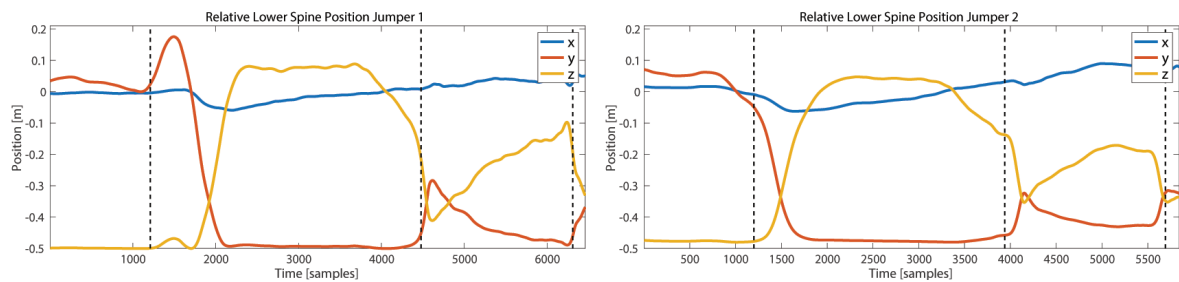


Figure 7.1: Data plot of the relative position of the lower back computed from two sample data captures and their respective phase annotations for the beginning of the in-run phase, the take-off and the landing (vertical black lines).

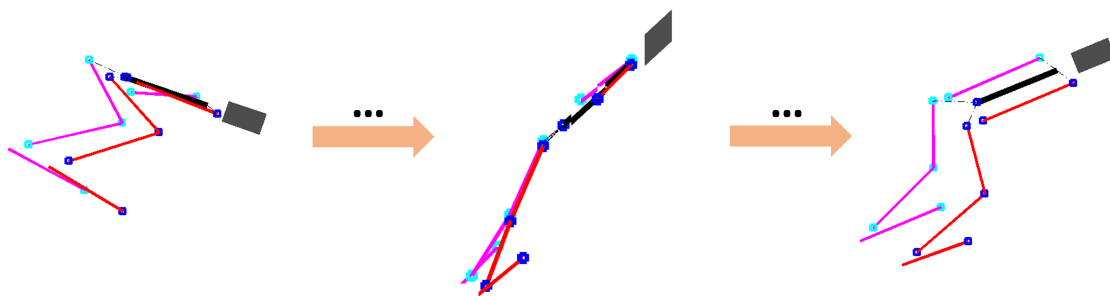


Figure 7.2: Screen shots of an animated figure visualization during in-run, flight and initiation of the landing of a ski jump computed from estimated joint positions along the kinematic chains of spine, arms and legs.

spectators) as plots of the temporal data evolution (Figure 7.1). For ski jumping for example, especially parameters that influence the aerodynamics and hence the length of a ski jump like the body-ski angle, the ski attack angle, the hip angle or the ski-opening angle might be useful.

Using segment joint positions and additionally measured lengths of body parts that are connecting the kinematic chains of interest, it is furthermore possible to create a full body motion visualization in animated figures over the complete flight – from the sitting position at the top of the jump hill through to the landing and outrun (Figure 7.2). Rendering a sequence of consecutive frames, it becomes then possible to create video sequences that could be watched on the computer or any other playback device.

Both visual feature transformations were furthermore also already used before to verify the accuracy of the field motion data (Section 6.1.2).

## 7.2 Transforming Data into Sound Features

The provision of auditive motion feedback to the athlete by sound (respectively movement sonification), is considered to be an effective additional source of information for motor control and motor learning [Eff05, EFW11]. So, it was for example shown that auditory information enhances human action observation systems of the brain [SMH<sup>+</sup>13]. In contrast to visual feedback, which is explored very well, there are only a few studies on efficient transformation of biological motion into auditory feedback [DB11]. Neural adaptation and learning processes evoked by auditive feedback are still under empirical examination with respect to the selection of suitable movement features, kinetic–acoustical mapping strategies and the number of regarded transformed feature dimensions. Efficient movement sonification strategies and principles for accurate display of the captured data are not commonly established yet. As a general rule, significant motion features should be built in such a way that they can be understood intuitively and reflect specific motion structures such as singularity within motion patterns or motion range. From the perspective of kinesiology, this means that the most relevant aspects within a motion - for example segment orientation, joint position data and motion velocity of the joint of interest - should be described. In the present study, the parameters position and velocity were chosen to represent the desired **acoustical kinematics**. They are part of the previously augmented motion data, but can be presented in various ways like pure axial coordinate values, pure angular coordinate values or a mix of both during the sonification process. All of those data representations offer a different level of complexity which might be more or less intuitive and useful for certain sonification tasks.

Finding the right data representation for a sonification strongly depends on the sonification purpose, the performed motion and the intended sound mapping. First, it is therefore necessary to choose the data representation most suitable for the intended sonification purpose. Various possibilities exist to process inertial motion data for further application in movement sonification [YH83]. Three primary data representations are introduced and their potential efficiencies within the movement sonification framework discussed here. In the second step, positional information in the chosen data representation is then transformed into sound parameters.

### 7.2.1 Data Representations for Sonification

Using a simple forward kinematics approach, joint positions are easily computed as Cartesian point coordinates along the global frame from the length and orientation of a chain of neighboring body limbs (Section 5.4). This computation defines every joint position  $p$  as a three dimensional vector so that  $p = [X_p \ Y_p \ Z_p]$  with  $X_p$ ,  $Y_p$  and  $Z_p$  containing the values along the corresponding axis. However, biological motion perception does not follow mathematical definitions. Instead of such absolute representation of joint position, a continuous relative change of related positions is perceived [TWL05]. For example, moving the hand along the

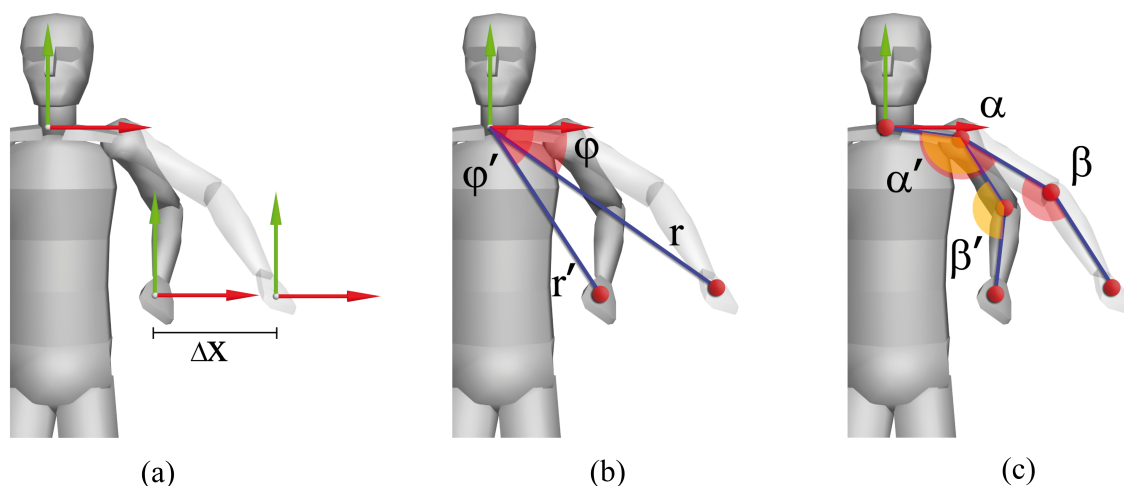


Figure 7.3: Defined coordinate systems for (a) Cartesian, (b) spherical coordinates and (c) angular representations. Changes in the position of a joint are differently displayed within each coordinate system. The definition for the coordinate systems is corresponding to the sensorimotor reference frames in humans.

horizontal axis is not only equivalent to a change in the hand's position along this axis, but also linked to positional and angular changes of further joints. Cartesian data representation uses only biological information on one selected joint (Figure 7.3a) and cannot display this information: moving the wrist along a horizontal line would only evoke a change in the x-coordinate data. When sonifying a biological movement for motor learning, it is consequently necessary to use another representation that includes the full motion characteristics of all related joints.

A data representation that is closer related to the principles of internal human motor control are spherical coordinates [YH83]. Here, joint position is defined by a radius  $r$  and the two angles azimuth  $\psi$  and inclination  $\theta$ . The radius represents the distance of a joint to the origin of the relative coordinate system, which is located in the middle of the actor's body in the present case. Every point  $p$  is then defined by a three dimensional vector so that  $p = [r \theta \psi]$ . Research has shown that spherical coordinates control arm movement in similar ways as the central nervous system [GTM02, SBGI10]: using angular movement features, more detailed and essential movement information can be displayed by only one joint (Figure 7.3 b). For the current example, moving the wrist along the horizontal axis is described by changes in the parameters  $\psi$  and  $r$ . Consequently, the positional data does not only represent the motion along this axis but also include a decrease of the hand's distance to the body center. This also means that additional information about the enclosed angle between elbow and radius is obtained.

A third strategy for the representation of positional data is to not involve any positional

information at all by using only angular movement features. To display the motion of a joint under this constraint, it is necessary to include the degree of freedom of every preceding related joint within the kinematic chain. This representation produces much more detailed information (and hence also a richer sound), but is also very complex: towards the end of a kinematic chain of several joints with two or three degrees of freedom, it might be necessary to display 10 or more parameters at the same time. To display the axis parallel horizontal sample motion of the wrist, all angles in shoulder, elbow and hand would need to be displayed, which means at least two angles at shoulder and elbow joint (Figure 7.3 c). The complexity of angular data representations can hence swell up very easily, and thus make motion feedback very difficult to perceive and understand.

Every data representation has its own advantages and disadvantages for respective use cases. The intention of a movement sonification in an augmented feedback system generally is to support neural motor skill acquisition processes. Therefore, it is recommendable to choose a data representation that conforms with the internal biological motion perception. As angular representations tend to be too complex to be perceived clearly, spherical coordinates were chosen for the transformation of motion information into sound parameters. They are satisfying for use in the next step with respect to both representation accuracy and amount of necessary data.

### 7.2.2 Sound Mapping Strategies

Sound can be produced in many different ways, such as by instruments or by the superimposition of oscillating sine waves of various frequencies. Here, it was chosen to display motion data streams as sound on the base of the MIDI standard. Its specification offers a consequent and well-defined way to control and generate sound that make it convenient to map motion data onto sound. Tones in MIDI are for example generated by sending a respective control demand, and sound properties easily influenced and changed by a variation of sound control messages. Furthermore, the timbre or constitution of a sound can easily be changed before or even during a performance with so called 'sound programs' simulating different sounds and instruments (similar as in an electrical keyboard).

MIDI offers a broad range of predefined standard control commands that leaves various possibilities to map motion data onto auditory features. They are amongst others attack and release time, timbre, tone frequency, velocity or sound effects as reverb and echo. The coarse resolution of any of such MIDI control messages consists of 128 steps in the interval [0, 127] to trigger sound properties. For example, every time the motion velocity within a motion performance reaches or exceeds the set maximal velocity, the corresponding MIDI controller could be of maximal value 127. For static phases with no motion velocity at all, the MIDI controller could in contrast be of minimal value 0.

As software for the manipulation of such sound parameters, I chose Miller Puckette's software

## Chapter 7. Making Sense of the Motion Data

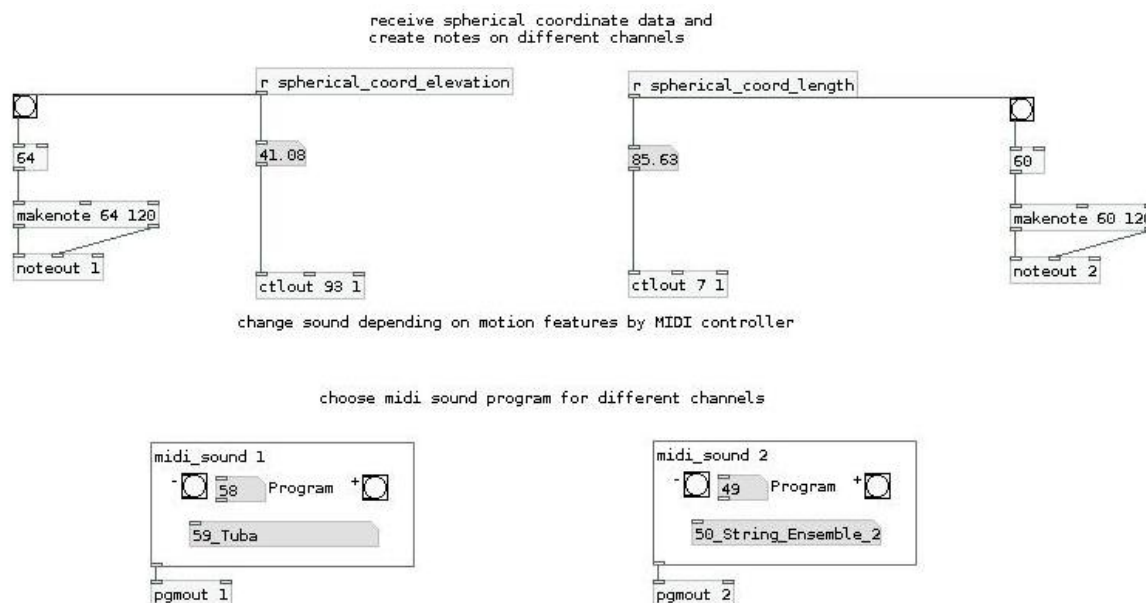


Figure 7.4: Sample PD patch to control sound by incoming motion data.

Pure Data (PD) [Pur] for electronic sound creation. PD is a graphical open source programming language and offers the possibility to send MIDI control messages that produce and influence sound within MIDI sound systems. Furthermore, it has been used for MIDI movement sonification before, for example to display rowing motion [Hen07]. Figure 7.4 shows a simple sample PD patch that creates MIDI notes and sends MIDI control messages to change sound properties in accordance with the corresponding motion feature. Here, spherical motion data (*spherical\_coord\_elevation* and *spherical\_coord\_length*) is constantly sent to create notes by the commands *makenote* and *noteout*. The MIDI controller 93 and 7 representing chorus and volume are constantly triggered by incoming data via the command *ctloud*, so that the resulting sound changes in real-time. Many other MIDI controllers can be accessed in the same way, leading to different sound results according to their MIDI specification [Rot95]. Sound mappings that have already been realized for sonification purposes are listed in [DB11].

To have access to a broad variety of simulated electronic sounds, the PD software output was connected to the Synth Modul 'SonicCell' (Roland Germany GmbH, Nauheim, Germany), which offered more than 300 predefined sound sets ranging from instruments like classical viola and flutes to percussion instruments and artificial sound creations. One frequently used sound was the sound called 'Jupiter Lead', a permanently held electronic sound creation that enables an easy modulation of the chosen sound parameters. Using PD software for internal sound manipulation of the Roland Synth Modul, the resulting system then displayed the selected acoustical kinematics in real-time. Consequently, a motion could be sonified for longer time periods of more than two hours, only restricted by hardware specifications such

as battery lifetime and others.

Various upper body motions by different motion actors were sonified and tested in first empirical studies: large and spacious movements such as arm rotation or throwing, as well as small and spatially centered motions such as drinking, grasping or writing. The sound parameters and their mappings were chosen under semantic aspects from a movement science related perspective and included the pitch (tone frequency), volume, brightness (spectral composition) and stereo effects (Table 7.1). All motions could be displayed well in real-time under different selected sound properties and sound mappings while maintaining characteristics of each motion. By mapping motion velocity onto volume, highly accelerated throwing was for example perceived as much louder than drinking. Under the implemented system, the chosen sound mappings could furthermore be freely combined to one-, two-, three- or four-dimensional auditory motion information.

Table 7.1: Description of the MIDI sound mappings chosen for experimental investigations on the effect of auditory feedback for motor learning in rehabilitation.

Feature	MIDI Controller	Mapped Motion Parameter
Pitch	tone bend	Inclination $\theta$ of a body joint (height information)
Channel Volume	controller 7	Motion velocity of a body joint, static motion - zero volume
Brightness	controller 74	Radius $r$ (distal information)
Pan (Stereo effect)	controller 10	Azimuth $\psi$ of a body joint (left-right information)

### 7.3 Transforming Data into Motion Features

For many motion analysis tasks, it is reasonable to include machine learning methods in the system's processing and computation pipeline. The creation of permanent, latent motion knowledge is for example very useful for performance surveillance, monitoring of aerodynamic conditions or motion evaluation. Generally, those problems are of fundamental design and include the retrieval of meaningful information from the sensor data and the identification of anomalies or specialties of further interest to the user. To make use of the raw multi-dimensional inertial sensor data in such scenario, good strategies for the extraction of the relevant motion features are necessary. Machine learning and data base retrieval technologies offer a vast variety of algorithms for speech and multimedia processing. Research in activity recognition from wearable sensor data for example has resulted in statistical raw-signal based features, event-based features, multilevel features derived from clustered statistical occurrences and kinematic body motion information [BBS14]. Many of the methods used in the context of sports data [Bac12] focus on low-level features and extract information directly from the raw sensor data [MF15, DMA14, GJ11b, PLY10, MCG<sup>+</sup>15, VDSBB<sup>+</sup>15]. For this work, I focused on both signal-based and body model features for two reasons. First, signal-based features are immediately available from the sensor data. Second, model-based

features as obtained from the augmented numeric motion data are closest related to the biomechanical descriptions of a motion performance. With the derived body kinematics, higher-level motion information like positional and temporal evolution of joints or relational information between body parts can be provided [HBMS11].

### 7.3.1 Segmenting Motion Data into Parts

Machine learning programs for human activity recognition usually contain a data segmentation step before the main computation to segment the data stream into correlated motion parts [KC14]. For this thesis, I developed a segmentation method for the principal ski jumping data of the field data base  $\mathcal{D}_R$ : in ski jumping, the style criteria are separated into the main jump phases flight, landing and outrun (Section 3.1.2). Consequently, it was sensible to first annotate the incoming inertial sensor data into the respective jump phases. I chose to implement a two-step phase identification that first approximated the start and end of the flight phase in a coarse way by the raw acceleration data of the ski mounted sensors. The main purpose of this step was to shorten the long data streams into smaller time frames, so that the following accurate segmentation could be performed faster and more efficiently. It furthermore increased the robustness towards outliers that satisfy the segmentation conditions outside of the actual phase timings. The second step was then to refine the first estimate by a more precise and accurate computation yielding the exact time annotations for all flight phases.

#### Coarse Phase Segmentation

The data of the two ski sensors is superimposed by high noise during ground contact as a cause of wobble and small oscillations of the ski surface. During flight in contrast, this noise is not present in the sensor data (Figure 7.5). This means that the aerial phase can be easily distinguished from the preceding and subsequent ground contact phases as the noise-free period in the middle of every jumping data stream. Implementing this relation, the aerial phase was then described as that phase where the function  $f_{SG} = std(a_{SKI})$  built from the standard deviation in the accelerometer data was below a certain (freely chosen) threshold  $t_f$ . To get a robust annotation for the start and end point,  $a_{SKI}$  constituted the sum of all acceleration data along all three sensor axes and the right and left ski sensor. As a result,  $f_{SG}$  contained significant peaks before and after the flight phase that could be used to annotate the flight interval: the start of the flight phase was assigned to the last peak in  $f_{SG}$  before the period below  $t_f$ , and the end of the flight phase to the first peak after the period below  $t_f$ .

### 7.3. Transforming Data into Motion Features

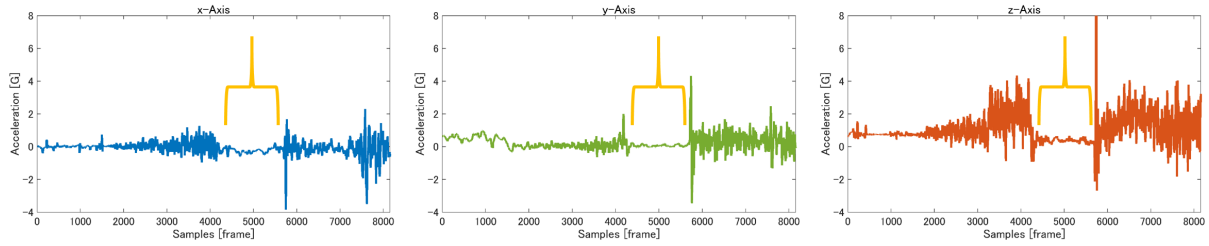


Figure 7.5: Raw acceleration data from the ski sensors was used to obtain a first coarse estimate on the start and end timing of the flight phase: noise superimposing the sensor signals during ground contact of the ski clearly separates in-run and landing from the flight phase.

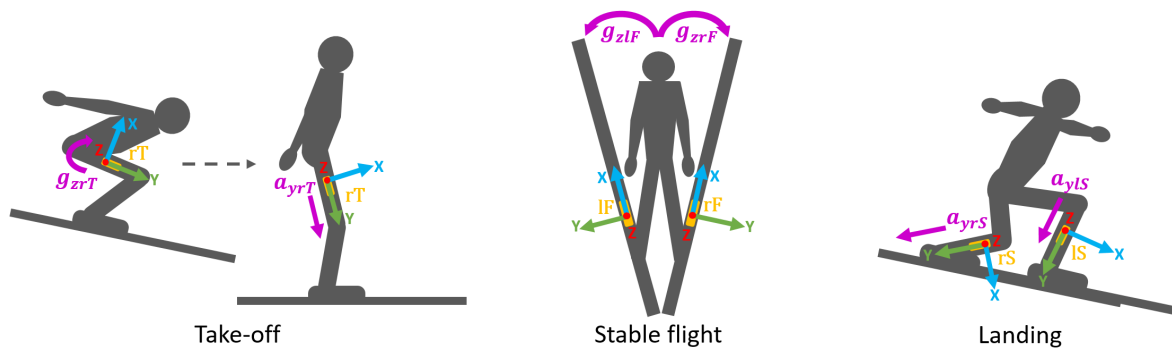


Figure 7.6: Characteristics of the different jump phases made it possible to segment the jump into different phases under a fine annotation level.

#### Fine Timing Annotation

In the second step, the coarse start and end timings of the flight phase were refined and complemented by the missing primary phase timings and sub-timings (Section 3.1.2). For this, I used the biomechanical descriptions of every phase and defined segmentation functions for the raw acceleration or the angular velocity data from various sensor locations. The beginning of the knee angle extension for example characterizes the initiation of the take-off, establishment and dissolving of the static v-opening characterize the start and end point of the stable flight phase, and high impact at the legs characterizes the moment of ground contact during landing (Figure 7.6). In concrete, the full segmentation functions were defined as follows:

- **Take-off Initiation** The take-off initiation is characterized by the start of an upward motion of the legs, where the knee angle of the sitting in-run position is extended towards the maximum at the instant of the take-off. With the sensor y-axis aligned in line with the bones of the legs, the z-axis was pointing towards the transversal axis. Therefore, I could describe the take-off initiation by the function  $f_{TOI} = abs(g_{zrT} + g_{zlT})$  of the summed absolute z-axis angular velocities of the sensors attached to lT and rT.



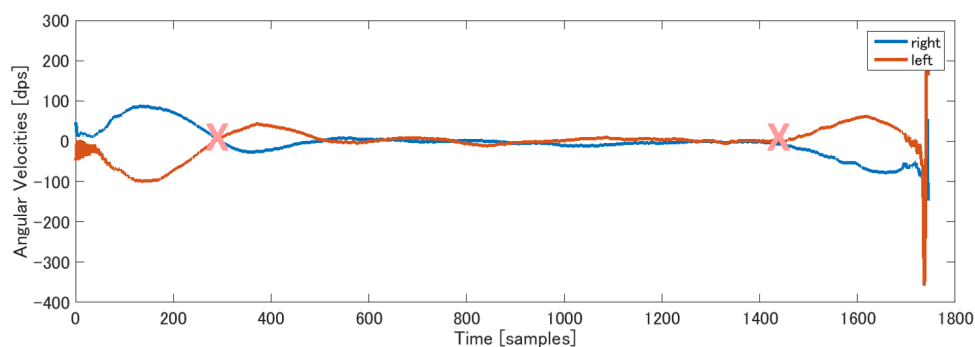


Figure 7.7: Determination of the start and end timing of the stable flight phase using the angular velocities at the z-axis of lF and rF. The selected phases depict the end, respectively the dissolution of the v-angle opening.

The take-off initiation timing  $t_{TOI}$  was finally determined as the first minimal peak before the maximal value of  $tf$  around the take-off timing.

- Take-off** In the moment of take-off, the legs are stretched and the knee angles extended to a maximum, with the highest impulse upwards from the in-run position. Consequently, the acceleration measured by the y-axis (pointing downwards) should also be maximal. I therefore determined the precise take-off timing by the maximum of the summed absolute y-axis acceleration of the sensors attached to lT and rT:  $t_{TO} = \max(\text{abs}(a_{yrT} + a_{ylT}))$ .
- Start and End of Stable Flight** During flight, a jumper's body posture should be static, so that no motion occurs. Such stable flight is characterized by a forward lean position with the skis held in a v-shape. Start and end of the stable flight can therefore be determined by lF and rF via the rotational motion that brings the skis into or out of the v-opening position (Figure 7.7). With the sensors' y-axes aligned with the length of the skis in forward direction, the z-axes are pointing downwards. Therefore, I described the start of the stable flight as the instant of no angular velocity around the z-axis, which represents the end of the ski opening motion. Averaged over both sensors attached to the skis, it was determined by  $t_{SFS} = \text{ceil}(t(g_{zrF} < 0) + t(g_{zlF} > 0))$ . In the same way, I described the end of the stable flight position by the dissolving of the v-ski angle, meaning the initiation of the landing. Averaged over both sensors attached to the skis, it was determined by  $t_{SFE} = \text{ceil}(t(g_{zrF} > 0) + t(g_{zlF} < 0))$ .
- Landing** In the moment an athlete gets in contact with the ground, a high impulse in downward hill direction is created that is reflecting in the data of the sensors mounted to the legs and skis. With the sensor y-axis aligned in line with the bones of the legs, the instant of landing was described by the summed absolute y-axis acceleration of the sensors attached to lS and rS. The maximum of this sum then determined the landing instant as  $t_{LD} = \max(\text{abs}(a_{yrS} + a_{ylS}))$ .

### 7.3. Transforming Data into Motion Features

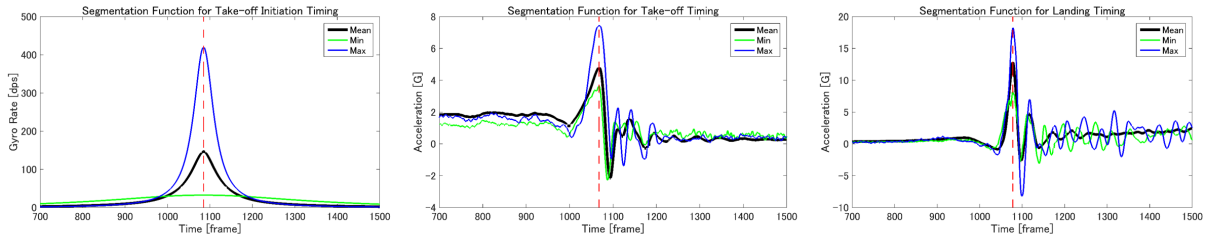


Figure 7.8: Aligning the segmentation functions  $f_{TOI}$ ,  $f_{TO}$  and  $f_{LD}$  of all jumps to a reference peak (red line) showed that the chosen strategies for phase segmentation (maximal peaks) were consistent among athletes and capture sessions. The mean over all curves (black) as well as the minimal peak (green) and maximal peak (blue) curves are shown. All other curves lie in between the extreme curves.

Using the previously determined coarse phase estimations, the defined segmentation functions only had to be considered within restricted time intervals around the respective point interest, meaning either the start or end of the flight phase or both. To determine for example the exact timing of take-off initiation and take-off itself, only a certain time before and after the coarse flight phase start annotation was relevant. To determine the beginning and end of the stable flight phase, only the coarse flight phase interval plus some margin buffer had to be respected. Lastly, to determine the exact instant of landing, it was only necessary to investigate a certain time before and after the coarse flight phase end annotation.

To verify the annotated timings, I captured the complete in-run slope area from the start gate to the take-off table with a wide angle Go Pro video camera positioned along the in-run. The video data was then synchronized to the sensor data from the start of the in-run motion, and take-off initialization, take-off and start of the stable flight manually annotated for all jumps. The manual annotations coincided with the sensor-annotated segmentations within the accuracy of the camera sampling rate of 60 Hz for all takes. Consequently, I came to the conclusions that the annotations were reliable for use in the subsequent retrieval step. I furthermore tested all data captures for consistency with respect to the chosen segmentation strategies for the instants  $t_{TOI}$ ,  $t_{TO}$  and  $t_{LD}$ . For this, I determined the position of all segmenting peaks within the respective segmentation functions and aligned them along the maximum of a reference jump that was chosen freely from the data set. As a result, I could see that for every function all jumps followed a uniform pattern that made all primary peaks occur at the position of the peak they were aligned to (Figure 7.8). In other words, the chosen segmentation properties showed to be consistent among jumps and athletes and hence useful for the proposed phase segmentation. Finally, this consistency confirmed the previous conclusion that the automatically annotated phase timing were reliable for a use in the following machine learning steps.

### 7.3.2 Computation of Motion Features

Variables like the number and placement of the sensors used, the length and especially the type of the motion to be evaluated have an influence on the formation of general motion descriptions and should be taken into account for the creation of efficient and meaningful feature extractors. This is important for any data base mining system: poor features can miss out on true hits, whereas too many or irrelevant features can lead to over selection and false hits [BBS14].

Before using features in the final machine learning environment and an evaluation of retrieval results, the usability and significance of a chosen feature set cannot be ensured completely. In this respect, it is sensible to test a learning application under multiple types of features to identify the most powerful setting for the intended target. For the establishment of the following system, I therefore designed three different feature sets: two general and one specific feature sets. Since the majority of all data captures in  $\mathcal{D}_R$  were ski jumps, all three feature sets were used in the ski jumping context in this thesis. However, the two general feature sets were designed in such a way that they could also be used for any other movement or sports data. They were formed by feature representation strategies as specified in various motion activity recognition literature and constituted of one discrete (descriptive statistics) feature set based on the raw and augmented signal data and one continuous (time-series) feature set based on the augmented body kinematics. The specific feature set was created from the augmented body kinematics under consideration of the semantics and biomechanical description of the target sport ski jumping.

#### General Feature Sets

Various motion descriptors that can be extracted from the sensor data and that are common in learning scenarios for motion pattern analysis were chosen to provide motion information for the jump phases  $A$  and  $L$ . Here, it turned out to be more efficient to consider a flight performance and eventual error in the motion execution from a whole body perspective than investigating every sensor location independently on its own. The data of every sensor was consequently combined to build two large sets of possible feature set.

The first general feature set  $\mathcal{F}_D$  was a set of discrete statistical descriptors, meaning it contained only one-dimensional data points that were obtained using standard descriptors for basic time-series data. They are: the mean value  $F_{D1}$ , the variance  $F_{D2}$ , the skewness  $F_{D3}$ , the kurtosis  $F_{D4}$ , 10 equally spaced samples from the autocorrelation sequence  $F_{D5}$ , the zero crossing rate (ZCR)  $F_{D6}$ , the mean crossing rate (MCR)  $F_{D7}$  and the power of the spectrum obtained with the FFT  $F_{D8}$ . The signal properties have been computed from the raw acceleration  $a$ , gyro rate  $g$  and magnetometer data  $m$  (processed in this order) as well as from the angular data in Euler angles  $\angle$  and the positional data  $p$  along all motion axes  $x$ ,  $y$  and  $z$ . This means that I obtained 120 discrete feature values for every sensor (Table 7.2),

### 7.3. Transforming Data into Motion Features

leading to a total of  $n_d = 1080$  available features with the 9-sensor based experimental motion measurement set up. All  $n_d$  features of  $\mathcal{F}_D$  were normalized to the interval  $[0, 1]$  by

$$F'_{Dn_d} = \frac{F_{Dn_d}}{|F_{Dn_d}|}. \quad (7.1)$$

This normalization ensured the standardization of every feature range and hence equalized the influence of every feature on the learning algorithms. Lastly, the discrete data points of all or selected features were united into a **feature vector**, whereas every feature represented one element of the vector.

Table 7.2: Description of the discrete (descriptive statistics) features  $\mathcal{F}_D$  with their feature ID for all sensor axes.

ID	Type	Description
$F_{D1}$	mean( $[a_x \ a_y \ a_z]$ , $[g_x \ g_y \ g_z]$ , $[m_x \ m_y \ m_z]$ , $[\angle_x \ \angle_y \ \angle_z]$ , $[p_x \ p_y \ p_z]$ )	Signal data mean value
$F_{D2}$	std( $[a_x \ a_y \ a_z]$ , $[g_x \ g_y \ g_z]$ , $[m_x \ m_y \ m_z]$ , $[\angle_x \ \angle_y \ \angle_z]$ , $[p_x \ p_y \ p_z]$ )	Signal data variance value
$F_{D3}$	skew( $[a_x \ a_y \ a_z]$ , $[g_x \ g_y \ g_z]$ , $[m_x \ m_y \ m_z]$ , $[\angle_x \ \angle_y \ \angle_z]$ , $[p_x \ p_y \ p_z]$ )	Signal data skewness value
$F_{D4}$	curt( $[a_x \ a_y \ a_z]$ , $[g_x \ g_y \ g_z]$ , $[m_x \ m_y \ m_z]$ , $[\angle_x \ \angle_y \ \angle_z]$ , $[p_x \ p_y \ p_z]$ )	Signal data kurtosis value
$F_{D5}$	autocorr( $[a_x \ a_y \ a_z]$ , $[g_x \ g_y \ g_z]$ , $[m_x \ m_y \ m_z]$ , $[\angle_x \ \angle_y \ \angle_z]$ , $[p_x \ p_y \ p_z]$ )	10 samples of signal autocorrelation sequence
$F_{D6}$	zcr( $[a_x \ a_y \ a_z]$ , $[g_x \ g_y \ g_z]$ , $[m_x \ m_y \ m_z]$ , $[\angle_x \ \angle_y \ \angle_z]$ , $[p_x \ p_y \ p_z]$ )	Zero crossing rate (ZCR)
$F_{D7}$	mcr( $[a_x \ a_y \ a_z]$ , $[g_x \ g_y \ g_z]$ , $[m_x \ m_y \ m_z]$ , $[\angle_x \ \angle_y \ \angle_z]$ , $[p_x \ p_y \ p_z]$ )	Mean crossing rate (MCR)
$F_{D8}$	pow(fft( $[a_x \ a_y \ a_z]$ , $[g_x \ g_y \ g_z]$ , $[m_x \ m_y \ m_z]$ , $[\angle_x \ \angle_y \ \angle_z]$ , $[p_x \ p_y \ p_z]$ ))	Power of the spectrum obtained with the signal FFT

Biomechanic specifications of a motion are mainly related to angular or positional differences between body segments and joints over time. One-dimensional discrete data points display those differences implicitly, whereas it cannot be excluded that differing signal progressions never result in the same or a similar output value. It is therefore reasonable to build features that can also represent the temporal evolution of a motion performance. Time-series features representing all those motion properties that are described by either positional and angular data or relations between body parts and body joints are gathered in the second general continuous feature set  $\mathcal{F}_C$ . Examples are the v-opening angle, the forward-lean angle of the human upper body or the knee angle as indicator of straight and bend legs.

For the formation of  $\mathcal{F}_C$ , I chose 2 orientation-based features  $F_{CO}$ , 3 position-based features  $F_{CP}$  and 3 additional types of relational features  $F_{CR}$  for every sensor location. In concrete, the

## Chapter 7. Making Sense of the Motion Data

features were formed as  $F_{CO} := (F_{C1}, F_{C2})^T$ ,  $F_{CP} := (F_{C3}, F_{C4}, F_{C5})^T$  and  $F_{CR} := (F_{C6}, F_{C7}, F_{C8})^T$  (Table 7.3). For  $F_{C6}$ , hip, knee, shoulder, ski elevation, ski opening and arm opening angle were used, whereas for every body segment the two spatially related, neighboring relative angles were determined. For rT this for example means that the angle between P and rT as well as the angle between rT and rS were computed, and for lF that the angle between lS and lF and the angle between lF and rF were computed. For  $F_{C7}$  and  $F_{C8}$ , the positional relations between right and left body parts (shoulder, hands, hip, feet, ski tips) along all three axes were used. Counting the number of all features and sensor axes, 23 features were available for sensor, leading to a total of  $n_c = 207$  features with the 9-sensor based experimental motion measurement set up. The  $n_c$  features of  $\mathcal{F}_C$  were rescaled to the interval  $[0, 1]$  by

$$F'_{Cn_c} = \frac{F_{Cn_c} - \min(F_{Cn_c})}{\max(F_{Cn_c}) - \min(F_{Cn_c})} \quad (7.2)$$

to standardize the range of the various features, as well as to scale out anthropometric differences such as different body length between athletes. The temporal sequences of all or selected continuous features could lastly be united and represented by so called **feature matrices** [MR06]. In those matrices, every row represents one feature. The temporal evolution is displayed within the columns that contain the sample-wise feature values (Figure 7.9).

Table 7.3: Description of the continuous (time-series) features  $\mathcal{F}_C$  with their feature ID for all sensor axes.

ID	Type	Description
$F_{C1}$	$\phi, \theta, \psi$	Roll, Pitch and Yaw
$F_{C2}$	$\Delta\phi, \Delta\theta, \Delta\psi$	Change in Roll, Pitch and Yaw
$F_{C3}$	$x_{rel}, y_{rel}, z_{rel}$	Segment end position in x,y,z
$F_{C4}$	$m_{x_{rel}}, m_{y_{rel}}, m_{z_{rel}}$	Slope of segment end position in x,y,z
$F_{C5}$	$\rho_{x_{rel}}, \rho_{y_{rel}}, \rho_{z_{rel}}$	Curvature of segment end position in x,y,z
$F_{C6}$	$\angle_{s1,s2}$	Angle between neighboring body segments $s1$ and $s2$
$F_{C7}$	$x_{j1,j2}, y_{j1,j2}, z_{j1,j2}$	Relative position differences of joints $j1$ and $j2$
$F_{C8}$	$\Delta x_{j1,j2}, \Delta y_{j1,j2}, \Delta z_{j1,j2}$	Change in relative position differences of joints $j1$ and $j2$

### Kinesiology-induced Feature Set

The general continuous feature set  $\mathcal{F}_C$  consisted of a relatively high number of probable motion features and it is unlikely that all of them would be relevant for the description of a ski jump and its respective style errors. With the evaluation of a ski jump being subject to assessment made from judges' observation, main points of interest for a motion rating are the proximity of a motion execution to the defined elementary bio-mechanical specifications. The augmented features from  $\mathcal{F}_C$  were therefore used to build a third, motion specific feature set  $\mathcal{F}_K$  that corresponds to the semantic biomechanical motion description.

### 7.3. Transforming Data into Motion Features

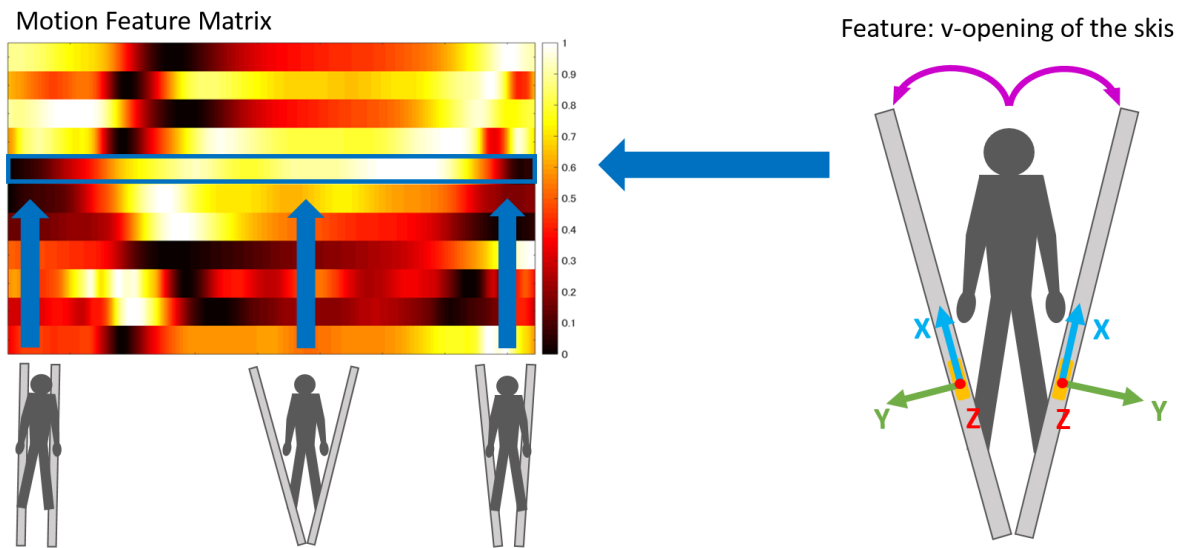


Figure 7.9: Visualization of a feature matrix and a sample feature ski opening (v-angle). Every row contains another motion feature with the temporal evolution sample-wise displayed in the columns.

Generally speaking, a ski jump performance is characterized by little motion to a large extent. Especially during flight, but also in landing and outrun, the absence of any irregularity is considered as good motion style. For the acquisition of high style points, it is important to convey an impression of safety and motor control, which is primarily influenced by a rigid body pose during flight and a safe landing. Consequently, it was especially necessary to select features that could depict all small variations in the data constituting the difference between a good and a worse jumping performance.

The final formation of the simple kinesiology-induced feature set  $\mathcal{F}_K$  was inspired by the style criteria from Table 3.1. Here, concrete technical specifications exist for the flight and landing. Relevant angles during flight are for example the body-ski angle  $\beta$ , the ski attack angle  $\alpha$  and the hip angle  $\gamma$  as well as the v-opening angle of the ski. Landing is particularly defined by the Telemark landing, during which the skis should not be further than two ski widths apart and the knee angle  $\Delta$  sufficiently large to display a bend knee position. For the remaining style criteria, I especially wanted to grasp insufficiency in the motion execution that is for example characterized by incompletely stretched legs, and instabilities that are for example described by arm movement during flight or body parts touching the ground during landing. For every style criteria, another combination of features was relevant (Table 7.4).

## Chapter 7. Making Sense of the Motion Data

Table 7.4: Description of the simple kinesiology-induced features  $\mathcal{F}_K$  with their feature ID and the represented style error.

ID	Type	Description	Error, style criteria $C$
$F_{K1}$	$\angle_{P,rS}, \angle_{P,lS}$	Hip angle $\gamma$	General flight and landing posture (A1, A2, A4, L2, L4)
$F_{K2}$	$\angle_{rT,rS}, \angle_{lT,lS}$	Knee angle $\Delta$ right and left	Straight knees during flight, Telemark position during landing (A2, A4, L1, L2, L3)
$F_{K3}$	$\phi_{rF}, \phi_{lF}$	Ski attack angle $\alpha$ right and left	Ski posture during flight, symmetry of skis (A1, A2, A5)
$F_{K4}$	$\angle_{rE,lF}$	V-opening skis	Ski posture during flight, symmetry of skis and distance during landing (A1, A2, A5, L4)
$F_{K5}$	$x_{rS,lS}, y_{rS,lS}, z_{rS,lS}$	Positional difference legs right and left	Posture and symmetry of legs during flight, posture of Telemark (A2, A4, L1, L2, L3, L4)
$F_{K6}$	$x_{rE,lF}, y_{rE,lF}, z_{rE,lF}$	Positional difference ski right and left	Ski posture during flight, symmetry of skis and distance during landing (A1, A2, A5, L4)
$F_{K7}$	$\angle_{P,rA}, \angle_{P,lA}$	Shoulder angle right and left	Posture and Symmetry of arms during flight and landing (A1, A2, A3, L4, L5)
$F_{K8}$	$\angle_{rA,lA}$	Angle between shoulders	Posture and Symmetry of arms during flight and landing (A1, A2, A3, L4, L5)
$F_{K9}$	$x_{rA,lA}, y_{rA,lA}, z_{rA,lA}$	Positional difference arm right and left	Posture and Symmetry of arms during flight and landing (A1, A2, A3, L4, L5)

## 8 Retrieving Auditory Motion Information

For the establishment of the intended motion information system, the previously implemented processing and learning methods need to be used in such a way that they make all relevant information perceptible by the target user. In other words, a system is required that translates the implicit information contained in the processed motion data into a universally understandable 'language', respectively level of data content – generally represented by some kind of intelligent data knowledge.

The creation and utilization of such system intelligence constitutes the fourth and last stage of the overall processing pipeline passed through in the course of this thesis. In dependence on the application system, this problem is designed and realized differently under consideration of specific constraints of the problem description. Consequently, an analysis of the resulting output to determine the efficiency of the previously implemented system also has to follow different methods and validation criteria. As first information type, I discuss auditory feedback in form of movement sonification using real motion data from  $\mathcal{D}_R$ . Movement sonification relies on the biological structures of the human brain with its corresponding internal motion knowledge to access and make sense of the provided motion information. Therefore, the present application considerably differs from the second application of performance assessment discussed in the following chapter.

### 8.1 Movement Sonification

The provision of auditory motion feedback is subject to internal biological motion perception evoked in certain areas of the human brain like the mirror neurons [LSS07, YRC13, Riz05]. Consequently, it is not necessary to develop and train any artificial motion knowledge for the final retrieval step. Instead, one can make use of existing, intuitive human knowledge learned over years or even decades of experience. However, this convenience does not come easy for analysis: the more an information retrieval process takes place internally, the more complicated it is to be quantified. Information on the power of chosen feature transformations, and the outcome of a retrieval process cannot be obtained directly. For analysis, it is therefore necessary to test the auditory feedback in experimental studies. Results of the studies using the implemented MIDI-based sonification system and sound mapping are shortly explained in the following.



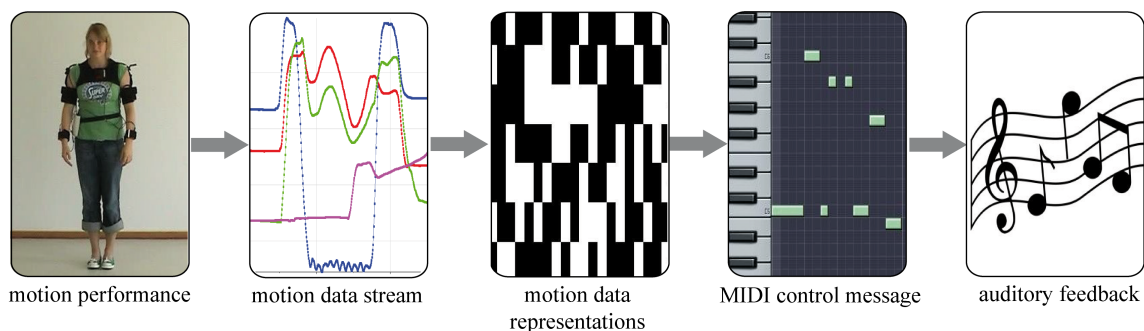


Figure 8.1: Schematic overview of the proposed sonification framework consisting of motion capturing procedures, motion data processing procedures and the final auditory display.

### General Specifications

Auditory and visual stimuli are perceived as originating from a single event when their intermodal delay lies within an approximate interval of  $t_{IM} = 100\text{ms}$  during the activation of multisensory areas within the central nervous system [SM93]. As a consequence of these neural mechanisms, the maximal acceptable delay for the emission of auditive information was set to  $t_{max} = 30\text{ms}$ . This benchmark ensured that subjects could perceive auditory display in real-time and merge it with feedback of other modalities during motor performance [SBD<sup>+</sup>09] (Figure 8.1). The sampling frequency was set to the (XSens internal) maximal rate of 100 Hz, which was dense enough to contain sufficient information for the primary target rehabilitation.

#### 8.1.1 Sonification for Rehabilitation

The effects of the selected sound mappings on motor learning and skill acquisition have been investigated in two empirical studies for rehabilitation as well as in a study on character writing by children. As general result, it could be shown that users were able to adapt themselves quickly to the auditory feedback by both intuitively understanding the represented sound mappings as well as by learning precise executions of a motion task.

In a first study, the informational content of the transformed acoustical kinematics was examined using an intermodal discrimination paradigm [VKF<sup>+</sup>13]. In particular, the intention was to find out whether humans were able to discriminate and intuitively understand the artificial movement specific sound sequences. For this, six common everyday upper limb actions – drawing a circle, stirring in a pot, pouring water, drinking from a glass, rasping one's nails and brushing one's teeth – were captured by five inertial XSens sensors mounted on shoulder, upper arm, lower arm, back of the hand and center of the right backs of the fingers of an actor's dominant hand. Body segment orientations were estimated and used to determine positional information of the distal finger tips relative to the body center under the forward

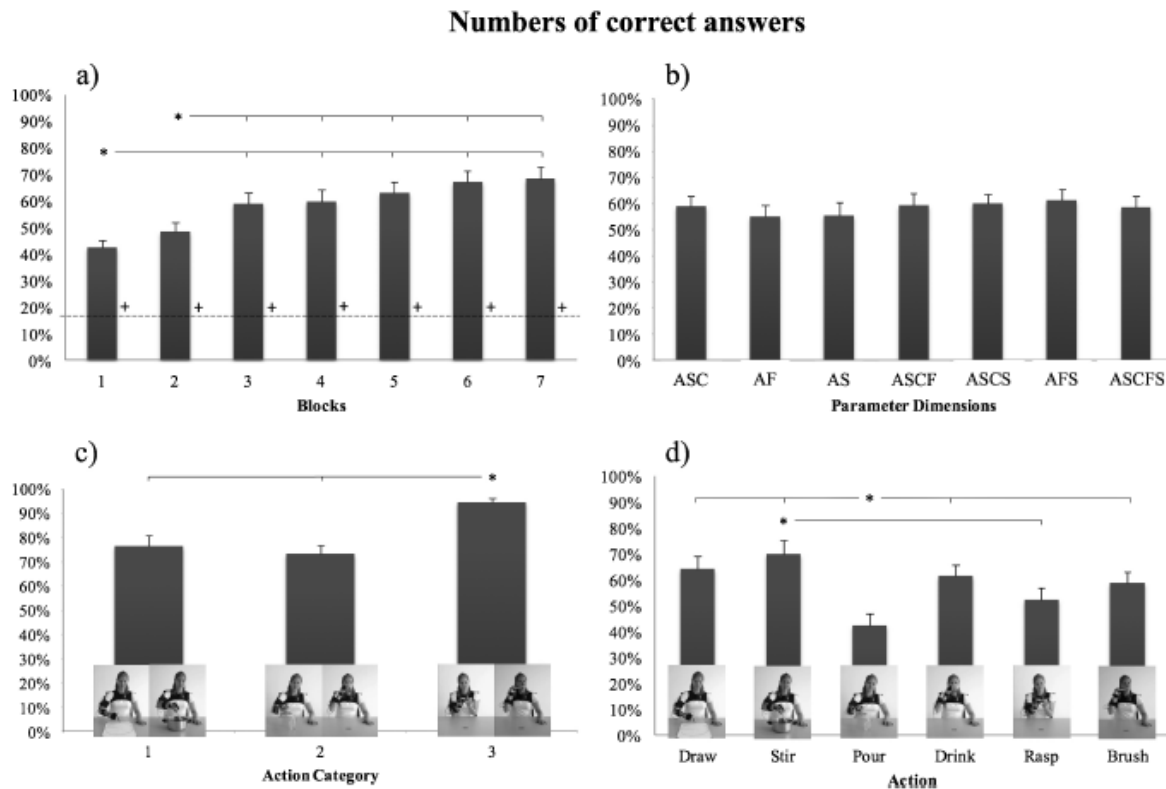


Figure 8.2: Identification rates of the sonification patterns with different dimensionalities over the course of empirical testing.

kinematic approach (Section 5.4). Represented in spherical coordinates (Section 7.2.1), the positional data was next transformed into the defined auditive motion representation. To evaluate dimensionality complexity and semantic significance of the present sound features, seven independent movement sonifications of differing feature combinations (from two up to four sonified parameters) were created.

In a repeated measure design, the six limb action sonifications were randomly presented to participants of the empirical study for identification. Subsequently, discrimination rates for correctly identified motion actions as well as confidence of choice were registered. Data indicated an immediate comprehensibility of the artificial movement acoustics as well as short term learning effects: already above chance level during the first trials, motion discrimination further improved with the progress of the study (Figure 8.2<sup>1</sup>). Comparing the seven sonification patterns, no differences between the encodings became evident in the discrimination rates. Even listening to low-dimensional sonifications resulted in high identification rates, indicating that each kind of sound feature mapping provided similar amounts

<sup>1</sup>Image taken from [VKF<sup>+</sup>13]

of information about a certain action pattern. This was likely due to the composition of the designed feature mappings that all contained amplitude as a transformation of motion velocity. The acoustically coded velocity information could therefore be assumed as highly efficient for intermodal pattern discrimination. As a main result, the study showed that the human brain allows for auditory pattern based action discrimination and perceptual learning.

After the perceptual impact of the chosen sound mapping was proven, the system was tested in a feasibility study with acute stroke patients [SKE14]. Here, the position of the wrist was sonified in real-time during the execution of goal-directed motion tasks of varying complexity. To assess the effect of movement sonification, motor and movement functions were tested before and after the intervention under a standardized medical test catalog. Analyses showed that auditive feedback yielded significant positive effects on the general motor skill of the patient's impaired arm. As a conclusion, the utilization of auditory feedback for motor learning could be shown as encouraging with respect to ambulatory use, as well as an application in more sport-related training.

In a different setting, the basic sonification approach was further developed to a system that encodes the kinematics of character writing obtained from an electronic writing tablet as sound [ESB<sup>+</sup>15]. This so-called SoundScript system creates real-time sound information on the writing trace and consequently enforces an integrated audio-visual perception of handwriting. The hope is that the system can stimulate the acceleration of the handwriting learning process in children in future. Data obtained in a pilot study gave promising results, indicating that writing kinematics can be reproduced more adequately under the additional display of auditive motion traces.

## 8.2 Discussion

Results of the first experimental studies showed that artificial movement acoustics based on kinematic movement parameters can be decoded by naive listeners. Discrimination rates of the performed actions were high from the first testing block, and increased over the duration of the empirical testing. Since no feedback on the correctness of their motion identifications was given to the participants, this enhancement of the discrimination rates was assumed to be a cause of increasing knowledge about sound sequences of concurring action patterns. Besides, errors in action identification were larger within than between categories. This confirmed that discrimination rates depended on the (dis)similarity of action structures. Moreover, discrimination rates were not related to the different dimensional sonifications. Since it was contained in all sound combinations, the acoustically coded velocity information was considered as main parameter for correct motion pattern identification: velocity (which was defined as the length of the action vector in three-dimensional space within a given time) reflected positional changes in time independent of action direction. Therefore, the implied

information about action structures might have been sufficient for discrimination by itself only.

With the second and third experimental study, the positive effect of auditory feedback on motor learning were shown, and the utilization of audio feedback in larger scale motor training scenarios encouraged. Considering all conclusions of the previous studies, similar auditory feature transformations are likely to be well applicable to sports and motor training. With motion velocity as intuitive and highly discriminative sound mapping, possibilities for future sonifications are numerous. They do not only apply to permanent, continuous sound information as used in most previous studies [DB15, CHU14, SH13, SOW11], but can also be expanded to auditory cues given before or during a motor performance. Auditory feedback can hence open up many possibilities for supporting the acquisition of motor skill in rehabilitation and high performance sport. Premotoric auditory cues could for example be applied in a priming context, fostering the development of motor precision. Two concrete examples for such sonifications are given in Section 10.1.1.



## 9 Retrieving Motion Style Information

For the motion rating application, the idea is to introduce algorithms that enable a technical evaluation of the quality of a motion performance which can then provide motion information to judges, but also athletes and coaches or other users. Different than auditory feedback, such intended error information constitutes an application problem bound to a technical solution – motion knowledge is not naturally available for use of automated information retrieval, but has to be built artificially. As a last step before the completion of the fundamental information system development, a computational method for this problem should be developed using real motion data from  $\mathcal{D}_R$ .

The basic idea for the development of a motion rating system was to define objective measures that score or rank different performances of subjective judged-sports on the base of intelligent machine motion knowledge (Figure 9.1) – and herewith exceed the possibilities of current grading systems (Section 3.3.4). In a general training and motor learning scenario, it is common to compare the athlete's current state of art to a predefined target outcome or performance skill. Similarly, performance knowledge of a machine could be created using the motion data of a reference (ideal) performance, to which the incoming motion data are then compared. In practice, however, is not possible to assess performances on the base of an absolute athlete-independent, ideal motion pattern serving as evaluation benchmark: a performance is subject to individual motion styles that are, amongst others, influenced by physical differences in the anthropometrics of every athlete. By using the previous normalized and re-scaled motion features, physical differences between athletes are partly compensated, so that variations as for example different body lengths do not reflect themselves in the motion data. Nevertheless, an universally valid, ideal reference motion cannot be defined. Therefore, I aim to evaluate motion performances in relation to each other under consideration of their feature values at the segmented primary motion phases.

In the following, I focus on the collection of ski jumping motions from  $\mathcal{D}_R$ , but all evaluation methods should be designed in such a way that they can be transferred to other sports in future. Before starting the final jump assessment step, it is necessary to introduce fundamental data definitions, to re-structure the main motion data as well as to implement the underlying functions. To get an overview into the topic, I first want to explain a possible semantic feature categorization system developed for assessment of relative performance qualities. Next, I illustrate and discuss the methods used for subsequent error recognition. Finally, multiple error classification strategies are designed and their recognition results validated at the end

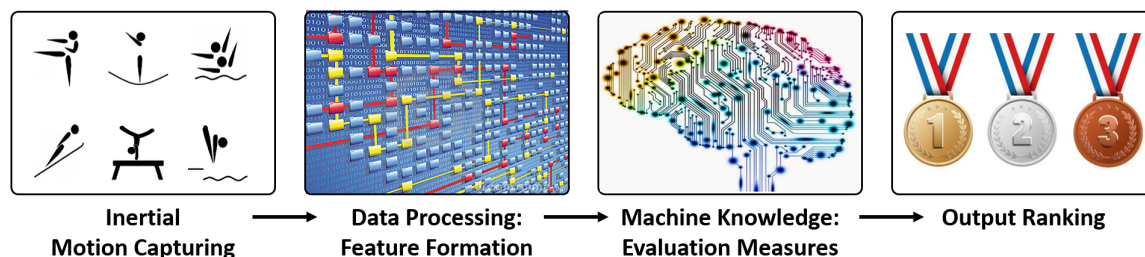


Figure 9.1: Flow of a general wearable motion rating and performance assessment system.

of this chapter.

## 9.1 Motion Feature Categories for Performance Assessment

From the style evaluation criteria in Section 3.1.2, one can see that a ski jump should be primarily assessed by the outer appearance of the succession of a jumper's movements from the take-off to the passing of the 'fall line' in the outrun. Particularly important motion aspects are precision, perfection, stability and general impression, separating the process of motion assessment into two evaluation strategies: verification of the correct motion execution under consideration of the principal technical motion determinants (e.g. the existence of the Telemark), and rating of the overall flight impression under consideration of aesthetic determinants. Following this categorization, I therefore introduced the two motion feature categories 'Technical Motion Features' and 'Aesthetic Motion Features'. Since the final rating system should offer the possibility of universal use in future judging applications, the categories describe the motion assessment task in a broad and general way. As required, the rating features could then be modified for a use in a specific motion. For this reason, both categories will be illustrated by not only the present ski jumping problem, but also by figure skating intended to function as inspiration for any probable follow-up system design.

### 9.1.1 Technical Motion Features

In the following,  $\mathcal{F}_T$  shall be the feature category containing all motion descriptors that extract kinematic quantities or display sequences of body movements within a performance under the principle of biomechanics. They can be computed for both performance- and result-oriented motions, as well as even target-oriented team sports. Therefore, they can also be used for various other information provision tasks like motion analysis and motion visualization.

For ski jumping,  $\mathcal{F}_T$  motion features depict all variables correlating to the skilled use of outer aerodynamic conditions with the goal of maximizing jump length, like for example the minimization of drag and the maximization of lift forces during in-run and flight. Particularly

## 9.1. Motion Feature Categories for Performance Assessment

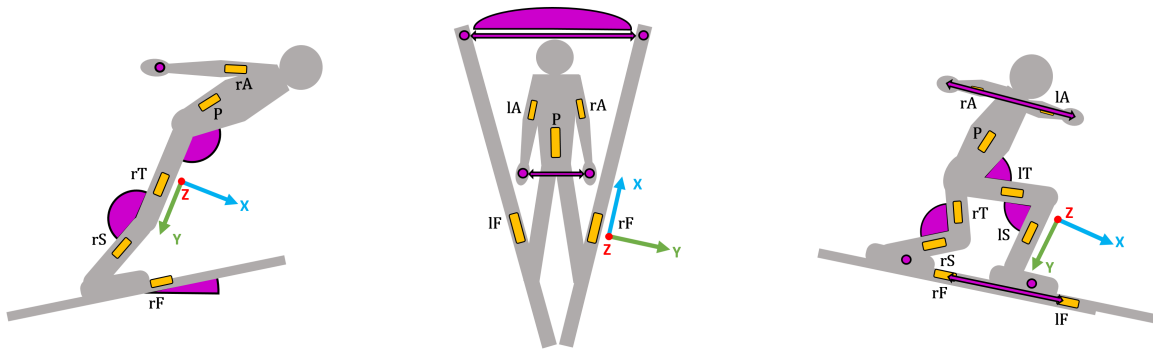


Figure 9.2: Visualization of technical motion features (purple) for the assessment of ski jump style.

relevant body angles during flight are the body-ski angle (conventionally referred to as  $\beta$ ), the ski attack angle (conventionally referred to as  $\alpha$ ), the hip angle (conventionally referred to as  $\gamma$ ) and the characteristic v-opening angle of the ski (here referred to as  $\nu$ ) (Figure 9.2). Biomechanical analyzes [SMY04, MRM<sup>+</sup>06, MS03] quantified the angles resulting in best aerodynamic conditions as  $\alpha \approx 35^\circ$ ,  $\beta \leq 10^\circ$ ,  $\gamma \approx 160^\circ$  and  $\nu = 35^\circ$ . However, their exact values vary per jumper, as every athlete uses an individual jump length maximization strategy dependent on individual motor abilities (including implicit motor knowledge), aerodynamic features of an athlete's anthropometrics and the equipment used. The Telemark landing is another technical part and is described well by the present angular, positional and relational motion features (Figure 9.2). By the moment of hitting the ground, one leg should be placed in front of the other with the skis not further than two ski widths apart. Furthermore important are appropriate flexibility (with knee and hip angles neither too small nor too large) and safety (no body part should be in contact with the ground) of the athlete.

In consideration of the previous aspects, I designed the general definition for the technical motion feature category. The design contains many motion features listed under  $\mathcal{F}_C$  and  $\mathcal{F}_K$  in Section 7.3. The features can flexibly be adapted to the individual needs of an assessed sport, as exemplary demonstrated for ice skating in the following.

### $F_{T1}$ Body Segment Orientation

The estimated segment orientations  ${}^S_E q$  give information on how specific body parts are oriented in the global space with respect to the Euler angles roll  $\phi$ , pitch  $\theta$  and yaw  $\psi$  around the motion axes x, y and z as in  $F_{C1}$ .

Inclination  $\theta_{IT}$  at the elevated left leg measured from a sensor attached to the thigh would be a relevant quality measure for charlotte spirals and camel positions in figure skating (Figure 9.3a). Heading  $\psi_{rF}$  at the (right) foot could be useful to detect incomplete jump rotations by the time of landing when the leg to land is the right one.

### $F_{T2}$ Angles Between Body Segments

The difference between two neighboring segment orientations  ${}^S_E q_{S1}$  and  ${}^S_E q_{S2}$  deter-



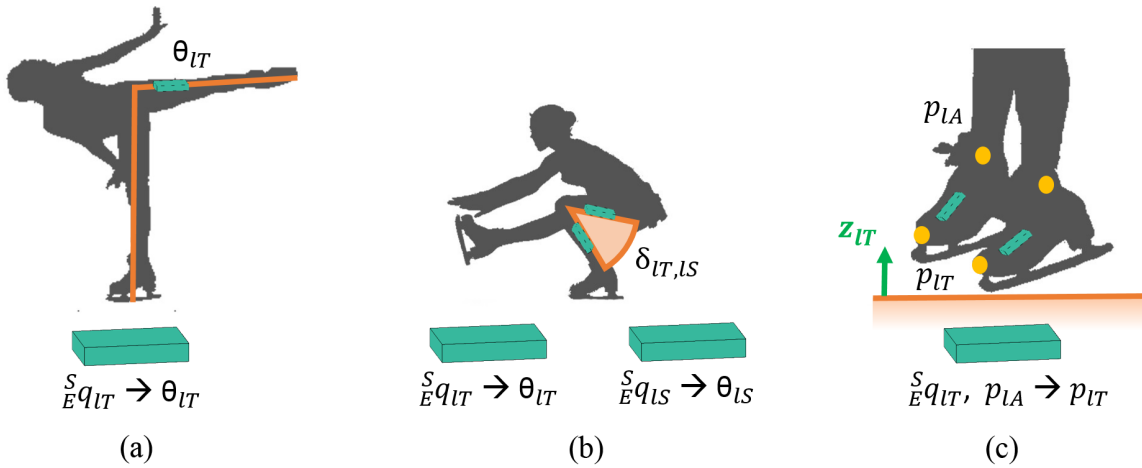


Figure 9.3: Illustration of a possible use for the technical motion features (a)  $F_{T1}$ , (b)  $F_{T2}$  and (c)  $F_{T3}$  with the proposed sample implementation in figure skating.

mine an angle  $\angle_{s1,s2}$  at the connecting body joint as in  $F_{C6}$ .

The knee bend angle  $\delta_{lT,lS}$  at the left standing leg could assess the depth of a left-sided sit spin in figure skating (Figure 9.3b).

**$F_{T3}$  Joint Positions**

The segment end positions  $p_j$  give information on the x, y and z positions  $x_j$ ,  $y_j$  and  $z_j$  of selected body joints in relation to the origin  $p_O$  of their respective kinematic chain as in  $F_{C3}$ .

Double footed landings in figure skating could be identified with the position  $z_{lF}$  of the right foot when the right leg is the leg to land (Figure 9.3c). Unwanted ice contact with the hands could be annotated from the positions  $z_{rF}$  and  $z_{lF}$  of the finger tips.

**$F_{T4}$  Relation Between Joint Positions**

The distances  $p_{j1,j2}$  between two joint positions (either within the same or a different kinematic chain) along x, y and z can be expressed in the spatial relations  $x_{j1,j2}$ ,  $y_{j1,j2}$  and  $z_{j1,j2}$  as in  $F_{C7}$ .

The positional difference  $z_{rT,rS}$  between right thigh and shank could measure the spread in the hip joint in right-sided charlotte spirals and camel positions in figure skating.  $z_{rH,rS}$  and  $z_{lH,lS}$  could indicate a general low positioning of the wrists in relation to the shoulder joints.

**$F_{T5}$  Temporal Course** Information on the temporal evolution within the complete technical course of a motion is automatically included in all previous features when generated from the raw sensor data as continuous features like  $\mathcal{F}_C$ .

The proposed design for  $\mathcal{F}_T$  allows for performance description relative to the principal kinematic factors and information retrieval tasks such as error recognition under coarse

## 9.1. Motion Feature Categories for Performance Assessment

---

and abstract reference descriptions. Due to individual style patterns,  $\mathcal{F}_T$  features cannot be used for analysis purposes that numerically compare single kinematic aspects between different athletes. Making use of the feature re-scaling, relative comparisons are possible that do set the kinematic parameters within the standard motion ranges per athlete. Furthermore, numerical performance monitoring by the assessment of differences between body angles or joint positions of single athletes over time can be deemed possible.

### 9.1.2 Aesthetic Motion Features

The feature category  $\mathcal{F}_A$  shall constitute the collection of features that help to unveil aspects of a performance's impression and beauty which are generally a matter of subjective perception. The fundamental idea behind this category is to find several quantifiable factors that impact the individual impression of an observer about a motion's aesthetic quality based on the information obtained with the technical motion features.

For ski jumping, aesthetic impression is the factor of style evaluation that cannot be described semantically. The official FIS rule book [FIS13] reads like follows on this matter:

The calculated points that should be given for the ideal performance of the jump are concerned with the utilization of the aerodynamic efficiency of body and ski, the posture of arms and legs, as well as the ski position during flight, the succession of movements during landing and the conduct during outrun. Also, flight, landing and outrun should convey an aesthetic overall impression.

Considering the motion progression of a ski jump, aesthetic impression is largely influenced by the impression of safety and sovereignty during almost the entire jump, and especially the aerial phase. In concrete, the athlete has to establish a static, rigid pose, with no motion and a wide forward lean of the upper body to make best use of the aerodynamic forces. A general description here is that anything visible is unaesthetic and should hence induce point reduction. For example, it might be reasonable to track the number of all motion actions happening during the ideally static phase. Especially large-scaled motions like balancing motion of the arms – which are also included in the official judging guidelines used for the subsequent retrieval tasks (Table 3.1) – should be kept minimal. Further benchmarks for the determination of aesthetic impression are body stiffness and a smooth transition between the flight phases. Sovereignty is furthermore conveyed by courage and high jumping skill, which are indicated by a wide forward lean angle, a wide ski opening and a high flight path. Especially the flight path might be an important influence on a jump's style rating: the assisting judges, whose scores were used for the ground truth evaluation, reported to rate jumps from an overall perspective from take-off to outrun, including the flight trajectory and distance to the slope. In this context, it usually holds that the higher the athlete stands in the air, the better the jump. This relation has been investigated and will be discussed in more

detail later.

Based on the previous considerations and feature description strategies generated for similar questions of aesthetic perception in non-motion multimedia data [ZZZ15, YLSC08], I designed the general aesthetic motion feature category in the next step. Since aesthetic impression is generally formed over the course of a motion, I came to propose the following aspects based upon the parameters dynamics, flow, density, clarity and neighboring relations that are again demonstrated under the example of figure skating.

### $F_{A1}$ **Motion Expression - Dynamics**

Assuming that a larger motion range, and therefore a higher spatial coverage, is more impressive to the human eye, the range  $rp_j$  of the position of certain body joints along  $rx_j$ ,  $ry_j$  and  $rz_j$  could describe motion expression. Assuming that among two executions of the same motion, the one of higher angular velocity appears to be more dynamic, the maximum angular velocities  $mAV_s$  reached within a performance at a body segment could describe motion expression.

The sequences  $\{rz_{rH,1}, rz_{rH,2}, \dots, rz_{rH,n}\}$  could rate the expression during a step combination of length  $n$  at the right wrist in vertical direction in figure skating. Similarly,  $\{rx_{rH,1}, rx_{rH,2}, \dots, rx_{rH,n}\}$  depicts the lateral direction, and  $\{mAV_{rH,1}, mAV_{rH,2}, \dots, mAV_{rH,n}\}$  the expression on base of the angular velocities.

### $F_{A2}$ **Motion Flow**

Skillful motion execution generally follows a smooth flow without sudden, unexpected events. Disturbances like sudden changes of directions and positions are displayed in the data in form of irregularities, curbs or data peaks. Positional difference of neighboring positions along all axes  $sp_j$  and the rotational difference of neighboring quaternions at a certain joint  $sr_j$  should not undergo any sudden large deviations from the mean  $sp_j$  and  $sr_j$  values of the selected time frame in smooth motions.

Stumbling might result in sudden counter movements at the upper extremities in figure skating. Those errors could then be retrieved as peaks in the sequence  $\{s_{rH,1}, s_{rH,2}, \dots, s_{rH,n}\}$  or  $\{s_{lH,1}, s_{lH,2}, \dots, s_{lH,n}\}$  of length  $n$ .

### $F_{A3}$ **Performance Density**

Counting the number of events  $nE_j$  that occur within a certain time frame at a specific body part gives a density measure, whereas the definition of an event depends largely on the specific requirements of a sport. After determining events that give a positive impression of skill and strength to an observer, it is first needed to classify them to be then able to detect their number of occurrences  $\sum nE_p$ .

Events that could be detected easily from the sensor data in figure skating are spin jumps represented as heading changes  $\psi_p$  of a sensor attached to the athlete's pelvis, or landings by counting the number of times the acceleration at the pelvis surpasses a certain threshold  $AccT$  within a defined time frame  $n$ .

### $F_{A4}$ Motion Clarity

The clarity of a motion performance shall be determined from the occurrences of 'noisy' motions in form of the sum of one or more translations in the x, y and z axes or rotational changes at a certain joint or body segment that is not directly related to the main performance. The easiest way to describe such sequences is by motion jitter  $\sum_{t=1}^n exAV_{rH,n}$  as the accumulation of extreme points  $exAV$  (and hence data peaks) in the respective angular velocities during the time frame n.

The motion of the arms could be noisy motion during a spin in figure skating.

## 9.2 Fundamental Information Retrieval Methods

The intended evaluation can be represented as a recognition problem assessing and weighting the presence or absence of a certain performance error. In other words, all ski jump data within  $\mathcal{D}_R$  shall be classified as either erroneous or non-erroneous, which is nothing else than a binary classification task. To verify machine learning methods, it is furthermore common to have at least two different data sets, of which one is used to train the learning methods and one to test the trained data. Information on the chosen basic strategy for data base separation as well as the implemented methods for error classification is given in the following.

### 9.2.1 General Data Base Separation

For all subsequent learning processes, the 85 ski jump captures with jump length and judge style annotation within  $\mathcal{D}_R$  should be split into a training and testing data subset per  $A$  and  $L$  style criteria (Table 3.1). Every jump was therefore separated into its relevant motion segments under the previously annotated key phase timings (Section 7.3.1). For the aerial phase  $A$ , this phase separation meant all samples from  $t_{TO} - 250$  frames until  $t_{LD} - 150$  frames. The landing  $L$  comprised all samples from  $t_{LD} - 300$  until  $t_{LD} + 400$  frames.

The general concept of the splitting process as performed for all subsequent retrieval tasks then looked as follows. First, I randomly assigned the data captures to a sub-training data base  $\mathcal{D}_{RF}$  and a sub-test data base  $\mathcal{D}_{RT}$  under consideration of the  $A$  and  $L$  phase-wise ground truth style annotations. For this separation, I created two labels: one group  $JF$  that contained all the jump data that were fined a point deduction in the collected judging score sheets and one group  $JN$  of all remaining jumps that were not fined a point deduction. For all determinants, the number of jumps  $n_{JF}$  from  $JF$  and  $n_{JN}$  from  $JN$  was identified and a data base separator  $r$  determined to randomly split the jumps into subsets. For an equal split,  $r$  was defined as  $r_F = 0.5 * n_{JF}$ , respectively  $r_N = 0.5 * n_{JN}$ .  $r_F$  jumps of  $JF$  and  $r_N$  jumps of  $JN$  were then assigned to  $\mathcal{D}_{RF}$ , and all remaining jumps were assigned to  $\mathcal{D}_{RT}$  for validation later (Figure 9.4). By this separation principle, both subsets could then be equally used as training and testing data in a two-fold or multi-fold validation, increasing robustness against bias

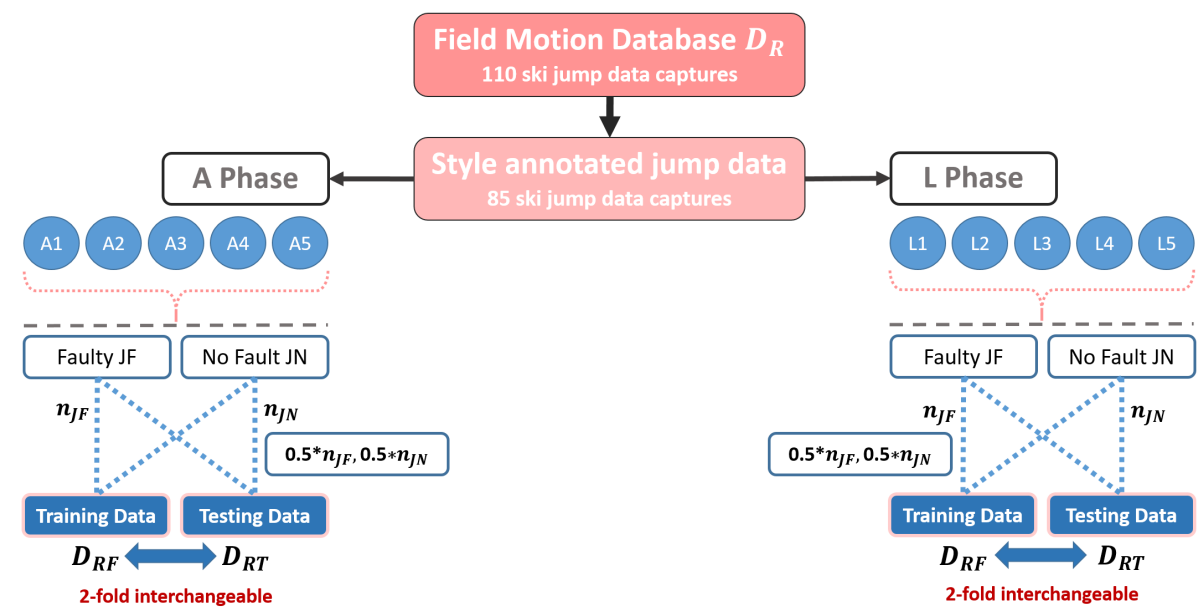


Figure 9.4: Schematic explanation of the data base preparation step separating the collected data captures into a training and a test data subset for the machine learning steps. Here, an equal split for 2-fold validation purposes is illustrated. The splitting process can be modified to any other desired multi-fold validation.

induced by the random data split.

## 9.2.2 Classification Methods for Error Recognition

Two different binary classification approaches were chosen and implemented for the present binary machine learning task - one similarity-induced method based on **Dynamic Time Warping (DTW)** and one kernel method based on a **support vector machine (SVM)**. The principal idea of both classifiers is to determine (and evaluate) commonalities between two or more motion performances. However, for numerical computations this is often not as simply defined as it can be expressed verbally: motions can undergo various variations, and especially if performed by different athletes or under different capture conditions, semantically similar motions do not need to be numerically similar. Performance data for example is often exposed to spatial variations caused by different capture locations or capture circumstances, variations caused by individual motion styles of different athletes as well as temporal variations caused by differences in timing and speed.

Since the main data in  $\mathcal{D}_R$  was captured at a single ski jump hill under constant conditions, and variations in heading were excluded by the developed magnetic heading compensation (Section 6.2.2), spatial variations could be neglected. Style variations on the other hand had to be considered as present in the motion data for the implementation of the classifiers. To

handle them in the best possible way, it is sensible to select robust feature representations that do not vary with different motion styles. Temporal variations cannot occur for the discrete features  $\mathcal{F}_D$ , and it was only necessary to compensate temporal differences within the time-serial feature sets  $\mathcal{F}_C$  and  $\mathcal{F}_K$ . Both classifiers respond to the variations in a different way that shall be explained in the following.

### Similarity-Based Classifier

The first classifier compares two different motion performances under the aspect of similarity. This means that a metric is defined that compares the similarity of the two feature vectors (in the discrete case) or every single column of the two feature matrices (in the continuous case). For the comparison of two feature matrices of different length, global, document-wise DTW can align the matrices so that they are brought to the same length: for motion performances of the same motion type, it can be assumed that motion feature sequences are of similar length, and temporal variations be excluded by computing local similarities.

The mathematical definition of global DTW shall be explained under a general scenario in the following. The optimal alignment between two time-dependent motion sequences  $X = (x_1, x_2, \dots, x_N)$  of length  $N$  and  $Y = (y_1, y_2, \dots, y_M)$  of length  $M$  has to be determined. Usually,  $X$  is associated to a matrix  $M_X := [x_1 x_2 \dots x_n] \in \mathbb{R}^{f \times N}$  and  $Y$  to a matrix  $M_Y := [y_1 y_2 \dots y_m] \in \mathbb{R}^{f \times M}$ , with the columns of  $M_X$  and  $M_Y$  representing  $f$  multidimensional data vectors of  $X$  and  $Y$ . The difference between two data vectors  $x, y$  is then determined by a *local cost measure* or *local distance measure*  $c$ . If the cost  $c(x, y)$  is small,  $x$  and  $y$  are called similar to each other, if the cost  $c(x, y)$  is large,  $x$  and  $y$  are different to each other. With computing the local cost measure for each pair of elements of  $X$  and  $Y$ , one obtains a *cost matrix*  $C \in \mathbb{R}^{N \times M}$  with  $C(n, m) := c(x_n, y_m)$ . For this thesis, the Euclidean  $L^2$  norm that defines the cost as  $c(x, y) := \|x - y\|$  has been used. Once the cost measure is defined, the next step is to find an alignment between  $X$  and  $Y$  of minimal overall cost. Such an alignment is represented by a *warping path*  $p_\ell = (n_\ell, m_\ell) \in [1 : N] \times [1 : M]$  with  $\ell \in [1 : L]$  where  $L$  is the length of the warping path. The cost of a warping path  $p$  between  $X$  and  $Y$  with respect to the local cost measure  $c$  is defined as  $c_p(X, Y) := \sum_{\ell=1}^L c(x_{n_\ell}, y_{m_\ell})$ . The warping path with minimal overall cost is then called the optimal warping path. It can be used as quantity to measure similarity of two feature sequences under the given cost measure  $c$ .

The optimal warping path can be determined by an accumulated cost matrix  $D \in \mathbb{R}^{N \times M}$  and has to satisfy three conditions - the boundary condition, the monotonicity condition and the step size condition. The boundary condition forces the warping path to start at position  $p_1 = [1, 1]$  and to end at position  $p_L = [N, M]$ , which means that the entire sequences  $X$  and  $Y$  will be aligned. The monotonicity condition assures the warping path to respect issues of timing and sequential time procession, so that going backward for example is not possible. The step size condition is closely related to the monotonicity condition and ensures that no element will be omitted and that there are no replications in the alignment (the classical step

## Chapter 9. Retrieving Motion Style Information

---

sizes to describe this requirement are  $[0,1]$ ,  $[1,0]$  and  $[1,1]$ ). Under the previous constraints,  $D$  has to satisfy the following requirements:

$$D(n, 1) = \sum_{k=1}^n c(x_k, y_1) \quad \text{for } n \in [1 : N], \quad (9.1)$$

$$D(1, m) = \sum_{k=1}^m c(x_1, y_k) \quad \text{for } n \in [1 : M] \text{ and} \quad (9.2)$$

$$D(n, m) = \min \{D(n-1, m-1), D(n-1, m), D(n, m-1)\} + C(n, m) \quad (9.3)$$

for  $1 < n \leq N$  and  $1 < m \leq M$ .

The accumulated cost  $D(N, M)$  - also referred to as DTW distance  $DTW(X, Y)$  - finally represents the cost of the optimal alignment of  $X$  and  $Y$  (and herewith the overall cost for the similarity measure between the two sequences  $X$  and  $Y$ ).

For the present error recognition, the presence and absence of a style error in a ski jump should be determined by computing the jump's similarity to a reference feature matrix. Precisely, two feature matrices  $R_{CE}$  for the erroneous and  $R_{CF}$  for the error-free jumps were built for all style criteria. The feature matrices contained the averaged values of all  $JF$  respectively  $JN$  jumps in the training data set  $\mathcal{D}_{RF}$ . The similarity  $MS$  between  $R_{CE}$  and  $R_{CF}$  to the feature matrices of all jumps in the test data set  $\mathcal{D}_{RT}$  was then measured under the global DTW similarity principle. For the discrete features, the two vectors  $v_1$  and  $v_2$  compared in the similarity (cost measure) were simply formed from the feature vector of the chosen reference jump and the feature vector of the compared jump. Their  $L^2$  norm then yielded the similarity  $MS_D$ . For the continuous features,  $v_1$  and  $v_2$  constituted the feature values of one sample within the reference jump feature matrix and the examined jump feature matrix. Summing up the frame-wise distances as defined for the global DTW, I obtained the accumulated cost matrix  $D$  whose entry  $D(n, m)$  was used as similarity measure  $MS_C$ .

Based on the  $MS_D$  or  $MS_C$  similarity measure, a jump was finally labeled as either faulty or non-faulty by a simple kNN-like classification metric with  $k = 1$ : the label of the similarity measure of smaller value was simply assigned to the examined jump. The  $MS_D$  and  $MS_C$  computations as well as their classification were repeated for all style criteria with the respective style reference matrices  $R_{CE}$  and  $R_{CF}$ .

### SVM-Based Classifier

The second classifier is a straight-forward implementation of the common binary SVM that assigns a label to an input data vector on the base of a trained separator (margin). In the

## 9.2. Fundamental Information Retrieval Methods

simplest definition of such SVM [FHT01, CST00], the training data is a set of points (vectors)  $x_j$  of specific categories  $y_j = \pm 1$  in a certain feature dimension  $d$ . Then, the primal function of a hyperplane separating points of different label is

$$f(x) = x' \beta + b = 0, \quad (9.4)$$

whereas  $b$  is a real number and  $\beta \in R^d$ . The best  $\beta$  and  $b$  values for a separating hyperplane are then found by a minimization problem that tries to assign  $y_j f(x_j) \geq 1$  to all data points  $(x_j, y_j)$ . All  $x_j$  for which  $y_j f(x_j) = 1$  are the so-called support vectors and located on the decision boundary. The parameters chosen for  $\beta$  and  $b$  determine the computation of a hyperplane and the classification of data points close by the separating margin. Those metrics in turn influence and affect the accuracy of an SVM classifier. Consequently, the SVM was first tested under the specific inertial sensor data input to determine the best settings for the present task, using data captures in  $\mathcal{D}_R$  that were not part of the main ski jump data captures. Best classification results were obtained with a Gaussian radial basis function (RBF) kernel and standardized input data. The kernel scale parameter was automatically set by a heuristic procedure based on sub-sampling and the margin parameter  $C$  was chosen as 1.

The main classification metrics were then computed using the feature descriptions of all  $JF$  or  $JN$  jumps in  $\mathcal{D}_{RF}$ , and the remaining  $JF$  and  $JN$  jumps in  $\mathcal{D}_{RT}$  labeled under the trained kernel settings. Here, it has to be noted that a SVM is conventionally based on a sequence of input observations, but does not accept any two-dimensional input sequences. In other words, the training data from  $\mathcal{F}_D$  could be used as SVM data input without any further data conversions by concatenating the feature values for every selected feature. For  $\mathcal{F}_C$  however, it was first necessary to include an additional data transformation that made the temporal information contained in the continuous data features representable within the observation input sequence.

For this feature transformation, I chose a weighted-sum singular value decomposition (SVD) algorithm that was introduced before for spatially invariant, but temporally varying motion data [LKP05]. This strategy represents the temporal data in a lower dimension. In concrete, the motion matrix  $A_k$  in the training data set was decomposed as

$$A_k = USV^T, \quad (9.5)$$

whereas  $U$  and  $V$  were two orthonormal matrices containing the principal components and coefficients and  $S$  was a diagonal matrix containing the singular values. The obtained first singular vector  $v_k$  was then projected to the first principal component. Lastly, a reduced feature vectors  $r_k$  was built by concatenating the projected singular vector  $t_k$  and the normalized singular value vector  $\vec{\lambda}_k$  of  $A_k$ . The resulting reduced feature vectors are close to each other if two motions are similar, and different if two motions are dissimilar. After feature transformation, the single feature vectors could be concatenated and used as both training and testing input data for the SVM in the same way as the  $\mathcal{F}_D$  features.



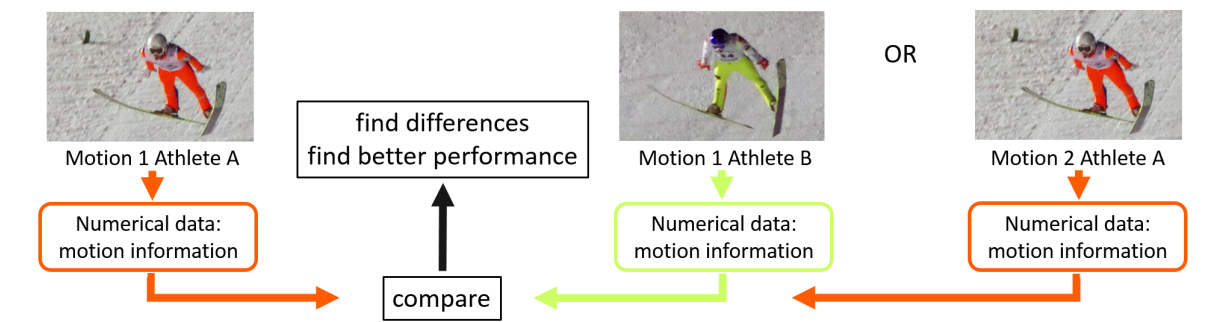


Figure 9.5: Flow of the evaluation system in ski jumping. Motions can be compared either among different athletes, giving a score and ranking for judging, or within one athlete to monitor different training sessions and the evolution of skills and jumping technology over time.

### 9.3 Ski Jump Style Assessment

To assess the quality and style of a ski jump, the existence of style errors or unfavorable motion behavior should be determined independently for every motion performance by learned machine motion knowledge. Their gravity can then be rated either quantitatively or qualitatively, and an error rating of a performance be obtained by summing up the single style error evaluations to an overall performance score in the next step. Sorting all performance assessments along each other, lastly a top-to-bottom ranking can be generated. Additionally, it might be sensible to include further information on the distance between two consecutive motions performances to the final ranking. This would allow to create groups of similar performance quality. For such distance information, measures are required that determine similarities between motion features of two different performances and numerically weigh or score the closeness between each other in an appropriate way.

Besides providing a competition score, such a functional evaluation and ranking method also enables the comparison of jumps from one individual athlete, showing trends in (recent) performances like the evolution of motor skills over time or the course of a training session. Such system data output can then also provide important information for training and performance surveillance. For the ski jumping scenario, the concrete work flow then looks as shown in Figure 9.5. In total, I obtained three different feature sets that were used for the subsequent retrieval task. For reference, a summary of their specifications and main definition is listed in Table 9.1 by the order they were introduced in this work.

One of the most important variables for the development of a performance rating system is the principal data annotation used as benchmark knowledge for the creation of semantic machine knowledge. In this thesis, the ground truth measure used for the training and validation of the performance rating methods is based on scores awarded by judges during the data capturing. As shortly mentioned in Section 9.1.2, judge's individual style impression might be correlating to the general technical motion execution, and it can contain bias due

Table 9.1: Overlook on all feature sets and feature selection strategies ordered by their occurrence in this thesis.

ID	Description	Specifications
$\mathcal{F}_D$	discrete feature set	Set of data points built from standard statistical data descriptors of both raw and processed signal data data. Multiple features are combined in feature vectors.
$\mathcal{F}_C$	continuous feature set	Set of time series built from body-model data descriptors of the processed signal data. Multiple features are combined in feature matrices.
$\mathcal{F}_K$	kinesiology-induced feature set	Set of time series built from body-model data descriptors of the processed signal data and reduced under supervised feature selection based on biomechanical motion definitions. Multiple features are combined in feature matrices.

to differences in individual perception. In the following, I therefore want to shortly discuss this issue.

#### Side note: The quality of the ground truth data

The idea for applying the chosen ground truth measure was to utilize style scores that are as close to the actual judging as possible. Whereas video data would enable judges to scroll back-and-forwards in single jumping sequences, and to a make their scores without time pressure (consequently reducing possible bias in perception), it cannot display all environmental information necessary for judging. Since the overall impression of a flight depends on multiple local parameters such as the flight curve and the distance to the slope, it is necessary to observe a jump within its natural environment on the ski jump hill for high-quality evaluation. For this reason, gravity and type of style errors were given in real-time from the usual position at the judge's tower.

Most of the parameters that define good flight style – like the ideal use of air pressure, an active take-off and the formation of an aerodynamic flying system with body and ski – also significantly influence the length of a jump. Judges reported that a longer jump enhances their impression of good style during flight. In reverse, this confession implies that a longer jump might yield higher style points, and that the length of jumps could serve as fundamental indicator for the quality of the captured flight performances. To verify this impression, I examined the correlation between lengths and style points of the present ski jump captures. To exclude the influences of poor landing style, I furthermore investigated the correlation

## Chapter 9. Retrieving Motion Style Information

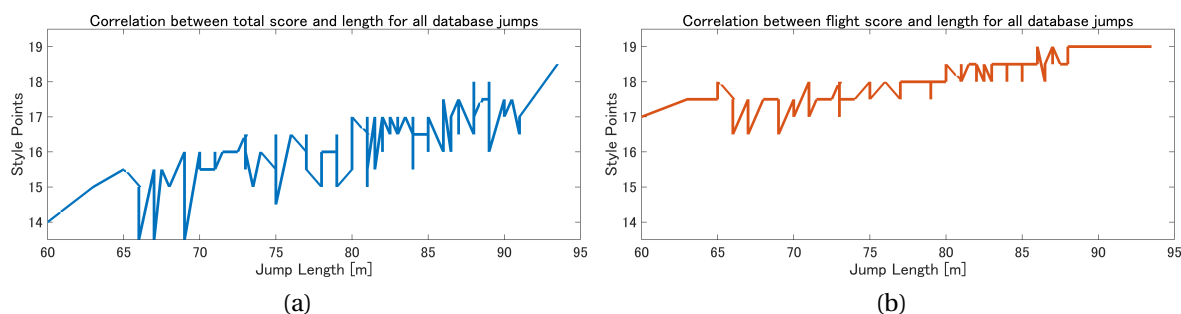


Figure 9.6: Correlation between length and flight style in the experimental data collected for this thesis. (a): style points with landing deductions, (b): style points for in-flight deductions only.

between aerial flight style and length only. The reason for this comparison is that landing, and particularly a missing Telemark, has a big influence on the overall points to be deducted. On the other hand, it is more difficult to land a Telemark in either very short distances at the steepest points of the landing slope (meaning far shorter jumps than the K-point) or in very long distances where the landing slope is flattening (meaning far longer than the K-point).

Although superimposed by natural outliers, both correlations show a linearly inclining function indicating that higher jump lengths indeed related to higher style points (Figure 9.6). Knowing this dependency, longer jumps generally correspond to fewer point deductions and can hence serve as a basic indicator for the quality of flight performances. Therefore, length should be used as additional evaluation metric later.

Lastly, using judges data as ground truth is not optimal for the general system development: the main reason for the development of an intelligent, fully automatic performance rating system is that grading is subject to individual bias. The discrimination between the different landing criteria as defined in Table 3.1 can for example be difficult and even be perceived differently between the human judges. Consequently, also the different feature representations within the training data base can be variate and as a result, the built average matrices functioning as evaluation measures not be significant enough. In other words, the data used to build a system of higher objectivity is based on subjectively made decisions. However, this shortcoming cannot be avoided, since no other measure for style assessment exists so far. For future investigations, it is therefore advisable to collect data of more than three judges at the same time, whereas the larger the number of judges would be, the higher the reliability of the ground truth measure would become. The data of all judges could then be averaged, so that the influence of outliers and individual bias is reduced. Practically, the acquisition of a high number of volunteering judges appears to be difficult to achieve though.

### 9.3.1 Style Error Recognition

A good and stable recognition of errors builds the foundation for any further style evaluations that weigh errors or award point deductions to determine a fixed style value. To start, I therefore implemented an error evaluation without the determination of point scores that could assess the presence or absence of style errors. Using the two implemented classification methods (Section 9.2.2), the presence and absence of style errors within every data capture in  $\mathcal{D}_{RT}$  shall be determined per style criteria and feature set (Section 7.3.2) in the following.

In general, both the DTW-based classifier and the SVM-based classifier offer different advantages and disadvantages that should impact the choice of their utilization in future applications. Whereas the DTW based-classifier gives a direct similarity measure between the compared data segments, it is slow due to the frame-wise comparison of the warping step. Furthermore, it is dependent on the input reference matrix that has to be built in a precomputation step. The SVM-based classifier on the other hand is much faster and, since it is designed for large clouds of data points, can handle the input feature sequences well. However, it is more dependent on the general kernel and vector machine settings and requires the definition of an additional distance measure for subsequent score computation. To demonstrate the differences, the classifiers are used interchangeably in the following.

#### Error Assessment with $\mathcal{F}_K$

First, I wanted to have a look on the **kinesiology-induced feature set**  $\mathcal{F}_K$  with a two-fold data base split validation. Using the DTW classifier, I labeled all data segments within  $\mathcal{D}_{RT}$  with the help of the precomputed reference matrices  $X_F$  for erroneous motions and  $X_N$  for error-free motions for every style criteria. In the next step, I compared the annotations with the ones made by the human judges. Every correct and incorrect labeling was count and the final error classification used to determine the overall values for precision  $P$ , recall  $R$  and the  $F_1$ -measure of the error recognition. In the present scenario, precision could be thought of as a measure of the classification's exactness, recall as a measure of the classification's completeness and  $F_1$  as combination of both precision and recall. In concrete, precision was the number of correctly classified errors  $n_{tp}$  divided by the number of all classified errors  $n_{tp} + n_{fp}$ , recall the number of correctly classified errors  $n_{tp}$  divided by the number of all elements that were actual errors  $n_{tp} + n_{fn}$  for every style criteria, and  $F_1$  the harmonic mean between  $P$  and  $R$ :

$$P = \frac{n_{tp}}{n_{tp} + n_{fp}}, \quad R = \frac{n_{tp}}{n_{tp} + n_{fn}}, \quad F_1 = 2 * \frac{P * R}{P + R}. \quad (9.6)$$

In general, a low precision indicates a large number of false positives ( $n_{fp}$ ), and a low recall many false negatives ( $n_{fn}$ ). Ideally, both should be close to 1 to show a good error recognition accuracy, which can be represented in a high  $F_1$ . The values were determined separately for both of the two validation cycles and were then averaged to yield the final accuracy measures.

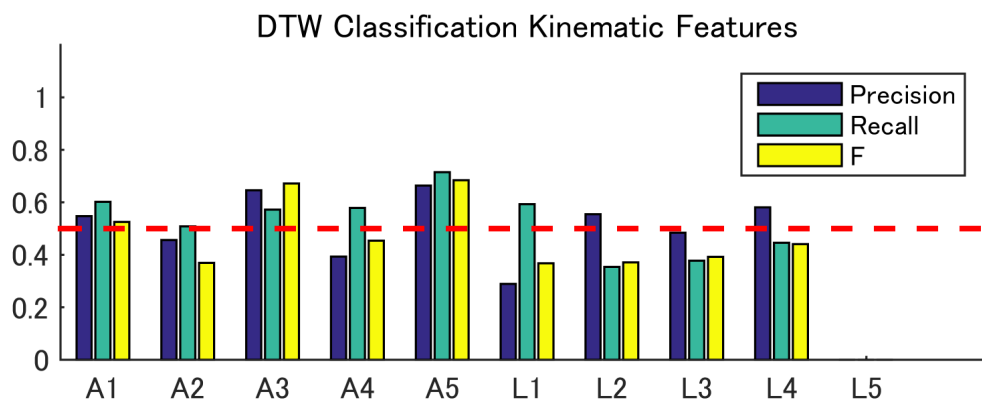


Figure 9.7: Precision and recall values and  $F_1$ -measure for the DTW error classification per style criteria. The red line represents the probability border of 50%.

The resulting  $P$  and  $R$  indicated an imprecise error recognition for most style criteria and did not show any remarkably good retrieval accuracy except  $A1$  (Figure 9.7). Only for four style errors (which were  $A1$ ,  $A2$ ,  $A3$  and  $L2$ ), all  $P$ ,  $R$  and  $F_1$  were higher than the chance rate. For the remaining style criteria, at least either one of  $P$  and  $R$  were low, indicating either many wrong error recognition or non-recognition of erroneous jumps within the two-fold error recognition cycle.

Considering the distribution of classification accuracy among the style criteria,  $A4$ ,  $A5$ ,  $L1$  and  $L5$  stood out as criteria of poor error recognition. For  $L5$  the reasons for the poor retrieval could be found in the consistence of the data base:  $L5$  was a non-frequent style error with by far less occurrences in the complete ski jump data set than any other error. Consequently, the number of available training data was not significant enough to build a good learning model for the testing under the two-fold data base split. Looking at the semantic description of the remaining affected style criteria, I assumed that not enough significant discriminative information that separated the erroneous and error-less label was represented within the training and/or test data sets.  $A1$ ,  $A2$  and  $A3$  that were of higher precision for example were subject to intuitive and relatively obvious (from the perspective of a human observer) error descriptions. The criteria  $A4$  and  $A5$  on the other hand focused on one aspect of the motion that might be subject to very small and subtle errors: during the flight of a ski jump, deviations from the perfect symmetric position at the legs and ski are generally bound to a very fine-scaled, small range due to aerodynamic constraints. Furthermore, (symmetric) position of legs is correlated to athlete-dependent style variations that might impede a generalization of the jump features. For  $L1$  on the other hand, misclassifications were likely evoked by the non-symmetrical landing position. Every athlete is free to choose either the left or right foot as principal (front) leg for the Telemark landing, and position can even vary within athletes over different jumps – a variation that was not considered within the feature transformations.

Next, the same error recognition process was repeated using the SVM under its respective classification principle. While it was possible to improve most of the  $P$ ,  $R$  and  $F_1$  values, it was

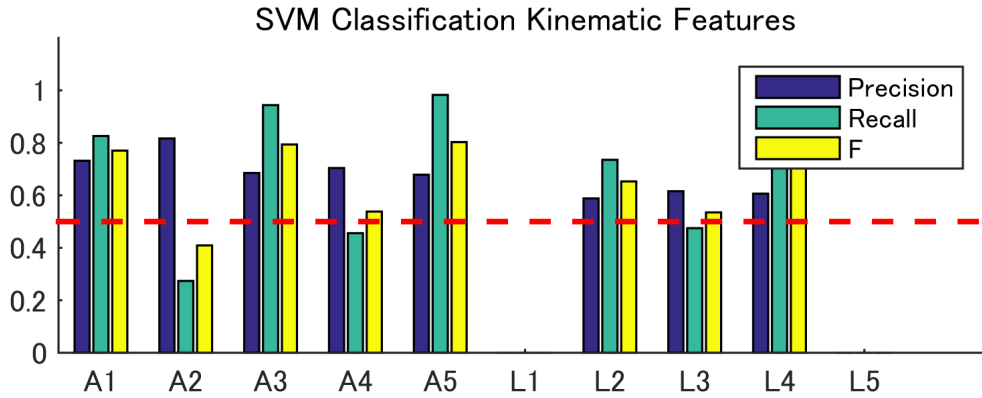


Figure 9.8: Precision and recall values and  $F_1$ -measure for the SVM error classification per style criteria and the probability border of 50% (red line).

not possible to determine the accuracy metrics for  $L1$  and  $L5$  (Figure 9.8). For both criteria, this was due to the fact that no significant classification model could be learned, so that no data segment in the test data was correctly recognized by the SVM. This, on the other hand, resulted in a division by zero in the precision's denominator, leading to  $P$  being not a number. Similarly,  $R$  resulted in a zero value. For criteria  $L5$ , I assumed this misclassification to be again a cause of the small number of available data segments with error. For  $L1$ , it was likely that the chosen kinematic features were not significant enough. This may either be due to bad feature selection, or the previously mentioned variations on the front leg of the Telemark landing position.

All in all, the results were encouraging that the designed system could be meaningful to retrieve errors. However, they also imposed the conclusion that the error recognition is style error and feature selection dependent. For a meaningful performance assessment, it is necessary to use a system with higher classification rates. To examine whether the semantically induced feature selection of  $\mathcal{F}_K$  was meaningful and whether better or differently distributed error classification results could be achieved with other features, I repeated the previous computations with the remaining more extensive feature sets in the next step.

#### Error Assessment with $\mathcal{F}_D$ and $\mathcal{F}_C$

To obtain a better balance between the number of available testing and training data, I chose  $k = 8$  instead of the described  $k = 2$  for the subsequent **k-fold cross-validation (CV)**. For the SVM classifier, I furthermore extended the validation process to a **k-fold nested cross-validation** functioning as regularization for the complexity of the classification model. This meant that the computation of classification precision for final evaluation was performed within two different k-fold CV steps: one external CV splitting the data base into k training and testing subsets, and an internal CV for parameter tuning on the current training subset only. The intention of this internal CV was to prevent over- or underfitting of the SVM. Given

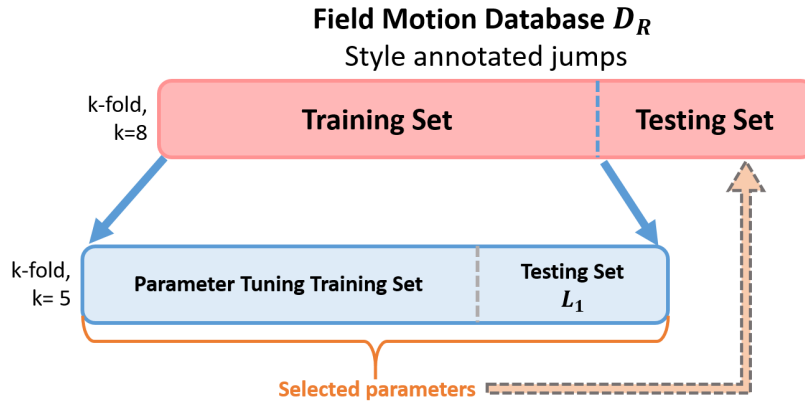


Figure 9.9: Scheme of the k-fold double-nested cross-validation used for error recognition along the different style criteria.

the number of data captures, I chose an internal k-value of  $k_i = 5$  for the inner model training and parameter tuning step here. I then determined the  $k_i$ -fold classification error for ten sets of random, initial Gaussian RBF kernel scale and margin parameter values. Lastly, I selected the parameters of the set of smallest error for the subsequent k-th error recognition of the outer CV (Figure 9.9).

As Figure 9.8 shows,  $P$  and  $R$  can be contradictory, so that  $P$  reaches high or full value, while  $R$  remains small. One way to combine the two accuracy measure was the previously introduced  $F_1$  score representing the harmonic mean between  $P$  and  $R$ . Another way of representing all relevant classification statistics would be to visualize the classification in a binary confusion matrix showing the true positives  $n_{tp}$ , false positives  $n_{fp}$ , true negatives  $n_{tn}$  and false negatives  $n_{fn}$ . In general, a good classification is then represented by high values along the diagonal axis:

$n_{tp}$	$n_{fp}$
$n_{fn}$	$n_{tn}$

In the data plots, high vales (with a max value 1) shall be denoted as black and low values (with a min value 0) as white. To exactly represent the recognition rates of every style error, I normalized the confusion matrix over the number of  $n_{JF}$  and  $n_{JN}$  for plotting. Besides confusion matrices, it is possible to use other accuracy numerical precision criteria instead of precision and recall. Measures related to the representation of confusion matrices are the classification accuracy  $CA$  and the error rate  $ER$ . They are defined as

$$CA = \frac{n_{tp} + n_{tn}}{n_{tp} + n_{tn} + n_{fp} + n_{fn}}, ER = \frac{n_{fp} + n_{fn}}{n_{tp} + n_{tn} + n_{fp} + n_{fn}}. \quad (9.7)$$

Containing information on both correctly classified jumps with errors and jumps without errors, the  $CA$  and  $ER$  metrics (which are oppositional and sum up to 1) as well as confusion matrices were used additionally to the  $P$ ,  $R$  and  $F_1$ -measures in the following investigations.

After running through the full proposed error classification, I obtained a similar distribution of the accuracy measures than with  $\mathcal{F}_K$ : all  $P$ ,  $R$ ,  $F_1$ ,  $CA$  and  $ER$  were obviously variant along the different style criteria for both the DTW classifier model as well as the SVM classifier model (Figure 9.10). Similarly as with the kinematic-induced features  $\mathcal{F}_K$ , data segments could be accurately classified under the style criteria  $A1$ ,  $A2$ ,  $A3$  and partly also  $A5$ , and less accurately under  $A4$  and all landing criteria. This disparity was also reflected within the inner parameter tuning CV. Despite the randomly chosen parameters of the classifier, the majority of all cross-validation losses (errors) was much smaller for certain style criteria (e.g.  $A1$ ) than for others, indicating that they were of higher discriminative power. Apart from the previously mentioned differences in semantic description and distinctiveness, two other reasons could be the cause here: one would be the general lack of sufficient discriminative data (so that the ideal separation between error-free and erroneous data captures could not be learned), the other one would be the specific lack of sufficient discriminative data (so that no definite separation between error-free and erroneous data captures could be learned). Whereas the former would result from the restricted number of motion takes within the used data base  $\mathcal{D}_R$ , the latter would result from the bias in the judges' ground truth data caused by individual perception of the flight performance. Especially for the poor landing classification, this assumption could hold true: all of the style criteria are concerned with the same main motion feature (meaning the landing process itself), and the recognition of a landing error might be difficult to separate into its certain error sub-categories represented as  $L1$ - $L5$ .

As a foremost unexpected observation, all of the computed data measures suggested that errors could be recognized better with the  $\mathcal{F}_D$  features than with the time-serial  $\mathcal{F}_C$  features. Continuously throughout all ten style criteria,  $P$ ,  $R$ ,  $F_1$  and  $CA$  values were larger here, and  $ER$  values smaller. Especially easy to spot was this difference at the  $CA$  and  $ER$  measures for the SVM classifier: classification accuracy was high with  $\mathcal{F}_D$  (ranging between 65 to 95%), whereas it was only  $\approx 50\%$  with  $\mathcal{F}_C$  (meaning around chance rate) and with certain landing criteria even smaller than the error rate. Here, an explanation could be that the transformation of the time-series data into a lower dimension did not represent enough information for the set up of a discriminative classification model. However, it should be emphasized that the  $CA$  and  $ER$  measures should not serve as single indicator for the quality of the present classifiers. This becomes particularly obvious when looking at the classification results for  $L5$ . Although no  $P$ ,  $R$  and  $F_1$  measures could be determined, classification reached a very good value for  $CA$  – misclassification of the error-free jumps was rare and the respective data segments had a recognition rate of close to 100%. The erroneous jumps on the other hand could not be retrieved at all, so that the actual error recognition rate of  $L5$  would be 0%. Visualizing the classification relations in the normalized confusion matrix, the differences in recognition rate became visible (Figure 9.11).



## Chapter 9. Retrieving Motion Style Information

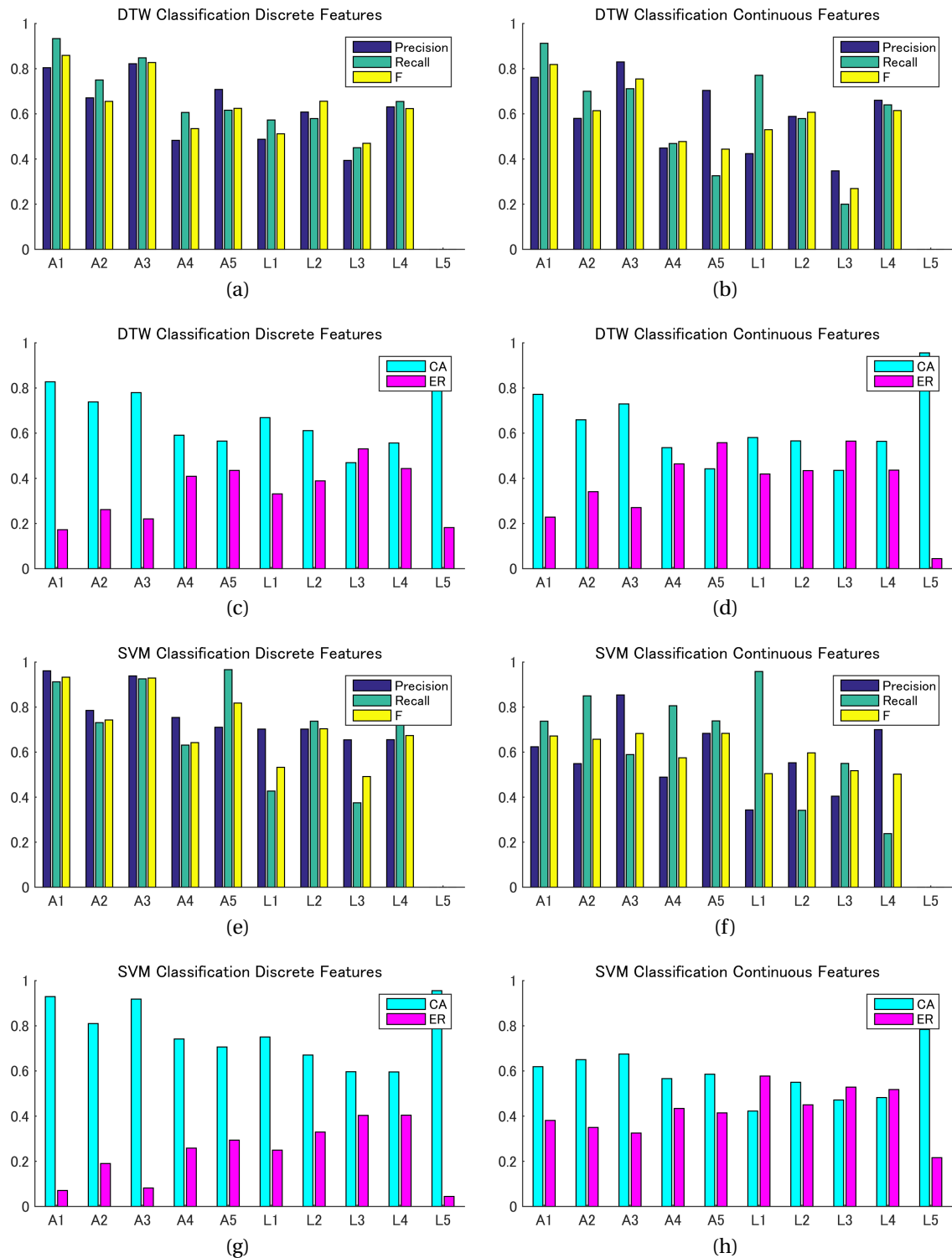


Figure 9.10: Accuracy measures for the error classification per style criteria using the DTW classifier ((a)-(d)) and the SVM classifier ((e)-(h)) for both  $\mathcal{F}_D$  and  $\mathcal{F}_C$ . Upper row each:  $P$ ,  $R$  and  $F_1$  values, lower row each:  $CA$  and  $ER$  values.

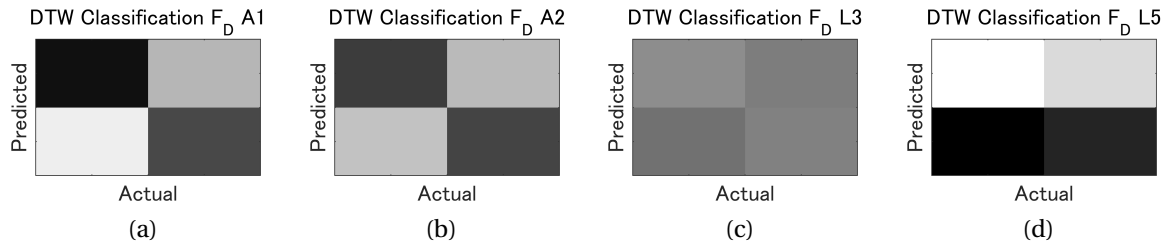


Figure 9.11: Sample normalized confusion matrices for the full feature classification with  $\mathcal{F}_D$  and DTW classification. From (a)-(d): confusion matrix for an accurate classification with  $A1$ , confusion matrix for an average classification with  $A2$ , confusion matrix for a poor classification with  $L3$  and confusion matrix for  $L5$ .

Despite this ambiguity, descriptive statistics seemed to offer an universal advantage over time-series data representations. These results indicated that for ski jumping, all the relevant motion information describing differences between data captures were fundamental, momentary signal properties that could be discovered well with basic analysis methods. Looking at the accuracy measures of single k-fold cycles for style criteria of good classification results, I could discover that classification accuracy was high in the majority of all cycles (usually in either 6 or 7 cycles), and less accurate in the remaining cycles. This confirmed the previous apprehension that bias in the judging data might influence and diminish the accuracy of the classifiers: with a higher number of misclassification, the data segments for testing might contain outliers that do not contain the same motion information in those cases.

#### Error Assessment with reduced $\mathcal{F}_D$ and $\mathcal{F}_C$

The previous error assessment showed that retrieval accuracy varied per style criteria under a similar distribution than for  $\mathcal{F}_K$ . It furthermore suggested that  $\mathcal{F}_D$  is better suited for the present classification task than  $\mathcal{F}_C$ . Especially the latter was not anticipated beforehand. Generally, the continuous time-serial features were assumed to be more precise for the assessment of a temporal sequence of body motion features. This imposed the question whether all of the chosen features were meaningful for the subsequent machine learning task, especially as the power of different features was unknown: learning algorithms are very sensitive to poor features that might not be able to display the information of interest for retrieval. In case that not all features are relevant to describe a certain motion characteristic, it can be useful to reduce the dimensionality of a feature set. Therefore, I repeated the described k-fold CV under three smaller feature sets that were built by reducing  $\mathcal{F}_D$  and  $\mathcal{F}_C$  under generic feature selection methods.

Generally, two approaches are possible to create valuable motion descriptors: defining relevant features individually on the base of expert knowledge on a motion's characteristics in a supervised environment, or defining relevant features from a set of possible features on

## Chapter 9. Retrieving Motion Style Information

---

the base of machine computations without any specific domain knowledge. The feature set  $\mathcal{F}_K$  was built under the former approach. Unsupervised feature selection was now applied to the two full general feature sets. Three different feature selection strategies were used and the resulting phase-wise feature selections validated with respect to their performance error classification to examine if a reduced sub-feature set could generate better results:

- FSS1*: The first feature selection strategy was a filter selection using leverage scores computed from a principal component analysis (PCA) [MD09]. In concrete, a PCA was used to reduce the dimensionality of the feature set and the most relevant features were then chosen by leveraging their relevance. This relevance was defined by the eigenvectors that retained 97% of the variation in the data and computed as the squared norm of the respective eigenvalues. The most and least significant features were revealed by sorting all feature leverage scores in descending order.
- FSS2*: The second feature selection strategy was performed by assigning correlations and their eigenvalues to clusters of similar variance [LCZT07] to select the most relevant features of large spread in lower dimension. This means that the points in the transformed space should be kept as far apart as possible to retain the variation in the original space and to select features that are distinctive from each other. Clustering was performed by using a binary decision tree built from the eigenvectors of the singular value decomposition (SVD) of the correlation matrices of all feature streams. The depth of the decision tree was again determined by the number of most dominant eigenvectors (retaining 97% of the variation in the data).
- FSS3*: The last strategy was a custom-made, logically-induced feature selection based on the idea of maximal relevance minimum variance: all those parts in the features that are reliably of high difference among all data takes (meaning of little variation over all takes) shall be identified and selected. For this algorithm, I first computed a mean matrix  $X$  over all data captures separately for  $JF$  and  $JN$ . In the second step, the features of highest difference in the mean values were identified, whereas features that underwent too many variations within the data base were excluded as unreliable.

Qualitative analysis of the three feature selections did not show any particular selection pattern. Amongst others, I for example determined the distribution of selected features for every reduced set of features. For this, I counted the number of occurrences at every style criteria and sensor location per feature category without distinguishing between sensor type and motion axes (Figure 9.12). Distribution of the selected features did not show significant peaks in distribution valid for all feature selections, which could indicate particularly high discriminative power of certain features. On the other hand also no feature could be excluded as completely irrelevant over all feature selections.

For quantitative analysis of all three feature selections, classification accuracy of the CV was analyzed under the same metrics as for the full feature CV before. To evaluate the effects a

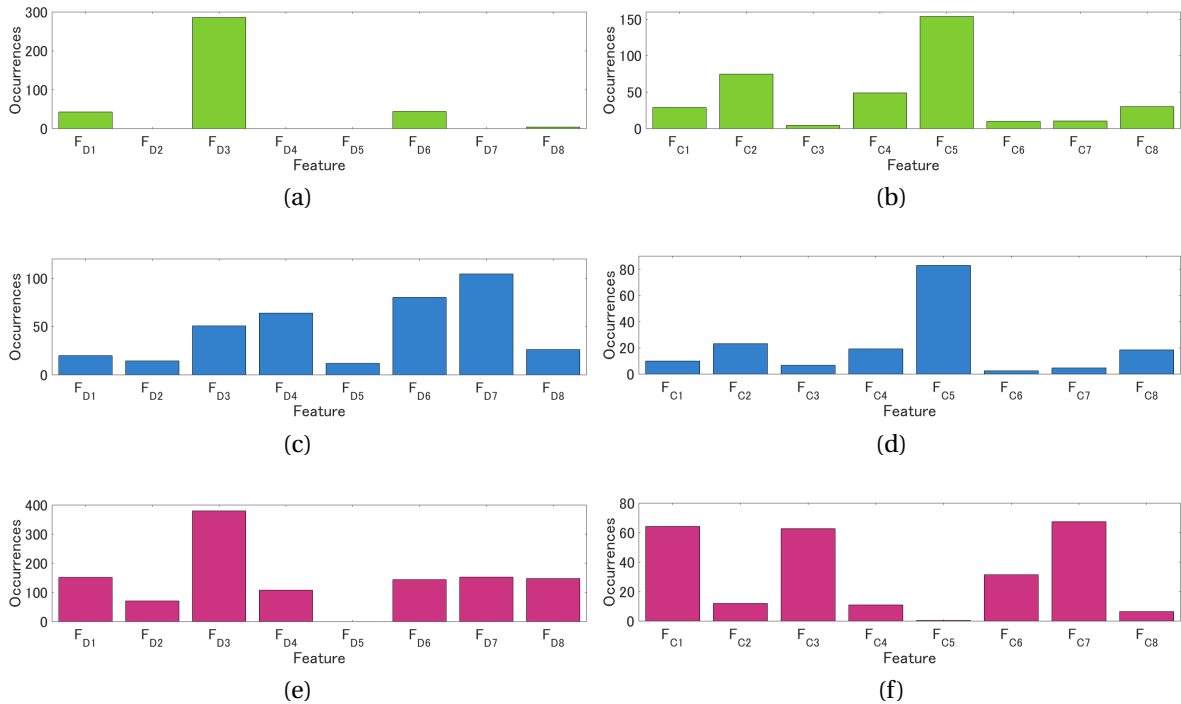


Figure 9.12: Visualization of the selected features for the reduced feature sets  $FSS1$  (green),  $FSS2$  (blue) and  $FSS3$  (magenta) over all sensor locations and style criteria in absolute occurrence. Left: discrete features  $\mathcal{F}_D$ . Right: continuous features  $\mathcal{F}_C$

of a feature selection on the error classification, I compared all sets  $FSS1$ ,  $FSS2$  and  $FSS3$  with the complete feature sets  $\mathcal{F}_D$  and  $\mathcal{F}_C$ , which I designated as  $FSS0$  for easier reference. Positive effects of the feature selection should easily be identified by improved evaluation measures, and eventual negative effects (caused by a bad feature selection) by degradation of the evaluation measures. Good retrieval under  $FSS0$  would furthermore give information whether all features contained relevant information, or whether the underlying data was so significant that irrelevant features might not have influenced the overall classification. Results did not show any significant improvements in error recognition for the three feature selections for both classification models. Instead, accuracy even diminished under certain style criteria throughout all reduced feature sets. As already presumed under  $FSS0$  beforehand, the accuracy metrics of both classifiers furthermore indicated that style errors during flight phase were of better recognition rate than style errors during landing. Differences in error recognition rates as a cause of different feature types were not discovered. For visualization, the  $P$ ,  $R$  and  $F_1$  measures averaged over all aerial and landing criteria shall be shown here with the DTW classifier (Figure 9.13). Distribution was similar for the SVM classifier.

As a result of both the qualitative and quantitative analysis, my first conclusion was that the two general feature sets  $\mathcal{F}_D$  and  $\mathcal{F}_C$  did not suffer considerably from irrelevant or bad feature sets. Assumptions on higher error recognition rates by use of the discrete feature

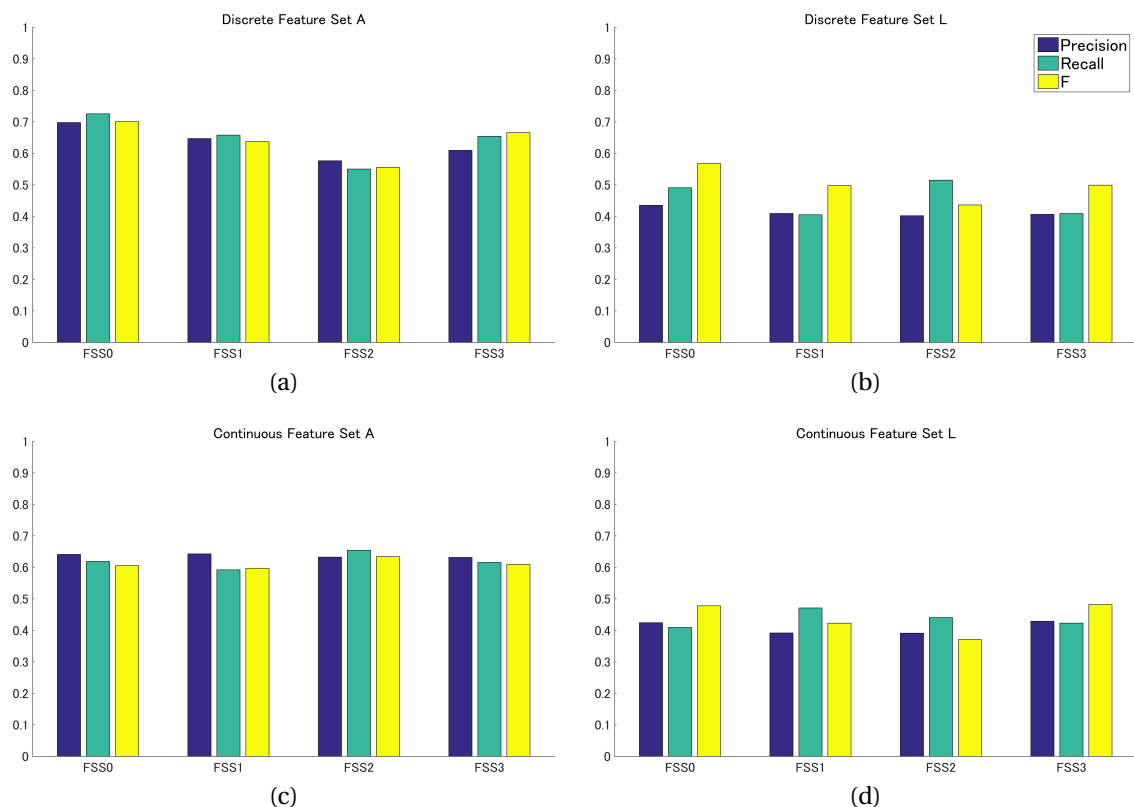


Figure 9.13:  $P$ ,  $R$  and  $F_1$  measure for  $k$ -fold CV of all sets of feature selections with the DTW classifier averaged over the jump phase for (a) and (b)  $\mathcal{F}_D$  and (c) and (d)  $\mathcal{F}_C$ .

types on the other hand could neither be confirmed nor invalidated, since accuracy measures were of similar values. Furthermore, I concluded that no feature reduction was available that would considerably improve the results of the style error classification. Consequently, it was not necessary to repeat the  $k$ -fold CV and its subsequent detailed analysis with a different, reduced feature set. However, it should be noted that classification accuracy might well be improved by good feature engineering. This could amongst others also be implemented by determining significant motion parameters from other ground truth input (e.g. video information using deep learning), but should not be further discussed in this thesis.

### Combined Landing Style Assessment

Within the previous evaluations, I discovered that errors in motion style during flight could be recognized more accurately than errors in landing. As responsible for this distinction I suspected outliers in the judging data caused by differences in clear separation between the five style criteria. By looking at the concrete judge scores, I could indeed already find discrepancies that seemed to support this hypothesis: while the official regulation required a minimum point deduction of 2.0 points for the  $L1$  error (Table 3.1), three of the 26 data

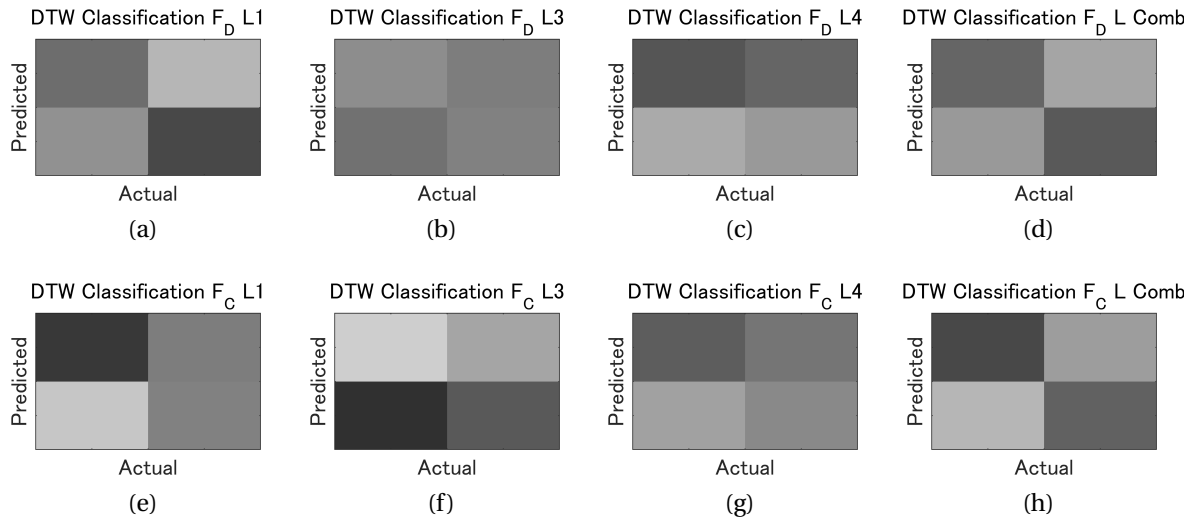


Figure 9.14: Confusion matrices for landing error recognition with DTW classification. From (a)-(d): confusion matrices for  $L1$ ,  $L3$ ,  $L4$  and the combination of  $L1$  and  $L3$  with  $\mathcal{F}_D$ . From (e)-(h): confusion matrices for  $L1$ ,  $L3$  and  $L4$  and the combination of  $L1$  and  $L3$  with  $\mathcal{F}_C$ .

captures annotated as  $L1$  error had an point deduction of less than 2.0 points. Besides, two data captures were awarded a point deduction for both  $L1$  and  $L3$ . Since both are directly related to the absence of the Telemark position ( $L1$  fines the complete absence of the Telemark,  $L3$  fines an insufficient execution of the Telemark), they should not occur simultaneously in practice. As last error recognition validation, I therefore classified the landing data segments under a combined metric respectively learned motion knowledge.

All of the 85 data captures within  $\mathcal{D}_R$  were awarded a point deduction in landing. This meant that I could not compare groups of combined style errors to jumps with a perfect landing. To evaluate whether a combined measure could be useful, I therefore divided the landing errors into two groups: the direct assessment of the Telemark execution by  $L1$  and  $L3$  and all other remaining landing style errors including  $L2$ ,  $L4$  and  $L5$ . After running through the k-fold CV under the  $L1 - L3$  error classification, one could presume that such combined measure might indeed be useful for the present task. Differences in classification accuracy were less obvious when compared to the error recognition of  $L1$ , but considerably visible when compared to the error recognition of the remaining jumps (Figure 9.14). Here, not only  $L3$  classification was enhanced. Also the recognition of the group with  $L2 - L4 - L5$  jumps (which served as counterpart to the group with  $L1 - L3$  jumps) was more accurate than in the single error recognition. Even better results could be obtained with the discrete features under the SVM classifier, where  $CA$  reached 94% correct classifications.

As a result, it should be noted that restructuring of the basic error annotations might generate better classification results when certain style errors cannot be clearly distinguished semantically. It was shown that the combination of error categories that are easy to intermix

can result in more distinct separation of affected and unaffected data takes. Here, a semantic grouping of  $L1 - L3$  and  $L2 - L4 - L5$  data segments was chosen, but also other combinations such as  $L1 - L2$  and  $L3 - L4 - L5$  or only  $L3 - L4$  could be possible and might yield even larger improvements. Testing the same assumption under a slightly different pairing  $L1 - L3$  and  $L2 - L4$  that excluded the  $L5$  errors, results could for example be slightly improved. In general, it should be stated that the better the interrelation between different grading criteria is known, the better a semantically meaningful combination can be built. Moreover, it is important to remember that all of the data captures used for the machine learning were annotated as superimposed by landing errors. Consequently, all landing data segment also were of semantically similar motion information content. It can be expected that much better classification results are achieved when jump segments with a landing error are compared to jump segments without a landing error. Considering that landing is one of the most difficult and error-prone part of a ski jump, the collection of data captures with perfect landing scores is however likely to be bound to performances of professional ski jump athletes.

### Leave-one-out (LOO) Error Assessment

The previous error recognitions include data of all participating athletes in both the training and testing data subset per CV cycle under a randomized distribution. While the CV neglects distribution effects caused by this randomization, it might still be possible that good accuracy results are mainly influenced by good error classification of one athlete's motion errors. For this reason, and to test the performance of the classifier with completely unknown motion data, I next performed a leave-one-out (LOO) classification. For this, I changed the basic CV implementation into a  $n_a$ -fold CV, whereas  $n_a$  constituted the number of participating athletes in the data collection (here  $n_a = 4$ ). In every cycle, the data of one athlete was retained as testing data, and the data of all remaining  $n_a - 1$  athletes used for training of the machine knowledge.

As first analysis, I determined the averaged accuracy measures  $P$ ,  $R$ ,  $F_1$ ,  $CA$  and  $ER$  over all LOO-CV cycles. The results were little satisfying: for most style criteria, the classification accuracy was around or even below the probability border of 50% (Figure 9.15). This indicated that the system was not capable of identifying motion errors of an athlete when his motion errors were not known and learned beforehand. In other words: every athlete seemed to have an individual motion style of a style error execution that was differing considerably from the motion style of all other athletes. In this context, I noted that the distribution of classification accuracy of the LOO-CV deviated to the ones previously obtained. In particular  $A1$  was of poor error recognition, whereas  $A5$  and  $L1$  were of similar classification accuracy as before. This under-performance of  $A1$  was likely to be a cause of the semantic description of every motion error.  $A1$  was defined very vaguely as instability and could be referred to any of the measured body parts arms, legs and skis. Consequently, it was indeed possible that a different type of body instability occurred per athlete, and that their uniform categorization into  $A1$  led to different error motion styles per actor.

### 9.3. Ski Jump Style Assessment

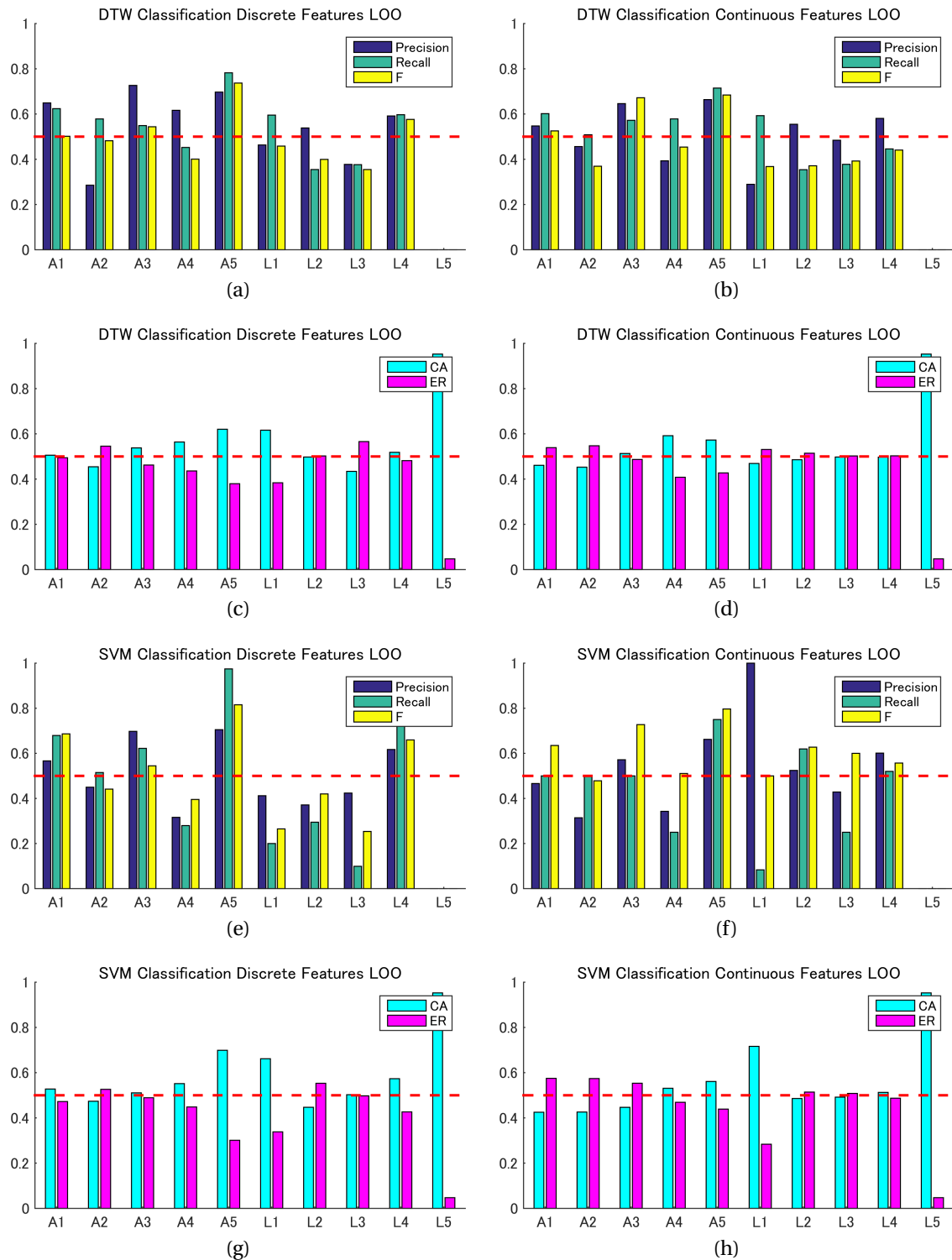


Figure 9.15: Accuracy measures for the LOO error classification per style criteria and the probability border of 50% using the DTW classifier ((a)-(d)) and the SVM classifier ((e)-(h)) for both  $\mathcal{F}_D$  and  $\mathcal{F}_C$ . Upper row each:  $P$ ,  $R$  and  $F_1$  values, lower row each:  $CA$  and  $ER$  values.



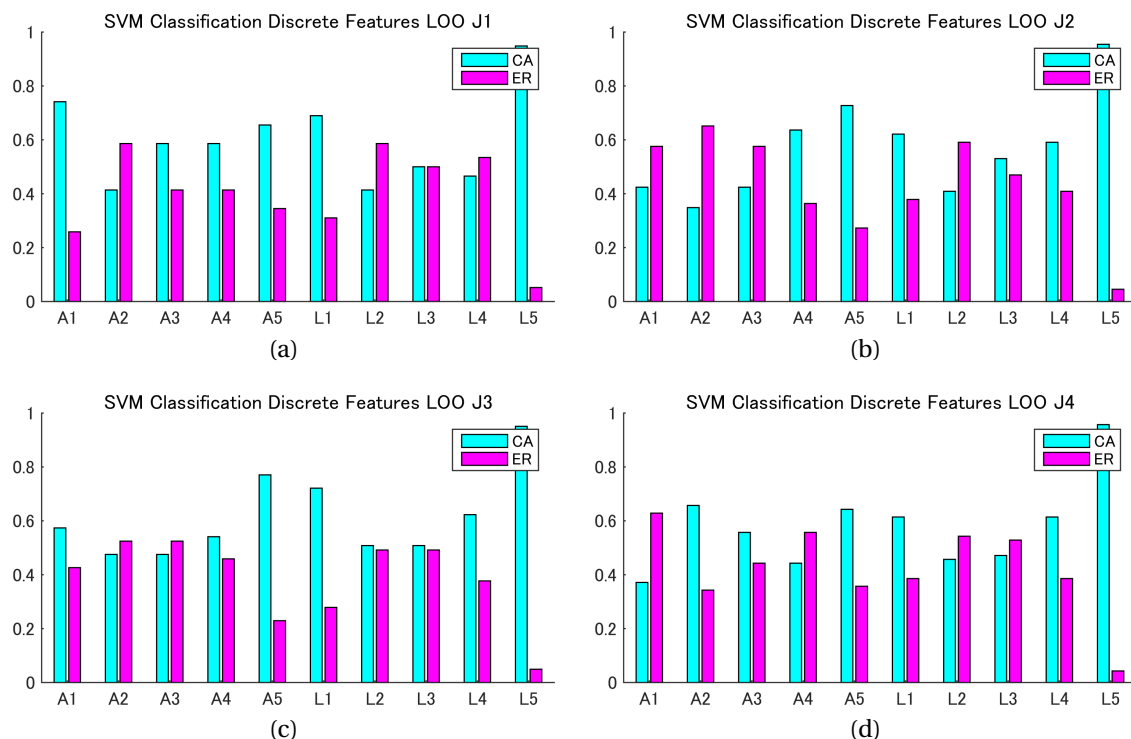


Figure 9.16: *CA* and *ER* for the LOO error classification per style criteria and CV cycle using the SVM classifier and  $\mathcal{F}_D$ .

Next, I therefore wanted to see whether error recognition was poor for all  $n_a$  CV cycles, or whether errors of certain athletes had a higher chance of correct error recognition. For this, I denoted the four jumpers as  $J1$ ,  $J2$ ,  $J3$  and  $J4$  and investigated the classification accuracy of their respective LOO-CV cycles separately. Indeed, accuracy metrics varied largely per cycles along all style criteria with both classifiers and  $\mathcal{F}_D$  and  $\mathcal{F}_C$ , suggesting that certain motion errors of certain athletes were easier to assess. In the present data collection, especially A1 of athlete  $J1$ , A2 of athlete  $J4$  and A5 of athlete  $J3$  had clearly higher classification accuracy than the same style errors in their respective three remaining counter cycles (Figure 9.16). Specific reasons for these particular discriminative strength were not found, but it could be assumed that differences in the motor execution between JF and JN jumps were particularly clearly defined in those motions. To investigate and explain any eventual relations, it might be useful to verify all motions from the collected video data in future.

### 9.3.2 Full Performance Quality Assessments

The previous style assessments were made on the assumption that relevant errors (meaning errors that have to be fined) of a motion performance can be put into single style criteria. However, judges reported a tendency to evaluate a performance under the complete impression of a jump within its environmental surroundings and including aspects such as

flight curve or distance to the landing slope. Earlier, I have already shown that style points correlated to the flight length (Figure 9.6). Consequently, the jumps should be tested under an overall performance quality aspect next, leaving behind the previous style criteria. Instead, I used the overall performance scores and jump lengths for grouping of the motion data streams. In consideration of the properties of the available data captures, jump quality was classified as good (G), medium (M) and poor (P) performance. Since the flight was considered as a whole motion performance, no phase separation was necessary. Therefore, motion data streams  $F$  for the complete jump were considered starting at  $t_{TOI} - 200$  frames and lasting until  $t_{LD} + 400$  frames.

Apart from the modified design specifications, the general classification principle remained the same in both scenarios. This meant that the classification accuracy was evaluated with a  $k$ -fold CV for the DTW classifier (with  $k = 8$ ) and a nested CV for the SVM classifier (with  $k = 8$  and an inner  $k_i = 5$ ).

#### Assessments Based on Overall Scores

In consideration of the overall jump scores from all data captures in  $\mathcal{D}_R$ , every jump with a score of 15.5 points or less was classified as P jump, every jump with a score of 16 or 16.5 points as M jump, and every jump with a score of 17.0 points or more as G jump. By this separation, a relatively equal split between all 85 data captures could be obtained. Herewith, the chosen threshold values of  $t_{pm} = 15.5$  and  $t_{mg} = 17.0$  points were a reflection of the skill level of the participating junior athletes. Including the motion data of more experienced, professional jumpers in the training and testing data base, other threshold values might need to be found (e.g.  $t_{pm} = 16.5$  and  $t_{mg} = 18.0$  points).

Analysis of the resulting performance quality assessments showed that accuracy measures were of similar level than for the previous classification under the ten style criteria (Figure 9.17). Especially good  $P$  measures were obtained by G jumps for the DTW based classification, whereas for the discrete features also the  $R$  and  $F_1$  measure were high. M jumps were of smallest retrieval accuracy for the discrete features, and P jumps for the continuous features. Given the mediocrity, it is not surprising that M jumps were recognized with less accuracy than the jumps within the outer boundary groups – their motion data is likely to be closer to both G and P jumps than the motion data of G jumps is to P. For this reason, I repeated the CV with only P and G jumps, to see whether the discrimination rate of jumps would increase. Comparing the classification accuracy of P and G under both CV, results could be improved.  $CA$  values rose from  $\approx 80\%$  to  $\approx 85\%$  for P and from  $\approx 75\%$  to  $\approx 80\%$  for G with the DTW classifier. For the SVM classification,  $CA$  was improved for P ( $\approx 80\%$  to  $\approx 90\%$ ), but diminished for G ( $\approx 80\%$  to  $\approx 72\%$ ). More evident became the positive effect however for  $P$ ,  $R$  and  $F_1$ : from values between 0.3 and 0.75, values grew tremendously (Table 9.2).

Classification accuracy brought me to the conclusion that in general, performance quality can

## Chapter 9. Retrieving Motion Style Information

Table 9.2:  $P$ ,  $R$  and  $F_1$  measures for classification of performance quality labeled under full flight scores with P, M, G and P and G only.

Type	$P P$	$R P$	$F_1 P$	$P G$	$R G$	$F_1 G$
P, M, G DTW	0.571	0.604	0.591	0.721	0.740	0.714
P, G DTW	0.875	0.688	0.857	0.829	0.865	0.839
P, M, G SVM	0.733	0.313	0.700	0.586	0.646	0.598
P, G SVM	0.875	0.625	0.810	0.908	0.958	0.931

be retrieved from the present data when a sufficient number of data takes is available. Besides, two further points could be verified that should be mentioned shortly. First,  $\mathcal{F}_D$  features again yielded better retrieval results in all  $P$ ,  $R$ ,  $F_1$ ,  $CA$  and  $ER$  than  $\mathcal{F}_C$  features. Averaging the metrics for the error assessment with full feature sets over all ten style criteria, and the full performance assessment over all three quality descriptors, in both cases significant differences in retrieval efficiency became obvious. For the DTW classifier, an error recognition under  $\mathcal{F}_C$  was 5-17% less accurate than an error recognition under  $\mathcal{F}_D$ . For the SVM classifier, an error recognition under  $\mathcal{F}_C$  was even 10-75% less accurate than an error recognition under  $\mathcal{F}_D$ . It should therefore be acknowledged that the discrete features were better suited for the given motion rating task. Second, results once again indicated the difficulty of classifying time-serial features with the SVM. While P jumps had the better classification accuracy with the SVM and  $\mathcal{F}_C$  features, M and G jumps had a better classification with the similarity-based DTW approach. Here, one could assume that errors of poorest performance quality were related to obvious data descriptions such as uncontrolled arm movement during flight. Style differences between M and G jumps on the other hand would then be subject to a finer, more detailed error assessment that could not be depicted in the dimension reduced  $\mathcal{F}_C$  feature input of the SVM. The normalized confusion matrices visualized this classification accuracy problem in an especially obvious way: especially M and G jumps could not be assigned to their class real labels in a reliable way, whereas they could be distinguished much better under the DTW classifier (Figure 9.18). P jumps could be recognized well as both either P or non P by both classifiers.

Concluding the current investigation, I want to state that the assessment of performance quality on the base of the overall jumps scores appeared to be another promising approach to the problem of motion performance assessment. However, results are dependent on the score thresholds chosen for annotation of the data captures. These on the other hand require a large amount of variant point scores within the underlying motion data base. Ideally – and with a sufficient number of data captures, every point score between 10 to 20 or 19.5 points (the perfect flight is difficult to achieve even for the best ski jumpers) should be used to build an own group for the learning of the fundamental artificial motion knowledge. In case of good classification accuracy, this performance quality assessment would then automatically include a numeric scoring for the creation of an overall ranking.

### 9.3. Ski Jump Style Assessment

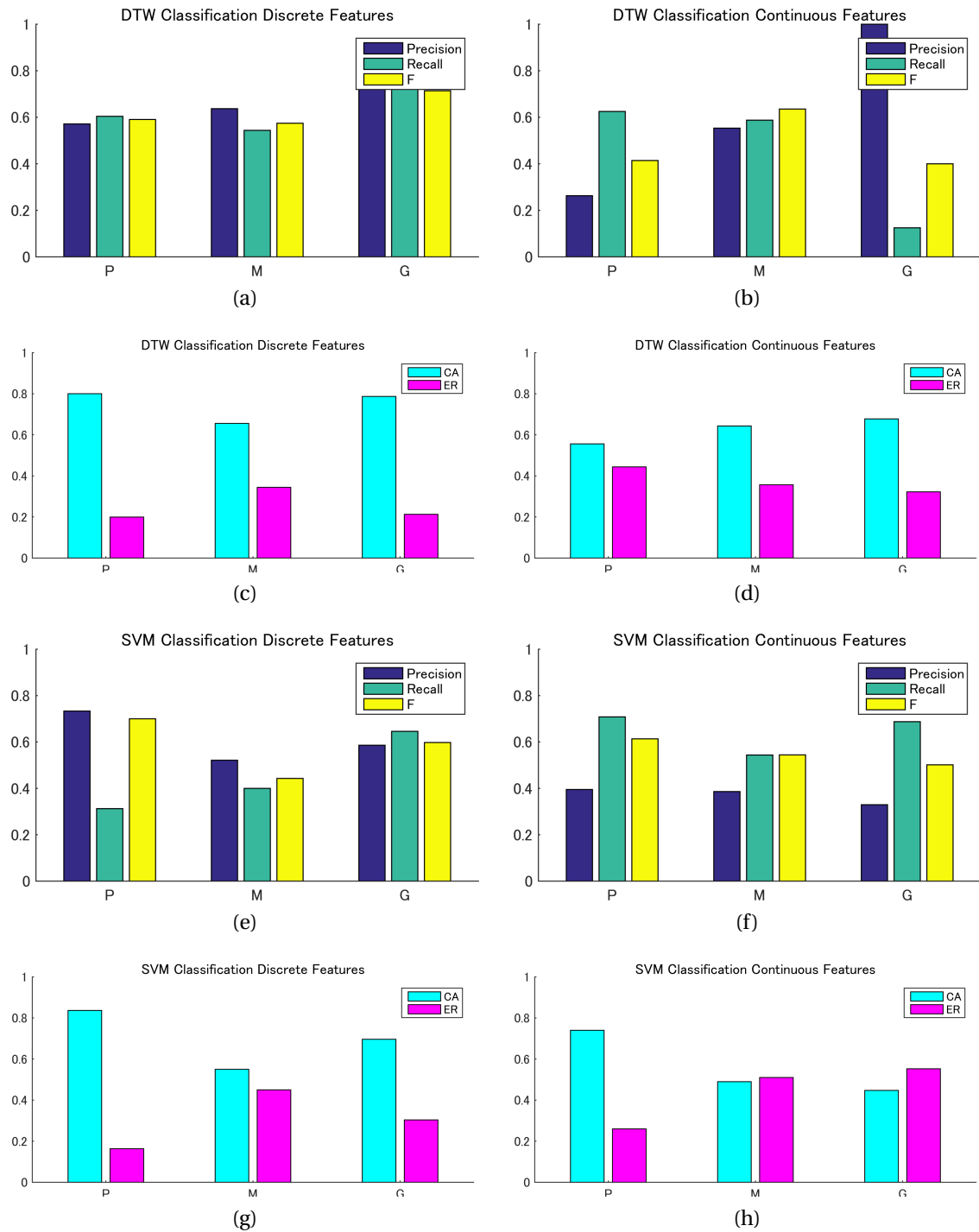


Figure 9.17: Accuracy measures for the classification of performance quality determined by overall flight scores using the DTW classifier ((a)-(d)) and the SVM classifier ((e)-(h)) for both  $\mathcal{F}_D$  and  $\mathcal{F}_C$ . Upper row each:  $P$ ,  $R$  and  $F_1$  values, lower row each:  $CA$  and  $ER$  values.

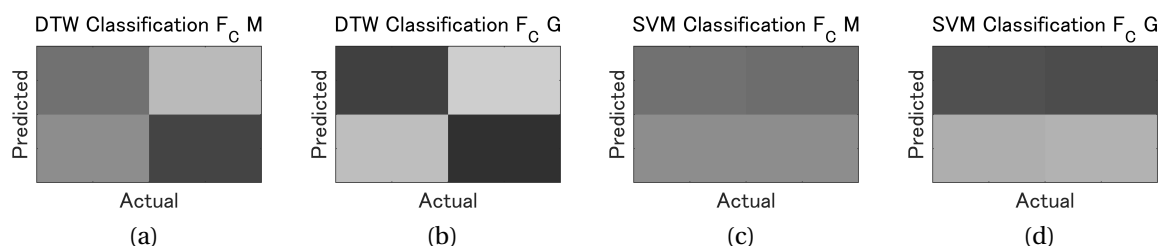


Figure 9.18: Confusion matrices for the classification of performance quality determined by overall flight scores with  $\mathcal{F}_C$  for M and G jumps with both DTW and SVM classification.

To put the results into relation, it should be stated that the resulting classifications have to be considered carefully: with all of the jumps performed by four different athletes only, the discrimination of performance quality on the base of the overall scores (and also length) is endangered to be less significant if the majority of poor or good jumps was executed by one single athlete. In such case, the test and training data would be suffer from less athlete-specific differences and classification results should be naturally higher.

### Assessment Based on Flight Length

Similar as before, I next assigned every jump to one of the three categories G, M and P, whereas I used the jump length as categorization criteria this time. Jump lengths ranged from 66 to 91 meters, whereas the majority of jumps ranged within an interval around 80 meters. Therefore, I chose  $t_{pm} = 76$  meters as threshold for the separation between P and M and  $t_{mg} = 84$  meters as threshold for the separation between M and G.

Again, no significant classification results were obtained with  $\mathcal{F}_C$ . Here, classification rates ranged around  $\approx 60\%$  for all groups. For  $\mathcal{F}_D$  however, accuracy measures reached much higher classification rates, and differences in accuracy distribution between the groups stood out more clearly than for the score based performance quality assessment. Classification rates of P jumps were  $\approx 90\%$ , classification rates of M jumps were were  $\approx 55\%$  and hence less significant, and classification rates of G jumps reached  $\approx 70\%$ . Consequently, P jumps showed to be particularly discriminative. Throughout  $P$ ,  $R$ ,  $F_1$ ,  $CA$  and  $ER$ , they were of extremely high respectively low accuracy measures (Figure 9.19). This imposes the conclusion that the underlying motion data of poor jumps were particularly discriminative. Since poor jumps are likely to be affected by errors in the motion performance, this would confirm that style errors were described by instantaneous events within the motion data (e.g. sudden motion of the arms after take-off). In total, it could be concluded that flight length serves as relative accurate indicator for motion style. This was also assumed before evaluation from the indications given by the volunteering judges. However, it should be repeated here that classification results have to be considered carefully in the given case, since P or G jumps might be performed by mostly one athlete.

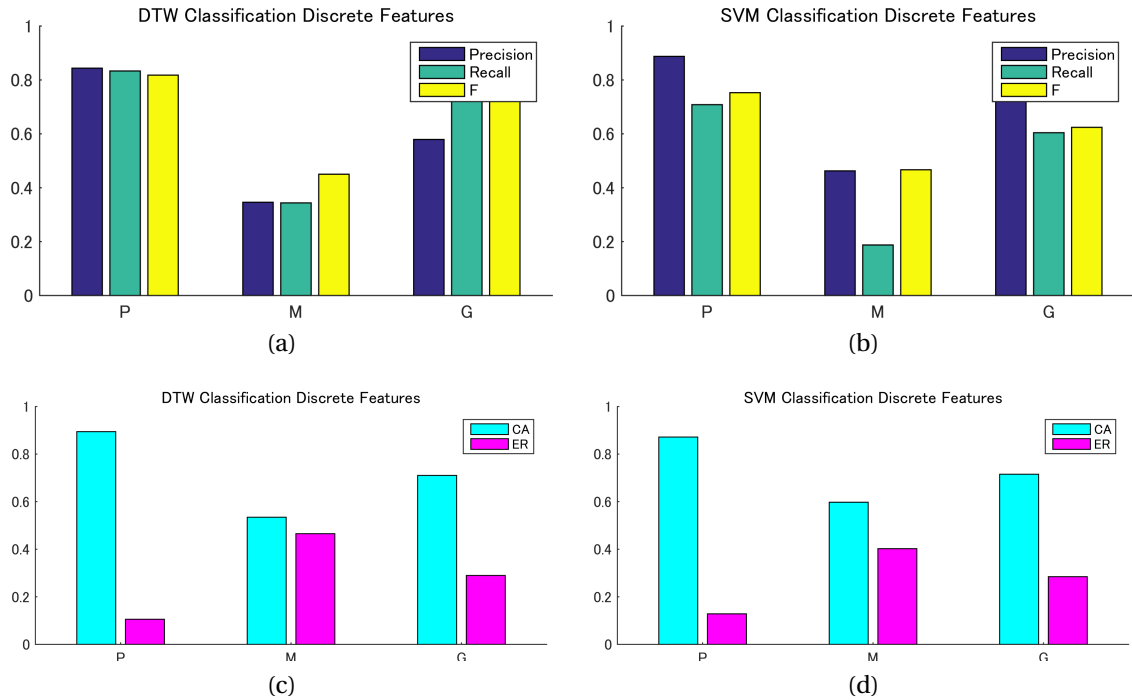


Figure 9.19: Accuracy metrics for the classification of performance quality determined by flight length with  $\mathcal{F}_D$ .

### 9.3.3 Feature Type Evaluation

Feature engineering is a very important part of any information retrieval process that considerably influences the performance of the complete learning system. No improvement in accuracy could be noted with any of the reduced feature sets obtained from three different feature selection strategies. However, in all of the previous style and error classifications, results suggested that errors were recognized better with the descriptive statistic feature set  $\mathcal{F}_D$  than with the body model feature set  $\mathcal{F}_C$ . To verify this assumption, I determined and compared the average accuracy metrics for both feature types and classifiers under both the criteria-wise error recognition and the overall flight quality assessment.

Independently of the chosen classifier and general performance evaluation strategy,  $P$ ,  $R$ ,  $F_1$  and  $CA$  values obtained with  $\mathcal{F}_D$  were larger than with  $\mathcal{F}_C$ , and  $ER$  values smaller, respectively. This observation held true for most CV cycles (Table 9.3), for each individual error category or quality label, and for all categories on average (Figure 9.20).

For the DTW classifier, an error recognition under the continuous feature set was 5-17% less accurate than an error recognition under the discrete feature set. For the SVM classifier, an error recognition under the continuous feature set was even 10-75% less accurate than an error recognition under the discrete feature set. Particularly large differences in the performance of the SVM classifier might be caused by the additional preprocessing step

## Chapter 9. Retrieving Motion Style Information

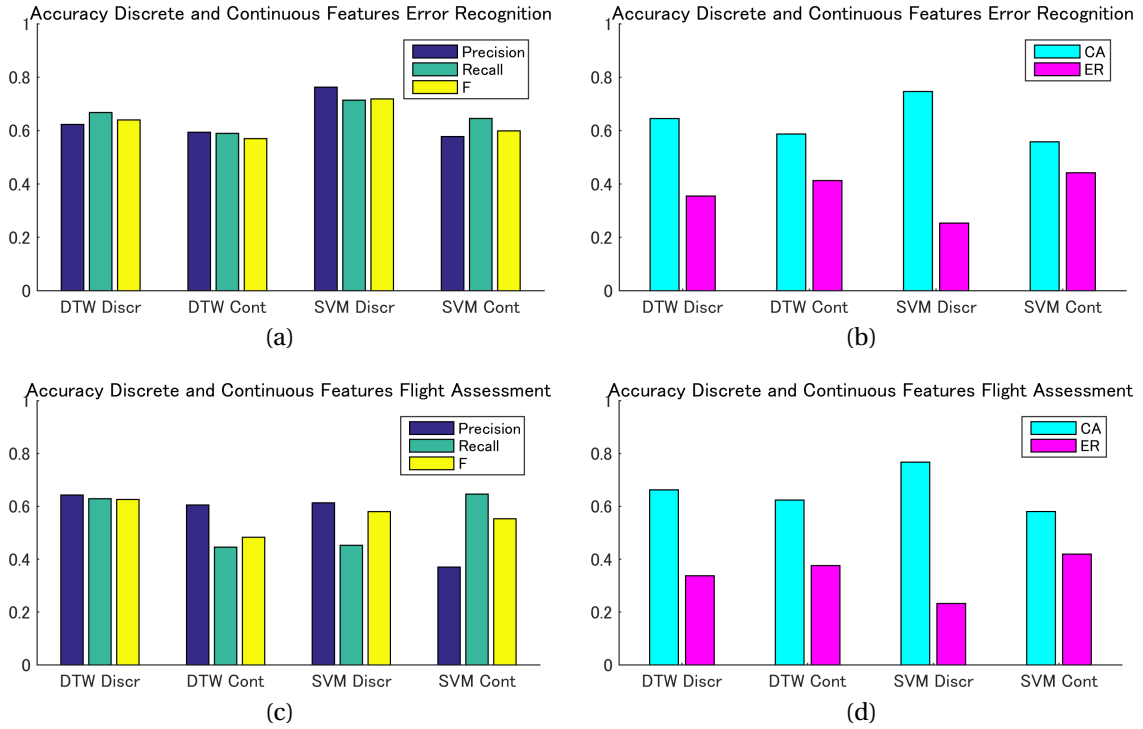


Figure 9.20: Comparison of the averaged accuracy values for the  $\mathcal{F}_D$  and  $\mathcal{F}_C$  feature sets with both classifiers. Top row: accuracy metrics for the basic, criteria wise error recognition. Bottom row: accuracy metrics for the overall flight quality assessment.

Table 9.3:  $CA$  values of the error recognition averaged over all error categories under the eight CV cycles.  $ER$  values can be determined as the difference between  $CA$  and 1.0.

k	$CA$ DTW $\mathcal{F}_D$	$CA$ DTW $\mathcal{F}_C$	$CA$ SVM $\mathcal{F}_D$	$CA$ SVM $\mathcal{F}_C$
1	0.6356	0.6767	0.7189	0.5833
2	0.7100	0.6336	0.7736	0.5682
3	0.5791	0.6145	0.7491	0.5800
4	0.7182	0.6364	0.7364	0.5727
5	0.6500	0.5645	0.7845	0.5218
6	0.7482	0.6636	0.8045	0.6082
7	0.6555	0.6073	0.7518	0.5909
8	0.6038	0.5955	0.8205	0.6197

that transformed the multidimensional feature matrices into a conventional input vector. However, this transformation could not be held responsible for all losses in performance quality, hence indicating the lower discriminative power of the continuous features. In other words, the present data collection indeed indicates that the most relevant motion information were fundamental, momentary signal properties that could be discovered well with basic analysis methods. This finding might be important for future system implementations:

for a robust recognition and identification of motion error it should consequently not be necessary to implement and run through an expensive preprocessing pipeline. Knowing that the estimation of body kinematics does not contribute any additional information content to the sensor data, the implementation of future hard-and software tools for motion error analysis could hence be drastically facilitated in future.

### 9.3.4 Numeric Style Error Assessment

The previous error recognition and performance quality assessments evaluated jump segments under the presence or absence of style errors, respectively a specific performance quality pattern. To enable a complete and functional scoring system, a quantitative evaluation is however not enough. In this case, it is furthermore necessary to enable discrimination within every group of errors or style quality. For the performance quality assessment based on overall scores, results indicated that under sufficient learning data, performances can be numerically rated in future. For the error recognition, it is necessary to develop further strategies that can award point deductions within a style category. The idea here would be to develop methods that can determine the gravity of every occurring error. Representing all of the previous error recognition retrieval tasks, the initial error recognition per style criteria shall be used next to investigate the probable set up of such numeric style error.

My idea to obtain a measure of error gravity was to compute the distance between the two categorization labels error ( $JF$ ) and non-error ( $JN$ ). Ideally, data segments that were awarded a higher point deduction (e.g. 1.5 points) should be more distant to the non-erroneous data segments than the data segments that were awarded a small error (e.g. 0.5 points). Two strategies are possible for such numeric error assessment. Strategy 1 computes the distance of every error classification to the error classifications of the respective other class under the previously classified labels. Strategy 2 uses regression instead of classification to directly obtain a numeric distance output from the error categorization process.

#### Strategy 1: Distance Assessment from Class Distance Measure

To be able to determine a distance measure of every error classification it was first necessary to mathematically define distance between variant data points for the two chosen classifiers. According to the definition of the present global standard DTW, the DTW distance  $DTW(X, Y)$  gives a measure of similarity for the two sequences  $X$  and  $Y$ . I therefore assumed that the accumulated cost  $D(N, M)$  could also serve as indicator for the error gravity: the larger for example the distance  $DTW(X, Y_1)$  than the distance  $DTW(X, Y_2)$ , the more serious the motion performance error referred to as gravity  $G$ :

$$G = DTW(X, Y_2) - DTW(X, Y_1), \quad (9.8)$$



## Chapter 9. Retrieving Motion Style Information

---

whereas  $X$  represents a test data segment and  $Y_2$  the reference matrix  $R_{CF}$  for error-free jumps and  $Y_1$  the reference matrix  $R_{CE}$  for erroneous jumps.

For the SVM, I hypothesized that a metric should be contained within the distance of a data point to the separating hyperplane. This means that the support vectors should be those feature points that were awarded the smallest error deduction (that means 2.0 points for  $L1$  and 0.5 points for all remaining style criteria). In the same way, larger point deductions would be further award from the boundaries. To determine the distance of every point, it is necessary to know the exact definition of the trained hyperplane. This shall be represented by a vector  $w$  built from the weight factors of every support vector. With  $K$  being the chosen kernel,  $x$  a support vector and  $\alpha$  the weight of the respective support vector,  $w$  is defined as

$$w^T = [(\sum_{i=1}^n \alpha_i K(x_i, x))^T b] \quad (9.9)$$

for the number of support vectors  $n$ .  $b$  represents a bias value that describes the intercept of the hyperplane in the normalized data space and is added to  $w$  as  $d + 1$ -th vector element, whereas  $d$  is the dimension of the feature vector. Contrary to the distance evaluation with DTW that was based on the distance of the testing data set, the distance evaluation of the SVM should be based on the distance of the training points to the hyperplane.

To examine whether the previous assumptions would hold true under the present motion data, I determined the distance with the DTW classifier and analyzed the support vectors of the SVM classifier. Since the classification results were better under  $\mathcal{F}_D$ , only the discrete features were considered in the following. Distance computations for all DTW classified test jumps over all k-fold CV cycles showed that the largest point deductions were not associated to the largest differences (Figure 9.21). For visualization, every list of distance measures was sorted in ascending order per style criteria.

Although the occurrence of point deductions did not correlate with the distance measure, it became obvious that most misclassifications (represented by negative values) were jump segments on the boundary, meaning segments of smallest possible point deduction (usually 0.5 points). This held especially for style criteria that had a larger variety of possible point deductions such as  $A1$ . It is natural to assume that the errors in the respective misclassified jumps have been too small to be recognized by the trained system. Considering the classifier's design, such misclassification might be caused by the lack of discriminative data. This, on the other hand, might be a result of the averaging process building the reference feature matrix or the bias in the ground truth data. Results consequently indicate that there might be a possibility for the assessment of distance in future data bases, however, this does not hold for the present collection of ski jump data.

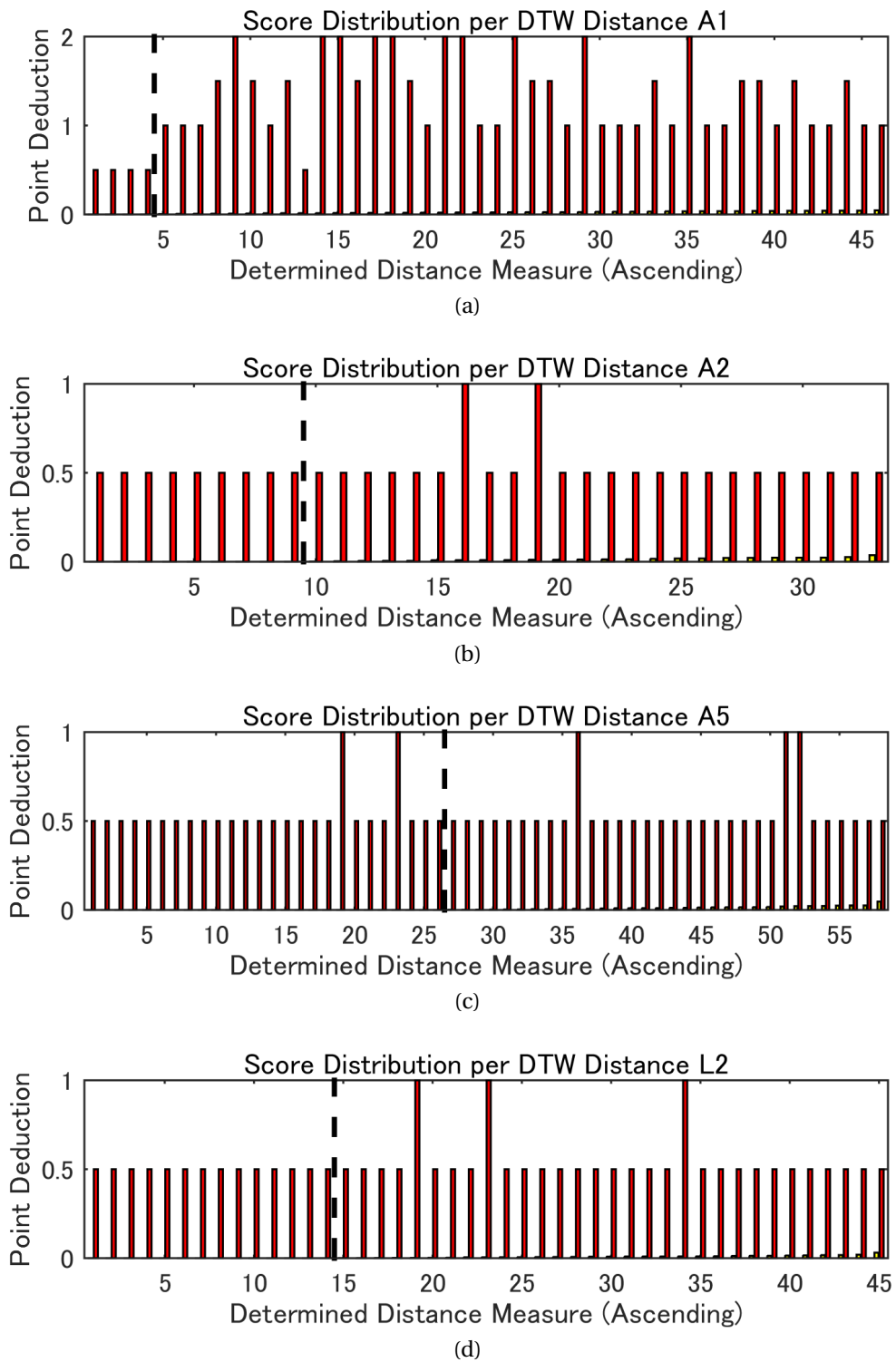


Figure 9.21: Sorted distance measures in ascending order with their correlating ground truth point deduction for sample style criteria under  $\mathcal{F}_D$ . The black line separates misclassifications and correct error recognitions.

Determining the support vectors of the training data per k-fold CV cycle gave me even less useful results. First, only  $\approx 10\%$  of the number of trained data did not function as support vectors. Second, the data points that did not function as support vectors were often data points that should have been labeled as support vectors and vice-versa. Consequently, my previous hypothesis was contradicted: under the given data, it was not possible to determine the gravity of points on the base of the distance to the hyperplane. Several reasons might be responsible for the large number of support vectors, which did not enable a distance measure. On the one hand, the SVM could be subject to overfitting – especially considering the sparsity of the SVM with the relatively small number of overall training data. On the other hand, the nested CV design with the previous kernel parameter optimization step commonly generates a very smooth classifier model with a large margin and many support vectors.

As a main conclusion, it should therefore be noted that it is recommended to supplement the data collection with a larger number of jumps and more robust ground truth judging data, and to then repeat the data analysis. In case of a powerful system design and discriminant available data, it should then be possible to better distinguish between the gravity of performance errors.

### Strategy 2: Distance Assessment by Regression Analysis

So far, I used the binary SVM to build a classification model and predict a label for every jump data segment. However, a SVM can also be employed to build a regression model. Regression analysis is a statistical process for estimating the relationships among variables and is widely used in predicting and forecasting. Simply said, it estimates a numeric value for an unknown jump segment in the testing data instead of a class label. As for SVM classification, the training data of a SVM regression model consists of predictor variables (here the feature inputs) and observed response values (here the ground truth error deduction points awarded by the judge).

Mathematically, a regression model is formulated as a convex optimization problem that has to be minimized. In concrete, a linear function  $f(x) = x'\beta + b$  should be found that deviates from a response value  $y_n$  by a value no greater than  $\epsilon$  for each training point  $x$ . At the same time,  $f(x)$  should be as flat as possible, which means that the  $f(x)$  with minimal norm value  $\beta'\beta$  should be found. The optimization problem is then defined as

$$J(\beta) = \frac{1}{2} \beta' \beta, \quad (9.10)$$

and the condition of all residuals having a value less than  $\epsilon$  as

$$\forall n : |y_n - (x_n' \beta + b)| \leq \epsilon. \quad (9.11)$$

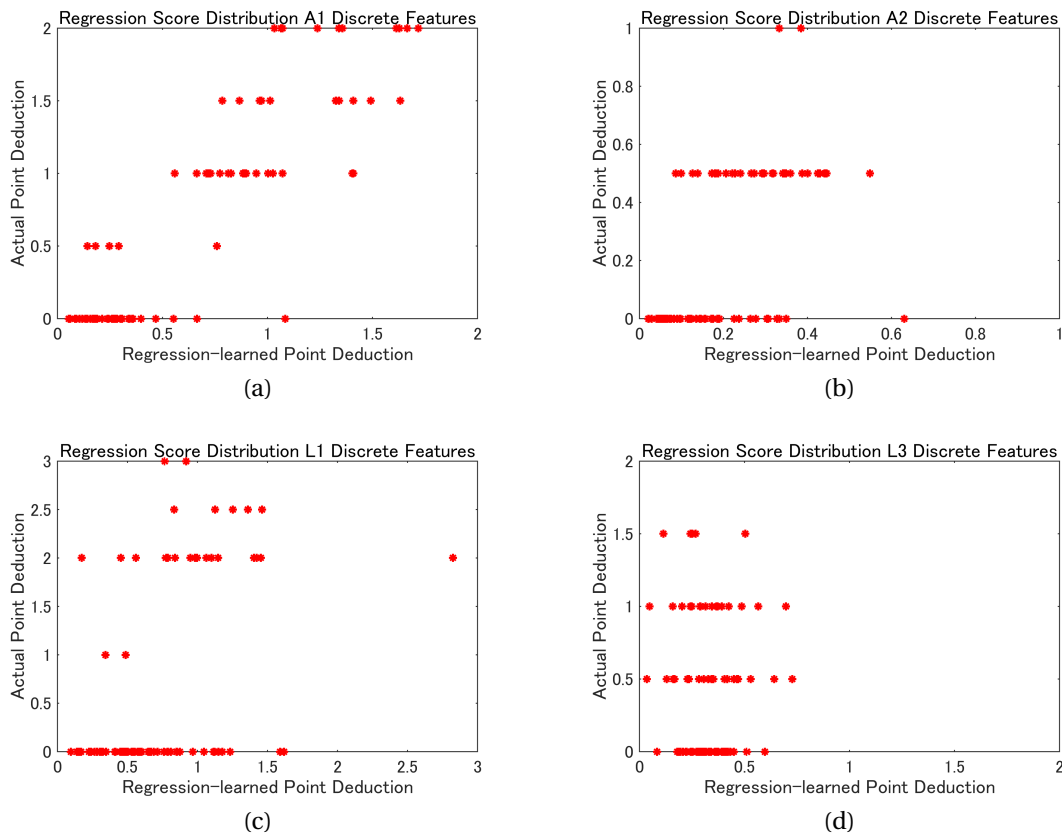


Figure 9.22: Estimated error values obtained from regression analysis in relation to the awarded ground truth data with  $\mathcal{F}_D$  for A1, A2, L1 and L3.

The present SVM regression was implemented in the same way as the basic nested SVM classification, whereas JN jumps were labeled with the no error value 0. Again, the SVM kernel parameters were trained in an inner CV cycle. Plotting the output of every machine per style criteria in relation to their ground truth data (Figure 9.22), I could discover similar patterns as for the basic style error classifications. This means that A1, A2, A3 and A5 showed linear relations between estimated and real point deduction values, whereas landing features did not show any correlations to the ground truth data.

In general, results are promising and encourage the conclusion that regression analysis could be used for error gravity determination in the future. Analysis of the regression and ground truth point values reveals high precision in the point forecast for multiple data points. However, also several aspects present themselves that should be resolved before a final conclusion can be drawn. First, it is likely that the general input data was too small to learn a completely meaningful regression model. In common forecasting, thousands or even millions of data points are used – in the present scenario, we used  $\approx 80$  data points per CV cycle. Second, the judges scores are awarded in steps by 0.5 points. To conform with this grading conventions, the regression estimates would need to be rounded in future. Third,

estimated values for error-free jumps hardly reach their actual zero value. Eventually, better overall results could be obtained by using a different training response value for JN jumps that is more distant to the actual error values. Lastly, grading conventions of  $L1$  require a minimum point deduction of 2.0 points. Output of the regression model should therefore also only contain values around 0 (for error-free jumps) and around 2.0 and more (for erroneous jumps). For this, a variation of the general SVM regression might be necessary.

### 9.4 Discussion

In the course of the current chapter, I developed an automatic system to evaluate and rate the style of a ski jump performance. For this, I first introduced a feature categorization system on the base of conventional judging guidelines. I then demonstrated the use of machine learning and binary classification method with the given problem and finally examined the implemented system methods for accuracy and reliability. I cross-validated the system under a variety of possible evaluation and retrieval aspects. Those were the existence of single style errors, the existence of style errors in a combination of possible errors, the quality of a complete jump as defined by overall score and length, and the computation of distance as a measure for error gravity.

Under the basic nested CV, error recognition results were accurate and reliable for the aerial flight criteria such as  $A1$ , and prone to misclassification for the landing criteria. For the latter, classification results could be improved by combining semantically similar style errors, indicating that the single style error annotations were difficult to distinguish in practice. Analysis with reduced sets of features furthermore showed that no improvements in accuracy could be achieved, and none of the chosen feature selection strategies could provide a feature set of better classification accuracy. However, the importance of feature engineering on the overall system performance shall be emphasized here: it cannot be excluded that error recognition might be drastically enhanced by different, unused feature transformations. For the sensitive landing criteria, I for example recommend to introduce further feature transformations that are unaffected by body-sided motion executions. A leave-one-out classification furthermore indicated the benefit of features that equalize athlete-dependent style variations well, so that motion errors are also classified well when tested with unlearned motion data.

For all discussed motion evaluation designs, the  $\mathcal{F}_D$  feature set obtained better retrieval results than the  $\mathcal{F}_C$  feature set, indicating the lower discriminative power of the continuous features. Since these were initially designed to better represent the essential biomechanical specifications of the underlying (ski jump) motion data, this finding is very unexpected at the first sight. However, it appears sensible when considering the semantic meaning of motion performance error: whereas different motion patterns and motion types (like different jumps of a trampoline sequence or performances in a skating routine) are described and

discriminated by their temporal evolution, a motion error is a mostly momentary event that superimposes the main temporal performance event. Therefore, it is also more likely to display itself under statistical descriptors that are specialized in finding data abnormalities than in temporal descriptions. This conclusion conforms to the (degraded) classification results obtained with the reduced feature sets – rather than the number and quality of feature extractors, the information content of the motion data itself appeared to be important. Respective error information should in conclusion be assumed to considerably superimpose the principal motion data structure in a large number of features, which is a characteristic most likely for outliers and data peaks. A similar correlation was also displayed in the classification results of the performance quality assessments, where P and G jumps could be discriminated well from each other. Especially poor jumps were accurately and reliably classified under the discrete features, affirming errors in a motion performance to be primarily instantaneous motion information easily retrievable by signal analysis methods. Consequently, it is also not surprising that the kinematic feature set  $\mathcal{F}_K$  consisting of a sparse set of continuous features could not generate satisfying error recognition results.

Results furthermore showed that the implemented SVM classifier was less suited for time-series features. This is likely to be a cause of the additional transformation necessary to bring the multidimensional temporal information into a lower dimensional feature space. Since the previous conclusions however suggested an advantage of the discrete features, it is recommended to implement the presented style assessment system for use under discrete features in future. Here, the SVM classifier can be used on equal terms with the DTW classifier, without loss of important information or eventually even better performance.

So far, I only used defined parameters for both classifiers. Although the SVM got trained as inner CV cycle within the nested CV, the main kernel setting remained the same – namely the Gaussian RBF kernel. Given all previous data analysis, it is likely that the present classification problems does not have a simple hyperplane as a useful separating criterion. In this case, other kernel might be better suited, such as a polynomial kernel or the sigmoid kernel. Similar presumptions can be made for the DTW classifier. Here, only standard step sizes ([0,1], [1,0] and [1,1]) were allowed, and the cost was determined using the Euclidean  $L^2$  norm. Different step sizes and cost measures might therefore yield to different (and eventually better) classification results. Consequently, much more possibility and freedom is left for system implementation, and an absolutely accurate and reliable style assessment might be obtained in future under different basic system properties.

Another way to improve error recognition might be to use a different classification model that is specialized in the classification of time-varying processes, such as a Hidden Markov Model (HMM). Research on activity recognition in surfing showed for instance that classifications of a common HMM classifier reached 8% better accuracies than the same classifications under a SVM classifier [HMS16]. For future system implementation, those result should be verified and eventually included in the final framework to ensure the utilization of the most accurate

algorithm available.

To summarize, results are promising that meaningful machine knowledge can be trained as basic input for the assessment of new incoming motion data in a mobile motion information system. Data can either be classified with respect to certain style errors, or with respect to the overall style performance under categories as good, poor or average. With a larger training data base, it might also be possible to obtain a finer graduation of the overall performance, or an estimate of the achieved style score of a performance. Besides, such extended data base could also enable the numeric determination of error gravity from an SVM regression analysis. Current results are promising that such distance evaluation can be learned, once more significant samples are available. In this case, the resulting system could then serve as quality indicator for training or for score ranking in competitions.

All in all, I consider the system a useful application for training and competition. Especially in amateur and junior ski jumping (where less technology-support is available and motion performances cannot be constantly supervised), the presented error recognition system constitutes an important contribution to the training and competition environment. Here, motion errors usually have a higher impact on correct motion technique and hence a jumper's safety due to a lack of experience and proficiency. Besides, motion errors can be expected to be more intense and herewith easier to discover by the learned machine motion knowledge. Although the classification results are not perfectly accurate for all style criteria or performance quality criteria, I believe the proposed system as very important for the development of mobile judging tools in future. As discussed before, no similar system design using real field data has ever been published before. The present analysis therefore represents the first investigation of this kind, and provides much new information as well as guidelines for development and implementation of the current and new system methods.

### 9.4.1 Outlook: Rating Further Sports

Judging bias in ski jumping is considered to be much smaller than judging bias in figure skating<sup>1</sup>. In fact, it is even discussed that ski jump style points are rather a protective measure for the athlete (to prevent any dangerous flight styles) than a measure for the evaluation of performance quality. Consequently, the developed rating system might also be better suited for different subjective, judged sports.

The general design of the processing framework allows for its quick adaptation to any kind of motion data. Body model based variations of the continuous motion features were listed in Section 9.1 under the example of figure skating. For the initial system re-implementation however, I recommend to use a different target sport which is spatially and temporally more restricted. Ideally, this sport is also subject to less aesthetic motion features than figure

---

<sup>1</sup>Information on this issue can be found here: <https://www.washingtonpost.com/news/monkey-cage/wp/2014/02/12/how-ski-jumping-gets-olympic-judging-right-and-figure-skating-gets-it-wrong/>

skating. Possible applications would be trampolining, water diving or any other gymnastic-related motion form. Another sample sport would be boxing, which just recently suffered from a big judging scandal during the Olympic Games in Rio de Janeiro<sup>2</sup>. Here, modifications of the grading system started a big controversy on the fairness in judging in boxing, which eventually even led to the suspension of all judges that were officiating during the Games in early October<sup>3</sup>.

For all of the above motion forms, I am confident that my proposed system would yield precise and applicable results with even higher accuracy than the ski jumping error classifications. While the differences within body posture and motion are very small in a ski jump, they are much larger in sports with gymnastic elements (e.g. in somersaults, spins and any other form of twists). Consequently, differences between performances and their respective error-free and erroneous motion data should also be larger, and herewith easier to display and retrieve. For boxing on the other hand, I believe that a wearable measurement and retrieval system should be particularly efficient since punches are the primary motion events. These should be relatively easy to discriminate and detect with respect to both frequency and power via discrete motion features built from both the raw and processed measurement data.

However, this characteristic of boxing brings me directly to the essence of the problem that is underlying all of its current fairness discussions: its so called '10-point must' grading system, which was employed during the Rio Games for the the first time in Olympic boxing history. In contrast to previous judging systems, this system offers a wider catalog of quality indicators for the scoring of a boxer's performance in a bout. Apart from the number and strength of quality blows landed on the opponent's target area, it is now also possible to evaluate domination by technical and tactical superiority, competitiveness and infringement of the rules<sup>4</sup>. These criteria all require subjective rating, and can hence be assumed to open the door to manipulation.

This evolution of boxing rating clearly opposes the most recent efforts of traditional judged sports that alter their grading system to include objective measures in the final score. Besides, this problem makes obvious that it is much easier to rate and evaluate a performance under technical motion features than under aesthetic ones. For this reason, also mainly technical motion parameters were used in this thesis. In near future, the current system should therefore definitely be extended and also include delicate, subjective performance parameters that make a sport prone to controversies on fraud and judging bias.

---

<sup>2</sup>A full article on this issue can be found here: <https://www.theguardian.com/sport/2016/aug/01/rio-2016-olympics-boxing-corruption-allegations>

<sup>3</sup>A full article on this issue can be found here: <https://www.washingtonpost.com/news/early-lead/wp/2016/10/06/every-boxing-referee-and-judge-from-the-rio-olympics-has-been-suspended/>

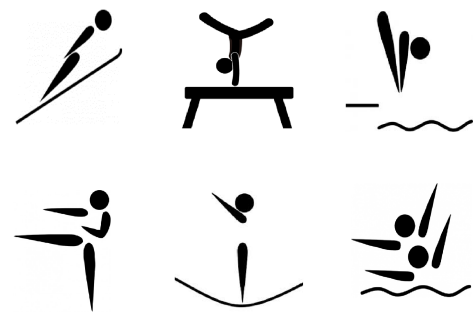
<sup>4</sup>Read more about the scoring rules here: <http://www.nbcolympics.com/news/boxing-101-rules-scoring>





# The Future of Training and Competitions

## Part IV





## 10 Information Provision

From the consumer and user perspective, the most important part of an augmented motion information system is the provision of the retrieved information to enhance motion understanding. The processed inertial sensor data can be used for the provision of motion information from several stages of the implemented system framework. So, it is for example already possible to provide a first, visual impression on a motion performance with the augmented kinematic motion information (Chapter 5). In the same way, information can be displayed after the augmented motion data has been transformed into meaningful feature representations (Chapter 7), or after the specific, relevant information has been automatically recognized and retrieved from the larger, general set of motion data (Chapter 9). One can see that the level of detail varies with the stage of data processing: whereas a data visualization is very general and motion information has to be understood intuitively, the latter information retrieval can be very directed and targeted. With respect to a future application in motion information systems, especially the latter is interesting.

As mentioned before, motion information can be processed both internally by multimodal integration in the human brain (as for the movement sonification) and by means of external modalities (as for the style error evaluation). Under the sport informatics based definition presented in this thesis, it can furthermore take on many different ways for the diverse group of users. In the following, a number of possible applications are given. For coarse organization, the applications shall be discussed with respect to their final utilization for different user groups, namely athlete (motion feedback) and judges (style knowledge) here.

### 10.1 Athlete Feedback

Motion feedback for athletes is the most common and conventional use case and subject to many investigations in sport scientific research. Here, the focus is usually put on the enhancement of motor skill acquisition and motor learning. In a technology-supported motor training environment, especially the development of automated, unsupervised training systems that provide additional motion information is important [KMH<sup>+</sup>13]. Implementing techniques that provide motion information on an easy-to-use basis which could not be obtained otherwise, the idea is to improve motor understanding, accelerate correct motor skill acquisition and eventually increase safety – or gain advantage in competition.

In compliance with the previously developed methods and the two chosen information types auditory feedback and performance ratings, I will illustrate four possible athlete feedback applications here.

### 10.1.1 Outlook: Auditory Feedback in Sports

Movement sonification has not only been proven to be useful for motor skill acquisition in health care and rehabilitation, but also for sport applications [DB15, SMBE09, EFW11, CHU14]. However, such auditory feedback systems are usually applied and evaluated in either a laboratory, or under environmentally restricted settings. This is because in competitive sports, it is difficult to set up a sonification system of several inertial sensors without influencing the motion performance, or at least detracting the athlete's attention. Especially in a fine motor skill and dangerous sports like ski jumping, athletes are very sensitive to any changes in their accustomed environment. With the reduced size and wireless waterproof design, the Logical Product sensors are auspicious to a future use in real-time movement sonification for sports training, given a wireless data transmission with immediate auditory display of the motion. The simplest method here would be to send the processed real-time sound feedback to the sensor-equipped athlete via wireless head phones, or to use a customized application in a smart phone device.

In the following, I want to give two ideas for future sonification applications, one for the present primary motion data ski jumping and one for the improvement of motor stability in long-distance result-oriented sports (Figure 10.1). In difference to the sound setting chosen for rehabilitation (Section 8.1), which were designed under general assumptions, they are developed under sport-specific aspects and in consideration of their target application. Consequently, their auditory information content is focused and directed to the immediate internal retrieval of specific core motion aspects.

#### Sonification of Ski Jumping

One of the key aspects in the execution of a ski jump is the take-off, since it decisively affects the flight curve and the overall jumping distance. Approaching the end of the in-run slope with a speed of  $\approx 25 \frac{m}{s}$ , the optimal time instant within a take-off should happen is of very short duration. Early or late take-off initiation can already reduce jump length by 5 meters or more. Furthermore, research showed that the posture during in-run drastically influences aerodynamic forces that can result in decreased take-off time or loss of take-off impulse [VKK01].

Providing additional information during the in-run phase consequently might be useful to support the athlete in the execution of an ideal take-off. Here, two sonification strategies for display of motion-specific information are probable: kinematic sound features related to

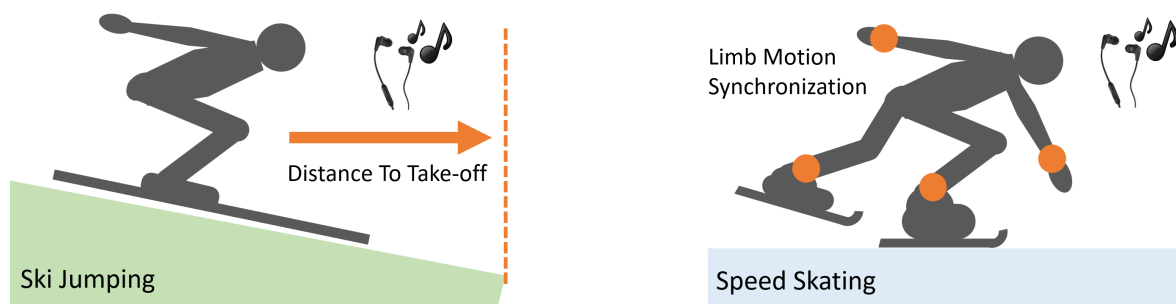


Figure 10.1: Probable sonification scenarios for the support of motor skill and motor performance in sports.

body posture on the one hand, and global sound features representing the distance to the take-off table and end of the in-run slope on the other hand. Knowing the velocity of the athlete-ski system and the in-run length, distal information could for example be provided by the increase or decrease of a permanent sound linear to the approach of the take-off table. Another idea would be to increase the attack frequency of a continuously generated tone as it is often employed in proximity sensors used for parking of automobiles.

The development of such sonification feedback system however is a very sensitive task requiring several assessment steps in wind-tunnel or other simulations before an in-field use. In particular, it is important to ensure that any negative impact on the take-off execution can be excluded: distracting the athlete from the main motion task by any sort of sonification could lead to mistakes in the motion execution resulting in problems during flight and severe injuries. Consequently, it is not planned to implement and realize such system in near future.

### Sonification for Motion Synchronization and Consistency

Another, more feasible sonification scenario is the support of motor synchronization and consistency in training of long-distance speed skating. Here, the idea is to sonify the main properties of the distal part of all extremities and hence rhythmify the overall skating performance: under the demonstrated pattern based action discrimination, it can be assumed that the brain can intuitively perceive differences and changes in the sound pattern during long-term skating. In other words, deceleration and asymmetries of the general motion pattern occurring over the course of a race or training run as a cause of fatigue could be made perceptible. As a result, it might be easier for the athlete to intuitively keep the initial rhythm and speed despite exhaustion.

Sonification of speed skating motion for training has been reported before [SOW11]. To date however, only force data of the skating shoe were transformed into auditory motion feedback. With the developed measurement framework capable to determine full-body kinematics from wearable devices, more sophisticated motion information can now be made available to the athlete. Wrist and ankle joints should be ideal to sonify the primary motion pattern of

continuously swinging arms and legs (either full body in the straight parts, or half-body in the curves). For synchronization of two or more extremities and the maintenance of speed, the two kinematic parameters velocity and distance to the body center (meaning the radius of spherical coordinates) should be sufficient to display all necessary information. One possible setting would be to encode velocity by any kind of spectral modulation (e.g. brightness) and the radial distance by volume. By this mapping, both the counter movement of the weaving left and right body limbs as well as a probable decrease in speed are represented in an intuitive way. Whereas the positional parameters would be encoded in the same way for all four extremities, every joint would be furthermore represented by its own, clearly distinguishable sound timbre. These different sound sources ensure that motion information of all extremities can be perceived simultaneously and then be discriminated by the athlete. The continuity in sound mapping on the other hand keeps the dimensionality of the sound mapping small, so that the implicit motion information is understood immediately.

Furthermore, possibilities for coaches to influence and control training could be increased by providing reference speed audio patterns to be reached and maintained by the athlete throughout a training session. Together with sending the athlete's real-time sonification, it could then for example be possible to send an additional sound stream for the target speed. If possible, the previously described setting shall be implemented and tested in the near future.

### 10.1.2 Motion and Style Feedback in Ski Jumping

Based on the large data base  $\mathcal{D}_R$  and the variety of implemented signal processing and machine learning methods, several motion feedback platforms of various level of detail are possible for athlete support in ski jumping. Of particular interest here is to assess relevant biomechanical parameters to retrieve information on motor style (defined by the criteria in Table 3.1) and performance quality. In contrast to the provision of auditory feedback, such motion and style feedback is acquired by the user in a self-controlled way. This means that the feedback parameters timing, distribution, frequency and content (Figure 2.3) are left subject to the individual decision of a user. While this might contradict insights from sport sciences, it correlates to the definition of motion information created for this thesis (Chapter 2) and the conditions of modern, connected times.

#### Data Visualization

The simplest motion feedback are data plots on the augmented motion data described in Section 7.1. Combining the data plot information with the animated stick figure visualization, it is possible to create multi-view displays that enhance the understanding of the temporal evolution of a motion. I want to give a small example here, visualizing the positional data of the lower spine for the complete flight in x-,y- and z- direction relative to the start of the kinematic chain at the spine top at the lower neck (Figure 10.2). Similar kinematic time-series

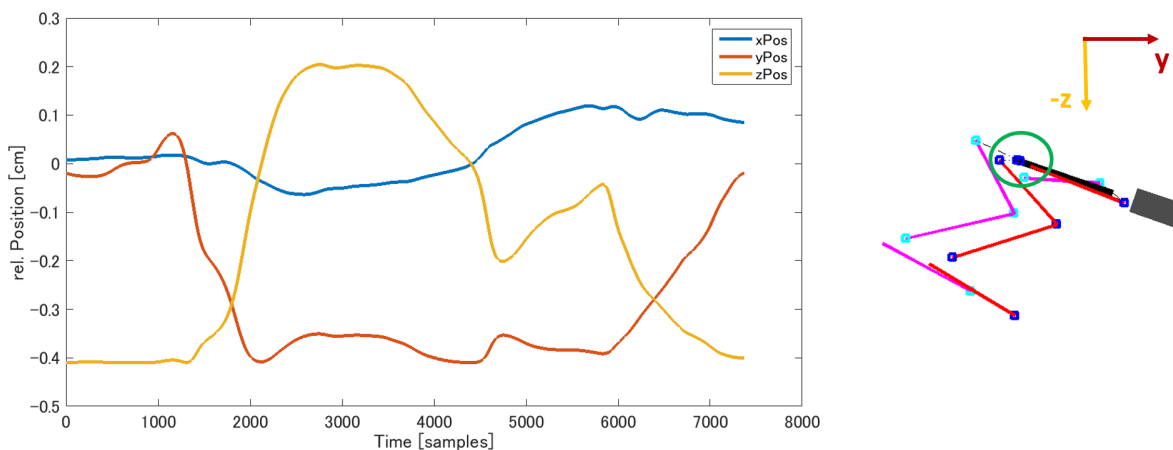


Figure 10.2: Visual feedback plot providing positional motion information, as for example on the relative end position of the spine during a ski jump. Additional video figure visualization enhances motion understanding.

data are available for multiple jump and athletes in  $\mathcal{D}_R$ . Amongst others, they can for example be compared to each other with respect to positions, pitching angle in the upper body during flight phases and landing and many more in a next step. In general, motion information presented to the athlete by visualization is likely to be based on technical motion features.

Especially the latter animated data plot is likely to be useful for future training and feedback systems: the human brain is able to intuitively understand motion patterns from even abstract data representations like point clouds and stick figures. This process is called biological motion perception [Joh73, TRS02]. In other words, such simple and sparse data visualization in form of an animated figure video plot can already be enough to provide first information and impression to athletes (and coaches). Adding visual time-synchronized information to the data plot (e.g. via a time mark running along the data plot), the comprehensibility of the data plots could be facilitated even more and motion information be made more accessible and intuitive even for users of less experience or expert knowledge.

### Automated Intelligent Style Training

Using the learned motion knowledge on jump style and errors, a wearable, automated framework for detailed assessment and training of motor style can be created. For ski jumping, I consider such a mobile feedback platform as particularly beneficial for junior and intermediate level athletes. Here, economic and logistic constraints influence the quality of the general training structures: for example it is common that many jumps are executed within a very short span of time. Consequently, responsible coaches often observe jumps from one perspective only (generally the coaches' stand), while the assessment of every single jump performance has to be instantaneous. Internal motor representations in intermediate level jumpers on the other hand are less stable than in professional athletes, making additional



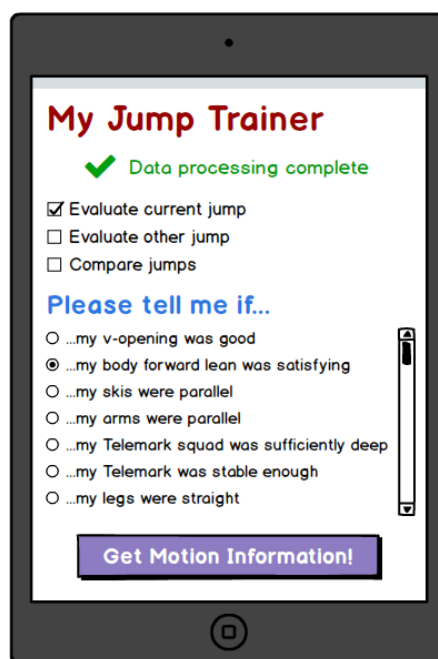


Figure 10.3: Example of a graphical user interface for the provision of directed motion feedback for ski jumping athletes.

information on previous motion performances very valuable. For good usability of such style training system, a graphical user interface should be programmed that can communicate with the athlete to give directed feedback on the motion (Figure 10.3).

To make best use of the previously implemented machine learning framework, the design of the athlete-system communication should be as follows. First, incoming sensor data of a current motion performance is received, processed and classified under the judging style criteria. Once the basic system computation is done, the athlete can ask for specific information on motion parts or motion properties by sending retrieval requests. Next, the respective information will be retrieved and delivered to the user.

Here, it is important to note that search criteria and keywords for communication with the training system were held general and intuitive by predefined search queries. Internally, those search queries were associated to one of the nine style criteria for information retrieval. A possible query in the user front end could for example be whether the arms have been held parallel during flight. In the back end this information would be labeled under the criteria  $A3$ , and the respective error recognition result for  $A3$  could therefore be used to display an either positive (in case of  $JN$ ) or negative (in case of  $JF$ ) output information (Figure 10.4).

From the validation of the underlying machine learning methods, one can conclude that such proposed system will be capable to identify style differences and errors well (Chapter 9). Previous results showed that it is possible to provide and directly deliver motion information by learned machine knowledge. Therefore, I believe that the previous system design is a

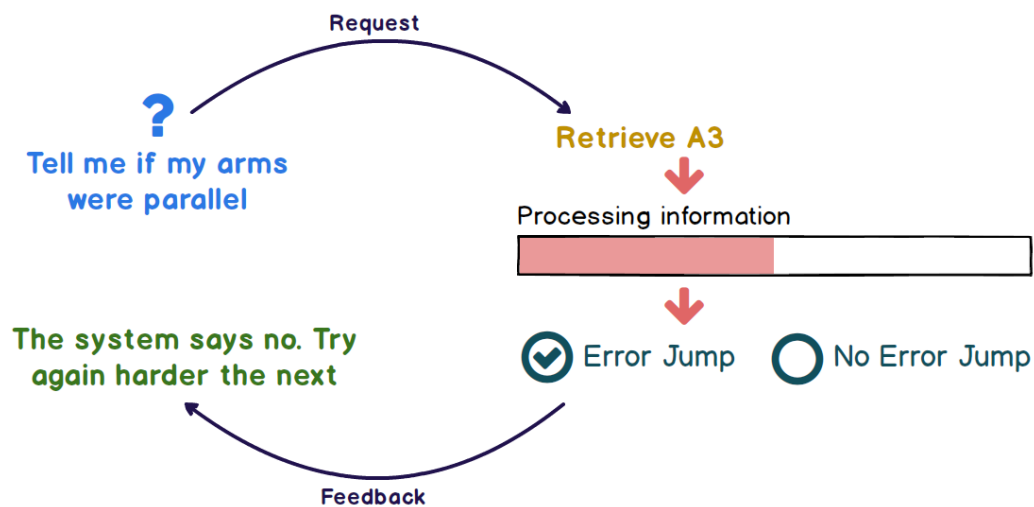


Figure 10.4: Principal front and back end processes establishing a dialog between athlete and motion style training application.

very promising and powerful approach to the question of future motor training systems. To enable a more specific training system for individual athletes, it might furthermore be reasonable to use different quality measures independent of universal style criteria. Alternatively, it is for example also possible to use the full flight performance quality assessment (Section 9.3.2) to display general feedback on the complete flight performance. Instead a concrete information on a specific aspect of the motion, the query would then simply be how good the flight performance was, or how good the current flight was in comparison to previous ones. The respective feedback information can simply be retrieved from a respectively trained motion knowledge, as demonstrated under the previous categories P, M and G. In dependence on the available training data, further categories for the classification of performance quality (enabling a finer separation between jumps) might also be feasible for system development. For the latter application, it should generally be useful to build individual motion knowledge for every athlete, so that the progression of motor skill over time could be monitored. However, this would require a large data base of jumps per athlete before a meaningful motion knowledge could be created – something which is difficult to organize in practice. On the other hand, it would also enable the inclusion of numerical parameters known to influence a ski jump performance (e.g. the body forward angle or the ski attack angle) that can otherwise not be respected due to individual differences in the ideal flight style influenced by every athlete's anthropometrics and motor skills. In reverse, the inclusion of motion data from professional, highly skillful athletes could be a very helpful indicator for junior athletes towards the acquisition of higher motor skills. Then for example, the distance and continuous approach or eventually also depart (in case of incorrect motor skill acquisition) to the system's learned G performances could be made understood in an easier and more intuitive way.

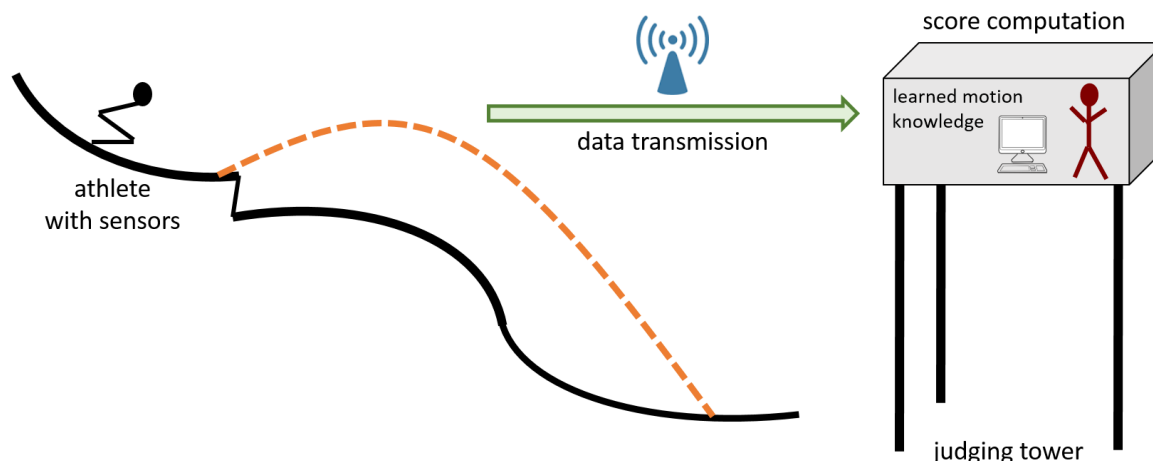


Figure 10.5: Technical implementation of a future online judging system at the ski jump hill.

## 10.2 Judging Knowledge

When developing a system for the provision of motion information to a use group different than athletes (and coaches), one usually follows a clear defined concrete intention that is much more specific than the support of motor skill acquisition. Conventionally, it got inspired by problems and constraints that occurred in daily situations and that require profound and detailed motion understanding. This can take on any possible form, such as the visualization of additional background information and content to the spectator, or precisely the chosen style assessment for judging support and increase of objectivity. As a last step of this work, it shall next be illustrated how such judging system can look like on the base of the previously developed methods.

The general idea for this performance scoring scenario is to implement an executable computer program file that awards point scores to a motion performance on the base of previously learned and stored motion knowledge. Incoming sensor data is transferred to the computer in either offline or – in case that stable data transmission via wireless network connections is enabled – online mode (Figure 10.5). For the former, this data transfer could be executed from a standard file load dialogue. For the latter, data could be sent out by the sensors and fetched on the fly by a receiving computer located in the judge's tower.

Designed and implemented with a common option window and dialog framework, the judging system executable should be intuitive and easy to use for any experienced computer user (Figure 10.6). Then, the computation of all relevant parameters can simply be started as full analysis including (a) the derivation of body kinematics, (b) the computation of error points per style criteria and (c) the determination of the resulting summed output score. Alternatively, it is also possible to execute all steps (a)-(c) independently. In the last step, the resulting rating is then presented to the user respectively judge. Possible motion information

## 10.2. Judging Knowledge

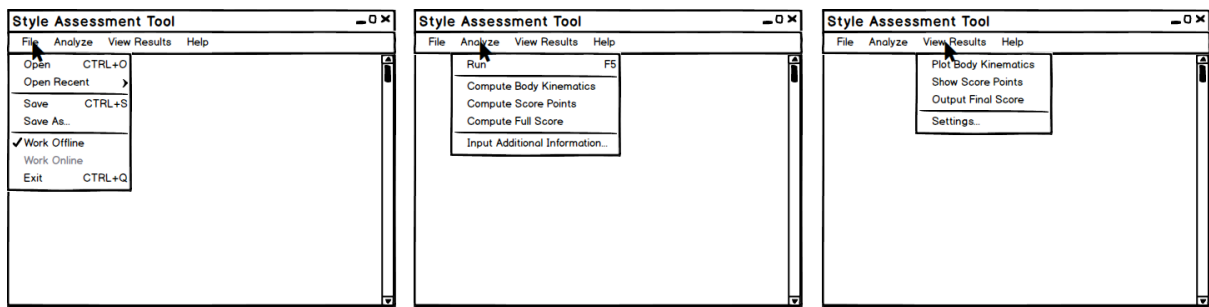


Figure 10.6: Illustration of a program interface and its possible functions for judging in ski jumping.

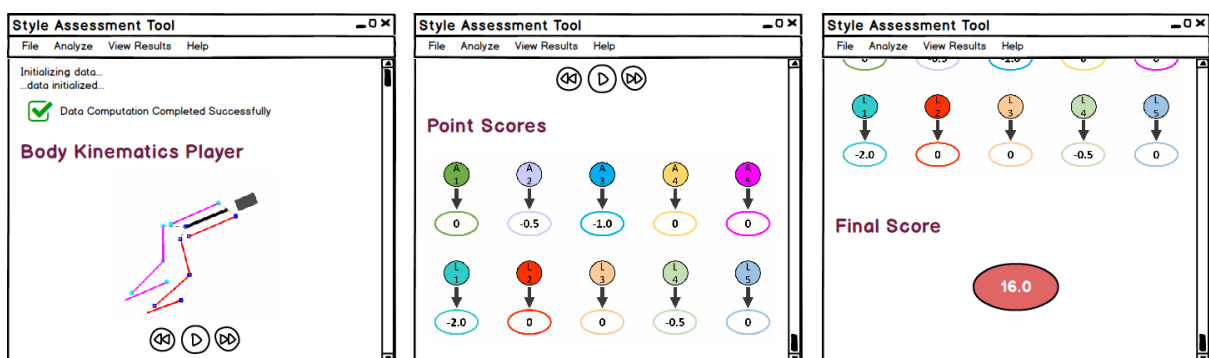


Figure 10.7: Illustration of a sample information output given by the judging program interface.

output are a video of the processed data in animated figures (Section 10.1.2), the error deduction scores per criteria and the resulting score (Figure 10.7). In the example, the point scores are listed under the error recognition approach to be then summed up to the overall point deduction. Under a reliable performance quality assessment with trained knowledge for the full standard point range (e.g. 13.0 to 20.0 points), it is additionally possible to directly retrieve the performance score.

By the provision of the video output, the system aims to improve the general circumstances of conventional judging, where a decision is made within a very short instant of time. Now, a jump can be watched repeatedly under arbitrary playback speed and abstract and uniform visualization parameters that do not distract from the main motion execution. The two score outputs (or one for use of the overall performance quality assessment) furthermore display the quality of the examined motion performance in numbers as result of the internal data processing.

One can see that the judging tool offers considerably less dialog options and possibilities of parameter choice than the previously demonstrated athlete feedback system. This system efficiency is due to the circumstance that the principal function of the system (determination of the final score) is very clear and more formulated more precisely. As a result, the communi-

cation between system and user is less ambiguous and does not require internal translations to increase usability. Furthermore, it is not dependent on self-controlled system use mechanisms. Instead, it is continuously employed for all situations that require a solution to the underlying problem, meaning competitions. Consequently, it is very target-oriented and can be expected to be beneficial without short comings or disadvantages once the reliability and accuracy of its output is confirmed.

### 10.3 Discussion

With the last chapter of this thesis, I have shown how the developed methods for retrieval of augmented motion information can be used to support humans involved in sport motion performances. I think that all presented applications with their implicit hardware and software solutions are promising designs for a future use in real sports, and could be implemented without additional effort as presented here.

For the applications based on artificial motion knowledge, a variety of possibilities for style and performance analysis were made available with this work. Consequently also various system implementations can be imagined, ranging from performance assessments with respect to specific motion aspects to temporal monitoring of overall skill acquisition to the awarding of style points for automatic judging. For all applications, however, one point remains particularly important: the availability of sufficient and variate motion data data for learning of the machine knowledge. It should therefore be emphasized that the first steps of the information provision pipeline – collection of numeric motion data and augmentation of the motion data – are essential and should not be taken easy, since they build the foundation for any subsequent analysis task.

The two biggest issues the proposed platforms have to face under the current state of technology are the provision of real-time information or feedback, as well as the correct handling and attachment of the motion sensors by the athletes required for a future independent system use. Whereas the former can be addressed by the establishment of a wireless data network for data transmission at the ski jump hill (or any other sporting venue), the latter is subject to the user. Consequently, possible sources of error should be held as small as possible. With the ongoing process of hardware enhancement, sensors would ideally be smaller and easier to use in future, such as for example by inclusion within the jump suit. I am convinced that as soon as those issues are solved, the systems could be implemented to full function. Then, they could even be marketed and brought into market by crowd funding or similar financial concepts.

# 11 Final Words

## 11.1 Summary and Conclusion

In this thesis, I illustrated the development of augmented motion information systems from wearable inertial sensor data for computer-assisted training and motion analysis. In contrast to the common, general expression of motion feedback in sport sciences, I designed and implemented my work under a broader, technological perspective. In concrete, this work comprised the provision of any kind of motion information to a variate group of end-users. This means that a system development is not only restricted to athletes and coaches, but also included judges, spectators or any other person involved in the (public) execution of a motion.

In both sports engineering and computer science, the awareness of the importance of CAT and augmented motion information systems has risen. This also led to a higher interest and effort for technological implementation. To address this research problem, various signal processing and machine learning methods were implemented in this thesis. They transformed the raw and sparse data obtained with inertial sensors into meaningful numeric motion representation or intelligent machine motion knowledge. This artificial motion knowledge can be used either additionally or as replacement for the internal, biological motion knowledge of a human and herewith increase the possibilities and objectivity of kinematic motion analysis. To summarize all algorithms and set them into relation to real world problems, I furthermore discussed how to employ the newly determined motion information in concrete applications to provide the desired system output to the user.

With the evolution of this thesis, I step-wise explained all stages that a general augmented motion information system has to pass through before the provision of a final data output (Figure 11.1). Those are (1) collection of numeric motion data, (2) augmentation of the numeric motion data, (3) sense-making of the augmented motion data and (4) retrieval of relevant motion information. Every step was illustrated in detail by the inertial capture data collected for this thesis and the chosen sample applications.

The main part of this work was developed using an extensive motion capture data base of ski jumping. As concrete application examples for the development of a functional motion information system, I presented two very different type of information: the provision of auditive feedback to athletes or patients in rehabilitation for support and acceleration of

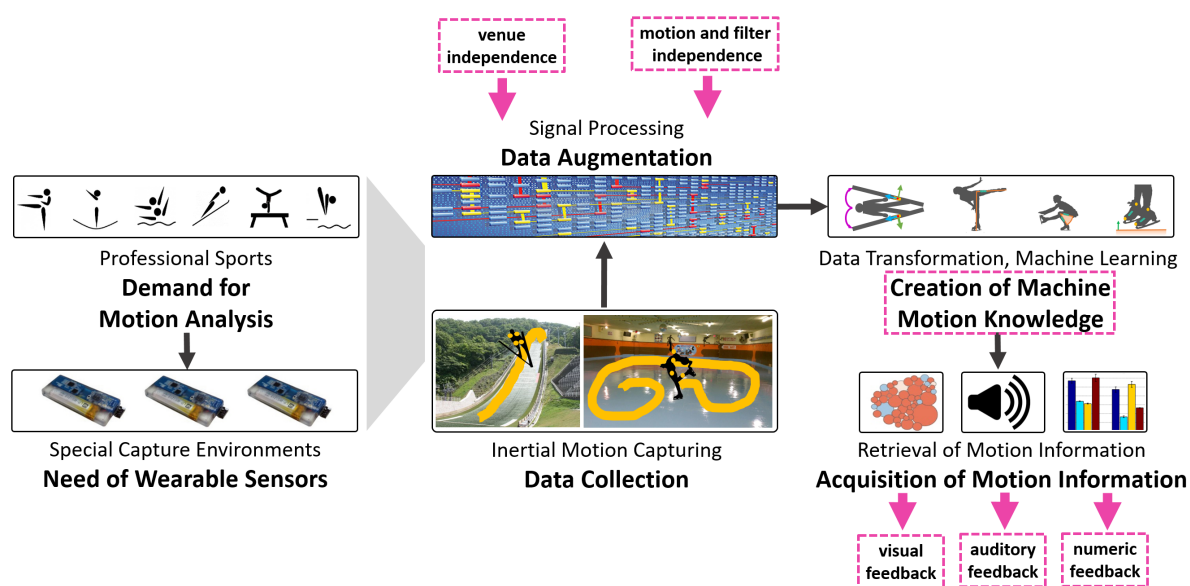


Figure 11.1: Recapitulation of the general design of the computer-based motion information system introduced in this thesis with the most important developments for system input and output highlighted in pink.

motor skill acquisition, and the provision of a style assessment and performance rating to (ski jump) judges for an increase of objectivity in scoring systems (Figure 11.3). I believe both of them to become very important applications in future augmented training scenarios and in the world of competitive and professional sports.

While correct and diligent work is important in all phases to generate a reliable and meaningful system output, the following points are particularly important for a general design of an augmented motion information system. They have been extensively examined and discussed with this work:

- The augmented numeric motion data has to be accurate and reliable, whereas sensor data is often imposed by hardware induced noise and bias. To increase the accuracy of a given data set, it might therefore be necessary to adapt the fundamental methods to the characteristics of a given task.
- Usability is very important for the future utilization of an augmented motion information system in sports: adaptation of the system methods for enhancement of the data accuracy for example might either require expert knowledge of the user, or the availability of further methodologies and strategies that can flexibly react to the system circumstances without specific user knowledge. In this work, I particularly engaged myself in the latter and developed two methods that can contribute to the enhancement of user-independent usability in future. One is a motion categorization system that

annotates the drift potential of certain motion patterns and that can amongst other be included in the estimation of sensor orientation in form of a two-step filter. The other one is a magnetic bias compensation that reduces random disturbances of the magnetic field data, and hence makes the inertial sensor data and their orientation estimates more reliable and robust towards local properties. As a result, it is not necessary to change computation settings within orientation estimation filters to tweak the resulting output estimates. Furthermore, the sensors can be employed more freely within any kind of sporting venues, such as ski jumping hills or snowboard half pipes, without the need to perform complicated field measurements for the calibration of the magnetic sensors.

- To make good use of the augmented motion data, it is necessary to define semantically and numerically meaningful feature transformations. Data analysis showed that those features might differ from one's own semantic ideas that are put into the system development. Consequently, the underlying motion data should also be investigated and verified with respect to their numerical data representation. In this respect and when suitable feature transformations are not known, it can help to investigate a large set of features under methods of unsupervised feature selection. Furthermore, it is generally recommendable to use features that can be universally applied and do not change their information content under different motion styles or varying spatial conditions.
- Auditory feedback is known to be effective for the support of motor skill acquisition. Experimental studies additionally showed that artificial movement acoustics based on kinematic movement parameters can be decoded by naive listeners. Especially the (dis)similarity of action structures was relevant for discrimination of different motion patterns: the human brain allows for auditory pattern based action discrimination and perceptual learning similar to visual biological motion perception. Acoustic kinematic features can therefore be both based on permanent, continuous sound information and directed auditory cues.
- Whereas auditive feedback is relying on internal motion knowledge built up by the user over years of experience, the assessment of style and error is bound to the existence of a newly learned intelligent machine knowledge. Ideally, this motion knowledge should be of similar power than biological human motion knowledge and imitate neural structures while being insensitive to bias and misperception. Using data annotations based on the official guidelines of a sport, it is possible to create intelligent machine knowledge that can retrieve motion information from an incoming data stream of augmented and transformed motion features. In this information retrieval and provision step, a fundamental ground truth is required that can be generated from (averaged, robust) human assessment if no other data is available.
- When using the style assessment of human judges as a ground truth data for the learning of artificial motion knowledge, one should be aware that the ground truth measure



is subject to bias. Therefore, outliers that influence the outcome of the overall classification accuracy can be present in the data. Ideally, judging based ground truth data is therefore made robust by averaging the point scores awarded by multiple independent judges.

- Assessing the quality and style of a motion performance is subject to different aspects of a motion. In most cases, those aspects can be assigned to one of two fundamental categories. Technical motion features that designate the biomechanical description of a motion execution can generally be measured quantitatively and are commonly known from kinesiology. Artistic motion features on the other hand are all those parts of a motion that influence the impression of beauty and motor skill and that cannot be quantified since they are subjective and perceived differently by every person. They are also those determinants of a performance score that are more difficult to retrieve and learn with neural network methodologies.
- For ski jumping, discrete motion features based on descriptive statistics (e.g. data mean, standard deviation, skewness and kurtosis) are more significant than time-serial data representations. Classification results indicated that the relevant motion information that describes style errors is defined by fundamental, momentary signal properties. These can be discovered well with basic analysis methods. The same is likely to hold for other sports, as well: whereas recognition of different motion patterns is more effective with time-serial features, error recognition might be better suited for the retrieval of errors.
- Besides error assessment, intelligent motion knowledge can be used for the provision of motion information in various different tasks (e.g. motion analysis). The methods developed and presented in this work can be modified for many similar applications, making use of either the internal biological motion knowledge, the newly learned artificial motion knowledge or both. The content of the desired motion information generally varies in dependence on the target user and his or her main field of interest for analysis. Commonly, all applications are used in a self-controlled way, meaning that the provision of feedback is regulated by the needs of the user himself.

Lastly want to recapitulate the innovations of this thesis (Figure 11.2), as well as the contributions to the existing state of art in research. They are the ...

**...full-body motion capturing of ski jumping motions and the determination of the relevant body kinematics**, which led to the currently most extensive inertial ski jump data base worldwide,

**...development of methods to enhance the usability of body kinematic estimators for the diverse group of future system users** represented by an intelligent drift compensation using elementary a-priori motion annotations for flexible use of orientation estimation filter with

## 11.1. Summary and Conclusion

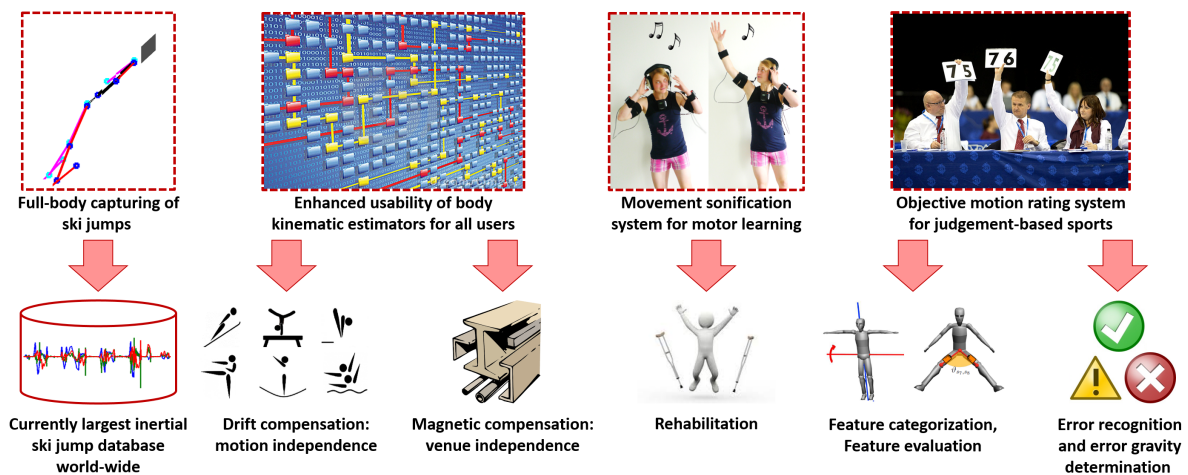


Figure 11.2: Recapitulation of the main innovations presented in this thesis.

sport motions and a magnetic compensation step for determination of body kinematics from data captured at variate sporting venues,

**...development and testing of real-time movement sonification system** for motor learning in rehabilitation,

**...development of the system environment and methods for a kinematic feature based motion rating system in subjective judging-based sports** including a motion feature categorization for motion rating scenarios, the testing of feature representations for motion rating by feature selection strategies and algorithms for error recognition and error assessment used for activity recognition in real sport motions with error gravity determination.

To summarize, one can see that this work addresses many different research problem, as well as scientific fields of research, including engineering (sensor hardware and data processing), mathematics (attitude data representations), computer science (machine learning, data visualization) and sport sciences (motor learning and multimodal integration of motor feedback). I believe that the combination of methods and strategies connecting the various fields of technology with each other and with the field of sport science is unique. While the basic methods used in this thesis are well-known in computer science, they have never been used on real sport motion data before: usually, machine learning methods are applied to recognize and evaluate constrained motion patterns defined by daily life situations and simulated in a laboratory setting for the implementation of the respective methods. Here, on the other hand, I used sport motions collected in their natural environments. Athletes were not asked to perform motions in a certain specific way to collect meaningful motion data. Instead, performances were used as is and learning methods had to be adapted to the obtained real data. In this regard, also various ways of problem solving were discovered and examined in this thesis. As far as it is known, no other work has been presented in a similar

## **Chapter 11. Final Words**

---

form anywhere else – approaches to augmented motion feedback provision from sports engineering or sport science research generally handle real motion data, but concentrated on certain selected body parts, low level features, neural networks from wavelet and frequency filters or pure analysis tasks only so far. Consequently, this thesis represents a valuable source of information for the development and implementation of future augmented motion information and feedback applications.

## 11.1. Summary and Conclusion

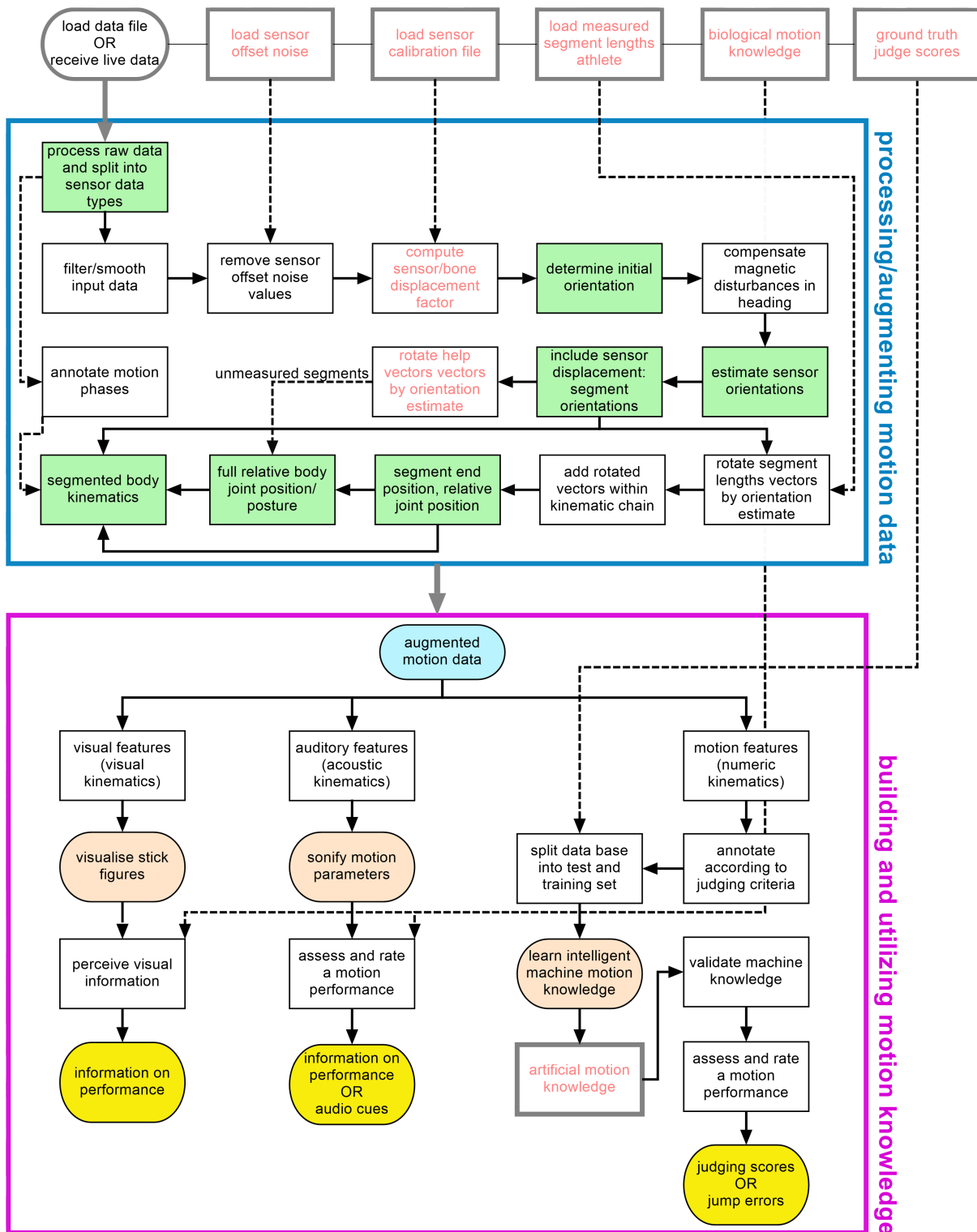


Figure 11.3: Flowchart of the complete, developed motion information system with processing methods and its final feedback output possibilities.

### 11.2 Outlook and Future Work

I believe that with the presented basic, elementary guidelines on the creation of computer-based motion information systems in the sports environment and the presented methods and technologies for data processing and machine learning, this work can serve as a handbook for future motion analysis tools. With the implementation and modification of conventional computer science method for use in real sport motion data, a new level of computational methods and data quality was provided that can considerably impact sport scientific research and motion analysis. Contributing to unique ways of motion analysis by the provision of enhanced motion information and wearable sensor based motion information, this work is intended to lead the way towards new applications that support training, performance improvement and talent recruiting in the future.

As the next step in the development of augmented motion information systems for training and motion analysis, the following points could further enhance the power and applicability of the present system. First, the currently existing methods for the determination of kinematic parameters could be extended to use with additional sensor data (e.g. a laser tracking system). Such increase in data input streams is for example reasonable for the FK pose estimation, which is at the moment only expressed in relation to the root joint. In other words, translational motions of the whole athlete-sensor system can currently not be determined. Here, the idea would be to introduce an additional method, so that the motion and displacement of the whole athlete-sensor system can be determined as a complete moving system.

Second, it might be reasonable to test both the DTW and the SVM classifiers under different basic settings, meaning a different kernel for the SVM and different step sizes and cost measures for the DTW. Then, one could evaluate whether the classification results can be improved under different method settings, and the functionality of the presented system design eventually be demonstrated even better. As discussed before, it might furthermore be reasonable to test further classification models, such as cluster methods, or methods that are developed for time-serial data like the HMM.

Third, it could be useful to demonstrate the sample information types in more than one application each. Respective ideas for implementation are presented in this thesis. Especially for movement sonification (that was developed for rehabilitation), it will be reasonable to illustrate the concept of audio clues with sports motion data sets. However, to prove the positive effects of such auditive motion feedback, it would also be necessary to set up empirical studies that can investigate eventual learning effects. This problem on the other hand is subject to (sport) psychological investigations and not in the scope of the presented work. A different case is the motion evaluation application, which can be executed under the established framework without additional investigations. Therefore, I hope that the system can be extended to a complete and universally useful evaluation program for many judged-sports in near future. Ideally, this system implementation can then also assess

performance under both technical and aesthetic aspects. Affected sample sports are certainly broadly available – may it be gymnastics, trampolining, water diving, snowboarding or, as most recently, boxing. In this context, I want to emphasize again that it is much easier to numerically grasp the quality of a motion with regard to technical motion descriptors than with regard to aesthetic impressions of a performance – a problem that also led to the current controversy in box in the first hand. Therefore, the main focus of my current work was put on the creation of methods to rate technical aspects of a motion. The development of methods that can 'translate' the aesthetic motion aspects of an artistic performance into numeric criteria (e.g. in gymnastics or figure skating) constitutes the next step and might be subject to further investigations after my PhD.

I am aware that the presented structural organization of the proposed style assessment system has two specific limitation. For my final conclusion, I want to highlight them another time: one is the bias within the collected judging scores that served as ground truth data, and one is the relatively restricted number of data captures used for testing and training of the intelligent machine knowledge.

As discussed before, a separation between different style criteria (as also the awarding of point deductions for certain style errors) can be subject to individual perception. Ideally, the system should therefore be tested under more objective ground truth data in the following. For sports that have a smaller field of activity than ski jumping (e.g. trampolining), it could theoretically be possible to capture motions with optical capture systems to search for and analyze differences in the data. However, a reference annotation is still required to identify the different style errors. Besides, sport motions are commonly not executed within sufficiently small motion capture volumes – and the results of the ones that can be captured are generally not based on subjective decision-making. Since consequently no other style evaluation except human judging is available, it is recommended to use a larger number of judges that simultaneously award point scores in the next experimentation. All scores could then be averaged to a final ground truth more robust against outliers and individual perception, which should also further increase the retrieval and classification results. Ideally, an even bigger motion data base would be made available at the same time: although the collected motion data base constitutes the largest known inertial full-body kinematic ski jump data base so far, the number of data captures for the creation of artificial motion knowledge could be even larger for future system use. In general machine learning applications, several hundreds or thousands of sample data are used to build the system knowledge.

To make the system fully valid for universal use, it would be furthermore necessary to collect additional data of different jumpers with varying skill levels. This would for example enable the introduction a larger number of categories for performance quality assessment: given the number of available motion data in the present motion data base, it was not reasonable to build more than three performance quality groups (G, M and P). Furthermore, a larger collection of ski jumps could serve to verify (or invalidate) the usefulness and accuracy of

## Chapter 11. Final Words

---

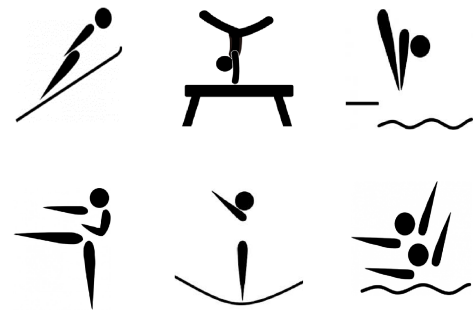
the developed numeric error assessment concept. This was not possible with the present restricted number of input data. Under the scope and financial possibilities of this research, it is however difficult to both plan, organize and generate such a huge data collection. I therefore deem the presented jump collection as sufficient for the implementation and first demonstration of the developed system pipeline.

As a last point, I want to state that the proposed platforms and interfaces for the provision of information involve man-machine interactions. When designing interfaces for technology support of humans, it is conventional to first validate the system in a beta version with a small group of test users. In case a system should be realized for actual training or style assessment, it is therefore reasonable to verify its effect and usability under real conditions in a feasibility study soon. Shortcomings in design and usability can then be discovered and corrected for implementation of the final user system. Before a final system could finally be brought to market, it is furthermore reasonable to collect even more data for the creation of the intelligent motion knowledge. This comprises additional data from both the same athletes and different athletes including female jumpers, as well as several judges to increase the robustness of the ground truth annotations. Under the developed learning concept from style guidelines, it would furthermore be necessary to collect a full range of style errors: with the current main ski jump data set, I could mainly acquire data for the style criteria *A1-L4*, while the number of *L5* errors in the data base turned out to be too small for the machine learning. Outrun errors could not be captured even once. However, this collection of missing data also brings the system to the end of technological possibilities. Additional error categories do not constitute a problem for the underlying system methods, since the new style errors can be handled in the same way as the existing ones. However, they constitute a problem from an ethical side – an athlete cannot be simply asked to intentionally perform a certain error (especially errors like fall) for the creation of sufficient learning data.

All in all, I believe that the innovative character of the machine learning pipeline for motion evaluation is so fundamental that its further development can and will be of great interest for many years to come in machine learning and sport engineering fields. I hope that this work will inspire further research, promoting the implementation and introduction of augmented motion information systems in sports. In particular, I hope that this work will contribute to the establishment of new objective motion assessment measures, employed to support the decision making and performance ranking in actual judging-based sports that are known to be prone to bias and error.

# Appendix

# Part V









## Author Publications

I published the majority of all work presented in this thesis as lead author in either peer-reviewed journal or peer-reviewed conference proceedings.

### Journal Publications:

The thesis includes the recognition of five journal papers referred to by their Roman numerals. The following two papers have been published or are accepted for publication as first author:

- I Brock, H., Ohgi, Y. Intelligent Drift Reduction in Inertial Sensor Orientation Estimates Using Elementary Motion Knowledge. SFC Journal. Vol.16 No.1. 2016. (Peer reviewed).
- II Brock, H., Ohgi, Y. Development of an inertial motion capture system for kinematic analysis of ski jumping. Proceedings of the Institution of Mechanical Engineers, Part P: Journal of Sports Engineering and Technology, 2016. (Peer reviewed). In print

A third paper is currently under review:

- III Brock, H., Ohgi, Y. System and Feature Engineering for Automated Style Error Recognition from Wearable Motion Sensor Data. Information 2016. (Peer reviewed).

Apart from the previous works, I have contributed to the following manuscripts:

- IV Vinken, P.M., Kroeger, D., Fehse, U., Schmitz, G., Brock, H. and Effenberg, A.O. (2013). Auditory Coding of Human Movement Kinematics. Multisensory Research, 26(6), 533 – 552. (Peer reviewed).
- V Helten, T., Brock, H., Müller, M. and Seidel H. (2011). Classification of trampoline jumps using inertial sensors. Sports Engineering, 14(2), 155 – 164. (Peer reviewed).

## Appendix A. Author Publications

---

**Division of work between authors:** Each authors' contribution at different stages of the reported studies is given in the following. Name lists are sorted alphabetically by surname and do not reflect any further weight in contribution.

### *Manuscript I*

This manuscript describes the algorithmic work and experiments done to improve the orientation estimates used for subsequent motion information provision methods. The study was designed and planned by Brock. Data was collected by Brock and analyzed and reported by Brock with advice from Ohgi.

### *Manuscript II*

This manuscript describes the development of a mobile system for the computer-based collection and processing of ski jumping motions free of error or magnetic bias. Brock and Ohgi planned and executed the main data acquisition. Data analysis was performed by Brock with advice from Ohgi, and results reported by Brock.

### *Manuscript III*

This manuscript illustrates the implemented system for assessment of motion style in ski jumping and presents results of its fundamental error classification. Brock and Ohgi planned and executed the data acquisition of the used ski jumping data. Data analysis and feature evaluation was performed by Brock with advice from Ohgi, and results reported by Brock.

### *Manuscript IV*

The study describes the results of an empirical study on the effect of the developed movement sonification system. The study details were planned by Brock, Effenberg, Kröger, Schmitz and Vinken. The sonification system was implemented by Brock, and sound mappings created by Brock, Effenberg, Kröger, Schmitz and Vinken. Data acquisition was executed by Kröger, Schmitz and Vinken. Data was analyzed by Fehse, Schmitz and Vinken and reported by Vinken under advice from Effenberg and Schmitz.

### *Manuscript V*

The manuscript is based on previous research on motion classification. The study details were planned by Brock, Helten and Müller. Data was collected by Brock and Helten. Brock and Helten analyzed the data with supervision from Müller and Seidel. Helten reported the results under advise of Müller and Seidel.

---

## Conference Publications

I have given five oral and one poster presentation at the following conferences:

- Brock, H., Schmitz, G., Baumann, J. and Effenberg, A.O. If motion sounds: Movement sonification based on inertial motion data. 9th Conference of the International Sports Engineering Association (ISEA), Boston, USA, 2012. (Peer reviewed).
- Brock, H., Ohgi Y. Evaluating Orientation Estimation Methods from Inertial Sensor Data for Sports Motion Analysis. International Association of Computer Science in Sports, IACSS Conference 2014, Darwin, NT, Australia, 2014.
- Brock, H., Ohgi Y. Estimating kinematics in ski jumping using inertial sensors. International Society of Skiing Safety, ISSS Congress 2015, San Vito, Italy, 2015.
- Brock, H., Ohgi Y. Towards Better Measurability - IMU-Based Feature Extractors For Motion Performance Evaluation. 10th International Symposium on Computer Science in Sport (ISCSS), Loughborough, UK, (2015). (Peer reviewed).
- Brock, H., Ohgi Y. Development of an automated motion evaluation system from wearable sensor devices for ski jumping. 11th International Conference on Sports Engineering (ISEA), Delft, Netherlands, July, 2016. (Peer reviewed).
- Brock, H., Ohgi Y. A Visual Feedback System for Full-Body Motion Analysis from Inertial Sensor Data. ASTN-Q Conference, Brisbane, Australia, August, 2016. (Peer reviewed).

I furthermore expect to present my work at one more conference this autumn:

- Brock, H., Ohgi Y. An Intelligent System for Motor Style Assessment and Training from Inertial Sensor Data in Intermediate Level Ski Jumping. 4th International Congress on Sport Sciences Research and Technology Support, icSports 2016. Porto, Portugal, November, 2016. (Peer reviewed).

## Awards

At the 11th International Conference on Sports Engineering (ISEA), Delft, Netherlands, I was awarded the Adidas Best Student Paper Award for my work on the automatic style assessment of ski jumping motion<sup>1</sup>).

---

<sup>1</sup>Image courtesy (pictures next page): Institute of Sports Engineering, Delft Technical University

# CERTIFICATE

THE JURY OF THE 2016 ISEA CONFERENCE  
THE ENGINEERING OF SPORT<sup>11</sup>  
HELD IN DELFT, THE NETHERLANDS

HAVE DECIDED TO GRANT THE

**ADIDAS BEST STUDENT PAPER AWARD**

TO

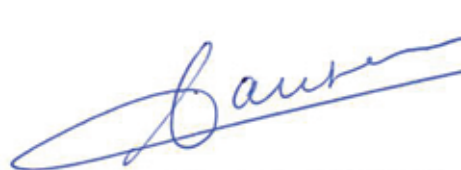
*Heike Brock, Yuji Ohgi  
and Kazuya Seo*

DEVELOPMENT OF AN AUTOMATED MOTION  
EVALUATION SYSTEM FROM WEARABLE  
SENSOR DEVICES FOR SKI JUMPING

ON BEHALF OF THE INTERNATIONAL JURY



PROF. DR. F.C.T. VAN DER HELM  
CONFERENCE CHAIR



DR. A.J. JANSEN  
PROGRAMME CHAIR



DR. A. SCHWAB  
CHAIRMAN AWARD COMMITTEE







## B System Promotion

In the following, I give information on all activities made in the course of my research work to promote the developed technology and systems outside of academic conferences and societies.

### Sonification System:

In summer 2011, the real-time movement sonification system has been presented at the German science fair 'Ideen Expo' in Hanover, Lower Saxony (Figure B.1<sup>1</sup>). The 'Ideen Expo' is a biannual educative fair for children and young adults established to present innovative systems and applications for the promotion of science and technology and the recruitment of new talent. It is held at the Hanover fair, venue of the 2000 World Exposition, and attracted more than 310.000 visitors in 2011.



Figure B.1: Presentation of the real-time sonification system at the 'Ideen Expo' science fair.

Besides, I have programmed a homepage for the movement sciences working group at Leibniz University, Hanover, to present the latest research outcomes on the provision of auditory feedback to the public in a suitable form (Figure B.2)<sup>2</sup>. The homepage was developed using WordPress [Wor], which offers high usability with a intuitive back end administration tool. The style of the homepage was then adapted on an individual basis using CSS-style sheets (e.g. background color, image slider and fontsize). It conformed to the most recent principles of fundamental internet security available in 2011.

<sup>1</sup>Image courtesy: Institute of Sport Science, Leibniz University Hanover

<sup>2</sup><http://sonification-online.com/en/>, Accessed 2016-10-06



## Appendix B. System Promotion

Home

Science in motion research group

Leibniz Universität Hannover

Home | News | Research | Members | Cooperations | Publications | Concluded Research | Media | Conference 2013

News

1

News  
current information  
about us and our research  
can be found here

2 3 4 5 6 7

Errorless Learning  
socSMCs  
SyncRow  
SoundSoccer  
Multisensorics  
Movement sonification

### Sonification Online

Motion, Sound and Multisensorics.

**Welcome to Sonification Online!**

**We are an interdisciplinary research group on multisensorics, motor cognition and motor control.**

**We hope you enjoy finding out more about our research.**

---

**More information**  
Alfred O. Effenberg  
Tel.: +49 (511) 762-5510  
Fax: +49 (511) 762-2196

**General Contact**  
mail@sonification-online.com  
Impressum

**Language**  
> Deutsch  
> English

Leibniz Universität Hannover - Institut für Sportwissenschaft. Am Moritzwinkel 6, 30167 Hannover.

Figure B.2: Screen shot of the homepage developed for the movement sciences group at the Leibniz University Hanover for promotion of auditory feedback system research.

## Ski Jump Measurement and Evaluation System:

I consider my research as unique and inspiring for similar system implementations in future. Therefore, I strove to present the work to a broader audience and larger platforms outside the field of sports engineering, such as for example the 'Wissenschaftlicher Gesprächskreis' (Scientific Discussion Group) of the German Academic Exchange Service (DAAD) and various research institutes all over the world (Table B.1).

Table B.1: Summary of all lectures and talks given during the PhD.

Date	Location	Description
2014/06/04	Tokyo, Japan	<i>Invited talk.</i> 'Wissenschaftlicher Gesprächskreis' (Scientific Discussion Group), DAAD <b>Title:</b> Menschliche Bewegung messen und verstehen - wie der Computer zum Sportzuschauer wird (German)
2016/07/07	Stuttgart, Germany	<i>Invited lecture.</i> University of Stuttgart. Faculty of Computer Science, Electrical Engineering and Information Technology – Department of Computer Science – Institute for Visualization and Interactive Systems (VIS), Socio-Cognitive Systems Group <b>Title:</b> Development of Signal Processing and Machine Learning Methods for Inertial Sensor Based Motion Feedback Systems
2016/08/05	Brisbane, Australia	<i>Invited lecture.</i> Griffith University. School of Engineering – Department of Electrical and Electronic Engineering – Sports and Biomedical Engineering Laboratories (SABEL labs), Queensland Academy of Sport <b>Title:</b> Towards Intelligent Motion Feedback Systems -The Use of Information Retrieval Methods in Sports
2016/08/11	Darwin, Australia	<i>Invited lecture.</i> Charles-Darwin University. Psychological and Clinical Sciences – Department of Exercise and Sport Science <b>Title:</b> Towards Intelligent Motion Feedback Systems -The Use of Information Retrieval Methods in Sports
2016/09/01	Rennes, France	<i>Invited lecture.</i> INRIA Research Institute Bretagne-Atlantic. MimeTIC Group (Analysis-Synthesis Approach for Virtual Human Simulation) <b>Title:</b> Towards Intelligent Motion Information Systems – Applying Information Retrieval to Sport Motion Data
2016/09/06	Bordeaux, France	<i>Invited lecture.</i> INRIA Research Institute South-West. Potioc Group (Popular Interaction) <b>Title:</b> Developing Intelligent Motion Information Systems for Performance Support in Sports

## Appendix B. System Promotion

---

Besides, I submitted the second part of my PhD research as a project to the 2016 **Student Project Competition of the International Sports Engineering Association (ISEA)**. This competition was open to undergraduate, masters, and PhD students of years 2015 and 2016 at any institution of higher education in the world, who had undertaken an individual project on a sports engineering topic. The judging of the submissions will be carried out by the members of the executive committee of the ISEA this fall. Judging criteria will be based on the originality of the project, the quality of the work and its presentation. Submission deadline was September 1<sup>st</sup>, and results of the screening are expected to be announced in early December. Comprising all my thesis work concerned with the retrieval of motion information (to be found in Part III and Part IV), my contribution had the project title 'Engineering Intelligent Wearable Motion Information Systems with Information Retrieval Methods – A Study Under the Example of Ski Jumping'. A large part of the discussed information was based on the performance evaluation system described in Chapter 9, which – in still relatively fundamental form – was already awarded the Best Student Paper Award at the last ISEA conference in Delft, Netherlands. However, the system was presented as a sample application within the larger task of developing intelligent motion information systems.

### Falling Walls Lab Tokyo 2016

Challenging was another public presentation which I gave at the Falling Walls Lab Tokyo at August 29, 2016. The Falling Walls Lab is a speech contest that offers an interdisciplinary forum for aspiring scientists and professionals from around the world to present their work. Official information<sup>3</sup> describes the Falling Walls Lab as follows:

The Falling Walls Lab is part of the annual, internationally renowned, conference for breakthroughs in science and society, the Falling Walls Conference. With the slogan "Share Your Idea!" the Falling Walls Lab offers hundreds emerging talents, entrepreneurs and innovators a stage to pitch their research work, initiatives or business models to their peers and a distinguished jury from academia and business.

In the course of the year, international Falling Walls Labs are organized by academic institutions throughout the world. The winners of each international Lab travel to the Falling Walls Lab Finale in Berlin, which takes place every year in November. At the Berlin Lab, 100 innovators receive the opportunity to present their work in front of a distinguished jury and attend the Falling Walls Conference the following day where they meet the world's top scientists. The three winners of the Berlin Lab will get the chance to present their ideas once more on the grand stage of the Falling Walls Conference to an international audience.

The intention of the event is to offer a platform for work and ideas of young researchers

---

<sup>3</sup><http://falling-walls.com/lab/faq1>

---

dedicated to innovation and new ideas. As the name suggests, a presentation at the Falling Walls Lab should discuss a currently existing wall (= a research problem), and an approach or idea on how to break down this wall. Coherently, the title of every presentation starts with 'Breaking the Wall of ...' and gives a sketch on the idea within 3 minutes. Such so-called 'elevator pitch' is a challenging restriction, but also emphasizes what is most essential about the idea: What it is, how it works and what it can be used for.

2016 was the first time a local sub-event of the Falling Walls Lab was launched in Tokyo. The contest was co-organized by EURAXESS Japan (pan-European initiative providing support services to European researchers located outside of Europe and researchers wishing to pursue their research careers in Europe) and the German Research and Innovation Forum Tokyo. A preselection of the participants was made on the base of a short submitted abstract in early August, leading to 16 presenters on the actual competition day (out of more than 30 applications). The short abstract and motivation that I submitted for application of participation are:

**Issue:** In many sports, the evaluation of motion performance quality is based on subjective decision by judges. To restrict bias, motion aesthetics should be translated into objective, computational measures.

**Idea:** Using wearable motion sensors, artificial machine knowledge on relevant motion aesthetics is learned. New performance data streams are then assessed and ranked by the learned motion knowledge.

**One-line description:** Fair play with modern technologies and algorithms.

**Statement of motivation:** Having been a competitive athlete, I know how bad it feels to become second in a competition where you (believe to) have been best. With ubiquitous motion sensing technologies, performances could soon be made comparable. Presenting my work in broad public will drastically draw attention to my research efforts, which in the end might alter traditional grading patterns and reanimate Olympic spirit.

Preparing my speech was a very interesting task which helped to rethink and rediscover my own work: while the presentation time was very short, the core point of the research had to be presented precisely and in a focused, yet entertaining way to the audience with various and diverse backgrounds. I titled my presentation as 'Breaking the Wall of Computational Motion Aesthetics'. Both my presentation style as well as my research topic got a lot of positive feedback from the audience at the end of the event. The full presentation was uploaded on Youtube by the responsible organizers of EURAXESS<sup>4</sup>.

---

<sup>4</sup><https://www.youtube.com/watch?v=PXjKp06io6U>

# FALLING WALLS LAB 2016 TOKYO

## CERTIFICATE OF PARTICIPATION

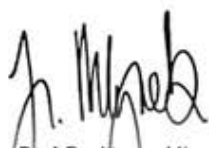
*We hereby proudly certify that*

**Heike Katrein BROCK**

*has participated in the Falling Walls Lab Tokyo*

*on 29 August 2016.*

The Falling Walls Lab is a challenging interdisciplinary platform that invites young academics, professionals and entrepreneurs from around the world to present their breakthroughs – research work, business ideas and initiatives – within 3 minutes each to an audience of industry experts, decision makers and scientists. A distinguished jury awards the best presentations. The Falling Walls Lab Tokyo is organised by the German Research & Innovation Forum Tokyo and EURAXESS Links Japan and is supported by the Falling Walls Foundation, A.T. Kearney and Festo.



Prof. Dr. Jürgen Mlynek  
Chairman of the Board of Trustees  
Falling Walls Foundation



Prof. Dr. Heinrich Menkhaus  
Chairman  
German JSPS Alumni Association



In cooperation with  
Founding Partner

**ATKearney** **FESTO**

Global Partner



Federal Foreign Office

German Research and  
Innovation Forum - Tokyo



Germany  
Land of Ideas



---

## Homepage and Code Sharing

Establishing the fundamental framework and sensor data processing methods necessary for the implementation of my information retrieval systems was a very tedious and time-consuming task, which took me more than 2 years until completion and verification. Talking with researchers and graduate students from other universities, I realized that many sport engineers are in a similar situation, especially when working with sensor measurement data from non-commercial systems.

To spread knowledge that I acquired within my PhD and to contribute to the sports engineering community, I therefore decided to make detailed information available to the public. For this, I programmed my own personal homepage (Figure B.3)<sup>5</sup>. It is dedicated on the use of wearable sensor data for motion information retrieval and contains simple, yet complete and intuitive descriptions of my work. The content of the homepage is divided into three main parts that contain essential explanations on the topics: motion sensor data collection, motion sensor data processing and motion information retrieval from sensor data. The homepage furthermore contains a link to a sample data base of ski jumps published under Creative Commons license and a link to essential code written in Matlab and posted on Github under GNU public license.

---

<sup>5</sup><http://motionsensorcomputing.com>, Accessed 2016-10-06

## Appendix B. System Promotion

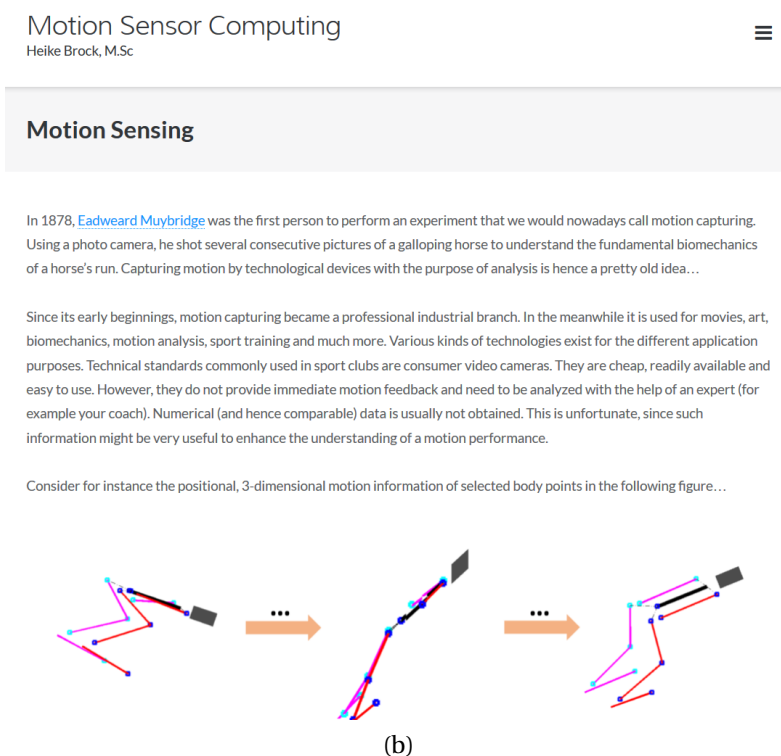
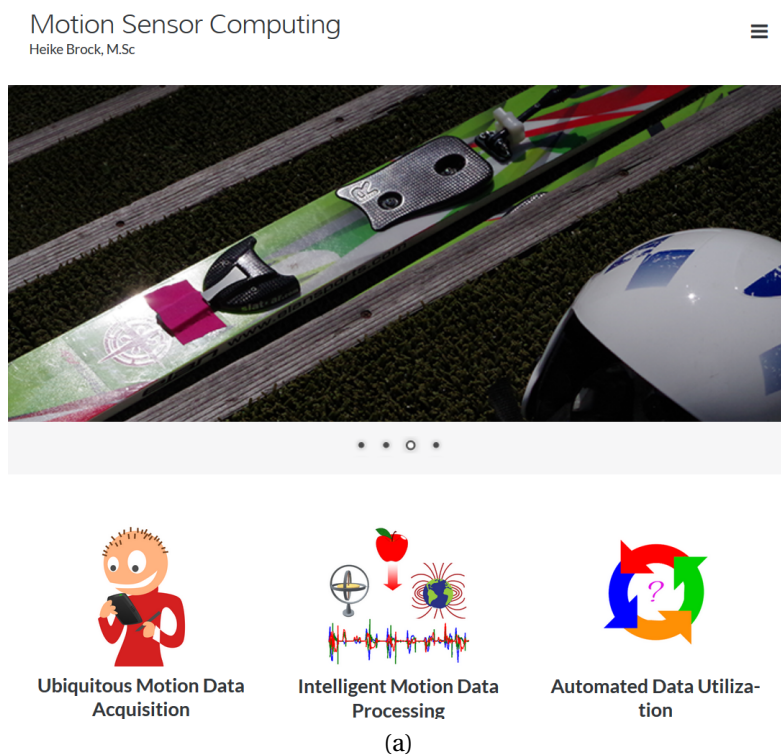


Figure B.3: Screen shots of the homepage developed for the promotion of my PhD work and the spread of knowledge on motion sensor data processing.

## Overview Ski Jump Data Base

A tabular overview on the captured data takes acquired during the main ski jumping experiment (Section 4.3) can be found here. Available sensor data was marked as o, missing sensor data as x. Data that was biased as a result of high landing impact at the ski is marked as yellow shimmed x. C-NP and C-LS represent the availability of the calibration files for the static normal pose (NP) and the rotational movement (LS).



Filename	S1	S2	S3	S4	S5	S6	S7	S8	S9	C_NP	C_LS	Quality	Group	Judge	Length
<b>25.07.</b>															
2507_A1_Sl	0	0	0	0	0	0	0	0	0	0	0	4	Test		
2507_A1_Sl	0	0	0	0	0	0	0	0	0	0	0	5	Test		
2507_A1_Sl	0	0	X	0	0	0	0	0	0	0	0				
2507_A1_Sl	0	0	0	0	0	0	0	0	0	0	0	4	Test		
2507_A1_Sl	0	0	0	0	X	0	0	0	0	0	0				
2507_A1_Sl	0	0	0	0	0	0	0	0	0	0	0	4	Test		
<b>2507_A2_Ig</b>															
2507_A2_Ig	0	0	0	0	0	0	0	0	0	0	0	5	Test		
2507_A2_Ig	0	0	0	0	0	0	0	0	0	0	0	4 Ski 2	Test		
2507_A2_Ig	0	0	0	0	0	0	0	0	0	0	0	5 Ski 2	Test		
2507_A2_Ig	0	0	0	0	0	0	0	0	0	0	0	5 Ski 3	Test		
2507_A2_Ig	0	0	0	0	0	0	0	0	0	0	0	5	Test		
<b>2507_A3_Ss</b>															
2507_A3_Ss	0	0	0	0	0	0	0	0	0	0	X	4	Test		
2507_A3_Ss	0	0	0	0	0	0	0	0	x	0	X				
2507_A3_Ss	0	0	0	0	0	0	0	0	x	0	X				
2507_A3_Ss	0	0	0	0	0	0	0	0	x	0	X				
2507_A3_Ss	0	0	0	0	0	0	0	0	x	0	X				
2507_A3_Ss	0	0	0	0	0	0	X	0	x	0	X				
<b>26.07.</b>															
<b>AM</b>															
2607_A1_Sl	0	0	0	0	0	0	0	0	0	0	0	4	Test		
2607_A1_Sl	0	0	0	0	0	0	0	0	0	0	0	4	Training	x	
2607_A1_Sl	0	0	0	0	0	0	0	0	0	0	0	3	Test	x	
2607_A1_Sl	0	0	0	0	0	0	0	0	0	0	0	4	Training	x	
2607_A1_Sl	0	0	0	0	0	0	0	0	0	0	0	4	Training	x	
2607_A1_Sl	0	0	0	0	0	0	0	0	0	0	0	4	Test	x	
<b>2607_A2_Ig</b>															
2607_A2_Ig	0	0	0	0	0	0	0	0	0	0	0	2	Test		
2607_A2_Ig	0	0	0	0	X	0	0	0	0	0	0			x	
2607_A2_Ig	0	0	0	0	0	0	0	0	0	0	0	2	Training	x	
2607_A2_Ig	0	0	0	0	X	0	0	0	0	0	0			x	
2607_A2_Ig	0	0	0	0	0	0	0	0	0	0	0	2	Training	x	
2607_A2_Ig	0	0	0	0	0	0	0	0	0	0	0	1	Training	x	
<b>2607_A3_Ss</b>															
2607_A3_Ss	0	0	0	0	0	X	0	0	0	0	0				
2607_A3_Ss	0	0	0	0	0	0	0	0	0	0	0	4	Training	x	
2607_A3_Ss	0	0	0	0	0	0	0	0	0	0	0	5	Test	x	
2607_A3_Ss	0	0	0	0	0	0	0	0	0	0	0	5	Training	x	
2607_A3_Ss	X	X	X	X	X	X	X	X	X	0	0			x	
2607_A3_Ss	0	0	0	0	0	0	0	0	0	0	0	3	Test	x	
<b>PM</b>															
2607_A1_Sl	0	0	0	0	0	0	0	0	0	0	0	4	Test		
2607_A1_Sl	0	0	0	0	0	0	0	0	0	0	0	5	Training	x	
2607_A1_Sl	X	0	0	0	0	0	0	0	0	0	0				
2607_A1_Sl	0	0	0	0	0	0	0	0	0	0	0	4	Training	x	
2607_A1_Sl	0	0	0	0	0	0	0	0	0	0	0	4	Test		
2607_A1_Sl	0	0	0	0	0	0	0	0	0	0	0	4	Training	x	
<b>2607_A2_Ig</b>															
2607_A2_Ig	0	0	0	0	0	0	0	X	0	0	0				
2607_A2_Ig	0	0	0	0	0	0	0	X	0	0	0			x	
2607_A2_Ig	0	0	0	0	0	0	0	X	0	0	0				
2607_A2_Ig	0	0	0	0	0	0	0	X	0	0	0			x	
2607_A2_Ig	0	0	0	0	0	0	0	X	0	0	0				
2607_A2_Ig	0	0	0	0	0	0	0	X	0	0	0			x	
<b>2607_A3_Ss</b>															
2607_A3_Ss	0	0	0	0	0	0	0	0	0	0	0	4	Test		
2607_A3_Ss	0	0	0	0	0	0	0	0	0	0	0	4	Training	x	
2607_A3_Ss	0	0	0	0	X	0	0	0	0	0	0				
2607_A3_Ss	0	0	0	0	0	0	0	0	0	0	0	5	Training	x	
2607_A3_Ss	0	0	0	0	0	0	0	0	0	0	0	5	Test		
2607_A3_Ss	0	0	0	0	0	0	0	0	0	0	0	5	Training	x	

**27.07.**

**AM**

2707_A1_Sl	0	0	0	0	0	X	0	0	0	X	X					x
2707_A1_Sl	0	0	0	0	X	0	0	0	0	X	X					x
2707_A1_Sl	0	0	0	0	0	0	0	0	0	X	X					x
2707_A1_Sl	0	0	0	0	0	0	0	0	0	X	X					x
2707_A1_Sl	0	0	0	0	0	0	0	0	0	X	X					x
2707_A1_Sl	0	0	0	0	0	0	0	0	0	X	X					x
2707_A1_Sl	0	0	0	0	X	0	0	0	0	X	X					x

2707_A2_Ig	0	0	0	0	0	0	0	0	0	X	0	4	Training			x
2707_A2_Ig	0	0	0	0	0	0	0	0	0	X	0	2	Test			x
2707_A2_Ig	0	0	0	0	0	0	0	0	0	X	0	2	Test			x
2707_A2_Ig	X	X	X	X	X	0	X	X	X	X	0					x
2707_A2_Ig	0	0	0	0	0	0	0	0	X	X	0					x
2707_A2_Ig	0	X	X	X	X	X	X	X	X	X	0					x
2707_A2_Ig	0	0	0	0	0	0	0	0	X	X	0					x

2707_A3_Ss	0	0	0	0	0	0	0	0	0	0	X	3	Test			x
2707_A3_Ss	0	0	0	0	0	0	0	0	0	0	X	4	Training			x
2707_A3_Ss	0	0	0	0	0	0	0	0	0	0	X	4	Test			x
2707_A3_Ss	0	0	0	0	0	0	0	0	0	0	X	5	Training			x
2707_A3_Ss	0	0	0	0	0	0	X	0	0	0	X				x	
2707_A3_Ss	0	0	0	0	0	0	0	0	0	0	X	4	Training			x
2707_A3_Ss	X	0	X	X	X	X	X	X	X	0	X					x

**PM**

2707_A1_Sl	0	0	0	0	0	0	0	0	0	0	0	4	Training			x
2707_A1_Sl	0	0	0	0	0	0	0	0	0	0	0	4	Test			x
2707_A1_Sl	0	X	X	X	0	X	X	X	X	0	0					x
2707_A1_Sl	0	0	0	0	0	0	0	0	0	0	0	3				x
2707_A1_Sl	0	0	0	0	0	0	0	0	0	0	0	3				

2707_A2_Ig	0	X	X	X	X	X	X	X	X	0	0					x
2707_A2_Ig	0	0	0	0	0	0	0	0	0	0	0	5	Training			x
2707_A2_Ig	0	0	0	0	0	0	0	0	0	0	0	3	Test			x
2707_A2_Ig	0	0	0	0	0	X	0	0	0	0	0					x
2707_A2_Ig	0	0	0	0	0	0	0	0	X	0	0					

2707_A3_Ss	0	0	0	0	0	0	0	0	0	0	0	4	Training			x
2707_A3_Ss	0	0	0	0	0	0	0	0	0	0	0	5	Training			x
2707_A3_Ss	0	0	0	0	0	0	0	0	0	0	0	4	Test			

Filename	S1	S2	S3	S4	S5	S6	S7	S8	S9	C_NP	C_LS	Quality	Group	Judge	Length
17.08															
1708_A1_S1	X	X	X	X	X	X	X	X	X	0	0				
1708_A1_S2	X	X	X	X	X	X	X	X	X	0	0				
1708_A1_S3	X	X	X	X	X	X	X	X	X	0	0				
1708_A3_S1	X	0	0	0	0	0	0	0	0	0	0				
1708_A3_S2	0	0	0	0	0	0	0	0	0	0	0	3	Test		
1708_A4_S1	0	0	0	0	0	0	0	0	0	0	0	3	Test		
18.08															
AM															
1808_A1_S1	0	0	0	X	0	0	0	X	X	0	0			x	87
1808_A1_S2	0	0	0	0	0	0	0	X	0	0	0			x	82
1808_A1_S3	0	0	0	0	0	0	0	0	0	0	0	4	Training	x	82.5
1808_A1_S4	0	0	0	0	0	0	0	0	0	0	0	4	Test	x	86.5
1808_A1_S5	X	X	X	X	X	X	X	X	X	0	0			x	79
1808_A1_S6	0	0	0	0	0	0	0	0	0	0	0	5	Training	x	81
1808_A1_S7	0	0	0	0	0	0	0	0	0	0	0	5	Test	x	82
1808_A1_S8	0	0	0	0	0	0	0	0	0	0	0	4	Training	x	85
1808_A1_S9	0	0	0	0	0	0	0	X	0	0	0				87
1808_A3_S1	X	X	X	X	X	X	X	X	X	0	0				
1808_A3_S2	X	0	0	0	0	0	0	0	X	0	0			x	87.5
1808_A3_S3	0	0	0	0	0	0	0	0	0	x	0	0		x	90.5
1808_A3_S4	0	0	0	0	0	0	0	0	0	x	0	0		x	85
1808_A3_S5	0	0	0	0	0	0	0	0	0	x	0	0		x	83
1808_A4_S1	0	0	0	0	0	0	0	0	0	0	0	4	Test		
1808_A4_S2	0	0	0	0	0	0	0	0	0	0	0	5	Training	x	86
1808_A4_S3	0	0	0	0	0	0	0	0	0	0	0	5	Training	x	81
1808_A4_S4	0	0	0	0	0	0	0	0	0	0	0	5	Test	x	84
1808_A4_S5	0	0	0	0	0	0	0	0	0	0	0	5	Training	x	84
1808_A4_S6	0	0	0	0	X	0	0	0	0	0	0			x	82
1808_A4_S7	0	0	0	0	0	X	0	0	0	0	0			x	89
1808_A4_S8	0	0	0	0	0	X	0	0	0	0	0			x	86.5
1808_A4_S9	0	0	0	X	0	0	0	X	X	0	0			x	88.5
PM															
1808_A1_S1	0	0	0	0	0	0	0	0	0	0	0	5	Training	x	81
1808_A1_S2	0	0	0	0	0	0	0	0	0	0	0	5	Training	x	89
1808_A1_S3	X	X	X	X	X	0	X	X	X	0	0			x	73
1808_A1_S4	0	0	0	0	0	0	0	0	0	0	0	4	Test	x	87
1808_A1_S5	0	0	0	0	0	0	0	0	0	0	0	4	Training	x	87
1808_A1_S6	0	0	0	0	0	0	0	0	0	0	0	5	Test	x	83
1808_A1_S7	0	0	X	0	0	0	0	0	0	0	0			x	85
1808_A1_S8	X	0	X	X	0	0	0	0	0	0	0			x	86
1808_A2_Ig1	0	0	0	0	0	0	0	0	0	0	0	4	Training	x	75
1808_A2_Ig2	0	0	0	0	0	X	0	0	0	0	0			x	69
1808_A2_Ig3	0	0	0	0	0	0	X	X	0	0	0			x	75
1808_A2_Ig4	0	0	0	0	0	0	0	0	0	0	0	5	Training	x	75
1808_A2_Ig5	0	0	0	0	0	0	0	0	0	0	0	4	Test	x	73.5
1808_A2_Ig6	0	0	0	0	0	0	0	0	0	0	0	4	Training	x	75
1808_A2_Ig7	0	0	0	0	0	0	0	0	0	0	0	3		x	
1808_A2_Ig8	0	0	0	0	0	0	0	0	0	0	0	4	Test	x	74
1808_A4_S1	0	0	0	0	0	0	0	0	0	0	0	4	Training	x	88
1808_A4_S2	0	0	0	0	0	0	0	0	0	0	0	5	Test	x	89
1808_A4_S3	0	0	0	0	0	0	0	0	0	0	0	5	Training	x	86
1808_A4_S4	0	0	0	0	0	0	0	0	0	0	0	5	Training	x	88
1808_A4_S5	0	0	0	0	0	0	0	0	0	0	0	5	Test	x	84
1808_A4_S6	0	0	0	0	0	0	0	X	0	0	0			x	
1808_A4_S7	0	0	0	0	0	0	X	X	0	0	0			x	91
1808_A4_S8	0	0	0	0	0	X	X	X	0	0	0			x	91

<b>19.08</b>																	
<b>AM</b>																	
1908_A2_Ig	0	0	0	0	0	0	0	0	0	0	0	4	Training	x	71.5		
1908_A2_Ig	0	0	0	0	0	0	0	0	0	0	0	5	Test	x	67		
1908_A2_Ig	0	0	0	0	0	0	0	0	0	0	0	5	Training	x	72		
1908_A2_Ig	0	0	0	0	0	0	0	0	0	0	0	4	Training	x	72.5		
1908_A2_Ig	0	0	0	0	0	0	0	0	0	0	0	4	Test	x	74		
1908_A2_Ig	0	0	0	0	X	0	0	0	0	0	0			x	71		
1908_A2_Ig	0	0	0	0	X	0	X	0	X	0	0			x	73		
1908_A2_Ig	0	0	0	0	0	X	X	0	0	0	0			x	71		
1908_A4_S	0	0	0	0	0	0	0	0	0	0	0	5	Training	x	81		
1908_A4_S	0	0	0	0	0	0	0	X	0	0	0			x	87		
1908_A4_S	0	0	0	0	0	0	0	X	0	0	0			x	87		
1908_A4_S	0	0	0	0	0	0	0	0	0	0	0	5	Training	x	81		
1908_A4_S	0	0	0	0	X	0	0	0	0	0	0			x	84		
1908_A4_S	0	0	0	0	0	0	0	0	0	0	0	5	Training	x	88		
1908_A4_S	0	0	0	0	0	0	0	0	0	0	0	5	Test	x	86		
1908_A4_S	0	0	0	0	0	0	0	0	X	0	0			x	84		
1908_A3_S	0	0	0	0	0	0	0	0	0	0	0	4	Training	x	82.5		
1908_A3_S	0	0	0	0	0	0	0	0	x	0	0			x	86		
1908_A3_S	0	0	0	0	0	0	0	0	x	0	0			x	82		
1908_A3_S	0	0	0	X	0	0	0	0	x	0	0			x	77		
1908_A3_S	0	0	0	0	0	0	0	0	x	0	0			x	82.5		
1908_A3_S	X	0	0	0	0	0	0	0	x	0	0			x	79		
1908_A3_S	0	0	0	0	0	0	0	0	x	0	0			x	88		
<b>PM</b>																	
1908_A1_S	0	0	0	0	0	0	0	0	0	0	0	4	Test	x	83		
1908_A1_S	0	0	0	0	0	0	0	0	0	0	0	4	Training	x	85		
1908_A1_S	0	0	0	0	0	0	0	0	0	0	0	4	Test	x	87		
1908_A1_S	0	0	0	0	0	0	0	0	0	0	0	4	Training	x	86		
1908_A1_S	0	0	0	0	0	0	0	0	0	0	0	4	Training	x	88		
1908_A1_S	0	0	0	0	0	0	0	0	0	0	0	4	Test	x	81.5		
1908_A1_S	0	0	0	0	0	0	0	0	0	0	0	4	Training	x	87.5		
1908_A4_S	0	0	0	0	0	0	0	X	0	0	0			x	78		
1908_A4_S	0	0	0	0	0	0	0	0	X	0	0			x	86		
1908_A4_S	0	0	0	0	0	0	0	0	X	0	0			x	89		
1908_A4_S	0	0	0	0	0	0	0	0	X	0	0			x	93.5		
1908_A4_S	0	0	0	0	0	0	0	0	X	0	0			x	89		
1908_A4_S	0	0	0	0	0	0	0	0	X	0	0			x	81.5		
1908_A4_S	0	0	0	0	0	0	0	0	X	0	0			x	83.5		
1908_A3_S	0	0	0	0	0	0	0	0	0	0	0	4	Training	x	80		
1908_A3_S	0	0	0	0	0	0	0	0	0	0	0	4	Training	x	86		
1908_A3_S	0	0	0	0	0	0	0	0	0	0	0	4	Test	x	87		
1908_A3_S	0	0	0	0	0	0	0	0	0	0	0	5	Training	x	86.5		
1908_A3_S	0	0	0	0	0	0	0	0	0	0	0	5	Test	x	90		
1908_A3_S	0	0	0	0	0	0	0	0	0	0	0	5	Training	x	87		
1908_A3_S	0	0	0	0	0	0	0	0	0	0	0	5	Training	x	75		
<b>20.08</b>																	
2008_A2_Ig	X	X	X	X	X	X	X	X	X	0	0			x	88		
2008_A2_Ig	X	X	X	X	X	X	X	X	X	0	0			x	70		
2008_A2_Ig	0	0	0	0	0	0	0	0	0	0	0	4	Training	x	67.5		
2008_A2_Ig	0	0	0	0	0	0	0	0	0	0	0	4	Test				
2008_A4_S	0	0	X	0	0	0	0	0	0	0	0			x	78		
2008_A4_S	0	0	0	0	0	0	0	0	0	0	0	4	Training	x	86.5		
2008_A4_S	0	0	0	0	0	0	0	0	0	0	0	4	Test	x	85		
2008_A3_S	0	0	0	0	0	0	0	0	0	0	0	4	Training	x	80		
2008_A3_S	0	0	0	X	0	0	0	0	0	0	0			x	84		
2008_A3_S	0	0	0	0	0	0	0	0	0	0	0	4	Training	x	82		



## **D** Judge Score Sheets

In the following, I want to show some sample scans of the judge score sheets collected during the ski jumping experiments (Section 4.3).

記録者名 サトウ 1 本目

日付 時刻 9:11 2015 / 8 / 18

被験者名 \_\_\_\_\_

出発No.	空中	着地	アウトラン	減点合計	B
	1.5	1.5	0	3.0	17.0

飛距離	87.5 m
-----	--------

No	空中での減点	max 5.0	被験者の減点
1	(ダイナミックな)飛行姿勢を形づくるとき、身体及びスキー板のコントロールが十分されていない	0.5-2.0	0.5
2	不安定(例: 不必要な腕の動き、身体のコントロールがされていない。膝が曲がっている。脚が完全に伸びていない)	0.5-1.0	
3	腕の位置が左右対称でない。および/またはバランスが取れていない	0.5-1.0	0.5
4	脚の位置が左右対称でない。および/またはバランスがとれていない	0.5-1.0	
5	スキー板のバラつき、および/またはスキー板の不揃い	0.5-1.0	0.5
	<b>着地での減点</b>	max 5.0	
1	着地動作全体を通し、(足が平行のまま)着地の瞬間にテレマーク姿勢を取ろうとしない。且つテレマーク姿勢が入らない。(ひとつの失敗として採点)	min 2.0	
2	空中姿勢からランディング姿勢への移行中、正確かつスムーズな動作に欠ける	0.5-1.0	0.5
3	着地の瞬間で、少なくとも最低限のテレマーク姿勢の入りや膝の曲がりが少ない	0.5-1.5	
4	スムーズなテレマーク姿勢による着地の衝撃吸収が不足している。または、着地の瞬間の後の不完全なテレマーク姿勢を着地手順の最後までに完全なテレマーク姿勢へ持っていく強さに欠ける(不安定、硬すぎる、またははっきりとしたテレマーク姿勢がない)	0.5-1.5	0.5
5	スキー動作全体のバランスを保つための腕の動きが不安定または、バランスが悪い	0.5-1.0	
6	スキー板のコントロール不足。(スキー板が平行でなく、板の間隔が2本以上ある)、および/または、両スキー板が滑走面に対し均一に接触していない(エッジが立っている)	0.5-1.0	
	<b>アウトランでの減点</b>	max 7.0	
1	アウトランにおける小さなミスがあった場合(瞬間的に不安定、両スキー板が滑走面に対し均一に接触していない、および/または平行でない。ブレーキをかける前、身体がまっすぐ立っていない状態)	0.5-1.5	
2	アウトランにおけるミスがあった場合。(スキーバランスの視覚的印象が乏しく、不安定。両スキー板が滑走面に対して、均一に接触していない、および/または平行でない。)身体がまっすぐ立っていない状態で転倒ラインの方向(真っ直ぐに滑る)から逸脱することを含む	2.0-2.5	
3	アウトランにおける大きなミスがあった場合。(不安定、転倒ライン上、またはラインの前の転びそうな姿勢、片手の雪面・マット・スキー板への接触)	3.0	
4	(両手・背中、および/または臀部がスキー板/雪面/マットに接触して移行カーブを通過し)、バランスおよびコントロールを失う。以上の減点は、この姿勢のまま転倒ラインを通過した時にも適用される	4.0-5.0	
5	転倒ライン手前または、転倒ライン上での転倒	7.0	

記録者名

セイ / 176

日付 時刻

9:13

2015/8/18

被験者名

出発No.	空中	着地	アウトラン	減点合計	B
	1.5	2.5	0	4.0	16.0

飛距離	86. m
-----	-------

No	空中での減点	max 5.0	被験者の減点
1	(ダイナミックな)飛行姿勢を形づくるとき、身体及びスキー板のコントロールが十分されていない	0.5-2.0	0.5
2	不安定(例: 不必要な腕の動き、身体のコントロールがされていない。膝が曲がっている。脚が完全に伸びていない)	0.5-1.0	
3	腕の位置が左右対称でない。および/またはバランスが取れていない	0.5-1.0	0.5
4	脚の位置が左右対称でない。および/またはバランスがとれていない	0.5-1.0	
5	スキー板のバラツシ、および/またはスキー板の不揃い	0.5-1.0	0.5
	着地での減点	max 5.0	
1	着地動作全体を通し、(足が平行なまま)着地の瞬間にテレマーク姿勢を取ろうとしない。且つテレマーク姿勢が入らない。(ひとつの失敗として採点)	min 2.0	2.0
2	空中姿勢からランディング姿勢への移行中、正確かつスムーズな動作に欠ける	0.5-1.0	0.5
3	着地の瞬間で、少なくとも最低限のテレマーク姿勢の入りや膝の曲がりがない	0.5-1.5	
4	スムーズなテレマーク姿勢による着地の衝撃吸収が不足している。または、着地の瞬間の後の不完全なテレマーク姿勢を着地手順の最後までに完全なテレマーク姿勢へ持っていく強さに欠ける(不安定、硬すぎる、またははっきりとしたテレマーク姿勢がない)	0.5-1.5	
5	スキー動作全体のバランスを保つための腕の動きが不安定または、バランスが悪い	0.5-1.0	
6	スキー板のコントロール不足。(スキー板が平行でなく、板の間隔が2本以上ある)、および/または、両スキー板が滑走面に対し均一に接触していない(エッジが立っている)	0.5-1.0	
	アウトランでの減点	max 7.0	
1	アウトランにおける小さなミスがあった場合(瞬間的に不安定、両スキー板が滑走面に対し均一に接触していない、および/または平行でない。ブレーキをかける前、身体がまっすぐ立っていない状態)	0.5-1.5	
2	アウトランにおけるミスがあった場合。(スキーバランスの視覚的印象が乏しく、不安定、両スキー板が滑走面に対して、均一に接触していない、および/または平行でない。)身体がまっすぐ立っていない状態で転倒ラインの方向(真っ直ぐに滑る)から逸脱することを含む	2.0-2.5	
3	アウトランにおける大きなミスがあった場合。(不安定、転倒ライン上、またはラインの前の転びそうな姿勢、片手の雪面・マット・スキー板への接触)	3.0	
4	(両手・背中、および/または臀部がスキー板/雪面/マットに接触して移行カーブを通過し)、バランスおよびコントロールを失う。以上の減点は、この姿勢のまま転倒ラインを通過した時にも適用される	4.0-5.0	
5	転倒ライン手前または、転倒ライン上での転倒	7.0	



記録者名

サトウ 4本目

日付 時刻

9:47

2015/8/18

被験者名

出発No.	空中	着地	アウトラン	減点合計	B
	2.0	1.5	0	3.5	16.5

飛距離	83 m
-----	------

No	空中での減点	max 5.0	被験者の減点
1	(ダイナミックな)飛行姿勢を形づくるとき、身体及びスキー板のコントロールが十分されていない	0.5-2.0	
2	不安定(例: 不必要な腕の動き、身体のコントロールがされていない。膝が曲がっている。脚が完全に伸びていない)	0.5-1.0	0.5
3	腕の位置が左右対称でない。および/またはバランスが取れていない	0.5-1.0	0.5
4	脚の位置が左右対称でない。および/またはバランスがとれていない	0.5-1.0	0.5
5	スキー板のバラつき、および/またはスキー板の不揃い	0.5-1.0	0.5
	<b>着地での減点</b>	max 5.0	
1	着地動作全体を通し、(足が平行なまま)着地の瞬間にテレマーク姿勢を取ろうとしない。且つテレマーク姿勢が入らない。(ひとつの失敗として採点)	min 2.0	
2	空中姿勢からランディング姿勢への移行中、正確かつスムーズな動作に欠ける	0.5-1.0	0.5
3	着地の瞬間で、少なくとも最低限のテレマーク姿勢の入りや膝の曲がりがない	0.5-1.5	
4	スムーズなテレマーク姿勢による着地の衝撃吸収が不足している。または、着地の瞬間の後の不完全なテレマーク姿勢を着地手順の最後までに完全なテレマーク姿勢へ持っていき強さに欠ける(不安定、硬すぎる、またははっきりとしたテレマーク姿勢がない)	0.5-1.5	1.0
5	スキー動作全体のバランスを保つための腕の動きが不安定または、バランスが悪い	0.5-1.0	
6	スキー板のコントロール不足。(スキー板が平行でなく、板の間隔が2本以上ある)、および/または、両スキー板が滑走面に対し均一に接触していない(エッジが立っている)	0.5-1.0	
	<b>アウトランでの減点</b>	max 7.0	
1	アウトランにおける小さなミスがあった場合(瞬間的に不安定、両スキー板が滑走面に対し均一に接触していない、および/または平行でない。ブレーキをかける前、身体がまっすぐ立っていない状態)	0.5-1.5	
2	アウトランにおけるミスがあった場合。(スキーバランスの視覚的印象が乏しく、不安定。両スキー板が滑走面に対して、均一に接触していない、および/または平行でない。)身体がまっすぐ立っていない状態で転倒ラインの方向(真っ直ぐに滑る)から逸脱することをさす	2.0-2.5	
3	アウトランにおける大きなミスがあった場合。(不安定、転倒ライン上、またはラインの前の転びそうな姿勢、片手の雪面・マット・スキー板への接触)	3.0	
4	(両手・背中、および/または臀部がスキー板/雪面/マットに接触して移行カーブを通過し)、バランスおよびコントロールを失う。以上の減点は、この姿勢のまま転倒ラインを通過した時にも適用される	4.0-5.0	
5	転倒ライン手前または、転倒ライン上での転倒	7.0	

記録者名

日付 時刻

15:17

2015 08 18

被験者名

セイ / 5年目

出発No.	空中	着地	アウトラン	減点合計	B
	2.0	2.5	0	4.5	15.5

飛距離	840 m
-----	-------

No	空中での減点	max 5.0	被験者の減点
1	(ダイナミックな)飛行姿勢を形づくるとき、身体及びスキー板のコントロールが十分されていない	0.5-2.0	0.5
2	不安定(例:不必要な腕の動き、身体のコントロールがされていない。膝が曲がっている。脚が完全に伸びていない)	0.5-1.0	0.5
3	腕の位置が左右対称でない。および/またはバランスが取れていない	0.5-1.0	0.5
4	脚の位置が左右対称でない。および/またはバランスがとれていない	0.5-1.0	
5	スキー板のバラつき、および/またはスキー板の不揃い	0.5-1.0	0.5
	着地での減点	max 5.0	
1	着地動作全体を通し、(足が平行なまま)着地の瞬間にテレマーク姿勢を取ろうとしない。且つテレマーク姿勢が入らない。(ひとつの失敗として採点)	min 2.0	2.5
2	空中姿勢からランディング姿勢への移行中、正確かつスムーズな動作に欠ける	0.5-1.0	
3	着地の瞬間で、少なくとも最低限のテレマーク姿勢の入りや膝の曲がりが少ない	0.5-1.5	
4	スムーズなテレマーク姿勢による着地の衝撃吸収が不足している。または、着地の瞬間の後の不完全なテレマーク姿勢を着地手順の最後までに完全なテレマーク姿勢へ持っていく強さに欠ける(不安定、硬すぎる、またははっきりとしたテレマーク姿勢がない)	0.5-1.5	
5	スキー動作全体のバランスを保つための腕の動きが不安定または、バランスが悪い	0.5-1.0	
6	スキー板のコントロール不足。(スキー板が平行でなく、板の間隔が2本以上ある)、および/または、両スキー板が滑走面に対し均一に接触していない(エッジが立っている)	0.5-1.0	
	アウトランでの減点	max 7.0	
1	アウトランにおける小さなミスがあった場合(瞬間的に不安定、両スキー板が滑走面に対し均一に接触していない、および/または平行でない。ブレーキをかける前、身体がまっすぐ立っていない状態)	0.5-1.5	
2	アウトランにおけるミスがあった場合。(スキーバランスの視覚的印象が乏しく、不安定。両スキー板が滑走面に対して、均一に接触していない、および/または平行でない。)身体がまっすぐ立っていない状態で転倒ラインの方向(真っ直ぐに滑る)から逸脱することを含む	2.0-2.5	
3	アウトランにおける大きなミスがあった場合。(不安定、転倒ライン上、またはラインの前の転びそうな姿勢、片手の雪面・マット・スキー板への接触)	3.0	
4	(両手・背中、および/または臀部がスキー板/雪面/マットに接触して移行カーブを通過し)、バランスおよびコントロールを失う。以上の減点は、この姿勢のまま転倒ラインを通過した時にも適用される	4.0-5.0	
5	転倒ライン手前または、転倒ライン上での転倒	7.0	

記録者名

日付 時刻

15:36

2015 08 18

被験者名

ミラキ

6本目

出発No.	空中	着地	アウトラン	減点合計	B
	1.5	1.5	0	3.0	17.0

飛距離	83 m
-----	------

No.	空中での減点	max 5.0	被験者の減点
1	(ダイナミックな)飛行姿勢を形づくるとき、身体及びスキー板のコントロールが十分されていない	0.5-2.0	
2	不安定(例:不必要な腕の動き、身体のコントロールがされていない。膝が曲がっている。脚が完全に伸びていない)	0.5-1.0	0.5
3	腕の位置が左右対称でない。および/またはバランスが取れていない	0.5-1.0	0.5
4	脚の位置が左右対称でない。および/またはバランスがとれていない	0.5-1.0	
5	スキー板のバラつき、および/またはスキー板の不揃い	0.5-1.0	0.5
	着地での減点	max 5.0	
1	着地動作全体を通し、(足が平行なまま)着地の瞬間にテレマーク姿勢を取らうとしない。且つテレマーク姿勢が入らない。(ひとつの失敗として採点)	min 2.0	
2	空中姿勢からランディング姿勢への移行中、正確かつスムーズな動作に欠ける	0.5-1.0	0.5
3	着地の瞬間で、少なくとも最低限のテレマーク姿勢の入りや膝の曲がりが少ない	0.5-1.5	0.5
4	スムーズなテレマーク姿勢による着地の衝撃吸収が不足している。または、着地の瞬間の後の不完全なテレマーク姿勢を着地手順の最後までに完全なテレマーク姿勢へ持っていく強さに欠ける(不安定、硬すぎる、またははっきりとしたテレマーク姿勢がない)	0.5-1.5	0.5
5	スキー動作全体のバランスを保つための腕の動きが不安定または、バランスが悪い	0.5-1.0	
6	スキー板のコントロール不足。(スキー板が平行でなく、板の間隔が2本以上ある)、および/または、両スキー板が滑走面に対し均一に接触していない(エッジが立っている)	0.5-1.0	
	アウトランでの減点	max 7.0	
1	アウトランにおける小さなミスがあった場合(瞬間的に不安定、両スキー板が滑走面に対し均一に接触していない、および/または平行でない。プレーキをかける前、身体がまっすぐ立っていない状態)	0.5-1.5	
2	アウトランにおけるミスがあった場合。(スキーバランスの視覚的印象が乏しく、不安定。両スキー板が滑走面に対して、均一に接触していない、および/または平行でない。)身体がまっすぐ立っていない状態で転倒ラインの方向(真っ直ぐに滑る)から逸脱することを含む	2.0-2.5	
3	アウトランにおける大きなミスがあった場合。(不安定、転倒ライン上、またはラインの前の転びそうな姿勢、片手の雪面・マット・スキー板への接触)	3.0	
4	(両手・背中、および/または臀部がスキー板/雪面/マットに接触して移行カーブを通過し)、バランスおよびコントロールを失う。以上の減点は、この姿勢のまま転倒ラインを通過した時にも適用される	4.0-5.0	
5	転倒ライン手前または、転倒ライン上での転倒	7.0	

# Bibliography

## Part VI







# Sensor Technology and Application

- [AB10] Kerem Altun and Billur Barshan. Human activity recognition using inertial/magnetic sensor units. In AlbertAli Salah, Theo Gevers, Nicu Sebe, and Alessandro Vinciarelli, editors, *Human Behavior Understanding*, volume 6219 of *Lecture Notes in Computer Science*, pages 38–51. Springer Berlin Heidelberg, 2010.
- [ADM<sup>+</sup>14] Amin Ahmadi, Francois Destelle, David Monaghan, Noel E O’Connor, Chris Richter, and Kieran Moran. A framework for comprehensive analysis of a swing in sports using low-cost inertial sensors. In *SENSORS, 2014 IEEE*, pages 2211–2214. IEEE, 2014.
- [AS10] AU Alahakone and A Senanayake. A real-time interactive biofeedback system for sports training and rehabilitation. *Proceedings of the Institution of Mechanical Engineers, Part P: Journal of Sports Engineering and Technology*, 224(2):181–190, 2010.
- [BAB<sup>+</sup>11] C.M.N. Brigante, N. Abbate, A. Basile, A.C. Faulisi, and S. Sessa. Towards miniaturization of a mems-based wearable motion capture system. *IEEE Transactions on Industrial Electronics*, 58(8):3234–3241, Aug 2011.
- [Bac12] Arnold Baca. Methods for recognition and classification of human motion patterns—a prerequisite for intelligent devices assisting in sports activities. *MATHMOD 2012, February 15-17, Vienna, Austria, 2012*.
- [BBCL15] Matthew A D Brodie, Tim R Beijer, Colleen G Canning, and Stephen R Lord. Head and pelvis stride-to-stride oscillations in gait: validation and interpretation of measurements from wearable accelerometers. *Physiological Measurement*, 36(5):857, 2015.
- [BBS14] Andreas Bulling, Ulf Blanke, and Bernt Schiele. A tutorial on human activity recognition using body-worn inertial sensors. *ACM Computing Survey*, 46(3):33:1–33:33, January 2014.
- [BKB14] Hans-Peter Brückner, Benjamin Krüger, and Holger Blume. Reliable orientation estimation for mobile motion capturing in medical rehabilitation sessions based on inertial measurement units. *Microelectronics Journal*, 45(12):1603–1611, 2014.
- [BLC<sup>+</sup>15] M. A. Brodie, S. R. Lord, M. J. Coppens, J. Annegarn, and K. Delbaere. Eight-week remote monitoring using a freely worn device reveals unstable gait

- patterns in older fallers. *IEEE Transactions on Biomedical Engineering*, 62(11):2588–2594, Nov 2015.
- [BLS<sup>+</sup>14] E. Bergamini, G. Ligorio, A. Summa, G. Vannozzi, A. Cappozzo, and A.M. Sabatini. Estimating orientation using magnetic and inertial sensors and different sensor fusion approaches: accuracy assessment in manual and locomotion tasks. *Sensors (Basel, Switzerland)*, 14(10):18625–18649, 2014.
- [BM14] P. Buonocunto and M. Marinoni. Tracking limbs motion using a wireless network of inertial measurement units. In *Industrial Embedded Systems (SIES), 2014 9th IEEE International Symposium on*, pages 66–76, June 2014.
- [BSDD14] B. Bouvier, A. Savescu, S. Duprey, and R. Dumas. Benefits of functional calibration for estimating elbow joint angles using magneto-inertial sensors: preliminary results. *Computer Methods in Biomechanics and Biomedical Engineering*, 17(SUPP1):108–109, 2014.
- [BWP08a] MA Brodie, A Walmsley, and W Page. Dynamic accuracy of inertial measurement units during simple pendulum motion: Technical note. *Computer Methods in Biomechanics and Biomedical Engineering*, 11(3):235–242, 2008.
- [BWP08b] Matthew Brodie, Alan Walmsley, and Wyatt Page. Fusion motion capture: a prototype system using inertial measurement units and gps for the biomechanical analysis of ski racing. *Sports Technology*, 1(1):17–28, 2008.
- [DCM<sup>+</sup>16] S.P. Davidson, S.M. Cain, R.S. McGinnis, R.R. Vitali, N.C. Perkins, and S.G. McLean. Quantifying warfighter performance in a target acquisition and aiming task using wireless inertial sensors. *Applied Ergonomics*, 56:27–33, 2016.
- [Die06] James Diebel. Representing attitude: Euler angles, unit quaternions, and rotation vectors, 2006.
- [DMA14] F. Dadashi, G.P. Millet, and K. Aminian. Estimation of front-crawl energy expenditure using wearable inertial measurement units. *IEEE Sensors Journal*, 14(4):1020–1027, April 2014.
- [dVVBvdH09] W.H.K. de Vries, H.E.J. Veeger, C.T.M. Baten, and F.C.T. van der Helm. Magnetic distortion in motion labs, implications for validating inertial magnetic sensors. *Gait & Posture*, 29(4):535 – 541, 2009.
- [ECM<sup>+</sup>08] M. Euston, P. Coote, R. Mahony, Jonghyuk Kim, and T. Hamel. A complementary filter for attitude estimation of a fixed-wing uav. In *IEEE/RSJ International Conference on Intelligent Robots and Systems, 2008. IROS 2008.*, pages 340–345, Sept 2008.

- [EMW14] Falko Eckardt, Andreas Münz, and Kerstin Witte. Application of a full body inertial measurement system in dressage riding. *Journal of Equine Veterinary Science*, 34(11–12):1294 – 1299, 2014.
- [ESHN08] Naser El-Sheimy, Haiying Hou, and Xiaoji Niu. Analysis and modeling of inertial sensors using allan variance. *IEEE Transactions on Instrumentation and Measurement*, 57(1):140–149, 2008.
- [FFC<sup>+</sup>15] Benedikt Fasel, Julien Favre, Julien Chardonens, Gérald Gremion, and Kamiar Aminian. An inertial sensor-based system for spatio-temporal analysis in classic cross-country skiing diagonal technique. *Journal of biomechanics*, 48(12):3199–3205, 2015.
- [FGM<sup>+</sup>16] S. Fantozzi, A. Giovanardi, F.A. Magalhães, R. Di Michele, M. Cortesi, and G. Gatta. Assessment of three-dimensional joint kinematics of the upper limb during simulated swimming using wearable inertial-magnetic measurement units. *Journal of Sports Sciences*, 34(11):1073–1080, 2016.
- [FSK<sup>+</sup>15] Benedikt Fasel, Jörg Spörri, Josef Kröll, Erich Müller, and Kamiar Aminian. Using inertial sensors for reconstructing 3d full-body movement in sports—possibilities and limitations on the example of alpine ski racing. In *33rd International Conference on Biomechanics in Sports*, number EPFL-CONF-209331, 2015.
- [GFF<sup>+</sup>14] Miguel F Gago, Vitor Fernandes, Jaime Ferreira, Hélder Silva, Luís Rocha, Estela Bicho, and Nuno Sousa. Postural stability analysis with inertial measurement units in alzheimer’s disease. *Dementia and geriatric cognitive disorders extra*, 4(1):22–30, 2014.
- [GJ11a] H. Ghasemzadeh and R. Jafari. Coordination analysis of human movements with body sensor networks: A signal processing model to evaluate baseball swings. *IEEE Sensors Journal*, 11(3):603–610, March 2011.
- [GJ11b] H. Ghasemzadeh and R. Jafari. Coordination analysis of human movements with body sensor networks: A signal processing model to evaluate baseball swings. *IEEE Sensors Journal*, 11(3):603–610, March 2011.
- [GLJ16] Sam Gleadhill, James Bruce Lee, and Daniel James. The development and validation of using inertial sensors to monitor postural change in resistance exercise. *Journal of Biomechanics*, 49(7):1259 – 1263, 2016.
- [GTNJ13] William H Gageler, David Thiel, Jonothan Neville, and Daniel A James. Feasibility of using virtual and body worn inertial sensors to detect whole-body decelerations during stopping. *Procedia Engineering*, 60:28–33, 2013.



- [HAW<sup>+</sup>10] H. Harms, O. Amft, R. Winkler, J. Schumm, M. Kusserow, and G. Troester. Ethos: Miniature orientation sensor for wearable human motion analysis. In *IEEE Sensors, 2010*, pages 1037–1042, Nov 2010.
- [HBMS11] Thomas Helten, Heike Brock, Meinard Müller, and Hans-Peter Seidel. Classification of trampoline jumps using inertial sensors. *Sports Engineering*, 14(2-4):155–164, 2011.
- [HDK13] Kiyoshi Hirose, Hitoshi Doki, and Akiko Kondo. Dynamic analysis and motion measurement of ski turns using inertial and force sensors. *Procedia Engineering*, 60(0):355 – 360, 2013. 6th Asia-Pacific Congress on Sports Technology (APCST).
- [HJ10] Jason William Harding and Daniel Arthur James. Performance assessment innovations for elite snowboarding. *Procedia Engineering*, 2(2):2919 – 2924, 2010. The Engineering of Sport 8 - Engineering Emotion.
- [HMHJ08] JasonW. Harding, ColinG. Mackintosh, AllanG. Hahn, and DanielA. James. Classification of aerial acrobatics in elite half-pipe snowboarding using body mounted inertial sensors (p237). In *The Engineering of Sport 7*, pages 447–456. Springer Paris, 2008.
- [HMS16] Hannes Hoettinger, Franziska Mally, and Anton Sabo. Activity recognition in surfing - a comparative study between hidden markov model and support vector machine. *Procedia Engineering*, 147:912 – 917, 2016. The Engineering of {SPORT} 11.
- [HMZ<sup>+</sup>13] F Hoflinger, Johannes Muller, Rui Zhang, Leonhard M Reindl, and Wolfram Burgard. A wireless micro inertial measurement unit (imu). *IEEE Transactions on Instrumentation and Measurement*, 62(9):2583–2595, 2013.
- [Hou05] Haiying Hou. *Modeling inertial sensors errors using Allan variance*. Library and Archives Canada= Bibliothèque et Archives Canada, 2005.
- [JSN<sup>+</sup>15] Thomas Jaitner, Marcus Schmidt, Kevin Nolte, Carl Rheinländer, Sebastian Wille, and Norbert Wehn. Vertical jump diagnosis for multiple athletes using a wearable inertial sensor unit. *Sports Technology*, pages 1–7, 2015.
- [KC14] Narayanan C. Krishnan and Diane J. Cook. Activity recognition on streaming sensor data. *Pervasive and Mobile Computing*, 10, Part B:138 – 154, 2014.
- [KCGC12] Daniel Kelly, Garrett F Coughlan, Brian S Green, and Brian Caulfield. Automatic detection of collisions in elite level rugby union using a wearable sensing device. *Sports Engineering*, 15(2):81–92, 2012.

- [KMH<sup>+</sup>13] Matthias Kranz, Andreas Möller, Nils Hammerla, Stefan Diewald, Thomas Plötz, Patrick Olivier, and Luis Roalter. The mobile fitness coach: Towards individualized skill assessment using personalized mobile devices. *Pervasive and Mobile Computing*, 9(2):203 – 215, 2013. Special Section: Mobile Interactions with the Real World.
- [KS16] M. Kok and T.B. Schon. Magnetometer calibration using inertial sensors. *IEEE Sensors Journal*, 16(14):5679–5689, 2016.
- [LBCP08] Daniel TH Lai, Rezaul Begg, Edgar Charry, and M Palaniswami. Frequency analysis of inertial sensor data for measuring toe clearance. In *Intelligent Sensors, Sensor Networks and Information Processing, 2008. ISSNIP 2008. International Conference on*, pages 303–308. IEEE, 2008.
- [LDJ<sup>+</sup>16] C.-G. Lee, N.-N. Dao, S. Jang, D. Kim, Y. Kim, and S. Cho. Gyro drift correction for an indirect kalman filter based sensor fusion driver. *Sensors (Switzerland)*, 16(6), 2016.
- [LKP05] Chuanjun Li, Latifur Khan, and Balakrishnan Prabhakaran. Real-time classification of variable length multi-attribute motions. *Knowledge and Information Systems*, 10(2):163–183, 2005.
- [Log] Logical Product. Sports sensing 9-axial waterproof inertial sensor. Accessed 2015-10-17.
- [LPR12] Jung Keun Lee, E.J. Park, and S.N. Robinovitch. Estimation of attitude and external acceleration using inertial sensor measurement during various dynamic conditions. *IEEE Transactions on Instrumentation and Measurement*, 61(8):2262–2273, Aug 2012.
- [LVB05] H.J. Luinge, P. H. Veltink, and C. T. M. Baten. Ambulatory measurement of arm orientation. *Journal of Biomechanics*, 40(1):78–85, 2005.
- [LZL<sup>+</sup>15] Tien Jung Lee, Shaghayegh Zihajehzadeh, Darrell Loh, Reynald Hoskinson, and Edward J Park. Automatic jump detection in skiing/snowboarding using head-mounted mems inertial and pressure sensors. *Proceedings of the Institution of Mechanical Engineers, Part P: Journal of Sports Engineering and Technology*, 229(4):278–287, 2015.
- [MBSS16] P. Muller, M.-A. Begin, T. Schauer, and T. Seel. Alignment-free, self-calibrating elbow angles measurement using inertial sensors. pages 583–586, 2016.
- [MCG<sup>+</sup>15] Robert Mooney, Gavin Corley, Alan Godfrey, Leo R Quinlan, and Gearóid ÓLaighin. Inertial sensor technology for elite swimming performance analysis: A systematic review. *Sensors*, 16(1):18, 2015.

- [MD09] Michael W Mahoney and Petros Drineas. Cur matrix decompositions for improved data analysis. *Proceedings of the National Academy of Sciences*, 106(3):697–702, 2009.
- [MF15] Bojan Milosevic and Elisabetta Farella. Wearable inertial sensor for jump performance analysis. In *Proceedings of the 2015 Workshop on Wearable Systems and Applications, WearSys '15*, pages 15–20, New York, NY, USA, 2015. ACM.
- [MFTW16] Benjamin Moeyersons, Franz Konstantin Fuss, Adin Ming Tan, and Yehuda Weizman. Biofeedback system for novice snowboarding. *Procedia Engineering*, 147:781 – 786, 2016. The Engineering of {SPORT} 11.
- [MHP08] R. Mahony, T. Hamel, and Jean-Michel Pflimlin. Nonlinear complementary filters on the special orthogonal group. *IEEE Transactions on Automatic Control*, 53(5):1203–1218, June 2008.
- [MHV11] S.O.H. Madgwick, A.J.L. Harrison, and R. Vaidyanathan. Estimation of imu and marg orientation using a gradient descent algorithm. In *2011 IEEE International Conference on Rehabilitation Robotics (ICORR)*, pages 1–7, June 2011.
- [MYB<sup>+</sup>01] J.L. Marins, X. Yun, E.R. Bachmann, R.B. McGhee, and M.J. Zyda. An extended kalman filter for quaternion-based orientation estimation using marg sensors. In *2001 IEEE/RSJ International Conference on Intelligent Robots and Systems, 2001. Proceedings.*, volume 4, pages 2003–2011 vol.4, 2001.
- [OBT16] A.P. Ompusunggu and A. Bey-Temsamani. 2-level error (drift) compensation for low-cost mems-based inertial measurement unit (imu). *Microsystem Technologies*, 22(7):1601–1612, 2016.
- [PLY10] J. Pansiot, B. Lo, and Guang-Zhong Yang. Swimming stroke kinematic analysis with bsn. In *2010 International Conference on Body Sensor Networks (BSN)*, pages 153–158, June 2010.
- [RLBV05] Daniel Roetenberg, Henk J Luinge, Chris Baten, and Peter H Veltink. Compensation of magnetic disturbances improves inertial and magnetic sensing of human body segment orientation. *IEEE Transactions on Neural Systems and Rehabilitation Engineering*, 13(3):395–405, 2005.
- [RLMLP16] X. Robert-Lachaine, H. Mecheri, C. Larue, and A. Plamondon. Validation of inertial measurement units with an optoelectronic system for whole-body motion analysis. *Medical and Biological Engineering and Computing*, pages 1–11, 2016.

- [RLS09] Daniel Roetenberg, Henk Luinge, and Per Slycke. Xsens MVN: Full 6DOF Human Motion Tracking Using Miniature Inertial Sensors. Technical report, xsens, 2009.
- [RPF15] E Ruffaldi, L Peppoloni, and A Filippeschi. Sensor fusion for complex articulated body tracking applied in rowing. *Proceedings of the Institution of Mechanical Engineers, Part P: Journal of Sports Engineering and Technology*, page 1754337115583199, 2015.
- [Sab06] A.M. Sabatini. Quaternion-based extended kalman filter for determining orientation by inertial and magnetic sensing. *IEEE Transactions on Biomedical Engineering*, 53(7):1346–1356, July 2006.
- [SGIA<sup>+</sup>15] Igor Setuain, Miriam González-Izal, Jesús Alfaro, Esteban Gorostiaga, and Mikel Izquierdo. Acceleration and orientation jumping performance differences among elite professional male handball players with or without previous {ACL} reconstruction: An inertial sensor unit-based study. *PM&R*, 7(12):1243 – 1253, 2015.
- [SNSK16] Olli Särkkä, Tuukka Nieminen, Saku Suuriniemi, and Lauri Kettunen. Augmented inertial measurements for analysis of javelin throwing mechanics. *Sports Engineering*, pages 1–9, 2016.
- [Stu12] Dennis Sturm. *Wireless Multi-Sensor Feedback Systems for Sports Performance Monitoring*. PhD thesis, PhD thesis, PhD Thesis, KTH Royal Institute of Technology, 2012.
- [Sup10] Matej Supej. 3d measurements of alpine skiing with an inertial sensor motion capture suit and gnss rtk system. *Journal of Sports Sciences*, 28(7):759–769, 2010. PMID: 20473823.
- [TGAT11] B. Tessedorf, F. Gravenhorst, B. Arnrich, and G. Troster. An imu-based sensor network to continuously monitor rowing technique on the water. In *2011 Seventh International Conference on Intelligent Sensors, Sensor Networks and Information Processing (ISSNIP)*, pages 253–258, Dec 2011.
- [TTM13] Shigeru Tadano, Ryo Takeda, and Hiroaki Miyagawa. Three dimensional gait analysis using wearable acceleration and gyro sensors based on quaternion calculations. *Sensors*, 13(7):9321–9343, 2013.
- [VDSBB<sup>+</sup>15] RMA Van Der Slikke, MAM Berger, DJJ Bregman, AH Lagerberg, and HEJ Veeger. Opportunities for measuring wheelchair kinematics in match settings; reliability of a three inertial sensor configuration. *Journal of biomechanics*, 48(12):3398–3405, 2015.
- [Vic] Vicon Nexus. Optical motion capture system. Accessed 2016-03-18.

- [WS13] Brian V Wright and Joel M Stager. Quantifying competitive swim training using accelerometer-based activity monitors. *Sports Engineering*, 16(3):155–164, 2013.
- [XSe] XSens. Mtw motion tracker. Accessed 2015-10-17.
- [YB06] X. Yun and E.R. Bachmann. Design, implementation, and experimental results of a quaternion-based kalman filter for human body motion tracking. *IEEE Transactions on Robotics*, 22(6):1216–1227, Dec 2006.
- [YB16] N. Yadav and C. Bleakley. Fast calibration of a 9-dof imu using a 3 dof position tracker and a semi-random motion sequence. *Measurement: Journal of the International Measurement Confederation*, 90:192–198, 2016.
- [YBM08] X. Yun, E.R. Bachmann, and R.B. McGhee. A simplified quaternion-based algorithm for orientation estimation from earth gravity and magnetic field measurements. *IEEE Transactions on Instrumentation and Measurement*, 57(3):638–650, March 2008.
- [YBMC07] X. Yun, E.R. Bachmann, H. Moore, and J. Calusdian. Self-contained position tracking of human movement using small inertial/magnetic sensor modules. In *IEEE International Conference on Robotics and Automation, 2007*, pages 2526–2533, April 2007.



# Ski Jumping

- [ABVK95] Anton Arndt, Cert-Peter Bruggemann, Mikko Virmavirta, and Paavo Komi. Techniques used by olympic ski jumpers in the transition from takeoff to early flight. *Journal of Applied Biomechanics*, 11(2), 1995.
- [BKTG10] M. Bächlin, M. Kusserow, G. Troster, and H. Gubelmann. Ski jump analysis of an olympic champion with wearable acceleration sensors. In *2010 International Symposium on Wearable Computers (ISWC)*, pages 1–2, Oct 2010.
- [CFC<sup>+</sup>13] Julien Chardonens, Julien Favre, Florian Cuendet, Gérald Gremion, and Kamiar Aminian. A system to measure the kinematics during the entire ski jump sequence using inertial sensors. *Journal of Biomechanics*, 46(1):56 – 62, 2013.
- [CFLC<sup>+</sup>12] Julien Chardonens, Julien Favre, Benoit Le Callennec, Florian Cuendet, Gérald Gremion, and Kamiar Aminian. Automatic measurement of key ski jumping phases and temporal events with a wearable system. *Journal of Sports Sciences*, 30(1):53–61, 2012.
- [FIS13] FIS. *The international ski competition rules (ICR). Book III. Ski jumping*. 2013.
- [Kei33] Alexander Keiller. *The Judging of Style in Ski Jumping*, pages 42–46. The Canadian Ski Annual, 1933.
- [MBG09a] Pascual Marqués-Bruna and Paul Grimshaw. Mechanics of flight in ski jumping: aerodynamic stability in roll and yaw. *Sports Technology*, 2(3-4):111–120, 2009.
- [MBG09b] Pascual Marqués-Bruna and Paul Grimshaw. Mechanics of flight in ski jumping: Aerodynamic stability in pitch. *Sports Technology*, 2(1-2):24–31, 2009.
- [MRM<sup>+</sup>06] W. Meile, E. Reisenberger, M. Mayer, B. Schmölzer, W. Müller, and G. Brenn. Aerodynamics of ski jumping: experiments and cfd simulations. *Experiments in Fluids*, 41(6):949–964, 2006.
- [MS03] Erich Müller and Hermann Schwameder. Biomechanical aspects of new techniques in alpine skiing and ski-jumping. *Journal of sports sciences*, 21(9):679–692, 2003.
- [Mül09] Wolfram Müller. Determinants of ski-jump performance and implications for health, safety and fairness. *Sports medicine*, 39(2):85–106, 2009.
- [OHMS08] Yuji Ohgi, Nobuyuki Hirai, Masahide Murakami, and Kazuya Seo. Aerodynamic study of ski jumping flight based on inertia sensors (171). In *The Engineering of Sport 7*, pages 157–164. Springer Paris, 2008.

## Ski Jumping

---

- [SM02] B Schmölzer and W Müller. The importance of being light: aerodynamic forces and weight in ski jumping. *Journal of Biomechanics*, 35(8):1059 – 1069, 2002.
- [SM05] B. Schmölzer and W. Müller. Individual flight styles in ski jumping: results obtained during olympic games competitions. *Journal of Biomechanics*, 38(5):1055 – 1065, 2005.
- [SMY04] K. Seo, M. Murakami, and K. Yoshida. Optimal flight technique for v-style ski jumping. *Sports Engineering*, 7(2):97–103, 2004.
- [SWM04] K. Seo, I. Watanabe, and M. Murakami. Aerodynamic force data for a v-style ski jumping flight. *Sports Engineering*, 7(1):31–39, 2004.
- [VIK<sup>+</sup>05] Mikko Virmavirta, Juha Isolehto, Paavo Komi, Gert-Peter Brüggemann, Erich Müller, and Hermann Schwameder. Characteristics of the early flight phase in the olympic ski jumping competition. *Journal of Biomechanics*, 38(11):2157 – 2163, 2005.
- [VKK01] Mikko Virmavirta, Juha Kivekäs, and Paavo V Komi. Take-off aerodynamics in ski jumping. *Journal of Biomechanics*, 34(4):465 – 470, 2001.



## System Development Sources

- [Ada03] Brett Adams. Where does computational media aesthetics fit? *IEEE Multimedia*, 10(2):18–27, 2003.
- [ARGB04] Tiziano Agostini, Giovanni Righi, Alessandra Galmonte, and Paolo Bruno. *Biomechanics and Sports: Proceedings of the XI Winter Universiads 2003*, chapter The Relevance of Auditory Information in Optimizing Hammer Throwers Performance, pages 67–74. Springer Vienna, Vienna, 2004.
- [BDP<sup>+</sup>12] Oresti Banos, Miguel Damas, Hector Pomares, Alberto Prieto, and Ignacio Rojas. Daily living activity recognition based on statistical feature quality group selection. *Expert Systems with Applications*, 39(9):8013 – 8021, 2012.
- [CCG<sup>+</sup>15] Guang Chen, Daniel Clarke, Manuel Giuliani, Andre Gaschler, and Alois Knoll. Combining unsupervised learning and discrimination for 3d action recognition. *Signal Processing*, 110:67 – 81, 2015. Machine learning and signal processing for human pose recovery and behavior analysis.
- [CGG<sup>+</sup>09] Yihua Chen, Eric K. Garcia, Maya R. Gupta, Ali Rahimi, and Luca Cazzanti. Similarity-based classification: Concepts and algorithms. *Journal of Machine Learning Research*, 10:747–776, June 2009.
- [CHU14] Daniel Cesarini, Thomas Hermann, and Bodo Ungerechts. A real-time auditory biofeedback system for sports swimming. In *Proceedings of the 20th International Conference on Auditory Display (ICAD 2014)*, 2014.
- [CST00] Nello Cristianini and John Shawe-Taylor. *An introduction to support vector machines and other kernel-based learning methods*. Cambridge university press, 2000.
- [DB11] Gaël Dubus and Roberto Bresin. Sonification of physical quantities throughout history: a meta-study of previous mapping strategies. In *The 17th International Conference on Auditory Display (ICAD 2011). June 20-24, 2011, Budapest, Hungary*. OPAKFI Egyesület, 2011.
- [DB15] Gaël Dubus and Roberto Bresin. Exploration and evaluation of a system for interactive sonification of elite rowing. *Sports Engineering*, 18(1):29–41, 2015.
- [Eff05] Alfred O Effenberg. Movement sonification: Effects on perception and action. *IEEE Multimedia*, (2):53–59, 2005.



## System Development Sources

---

- [EFW11] Alfred Effenberg, Ursula Fehse, and Andreas Weber. Movement sonification: Audiovisual benefits on motor learning. In *BIO Web of Conferences*, volume 1, page 00022. EDP Sciences, 2011.
- [ESB<sup>+</sup>15] Alfred Oliver Effenberg, Gerd Schmitz, Florian Baumann, Bodo Rosenhahn, and Daniela Kroeger. SoundscripT—supporting the acquisition of character writing by multisensory integration. *The Open Psychology Journal*, 8(1), 2015.
- [FHT01] Jerome Friedman, Trevor Hastie, and Robert Tibshirani. *The elements of statistical learning*, volume 1. Springer series in statistics Springer, Berlin, 2001.
- [FZP03] Yazhong Feng, Yueting Zhuang, and Yunhe Pan. Music information retrieval by detecting mood via computational media aesthetics. In *IEEE/WIC International Conference on Web Intelligence, 2003. WI 2003. Proceedings.*, pages 235–241, Oct 2003.
- [GTM02] Michael SA Graziano, Charlotte SR Taylor, and Tirin Moore. Complex movements evoked by microstimulation of precentral cortex. *Neuron*, 34(5):841–851, 2002.
- [Hen07] Christoph Henkelmann. Improving the aesthetic quality of realtime motion data sonification. *Computer Graphics Technical Report CG-2007-4, University of Bonn*, 2007.
- [HHFS10] Jessica Hummel, Thomas Hermann, Christopher Frauenberger, and Tony Stockman. Interactive sonification of german wheel sports. In *Proceedings of ISON 2010-Interactive Sonification Workshop: Human Interaction with Auditory Displays*, 2010.
- [HSSL13] Mehrtash T. Harandi, Conrad Sanderson, Sareh Shirazi, and Brian C. Lovell. Kernel analysis on grassmann manifolds for action recognition. *Pattern Recognition Letters*, 34(15):1906 – 1915, 2013. Smart Approaches for Human Action Recognition.
- [JKBH15] Min Jiang, Jun Kong, George Bebis, and Hongtao Huo. Informative joints based human action recognition using skeleton contexts. *Signal Processing: Image Communication*, 33:29 – 40, 2015.
- [Joh73] Gunnar Johansson. Visual perception of biological motion and a model for its analysis. *Perception & psychophysics*, 14(2):201–211, 1973.
- [LCZT07] Yijuan Lu, Ira Cohen, Xiang Sean Zhou, and Qi Tian. Feature selection using principal feature analysis. In *Proceedings of the 15th international conference on Multimedia*, pages 301–304. ACM, 2007.
- [LSS07] Amir Lahav, Elliot Saltzman, and Gottfried Schlaug. Action representation of sound: audiomotor recognition network while listening to newly acquired actions. *The journal of neuroscience*, 27(2):308–314, 2007.

- [MA07] Richard A Magill and David Anderson. *Motor learning and control: Concepts and applications*, volume 11. McGraw-Hill New York, 2007.
- [MGSR<sup>+</sup>15] Jill L McNitt-Gray, Kathleen Sand, Christopher Ramos, Travis Peterson, Laura Held, and Korkut Brown. Using technology and engineering to facilitate skill acquisition and improvements in performance. *Proceedings of the Institution of Mechanical Engineers, Part P: Journal of Sports Engineering and Technology*, page 1754337114565381, 2015.
- [MR06] Meinard Müller and Tido Röder. Motion templates for automatic classification and retrieval of motion capture data. In *Proceedings of the 2006 ACM SIGGRAPH/Eurographics symposium on Computer animation*, pages 137–146. Eurographics Association, 2006.
- [MRM<sup>+</sup>05] Bill Manaris, Juan Romero, Penousal Machado, Dwight Krehbiel, Timothy Hirzel, Walter Pharr, and Robert B. Davis. Zipf’s law, music classification, and aesthetics. *Computer Music Journal*, 29(1):55–69, February 2005.
- [MSD<sup>+</sup>13] Gregory D Myer, Benjamin W Stroube, Christopher A DiCesare, Jensen L Brent, Kevin R Ford, Robert S Heidt, and Timothy E Hewett. Augmented feedback supports skill transfer and reduces high-risk injury landing mechanics a double-blind, randomized controlled laboratory study. *The American journal of sports medicine*, 41(3):669–677, 2013.
- [NDV01] F Nack, C. Dorai, and S. Venkatesh. Computational media aesthetics: finding meaning beautiful. *IEEE MultiMedia*, 8(4):10–12, Oct 2001.
- [PDLM15] Hossein Pazhoumand-Dar, Chiou-Peng Lam, and Martin Masek. Joint movement similarities for robust 3d action recognition using skeletal data. *Journal of Visual Communication and Image Representation*, 30:10 – 21, 2015.
- [PFBH13] Elissa Phillips, Damian Farrow, Kevin Ball, and Richard Helmer. Harnessing and understanding feedback technology in applied settings. *Sports Medicine*, 43(10):919–925, 2013.
- [PH06] Henning Plessner and Thomas Haar. Sports performance judgments from a social cognitive perspective. *Psychology of sport and exercise*, 7(6):555–575, 2006.
- [Pur] PureData (PD). Visual sound programming language. Accessed 2016-05-19.
- [PvSMW15] G. I. Parisi, F. von Stosch, S. Magg, and S. Wermter. Learning human motion feedback with neural self-organization. In *2015 International Joint Conference on Neural Networks (IJCNN)*, pages 1–6, July 2015.
- [Riz05] Giacomo Rizzolatti. The mirror neuron system and its function in humans. *Anatomy and embryology*, 210(5):419–421, 2005.

## System Development Sources

---

- [Rot95] Joseph Rothstein. *MIDI: A comprehensive introduction*, volume 7. AR Editions, Inc., 1995.
- [SBD<sup>+</sup>09] Lukas Scheef, Henning Boecker, Marcel Daamen, Ursula Fehse, Martin W Landsberg, Dirk-Oliver Granath, Heinz Mechling, and Alfred O Effenberg. Multimodal motion processing in area v5/mt: evidence from an artificial class of audio-visual events. *Brain research*, 1252:94–104, 2009.
- [SBGI10] Gerd Schmitz, Otmar Bock, Valentina Grigorova, and Milena Ilieva. Adaptation of eye and hand movements to target displacements of different size. *Experimental brain research*, 203(2):479–484, 2010.
- [SBKF<sup>+</sup>13] Cassandra Sampaio-Baptista, Alexandre A Khrapitchev, Sean Foxley, Theresa Schlagheck, Jan Scholz, Saad Jbabdi, Gabriele C DeLuca, Karla L Miller, Amy Taylor, Nagheme Thomas, et al. Motor skill learning induces changes in white matter microstructure and myelination. *The Journal of Neuroscience*, 33(50):19499–19503, 2013.
- [Sch75] Richard A Schmidt. A schema theory of discrete motor skill learning. *Psychological review*, 82(4):225, 1975.
- [SH13] Gabriela Seibert and Daniel Hug. Bringing musicality to movement sonification: Design and evaluation of an auditory swimming coach. In *Proceedings of the 8th Audio Mostly Conference, AM '13*, pages 17:1–17:6, New York, NY, USA, 2013. ACM.
- [SKE14] Gerd Schmitz, Daniela Kroeger, and Alfred O Effenberg. A mobile sonification system for stroke rehabilitation. 2014.
- [SKM12] Lior Shmuelof, John W Krakauer, and Pietro Mazzoni. How is a motor skill learned? change and invariance at the levels of task success and trajectory control. *Journal of neurophysiology*, 108(2):578–594, 2012.
- [SL88] Richard A Schmidt and Tim Lee. *Motor control and learning*. Human kinetics, 1988.
- [SM93] Barry E Stein and M Alex Meredith. *The merging of the senses*. The MIT Press, 1993.
- [SMBE09] Nina Schaffert, Klaus Mattes, Stephen Barrass, and Alfred O Effenberg. Exploring function and aesthetics in sonifications for elite sports. In *Proceedings of the 2nd International Conference on Music Communication Science (ICoMCS2)*, pages 83–86, 2009.
- [SMH<sup>+</sup>13] Gerd Schmitz, Bahram Mohammadi, Anke Hammer, Marcus Heldmann, Amir Samii, Thomas F Münte, and Alfred O. Effenberg. Observation of sonified movements engages a basal ganglia frontocortical network. *BMC Neuroscience*, 14(1):1–11, 2013.

- [SO08] J. Shin and S. Ozawa. A study on motion analysis of an artistic gymnastics by using dynamic image processing - for a development of automatic scoring system of horizontal bar. In *IEEE International Conference on Systems, Man and Cybernetics, 2008. SMC 2008.*, pages 1037–1042, Oct 2008.
- [SOW11] Jelle Stienstra, Kees Overbeeke, and Stephan Wensveen. Embodying complexity through movement sonification: Case study on empowering the speed-skater. In *Proceedings of the 9th ACM SIGCHI Italian Chapter International Conference on Computer-Human Interaction: Facing Complexity*, CHIItaly, pages 39–44, New York, NY, USA, 2011. ACM.
- [SRRW12] Roland Sigrist, Georg Rauter, Robert Riener, and Peter Wolf. Augmented visual, auditory, haptic, and multimodal feedback in motor learning: A review. *Psychonomic Bulletin & Review*, 20(1):21–53, 2012.
- [SSW84] Alan W Salmoni, Richard A Schmidt, and Charles B Walter. Knowledge of results and motor learning: a review and critical reappraisal. *Psychological bulletin*, 95(3):355, 1984.
- [Ste14] George E Stelmach. *Information processing in motor control and learning*. Academic Press, 2014.
- [SW76] Claude E Shannon and Warren Weaver. *Mathematische grundlagen der informationstheorie*, 1976.
- [SW08] Richard A Schmidt and Craig A Wrisberg. *Motor learning and performance: A situation-based learning approach*. Human Kinetics, 2008.
- [SWDS15] Rim Slama, Hazem Wannous, Mohamed Daoudi, and Anuj Srivastava. Accurate 3d action recognition using learning on the grassmann manifold. *Pattern Recognition*, 48(2):556 – 567, 2015.
- [TRS02] Ian M Thornton, Ronald A Rensink, and Maggie Shiffrar. Active versus passive processing of biological motion. *Perception*, 31(7):837–853, 2002.
- [TWL05] Nikolaus F Troje, Cord Westhoff, and Mikhail Lavrov. Person identification from biological motion: Effects of structural and kinematic cues. *Perception & Psychophysics*, 67(4):667–675, 2005.
- [VKF<sup>+</sup>13] Pia M Vinken, Daniela Kröger, Ursula Fehse, Gerd Schmitz, Heike Brock, and Alfred O Effenberg. Auditory coding of human movement kinematics. *Multisensory research*, 26(6):533–552, 2013.
- [WDFJ13] Yanran Wang, Qi Dai, Rui Feng, and Yu-Gang Jiang. Beauty is here: Evaluating aesthetics in videos using multimodal features and free training data. In *Proceedings of the 21st ACM International Conference on Multimedia*, MM '13, pages 369–372, New York, NY, USA, 2013. ACM.

## System Development Sources

---

- [WH79] Stephen A Wallace and Richard W Hagler. Knowledge of performance and the learning of a closed motor skill. *Research Quarterly. American Alliance for Health, Physical Education, Recreation and Dance*, 50(2):265–271, 1979.
- [Wie49] Norbert Wiener. Kybernetik. *Physikalische Blätter*, 5(8):355–362, 1949.
- [Wor] WordPress. Software for website creation. Accessed 2016-05-19.
- [XL15] Jian Xiang and Ronghua Liang. Motion recognition and synthesis based on 3d sparse representation. *Signal Processing*, 110:82 – 93, 2015. Machine learning and signal processing for human pose recovery and behavior analysis.
- [YA13] Kazuma Yanagisawa and Kakuro Amasaka. Constructing a scoring support approach model for classical ballet: Combining motion capture and statistical science. *Journal of Business & Economics Research (Online)*, 11(6):241, 2013.
- [YH83] BL Yen and TS Huang. Determining 3-d motion and structure of a rigid body using the spherical projection. *Computer Vision, Graphics, and Image Processing*, 21(1):21–32, 1983.
- [YKT<sup>+</sup>15] Shinichi Yamagiwa, Yoshinobu Kawahara, Noriyuki Tabuchi, Yoshinobu Watanabe, and Takeshi Naruo. Skill grouping method: Mining and clustering skill differences from body movement bigdata. In *IEEE International Conference on Big Data (Big Data)*, 2015, pages 2525–2534. IEEE, 2015.
- [YLC09] Yi-Hsuan Yang, Yu-Ching Lin, and Homer Chen. Personalized music emotion recognition. In *Proceedings of the 32nd international ACM SIGIR conference on Research and development in information retrieval*, pages 748–749. ACM, 2009.
- [YLSC08] Yi-Hsuan Yang, Yu-Ching Lin, Ya-Fan Su, and H.H. Chen. A regression approach to music emotion recognition. *IEEE Transactions on Audio, Speech, and Language Processing*, 16(2):448–457, Feb 2008.
- [YOS14] Shinichi Yamagiwa, Hiroyuki Ohshima, and Kazuki Shirakawa. Development of skill scoring system for ski and snowboard. In *International Congress on Sports Science Research and Technology Support*, pages 1–15. Springer, 2014.
- [YRC13] William Young, Matthew Rodger, and Cathy M Craig. Perceiving and reenacting spatiotemporal characteristics of walking sounds. *Journal of Experimental Psychology: Human Perception and Performance*, 39(2):464, 2013.
- [YYC11] Chun-Yu Yang, Hsin-Ho Yeh, and Chu-Song Chen. Video aesthetic quality assessment by combining semantically independent and dependent features. In *2011 IEEE International Conference on Acoustics, Speech and Signal Processing (ICASSP)*, pages 1165–1168, May 2011.
- [ZB15] Maryam Ziaefard and Robert Bergevin. Semantic human activity recognition: A literature review. *Pattern Recognition*, 48(8):2329 – 2345, 2015.

- [ZBMM06] Hao Zhang, A. C. Berg, M. Maire, and J. Malik. Svm-knn: Discriminative nearest neighbor classification for visual category recognition. In *2006 IEEE Computer Society Conference on Computer Vision and Pattern Recognition*, volume 2, pages 2126–2136, 2006.
- [Zit06] Eric Zitzewitz. Nationalism in winter sports judging and its lessons for organizational decision making. *Journal of Economics and Management Strategy*, 15(1):67–99, 2006.
- [Zit14] Eric Zitzewitz. Does transparency reduce favoritism and corruption? evidence from the reform of figure skating judging. *Journal of Sports Economics*, 15(1):3–30, 2014.
- [ZZZ15] Ying Zhang, Luming Zhang, and Roger Zimmermann. Aesthetics-guided summarization from multiple user generated videos. *ACM Transactions on Multimedia Computing, Communications and Applications*, 11(2):24:1–24:23, January 2015.